Zhenfeng Xi   *Editor*

Organo-di-Metallic Compounds (or Reagents)

Synergistic Effects and Synthetic Applications

Springer

47
Topics in Organometallic Chemistry

Aims and Scope

The series *Topics in Organometallic Chemistry* presents critical overviews of research results in organometallic chemistry. As our understanding of organometallic structure, properties and mechanisms increases, new ways are opened for the design of organometallic compounds and reactions tailored to the needs of such diverse areas as organic synthesis, medical research, biology and materials science. Thus the scope of coverage includes a broad range of topics of pure and applied organometallic chemistry, where new breakthroughs are being achieved that are of significance to a larger scientific audience.

The individual volumes of *Topics in Organometallic Chemistry* are thematic. Review articles are generally invited by the volume editors. All chapters from *Topics in Organometallic Chemistry* are published OnlineFirst with an individual DOI. In references, *Topics in Organometallic Chemistry* is abbreviated as Top Organomet Chem and cited as a journal.

More information about this series at
http://www.springer.com/series/3418

Zhenfeng Xi
Editor

Organo-di-Metallic Compounds (or Reagents)

Synergistic Effects and Synthetic Applications

With contributions by

G. Barozzino-Consiglio · N. Duguet · M. Fustier-Boutignon ·
A. Harrison-Marchand · J. Maddaluno · N. Mézailles ·
R.E. Mulvey · H. Oulyadi · S.D. Robertson · M. Uchiyama ·
C. Wang · Z. Xi · S. Zhang · W.-X. Zhang

Springer

Editor
Zhenfeng Xi
College of Chemistry
Peking University
Beijing
China

Printed on acid-free paper

Preface

Synergy, gathering synergistic effects, and cooperative effects, have become phrases frequently used in the chemical literature and frequently heard at oral presentations at various chemical conferences. As a powerful synthetic strategy, synergy results in new structural bonding modes, new reaction patterns and synthetic methods which are not accessible by simply mixing up two or more reagents even when they are reaction partners.

Dianions present in the same derivative frequently appear as important synthetic intermediates and often show synergistic effects inside the same molecule and toward useful transformations of substrates. This volume deals with dianionic compounds which contain carbon anions with various metals (such as Li, Mg, Ca, Ba, Al, Fe, Zn, Cu, rare earth metals, etc.). Synthesis and structures of dianionic compounds containing two identical or different metals are briefly introduced. Their synthetic applications based on their synergistic effects are focused especially on making organic compounds and organometallic compounds via novel improved processes.

Five research groups with expertise in the field summarize recent fascinating developments, including 1,4-dilithio-1,3-butadienes and their transmetallated organo-di-metallic compounds, mixed dimers of lithium amide/alkyllithium, *gem*-diorganometallic compounds, alkali-metal mixed-metal ate compounds, and lithium zincates.

The primary purpose of this volume is to demonstrate the unique structures and synthetic innovations of organo-di-metallic compounds and to initiate new ideas leading to further synthetic strategy in the future. This volume should be useful to researchers in organic and organometallic chemistry and catalysis both from academia and industry. Moreover, young researchers, doctorate students and postdoctoral researchers should be motivated by these innovations in chemistry.

I gratefully acknowledge the cooperative contributions by all authors. Without their expertise and efforts this volume would not have been possible. I would also like to thank Prof. Dixneuf for his encouragement and help throughout the preparation of this volume.

Beijing, China   Zhenfeng Xi
May 2014

Contents

Organo-*di*-Lithio Reagents: Cooperative Effect and Synthetic Applications

Shaoguang Zhang, Wen-Xiong Zhang, and Zhenfeng Xi[*]

Abstract The development of organometallic reagents remains one of the most important frontiers in synthetic chemistry. In this review, we summarize our research on the structures, reactions, and synthetic applications of 1,4-dilithio-1,3-butadienes as organo-*di*-lithio reagents. The 1,4-dilithio-1,3-butadienes bearing a wide variety of substitution patterns on the butadienyl skeleton can be readily prepared in high efficiency. The configuration has been predicted and demonstrated to favor a double dilithium bridging structure in both solution and solid states. The two Li atoms are bridged by a butadiene moiety and are in close proximity. By taking advantage of this unique configuration, we have developed useful and interesting synthetic methodologies. Three types of reactions of 1,4-dilithio-1,3-butadienes have been developed and are discussed: intramolecular reaction, intermolecular reaction, and transmetallation. First, intramolecular reaction is introduced as a result of the intra-cooperative effect among the two C–Li moieties, the butadienyl bridge, and the substituents. A useful transformation from silylated 1,4-dilithio-1,3-butadienes to α-lithio siloles is described. Second, we discuss an intermolecular reaction that results from the inter-cooperative effect of the two C–Li moieties toward substrates. The intermolecular reactions are featured with formation of oxy-cyclopentadienyl dilithium via the reaction of di-lithio reagents with CO and formation of a series of *N*-heterocycles via the reaction of di-lithio reagents with nitriles. Third, we discuss transmetallation of di-lithio reagents with aluminum, copper, iron, zinc, or barium salts to generate diversified organo-*di*-metallic or metallacyclic compounds. The dimetallic 1,4-dilithio-1,3-butadienes and their transmetallated derivatives provide unique synthetic organometallic reagents that are different from monometallic reagents, both in terms of reactivity and in synthetic application. These organo-*di*-metallic reagents provide the access to interesting and useful compounds that are not available by other means, such as

S. Zhang, W.-X. Zhang, and Z. Xi* (✉)
College of Chemistry, Peking University, Beijing 100871, China
e-mail: zfxi@pku.edu.cn

N-, O-, and Si-containing heterocycles, strained ring systems, metal-containing macrocycles, and metal complexes bearing new types of ligand.

Keywords Cooperative effect · 1,4-Dilithio-1,3-butadiene · Intermolecular reaction · Intramolecular reaction · Structure · Transmetallation

Contents

Abbreviations

Ac	Acetyl
Ad	Adamantyl
Ar	Aryl
Bn	Benzyl
Bu	Butyl
cat	Catalyst
cod	Cyclooctadiene
COT	Cyclooctatetraene
Cp	Cyclopentadienyl
DMAD	Dimethyl azodicarboxylate
DME	1,2-Dimethoxyethane

DMF	Dimethylformamide
DMPU	1,3-Dimethyl-3,4,5,6-tetrahydro-2(1H)-pyrimidinone
DMSO	Dimethyl sulfoxide
dppe	1,2-Bis(diphenylphosphino)ethane
ee	Enantiomer excess
equiv	Equivalent(s)
Et	Ethyl
h	Hour(s)
Hex	Hexyl
HMPA	Hexamethylphosphoric triamide
i-Pr	Isopropyl
LDA	Lithium diisopropylamide
Me	Methyl
min	Minute(s)
mol	Mole(s)
NBS	*N*-bromosuccinimide
NCS	*N*-chlorosuccinimide
Nu	Nucleophile
Ph	Phenyl
Pr	Propyl
py	Pyridine
rt	Room temperature
s	Second(s)
TBAF	Tetrabutylammonium fluoride
t-Bu	*Tert*-butyl
THF	Tetrahydrofuran
TIPS	Triisopropylsilyl
TMEDA	*N,N,N′,N′*-Tetramethyl- 1,2-ethylenediamine
TMS	Trimethylsilyl
Tol	4-Methylphenyl
Ts	4-toluenesulfonyl

1 Introduction

The development of practical and efficient organometallic reagents has greatly accelerated the advancement of synthesis and related subjects. Consequently, the research and development of organometallic reagents continues to be one of the most important areas in synthetic chemistry. Among all types of organometallic reagents, organolithium compounds are a class of important reagents in preparative chemistry since the pioneering work of Schlenk [1–6]. In contrast to mono-lithium compounds, much less investigations were carried out on the structures, reactivities, and aggregation states of organo-*di*-lithium compounds [7–21].
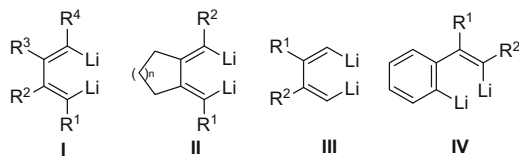
Fig. 1 Representative skeletons of di-lithio reagents. R^1, R^2, R^3, R^4 can be H, alkyl, alkenyl, aryl, silyl, etc.; the substituents and the size of the ring may be different

Conceptually, when two carbon–metal bonds are in the same molecule and in close proximity, these two carbon–metal moieties may exhibit novel reactivity. A few of 1,4-dilithio compounds are developed and used as 1,4-dianion precursors for the preparation of main group metallole [22]. Besides, some dilithium or even polylithium compounds show interesting reactivity [7–21]. For example, bis (2-lithioallyl)amines [15], 2,9-dilithio-1,4,6,9-decatetraenes [16], 3,4-dilithio-2,4-hexadienes [17], and lithiophenylalkyllithiums [18–20] have been prepared and their reactivities toward carbonyl compounds have been reported.

In 1999, we occasionally found that substituted 1,4-dilithio-1,3-butadienes (Fig. 1, di-lithio reagents for short) exhibit different reactivity patterns compared with their mono-lithium analogs toward organic carbonyl compounds [12–14]. We gradually recognized that the cooperative effect between the two C–Li moieties and the butadienyl bridge is essential for realizing such reaction patterns.

Shown in Fig. 1 are four representative skeletons of di-lithio reagents. A wide variety of substituents on the butadienyl skeleton can be readily introduced. Herein we would like to discuss our results on the chemistry of di-lithio reagents in our group. We focus on three major reaction patterns: (1) intramolecular reactions, (2) intermolecular reactions, and (3) transmetallations. Some reactions of di-lithio reagents which did not show the cooperative effect of two C–Li bonds will not be included in this review. The reactions illustrate the cooperative reactivity of these di-lithio reagents as well as the effect of substituents on the butadienyl skeleton. Additionally, these organo-*di*-metallic reagents provide access to interesting and useful compounds which could not be easily synthesized by other means, such as *N*-, *O*-, and *Si*-containing heterocycles, strained ring systems, functional polycyclic skeletons, metal-containing macrocycles, and metal complexes bearing new types of ligand.

2 Preparation and Structures of 1,4-Dilithio-1,3-Butadienes

1,2,3,4-Tetraphenyl-1,4-dilithio-1,3-butadiene as the first all-substituted 1,4-dilithio-1,3-butadiene compound was prepared by Schlenk and Bergmann in 1928 by reaction of diphenylacetylene with Li [23, 24]. Di-lithio reagents **1** have been predicated and structurally demonstrated to favor a double dilithium bridged
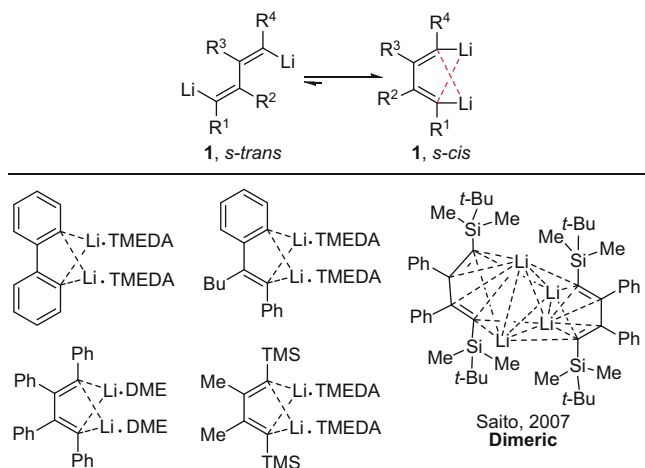
Scheme 1 Selected examples of structures of 1,4-dilithio-1,3-butadienes, which favor a double dilithium bridged structure (*s-cis* configuration) in both solution and solid states

structure (*s-cis* configuration) in both solution and solid states. In 1980, Kos and Schleyer reported an initial ab initio MO study of **1**, which showed that a symmetrically bridged structure (*s-cis*) was energetically favored over non-bridged conformations (Scheme 1) [25]. The theoretical predictions with double lithium bridges were confirmed by single-crystal X-ray structure of 2,2′-dilithiobiphenyl in 1982 [26]. Later, X-ray structures of the aryl or Si-substituted 1,4-dilithio-1,3-butadienes with coordinated TMEDA or DME again confirmed the double dilithium bridge adopting a monomeric fashion in the solid state structures [27, 28]. In 2007, Saito et al. reported a dimeric structure of a silyl-substituted di-lithio compounds [29].

Since we found 1,4-dilithio-1,3-butadienes demonstrate different reaction patterns from commonly used mono-lithium reagents, we have tried to establish an efficient synthetic method to obtain pure di-lithio compounds, aiming at developing such compounds as useful organo-*di*-lithio reagents and characterizing their single-crystal structures [30–33]. Until now, several types of well-defined 1,4-dilithio-1,3-butadienes **1** (Types **I**, **II**, **III**, **IV** in Fig. 1) have already been designed and prepared readily in high efficiency with a wide variety of substitution patterns on the butadienyl skeleton. According to their X-ray crystal structures, these organo-*di*-lithio compounds could be divided into four types: trimeric all-alkyl substituted 1,4-dilithio-1,3-butadienes **1a** (*Type I*), dimeric 1,4-dilithio-1,3-butadienes **1b–d** (*Type II*), monomeric 1,4-dilithio-1,3-butadienes **1e** (*Type III*), and 3-D brickwall coordination polymer of dimeric 1,4-dilithio-1,3-butadienes **1f** (*Type IV*) [30–33]. All examples of di-lithio compounds **1** clearly showed the dilithium bridge in X-ray structures.

1,2,3,4-Tetraethyl-1,4-dilithio-1,3-butadienes **1a** (*Type I*, Scheme 2) was generated in situ from its corresponding 1,4-diiodo-1,3-butadiene **2a** and 4 equiv of
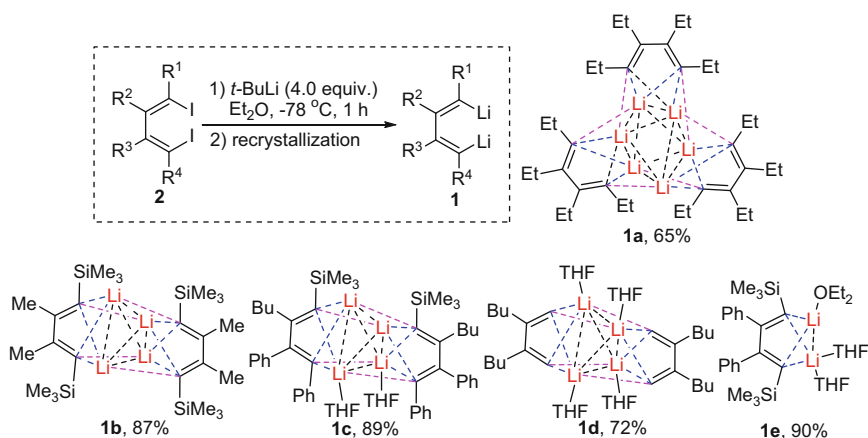
Scheme 2 Preparation and isolation of organo-*di*-lithium reagents

t-BuLi in diethyl ether at –78°C for 1 h [30]. The pure **1a** was obtained in 65% yield by extracting the in situ generated **1a** with hexane and recrystallization in hexane after filtration of LiI. X-ray structure of **1a** revealed a trimeric pattern with a Li_6 pseudooctahedron [30]. This result provides the first structural information of more general all-alkyl substituted **1** in higher aggregation states.

Under similar procedure, di-lithio compounds **1b–d** (*Type II*, Scheme 2) could be obtained in high yield as a dimer in the solid state [30–32]. The aggregation states and coordination environment of Li atom depend on the substitution pattern and steric hindrance on butadiene skeleton. In the crystal structure of **1a** and **1b**, no external ligand is coordinated to Li atom, while in the crystal structure of **1c**, THF ligands are only coordinated to the less-hindered, α-phenyl-substituted Li atom. In the crystal structure of **1d**, each Li atom is coordinated by one THF ligand. We suggest that Li atom in **1d** is much less hindered and easier to accept THF coordination because of only hydrogens on 1,4-position of butadiene skeleton [32].

In contrast with the dimeric structure of **1b**, an X-ray structural analysis of 1,4-bis(silyl)-2,3-diphenyl-1,4-dilithio-1,3-diene **1e** revealed a monomeric pattern with a double dilithium bridge (*Type III*, Scheme 2), despite no chelating ligands such as TMEDA were used [33]. Two Li atoms were coordinated with two THF and one Et_2O, respectively.

In the presence of TMEDA, a 3-D brickwall coordination polymer of TMEDA-supported dimeric, less bulky 2,3-dialkyl-1,4-dilithio-1,3-butadiene **1f** was formed, which has been confirmed by X-ray analysis (*Type IV*, Scheme 3) [32]. The expected TMEDA-chelated monomeric structure **1f'** as a deaggregation product was not formed. As shown in Fig. 2 and Scheme 3, in monolayer of 3-D brickwall polymeric structure of **1f**, six Li_4 cores and six TMEDA bridges composed a chair-like macrocyclic unit. The macrocyclic unit extends to form 2-D brickwall mono-layer via N-Li coordination. The brickwall monolayers are linked by TMEDA molecules to form the 3-D network, also forming chair-like Li_4-TMEDA
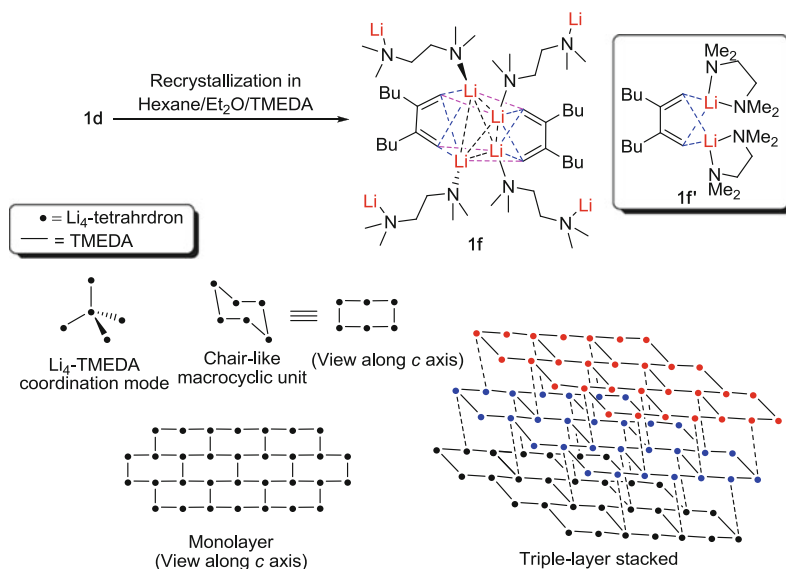
Scheme 3 Preparation of **1f** and diagrams of Li$_4$-TMEDA coordination mode, monolayer structure, and layer-by-layer stacked structure
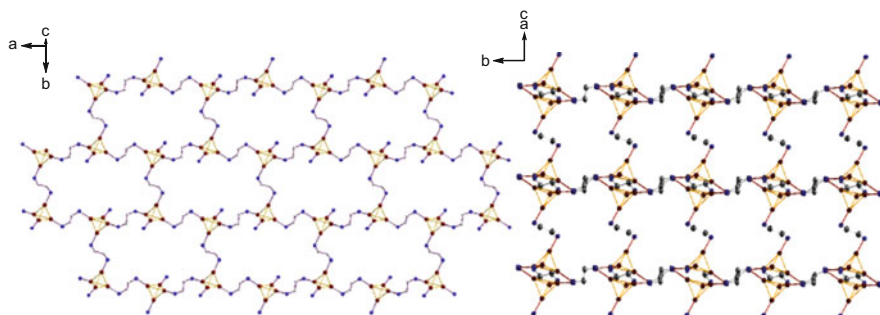
Fig. 2 (*Left*) Two-dimensional brickwall motif in crystalline **1f** via N-Li coordination. (*Right*) Layer-by-layer stacked network in crystalline **1f**. Hydrogen atoms, butyls, butadiene skeletons, and methyls on TMEDAs are omitted for clarity. C *gray*, N *blue*, Li *dark red*

macrocycles. TMEDAs behave as bridging coordinating ligands rather than intramolecular chelating ligands. The Li$_4$-tetrahedron core was stable toward the deaggregation of TMEDA probably because of the small steric hindrance on the butadiene skeleton.

Most of such derivatives can be obtained in this group as fine crystalline compounds in good to excellent isolated yields with gram scale, which are kept in cooler and used when needed as reagents.

The lithium bridge in the solid states and in solution enables these di-lithio reagents to show cooperative effect, by which both two C–Li bonds react with the substrates, giving several types of cyclic or acyclic organic compounds as well as

organometallic complexes, depending on the substitution pattern on the butadienyl skeletons and the substrates used.

3 Intramolecular Reaction Pattern: Formation of α-Lithio Siloles from Silyl-Substituted Di-lithio Reagents via E/Z Isomerization Followed by Nucleophilic Attack

3.1 Reaction and Mechanistic Aspects

Normally, di-lithio reagents were generated at low temperature. When the reaction mixture was warmed to higher temperature, functionalized substituents on the butadienyl skeletons of di-lithio reagents might trigger intramolecular reaction among the C–Li bonds and substituents and thus resulted in intramolecular cyclization or other reaction types. As a typical example, the intramolecular cyclization of silyl-substituted 1,4-dilithio-1,3-butadienes **1** affording lithio silole derivatives is introduced. When the reaction mixture of silyl-substituted **1** was heated to reflux in Et$_2$O, intramolecular cyclization took place to efficiently afford α-lithio siloles **6** (Scheme 4) [34–36]. The lithio siloles **6** obtained by this reaction are more general in terms of substitution patterns.

This was the first intramolecular reaction pattern of such di-lithio compounds. Mechanistic investigation demonstrated that an *E/Z* isomerization of one of those 1-silyl-1-lithio alkene moieties in **1** took place, followed by intramolecular cyclization along with cleavage of Si–Me bond and elimination of MeLi (Scheme 4) [37, 38]. The released MeLi moiety can be readily trapped by various electrophiles. Organolithium-mediated cleavage of Si–C bond from SiR^{1}R^{2}R^3 group is an interesting and fundamental topic for silicon chemistry [39, 40]. An X-ray single-crystal structure of **6a** reveals that it adopts a dimeric fashion through two lithium bridges, in which two carbon atoms and one Et$_2$O are bonded to each lithium atom. The distance between two Li atoms is 2.258 Å, which suggests a strong Li–Li interaction [36].

3.2 Synthetic Applications

Synthesis and applications of functionalized siloles have become ever more attractive in recent years, since these types of compounds have practical applications including π-conjugated organic materials of electronic and optoelectronic devices [41, 42]. As well documented, substituents on siloles have a remarkable impact on the property of siloles. Therefore, it is important to realize the multi-substituted pattern of produced functional siloles. When treated with a wide variety of electrophiles such as iodine, methyl iodide, ketone, aldehyde, CO$_2$, chlorosilane, or acid
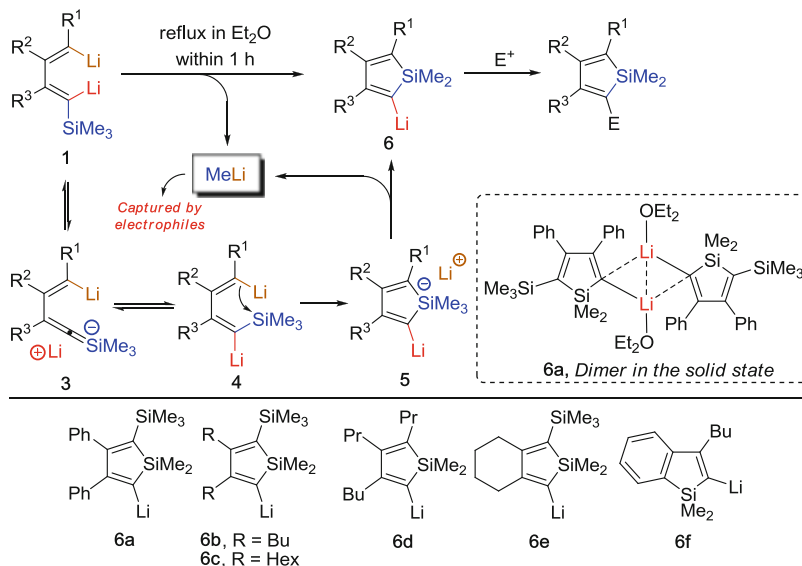
Scheme 4 Intramolecular cyclization of silyl-substituted 1,4-dilithio-1,3-butadienes to afford α-lithio siloles via E/Z isomerization and nucleophilic attack
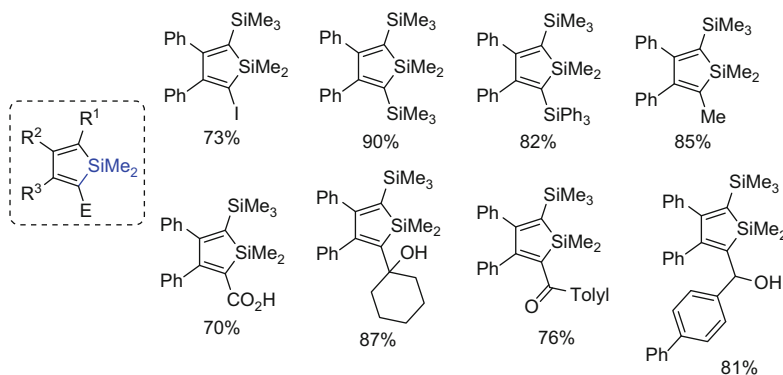
Fig. 3 Various silole-containing compounds available from this methodology

chloride, lithio siloles **6** are readily transformed into diversified silole-containing compounds (Fig. 3) [34–36].

Linear and planar poly- or oligo-silole systems are among mostly used silole systems with elongated conjugation.[19] Our protocol was further successfully used to prepare di-lithio bis-silole derivatives bearing different substituents (Scheme 5). For example, the linked tetra-lithio reagent **7** could be readily transformed to linked di-lithio bis-silole derivatives **8**, which could afford interesting but otherwise unavailable bridged bis-siloles **9** upon treatment with electrophiles. Thus,
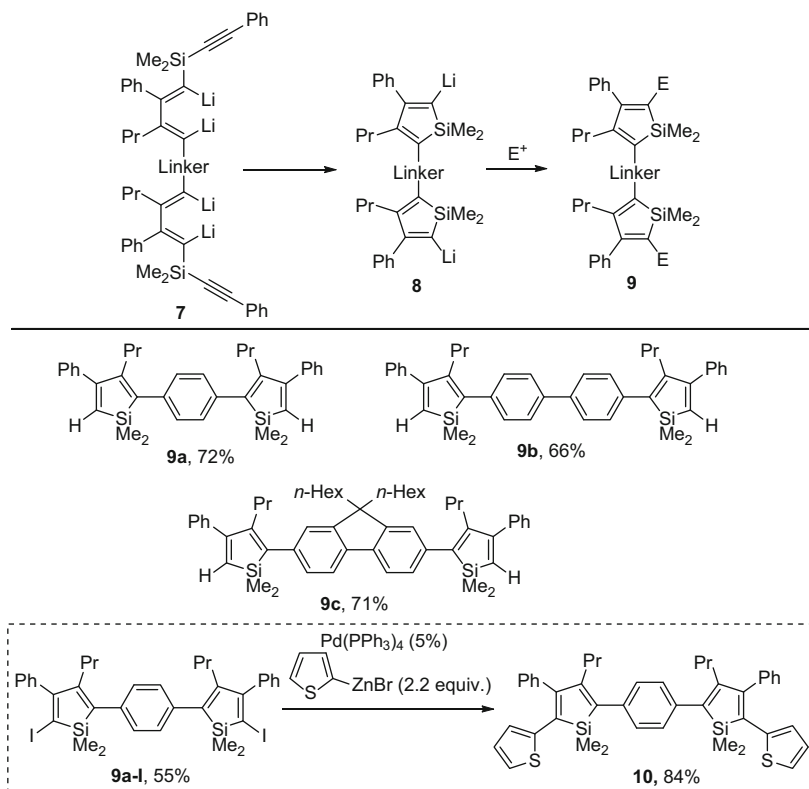
Scheme 5 From linked tetra-lithio reagents to linked bis-siloles

phenyl-linked bis-silole **9a**, biphenyl linked bis-silole **9b**, and fluorenyl linked bis-silole **9c** could all be obtained in good yields [35, 36]. When di-lithio bis-silole derivative **8** was treated with iodine, the bis-iodonated phenyl-linked bis-silole **9a–I** was obtained in 55% isolated yield. This functionalized **9a–I** could be further utilized to afford the product **10** with elongated conjugation in 84% yield by Negishi coupling (Scheme 5) [36].

4   Intermolecular Reaction Pattern

As mentioned above, the double dilithium bridge in 1,4-dilithio-1,3-butadiene **1** exists both in the solid states and in solution. When these di-lithio reagents are allowed to react with other substrates, the two C–Li bonds would work together to show cooperative effect, and a variety of cyclic or acyclic compounds could be thus generated. Formation of cyclic compounds from the reactions of polylithium reagents has been reported. For example, bis(2-lithioallyl) amines as

non-conjugated di-lithio reagents were reported by Barluenga to react with carboxylic esters to afford cyclic alcohols after hydrolysis [15]. A dilithiated-dihydropyrrole was proposed as the key intermediate, which was generated via intramolecular carbolithiation of a lithiated double bond. Similarly, the reaction of 2,9-dilithio-1,4,6,9-decatetraenes with acyl halides or carboxylic esters gave nine-membered carbocycles [16]. The conjugated diene moiety probably fixes the skeleton and makes the two alkenyllithium moieties in close proximity.

4.1 Reactions with Carbonyl Compounds: Formation of Cyclopentadiene or 2,5-Dihydrofuran Derivatives

In general, two types of C–C bond formation reactions are known via the deoxygenation of the C=O bonds in carbonyl compounds (Scheme 6, *Type I* and *Type II*). The formation of cyclopentadiene derivatives from 1,4-dilithio-1,3-dienes and aldehydes or ketones via direct cyclo-dialkenylation represents a new pattern of C–C bond formation involving carbonyl compounds (Scheme 6, *Type III*). When 1,4-dilithio-1,3-diene derivative was treated with 1 equivalent of cyclohexanone at $-78°C$ for 30 min, multi-substituted cyclopentadiene **13** could be isolated in high isolated yield (Scheme 7) [43, 44]. Both ketones and aldehydes could be applied in the reaction and a variety of cyclopentadiene derivatives of diverse structures could be prepared, such as spiro compounds and tetrahydroindene derivatives (Scheme 7) [43, 44]. Reactions of **1** with ketones give higher yields than the reactions with aldehydes, probably due to higher reactivity of aldehydes than ketones toward organolithium reagents. From the mechanistic aspect, chelation of the two C–Li bonds with the carbonyl group is proposed to be involved in this reaction (Scheme 7). First, nucleophilic addition of one of the two alkenyllithium moieties in **11** with the chelated carbonyl group gives **12**, which then undergoes an intramolecular nucleophilic attack by another alkenyllithium moiety to give the cyclopentadiene derivatives, with elimination of lithium oxide.

When two equivalents of aldehydes were allowed to react with di-lithio reagent **1** at room temperature, 2,5-dihydrofuran derivatives **15** were formed with high stereoselectivity (Scheme 8) [45]. The formation of cyclopentadiene derivatives was not observed in most cases. Depending on the bulkiness of the ketones, analogous reactions with ketones afforded mixtures of 2,5-dihydrofurans and cyclopentadienes. 1,6-Dialkoxide **14** is assumed to be the intermediate in this reaction (Scheme 8). Several experimental results indicated that intramolecular nucleophilic attack followed by elimination of Li_2O might be the reaction pathway leading to the final product (*path a*); however, since 1,6-diols **16** were isolated in some cases, the acid-promoted allylic rearrangement and sequential cyclization leading to 2,5-dihydrofurans (*path b*) could not be ruled out.
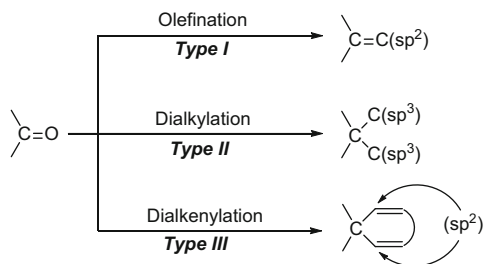
Scheme 6 Types of C=C bond forming reactions via cleavage of the C=O double bonds in carbonyl compounds
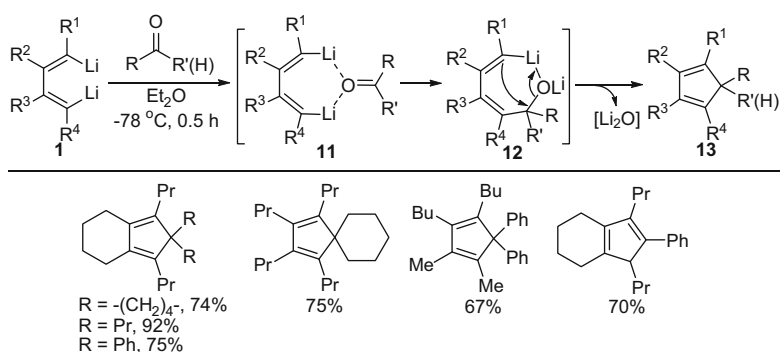
Scheme 7 Reaction of 1,4-dilithio-1,3-diene derivatives with carbonyl compounds affording cyclopentadienes and proposed reaction mechanism
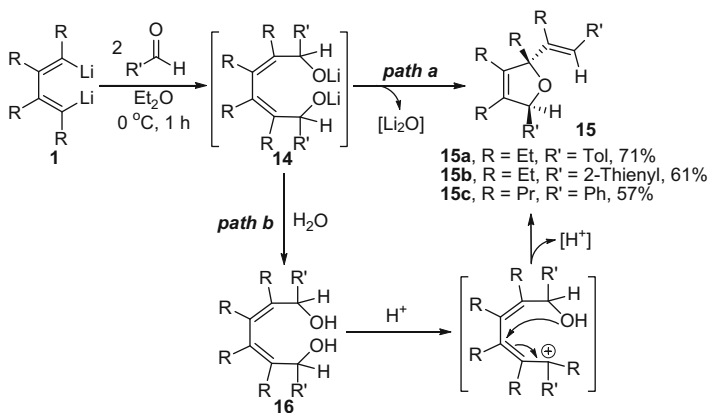
Scheme 8 Reaction of 1,4-dilithio-1,3-diene derivatives with aldehydes affording 2,5-dihydrofuran derivatives and proposed reaction mechanism

4.2 Reactions with Oxalate: Synthesis of 2,6-Dioxabicyclo [3.3.0]-Octa-3,7- Dienes or o-Benzoquinones

o-Benzoquinones are useful building blocks for synthesis of a variety of functionalized compounds [46, 47]. On the other hand, dioxabicyclo[3.3.0]-octacycles have also been found in many biologically active compounds [48]. Thus, development of synthetic methods toward these skeletons has been of interest. Reactions of 1,4-dilithio-1,3-dienes **1** with dimethyl oxalates afforded multi-substituted *o*-benzoquinones **18** or stereodefined 2,6-dioxabicyclo[3.3.0]-octa-3,7-dienes **19** in good yields (Scheme 9) [49]. The yields and chemoselectivity of this reaction toward two types of products could be influenced by the substitution patterns on skeleton of di-lithio reagents **1** as well as the order of addition of the substrates. The reaction mode of di-lithio reagents **1** toward oxalate showed cooperative effect, and the linear product **17** resulted from reaction of each C–Li bond with one oxalate independently was not observed.

4.3 Reactions with CO_2 and CS_2

The reactions of carbon dioxide and carbon disulfide with organolithium reagents have attracted much attention and have been applied in various organic synthesis. Reaction of carbon dioxide with organolithium compounds normally affords carboxylic acids after hydrolysis [50]. The formation of unsymmetrical ketones was reported from the reaction of CO_2 and two organolithium compounds via an intermolecular reaction pathway [51]. When 1,4-dilithio-1,3-dienes **1** was treated with CO_2, cyclopentadienone derivatives **20** with various substituents could be prepared in high yields in one-pot within several minutes via cleavage of one of the C=O double bonds (Scheme 10) [52]. The experimental results indicate that this intermolecular reaction pattern affords cyclopentadienones in the reaction mixture before hydrolysis.

However, when the 1,4-dilithio-1,3-dienes **1** were treated with CS_2, the corresponding cyclopentadienethiones **23** were not isolated. Instead, multi-substituted thiophene derivatives **21** or thiopyran-2-thione derivatives **22** were generated in good yields via cleavage of C=S double bonds or cycloaddition reactions, respectively, depending on the substitution patterns on the di-lithio compounds **1** [53, 54].The proposed intermediates in the reaction of **1** with CO_2 or CS_2 are shown in Scheme 10.
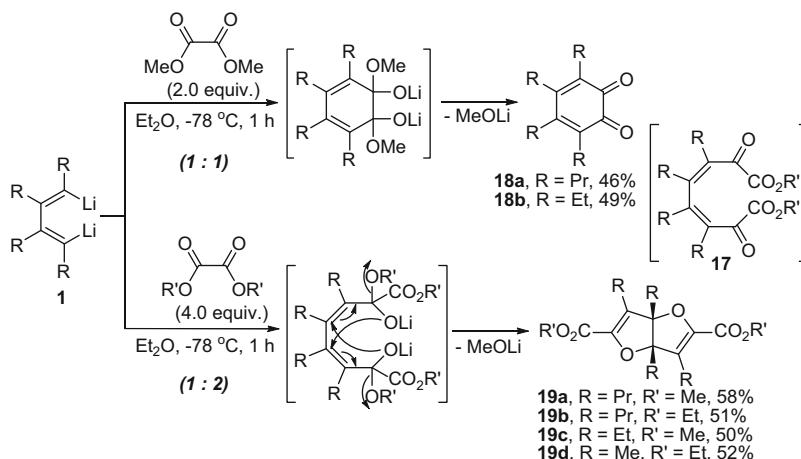
Scheme 9 Reaction of 1,4-dilithio-1,3-dienes with dimethyl oxalates affording multiply substituted *o*-benzoquinones or stereodefined 2,6-dioxabicyclo[3.3.0]-octa-3,7-dienes
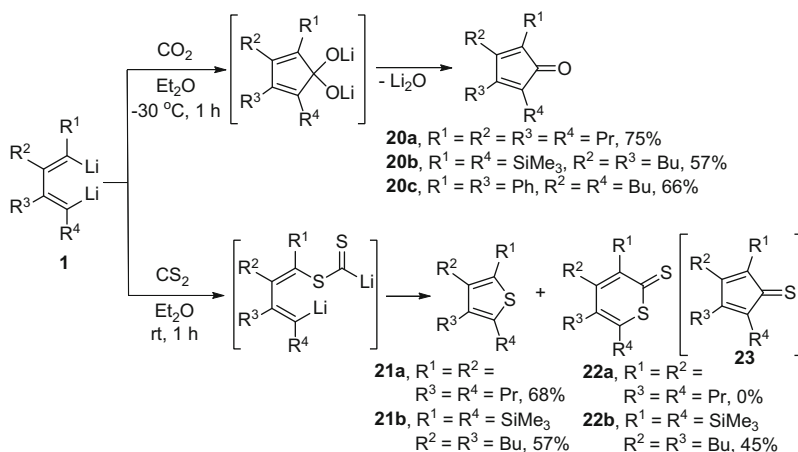
Scheme 10 Reactions of 1,4-dilithio-1,3-dienes with CO_2 and CS_2

4.4 Reactions with Isothiocyanates: Formation of Iminocyclopentadiene Derivatives via Cleavage of C=S Bond

Addition of organolithium reagents to isothiocyanates has been a fundamental protocol for the preparation of a wide variety of *S*-, *N*-, and *O*-containing linear and cyclic compounds. Isothiocyanates reacted with 1,4-dilithio-1,3-butadienes **1** to afford iminocyclopentadiene or indenimine derivatives in excellent isolated yields
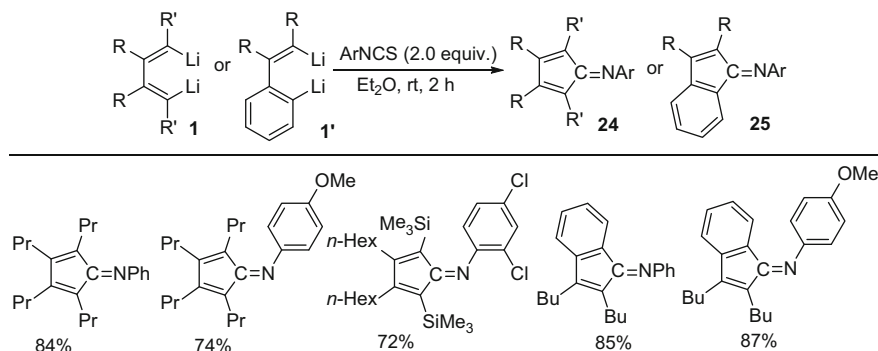
Scheme 11 Formation of iminocyclopentadienes and indenimines from the reaction of 1,4-dilithio-1,3-dienes with isothiocyanates

and high selectivity (Scheme 11) [55]. Aromatic isothiocyanates could be well applied in the reaction and cleavage of the C=S double bond of an isothiocyanate molecule took place via a successive inter-intramolecular carbophilic addition. As comparison, the reaction of isocyanates with 1,4-dilithio-butadienes afforded a number of products, probably due to the high reactivity of isocyanates toward 1,4-dilithio-butadienes.

4.5 Reaction with C_6F_6: Synthesis of Fluorinated Naphthalene Derivatives

Reaction of 1,4-dilithio-1,3-dienes **1** with 1.1 or 1.2 equiv of C_6F_6 at room temperature afforded the multi-substituted partially fluorinated naphthalene derivatives **26** in good to high isolated yields (Scheme 12) [56]. The reaction is assumed to proceed via double nucleophilic substitution. The naphthalene derivatives with different substitution patterns could be prepared conveniently by this method. Instead of nucleophilic substitution, when di-lithio reagents **1** were treated with hexachlorobenzene, chloropentafluorobenzene, or bromopentafluorobenzene, chlorine–lithium or bromine–lithium exchange reactions took place to afford the 1,4-dichloro- or 1,4-dibromo-1,3-diene derivatives. Preliminary results demonstrate that these partially fluorinated multi-substituted naphthalene derivatives show unique stacking fashions.

4.6 Carbonylation with CO

The reaction of organolithium reagents with CO is a fundamental reaction in organic chemistry and organometallic chemistry. This reaction gives acyllithium

Scheme 12 Reaction of dilithiobutadienes **1** with C_6F_6 affording partially fluorinated aromatic compounds **26**

26a, $R^1 = R^2 = Et$, 68%
26b, $R^1 = Bu$, $R^2 = (CH_2)_4$, 74%
26c, $R^1 = H$, $R^2 = n\text{-Hex}$, 72%

27a, $R^1 = R^2 = Et$, 54%
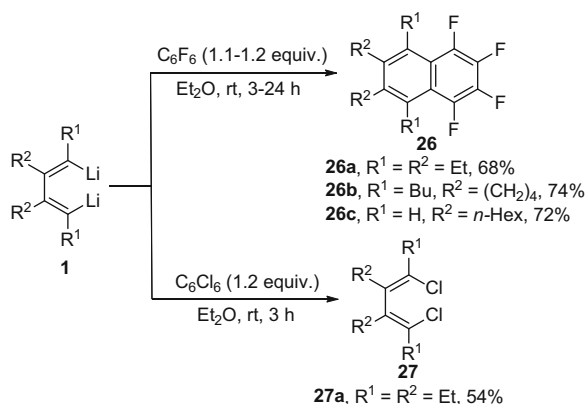
intermediate **28** as a useful intermediate for synthesis of carbonyl compounds. However, since **28** is too reactive even at low temperature, its application has been much limited. Both the direct application such as intermolecular trapping reaction (*Type I*, Scheme 13) [57] and the indirect application generating more stable intermediates such as enolate or ynolate lithium compounds via an intramolecular reaction pattern (*Type II*, Scheme 13) have been developed to broaden the application [58]. With the consideration of the cooperative effect of di-lithio compounds **1** with substrates, we envisioned that carbonylation of one C–Li bond in di-lithio compound **1** would form an acyllithium intermediate, which might be stabilized by interaction with the adjacent remaining CpLi moiety (*Type III*, Scheme 13). The acyllithium moiety **29** was indeed properly stabilized and its reaction selectivity could be under control [31, 59].

4.6.1 Synthesis of 3-Cyclopentenone Derivatives

The reaction of di-lithio reagents **1** with CO at $-78\,^\circ$C for 1 h afforded *trans*-3-cyclopenten-1-one **30** in an excellent isolated yield and with *trans* selectivity after hydrolysis (Scheme 14) [59]. Deuteriolysis of the reaction mixture afforded dideuterated products with more than 98% of deuterium incorporation. This reaction featured high efficiency and regio- and stereoselectivity, which showed an unprecedented pattern of highly selective and efficient carbonylation of organolithium reagents.

4.6.2 Isolation of Oxy-Cyclopentadienyl Dianions and Application

In this reaction, carbonylation of di-lithio reagents **1** was assumed to give an acyclic carbonyllithium species **29** as the first reaction intermediate, which immediately undergoes cycloaddition reaction followed by sequential rearrangement to afford cyclic dianions, such as **31-A** to **31-F** (Fig. 4). We isolated and characterized the
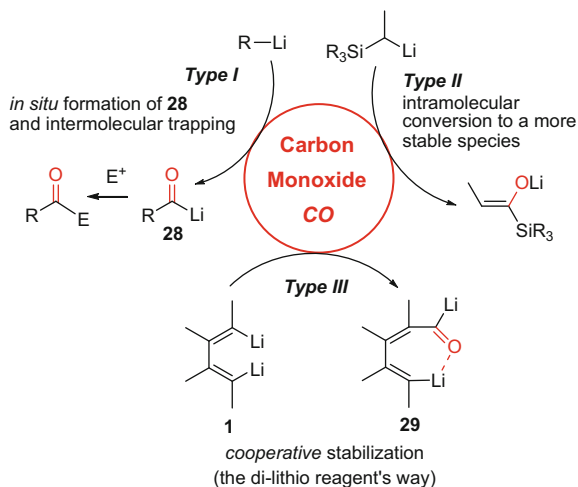
Scheme 13 Strategies to use acyllithium intermediates
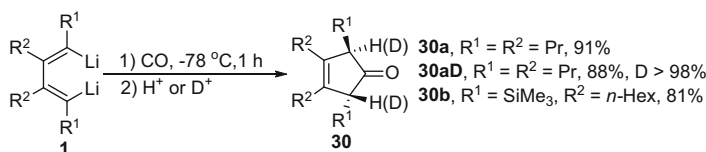
Scheme 14 Formation of cyclopentenones from the reaction of 1,4-dilithio-1,3-dienes with CO

reaction intermediates and found the oxy-cyclopentadienyl dilithium **31-D** (OCp for short) is the intermediate obtained in the solid state (Scheme 15) [31]. X-ray crystal structures show that two Cp rings are connected through a "Li_2O_2" four-membered ring (Fig. 5). Each Cp ring is coordinated to a lithium atom in an η^5-mode. Solution NMR of products **31** also supports that the oxy-cyclopentadienyl dilithium species is the intermediate [31].

Since other intermediates **31A–F** could be considered as resonance structures of OCp dianion **31-D**, an equilibrium among these intermediates might exist. Specific substrates might differentiate the reaction site such as C or O and move the equilibrium, thus to afford different products.

The isolation and reactivity investigation of such cyclic dianion species are of general interest in both organic synthesis and organometallic chemistry, which are not only beneficial for in-depth understanding of reaction mechanisms, but can also lead to discovery of synthetically useful reactions. Because of the concomitant of the CpLi moiety, the exocyclic oxy anion, and those multi-reactive sites, these OCp dianions **31** are structurally unique and of novel reaction chemistry toward organic substrates and organometallic compounds (Scheme 16).

When **31** was treated with 2 equivalents of electrophiles such as MeI, Me_2SO_4, allylic bromide, benzyl halides, or propargyl halides, 3-cyclopentenone derivatives
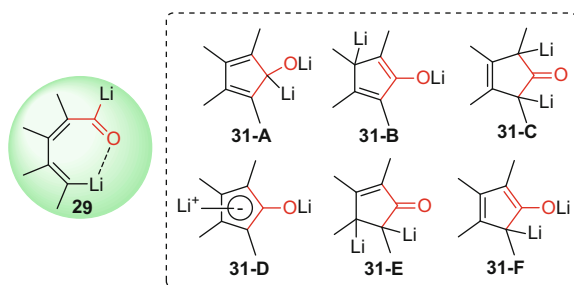
Fig. 4 Possible cyclic dianion intermediates **31A–F**

31a, R^1 = SiMe$_3$, R^2 = Me, 80%
31b, R^1 = SiMe$_3$, R^2 = Ph, 75%
31c, R^1 = R^2 = Et, 79%
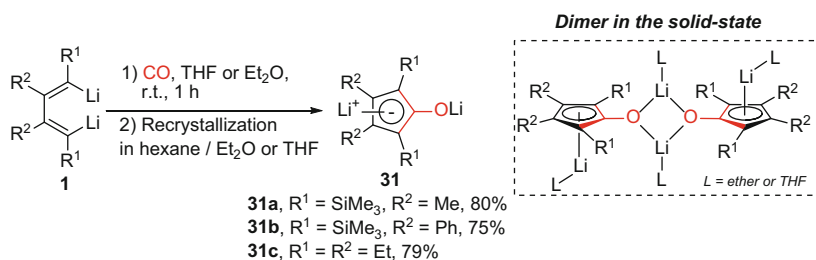
Scheme 15 Isolation of the intermediate **31**
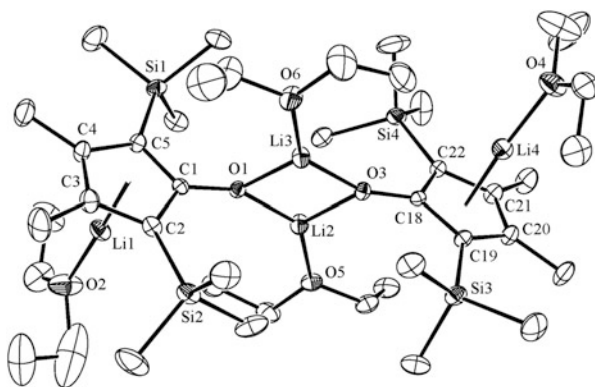
Fig. 5 The crystal structure of **31a**
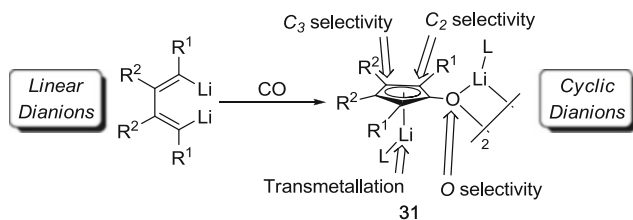
Scheme 16 Reaction modes of cyclic dianion **31**
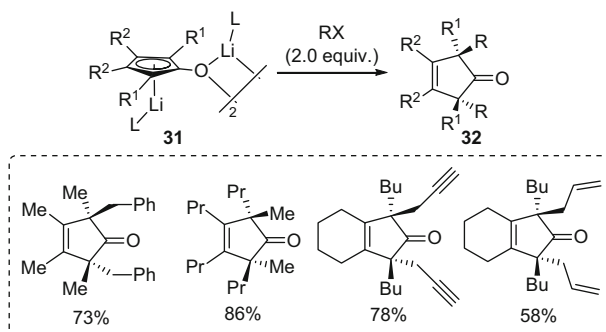
Scheme 17 Reaction of cyclic dianion **31** with electrophiles: selective synthesis of multi-substituted 3-cyclopentenone

32 were obtained in good to excellent yield with perfect chemo-, regio-, and stereoselectivity (Scheme 17) [59].

It should be noted that when electrophiles are acid chloride (RCOCl), the reaction affords different products (Scheme 18). Double-acylated cyclopentadienes **33** were resulted from reactions of **31** and two identical acid chlorides, while mixed double-acylated ones **34** were generated from one *t*-BuCOCl and one smaller acid chloride, respectively, in good to excellent isolated yields [31].

Besides, when silyl-substituted OCp dianions **31** were subjected into the reactions with acid chlorides, silyl-shift reaction might occur depending on the reaction condition and the structures of acid chlorides used. When the OCp dianion **31** was treated with one equivalent of electron-deficient, bulky 2,4,6-trichlorobenzoyl chloride (ArCOCl), the *O*-acylated intermediate **35** was isolated in 65% isolated yield. Recrystallization of **35** with TMEDA afforded the single-crystals **35-TMEDA**, whose structure was determined by single-crystal X-ray structural analysis as a monomeric CpLi compound [60]. Electrophilic trapping of **35** with trichloroacetic chloride led to double-acylated product **34c**. However, hydrolysis of the isolated intermediates **35** with water afforded cyclopentadiene derivative **37** as silyl-shift product in a quantitative yield. These results demonstrated that compounds **37** might be formed upon protonation of **35**.

Moreover, THF solvent could also trigger the silyl-shift reaction and compound **35** slowly transformed into a different compound **36** within 3 days in THF. Recrystallization of **36** with TMEDA afforded the suitable single-crystals **36-TMEDA**, which was determined by single-crystal X-ray structural analysis as a monomeric chelate enolate lithium structure [60]. Hydrolysis of the isolated intermediate **36** afforded its corresponding *gem*-bis(trimethylsilyl) cyclopentenones derivative **38** containing a stable enol moiety in a quantitative yield. No double-acylated product was obtained even when two equivalents of ArCOCl were used.

Furthermore, expecting these OCp dianions **31** as precursors and/or ligands for transition metal complexes, we also investigated their reactivity with Ni(dppe)Cl$_2$, which afforded the cyclopentadienone-nickel complexes **39** in high isolated yields
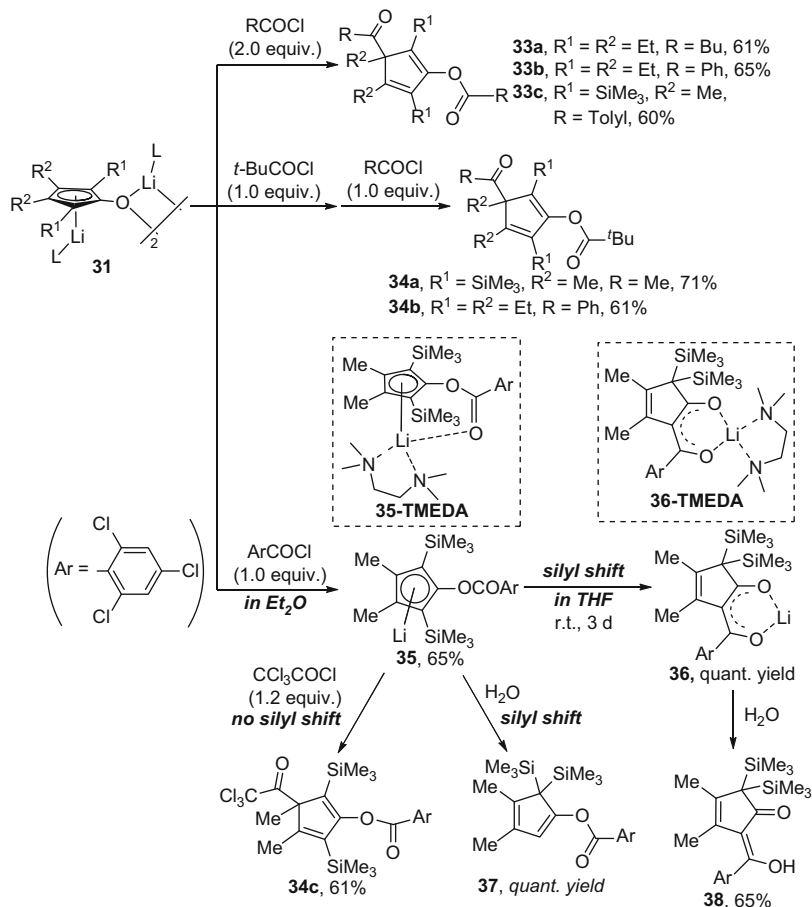
Scheme 18 Reaction of cyclic dianion **31** with acid chlorides: selective synthesis of multi-substituted cyclopentadiene and *gem*-bis(trimethylsilyl) cyclopentenones

(Scheme 19) [31]. Recently, utilization of OCp dianion **31** for synthesis of metallocene complexes has been achieved [61].

4.7 Reaction with Nitriles

The addition reaction of organolithiums to nitriles to provide *N*-lithioketimines is among the fundamental processes in organometallic chemistry. Generally, the intermolecular trapping of *N*-lithioketimines with organohalides or protons yields imines and ketones. While the trapping of *N*-lithioketimines with intramolecular organohalides provides a useful route to construct *N*-containing heterocycles
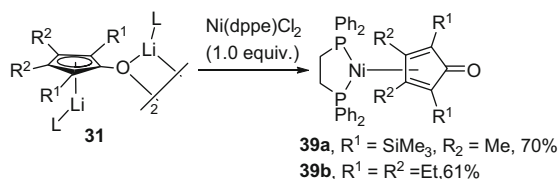
Scheme 19 Transmetallation of cyclic dianion **31**

[1–6]. Our results showed that the reaction of organo-*di*-lithium reagents with nitriles demonstrates new types of reaction and affords pyridines, cyclopentadienylamines, Δ^1-bipyrrolines, siloles, and (*Z,Z*)-dienylsilanes, depending on the substitution patterns (including the size of the fused ring) on the butadienyl skeletons of **1**. Furthermore, the reaction of 1,4-unsubstituted di-lithio compounds **1** with nitriles could direct the synthesis of theoretically interesting 2,6-diazasemibullvalenes, which feature polycyclic strained skeleton and intramolecular aza-Cope rearrangement and have been considered as potential homoaromatic molecules.

4.7.1 Formation of Pyridines, Pyrroles, Δ^1-Bipyrrolines, Siloles, and (Z, Z)-Dienylsilanes: Remarkable Effect of Substitution Patterns on the Butadienyl Skeletons

When 1,2,3,4-tetra-substituted-1,4-dilithio-1,3-dienes **1** were treated with nitriles in the presence of HMPA, all-substituted pyridine derivatives **40** were formed in high isolated yields (Scheme 20). When 2-cyanopyridine was used, its reaction afforded 2,2′-bipyridine derivatives in high isolated yields. Similarly, 2,3-dialkyl or diaryl substituted di-lithio reagents generated trisubstituted pyridines [62, 63]. When the reaction of **1** with 2-cyanopyridine was carried out at −60°C in the presence of HMPA, cyclopentadienylamine **42** was isolated in 29% yield, along with 34% yield of pyridine **40a** (Scheme 21). However, when 1,4-unsubstituted di-lithio reagents were used to react with aromatic nitriles or aliphatic nitriles without α-hydrogens, tricyclic Δ^1-bipyrrolines **44** were isolated as sole products after quenching. We assumed that 1-azaallylic dianions **43** would be the possible intermediates before quenching (for a recent review on 1-azaallylic anions, see [64]). As far as we are aware, this is the first synthesis of tricyclic Δ^1-bipyrrolines (Scheme 22).

Mechanisms on the reactions of 1,4-dilithio-1,3-butadienes and nitriles were explored through DFT calculations [65]. The computational results again support that the selectivity of these reactions is strongly affected by the structures of the substrates. As the first step of all reaction pathways, one C–Li bond reacts with the nitrile to give the *N*-lithio ketimine intermediate.

When tetra-alkyl substituted 1,4-dilithio-1,3-dienes and 2-cyanopyridine are used, the *N*-lithio ketimine intermediate undergoes 5-exo cyclization to give the cyclopentadienyl amine **42** as the kinetic product because of the coordination of the pyridyl *N*-atom to the lithium atoms.
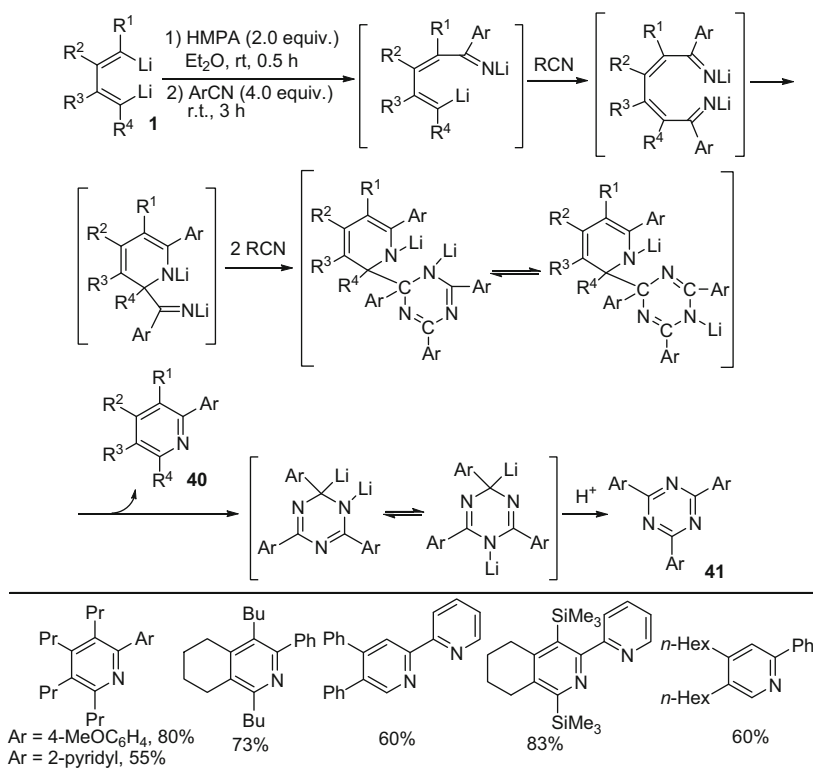
Scheme 20 Formation of pyridine derivatives: substituent-dependent
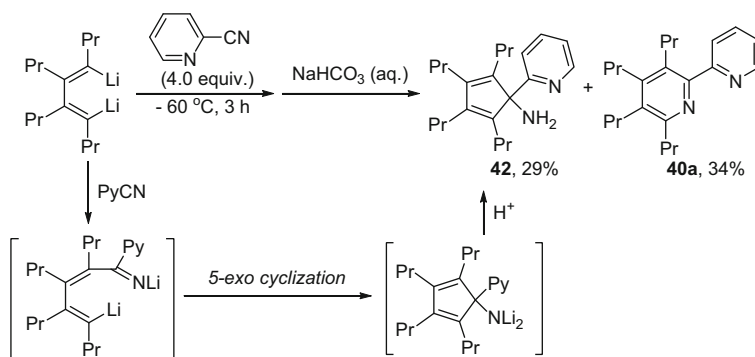
Scheme 21 Formation of cyclopentadienylamine derivatives

When tetra-alkyl substituted 1,4-dilithio-1,3-dienes and aryl nitriles are used, the *N*-lithio ketimine intermediate undergoes insertion of a second nitrile into the C–Li bond to afford the 1,8-dilithio bis-ketimine intermediate. 1,8-Dilithio bis-ketimine
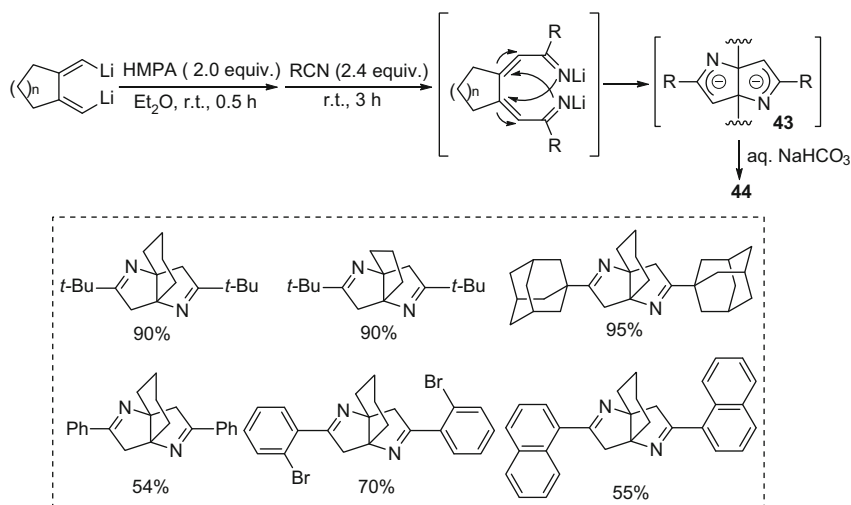
Scheme 22 Synthesis of tricyclic Δ^1-pyrroline derivatives: substituent-dependent

intermediate undergoes a 1,6-cyclization, followed by insertion of two nitriles, electrocyclization, and fragmentation to generate pyridine **40** and triazine dilithium intermediate through thermodynamically favored pathways. Quenching of triazine dilithium intermediate with water gives rise to triazine **41**.

When cyclic 1,4-dilithio butadiene and tertiary aliphatic nitriles are used, the 1,8-dilithio bis-ketimine intermediate undergoes two sequential 1,5-cyclization steps with a lower energy barrier, generating tricyclic Δ^1-bipyrrolines **44**. The calculation results clearly show the mechanism details and are in good agreement with the experimental observations [65].

Besides, the types of nitrile used in the abovementioned reaction have also strong impact on the reaction patterns. When 1,2,3,4-tetra-substituted di-lithio reagents were treated with Me$_3$SiCN, a tandem silylation-intramolecular substitution process readily occurred to yield siloles **45**, while the reaction of 2,3-di-substituted di-lithio reagents with Me$_3$SiCN gave rise to the first synthesis of (*Z*, *Z*)-dienylsilanes **46** with high stereoselectivity (Scheme 23) [63]. In this reaction, the normal reaction pattern that nitriles are attacked at C≡N triple bond by mono-Li reagents was not found. Instead, cleavage of Si–C bond in Si–CN moiety was observed.

All these results revealed that the substitution patterns of di-lithio reagents and the nature of nitriles played key roles in the formation of pyridines, cyclopentadienylamine, tricyclic Δ^1-bipyrrolines, siloles, and (Z,Z)-dienylsilanes.
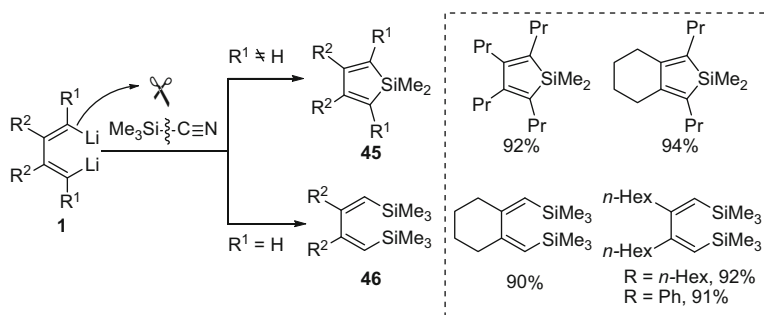
Scheme 23 Formation of siloles and (*Z,Z*)-dienylsilanes

4.7.2 Synthesis of 2,6-Diazasemibullvalenes

2,6-Diazasemibullvalene (NSBV) and its all-carbon analog semibullvalene (SBV) have long been of fundamental interest both theoretically and experimentally, because of their unique strained ring systems, their intramolecular skeletal rearrangements, as well as their rapid degenerate Cope rearrangement and predicted existence of homoaromatic delocalized structure [66–69]. However, little is known experimentally on the synthesis, structures, and reaction chemistry of 2,6-diazasemibullvalenes [68, 69]. Based on the reaction of 1,4-unsubstituted di-lithio reagents **1** and nitriles without α-hydrogen, we developed two preparative methods and isolated a series of NSBVs via oxidant-induced intramolecular C–N bond formation of 1-azaallylic dianion **43** [63, 70].

Method A represents a one-pot synthesis of NSBVs **45** (Scheme 24). Reaction of **1** with 2.4 equiv of nitrile readily afforded the dianion **43** [63]. Addition of di-*tert*-butyl peroxide ((*t*-BuO)$_2$, 4.0 equiv) as oxidant led to 1,5-bridged-2,6-diazasemibullvalenes **45a–45f** with different substituents at 3,7-position (Type I, Type II) in moderate yields [70]. *Method B* represents a stepwise synthesis of NSBV **45** (Scheme 24). The dianions **43** could be readily in situ generated via di-lithiation of Δ^1-bipyrrolines **44**. Sequential addition of phenyliodine diacetate (PhI(OAc)$_2$) as oxidant afforded their corresponding NSBVs **45** in good isolated yields. For the synthesis of Type I NSBV derivatives, *Method B* was found to be more efficient than *Method A*. 1,5-Dialkyl substituted Δ^1-bipyrrolines **44** could also be converted to their corresponding non-bridged NSBVs **45g** and **45h** (Type III) in 72% and 73% isolated yield, respectively [70].

This synthesis of NSBV **45** greatly highlights the synthetic value of 1,4-dilithio-1,3-butadienes. Besides, the established experimental models of NSBV **45** benefited us to study the structures, reactivities, and theoretical chemistry. Furthermore, NSBV has shown diversified reaction chemistry such as insertion reaction, cycloaddition, and oxidation, affording diverse and interesting "bowl-shape" or "cage-shape" *N*-containing polycyclic frameworks [70–72]. We suggest that the rigid ring skeletons of NSBV **45** as well as intramolecular aza-Cope rearrangement contribute to the highly reactive nature and novel reaction patterns of NSBV **45** (Scheme 25).

1,4-Dilithio-1,3-diene	NSBV	Isolated Yield (%)	
		Method A	Method B
Type I	**45a**, R' = *t*-Bu	66 *b*	83 *c*
	45b, R' = Ad	53 *b*	68 *c*
	45c, R' = Et₂MeC	43 *b*	72 *c*
	45d, R' = BuMe₂C	30 *b*	83 *c*
	45e, R' = EtMe₂C	51 *b*	72 *c*
Type II	**45f**, R' = *t*-Bu	51 *d*	
Type III	**45g**, R = Me, R' = *t*-Bu		72 *d*
	45h, R = Bu, R' = *t*-Bu		73 *d*

a. HMPA (2.0 equiv.), rt, 0.5 h; **R'**CN (2.4 equiv.), reflux, 3 h; NaHCO₃ (aq.);
b. [O] = (*t*-BuO)₂ (4.0 equiv.); *c*. [O] = PhI(OAc)₂ (1.0 equiv.);
d. [O] = *t*-BuOCl (1.0 equiv.)
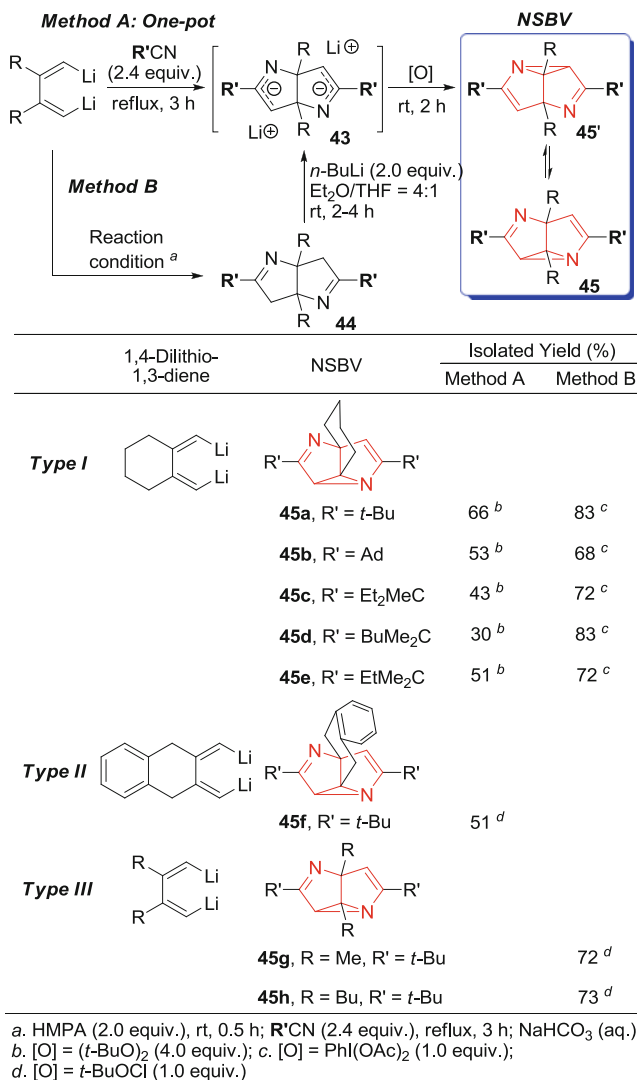
Scheme 24 Synthesis of 2,6-diazasemibullvalenes from 1,4-dilithio-1,3-butadienes and nitriles

4.8   Reaction with Diazo Compounds: Synthesis of 1-Imino-Pyrrole Derivatives

1,4-Dilithio-1,3-dienes **1** could react with diaryl diazomethanes to give multi-substituted 1-imino-pyrrole or indole derivatives **46** in high yields [73]. In this reaction, diaryl diazomethanes reacted as electrophiles. Besides, synthetic methods for *N*-imino-pyrrole and indole derivatives are limited. Only when 2,3-cyclic-1,4-diphenyl-1,4-dilithio-1,3-butadiene **1** were treated with 2.2 equivalents of
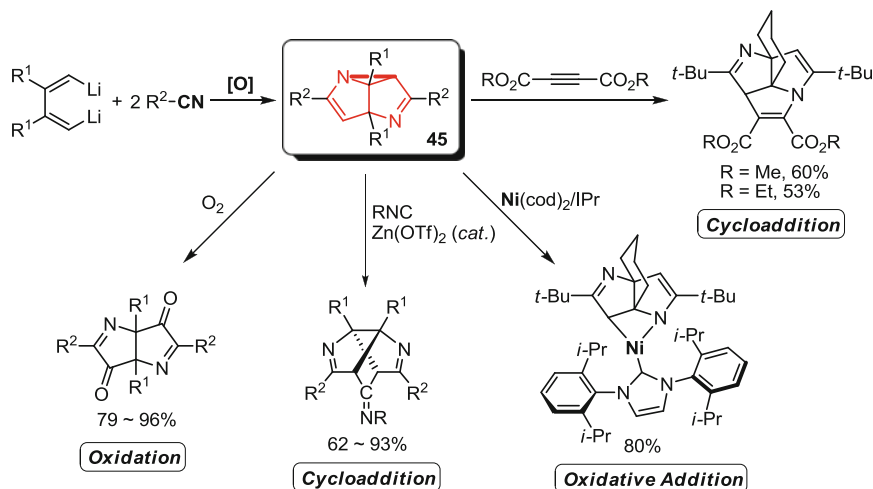
Scheme 25 Reaction chemistry of 2,6-diazasemibullvalenes

diphenyldiazomethane, the unexpected bis(diazo) compound **47** was obtained in 83% isolated yield. Formation of its corresponding tetrahydroisoindole derivative was not observed (Scheme 26).

Mechanistic investigation revealed that two diazo compounds reacted with one di-lithio reagent affording the intermediate **48** (Scheme 27), which was isolated and characterized by NMR spectrum. Quenching intermediate **48** with H_2O under N_2 afforded the product **49. 49** could be oxidized to afford the 1-imino-pyrrole **46b** and the diazo compound **50** [73]. Furthermore, an unprecedented Zn-complex **51** was obtained via transmetalation of the intermediate **48** with $ZnCl_2$. In this Zn-complex, *trans*-μ_2-η^1:η^1 coordination mode in the solid state was observed.

5 Transmetallation and Further Applications

Transmetallation is one of the fundamental and valuable reactions in organometallic chemistry. The transmetallation reactions of organolithium compounds could afford a wide variety of different organometallic compounds. Thus, we expect more interesting reaction and applications of transmetallation of organo-*di*-lithium reagents with other metals salts, including copper, iron, zinc, aluminum, and barium. We envision that the cooperative effect of two metal–carbon bonds might also lead to new reactions. Indeed, these reactions not only give diverse organometallic compounds, but also show value in synthetic chemistry. Moreover, the reactivities of thus generated organo-*di*-metallic compounds show different patterns compared with that of organo-*di*-lithium reagents.
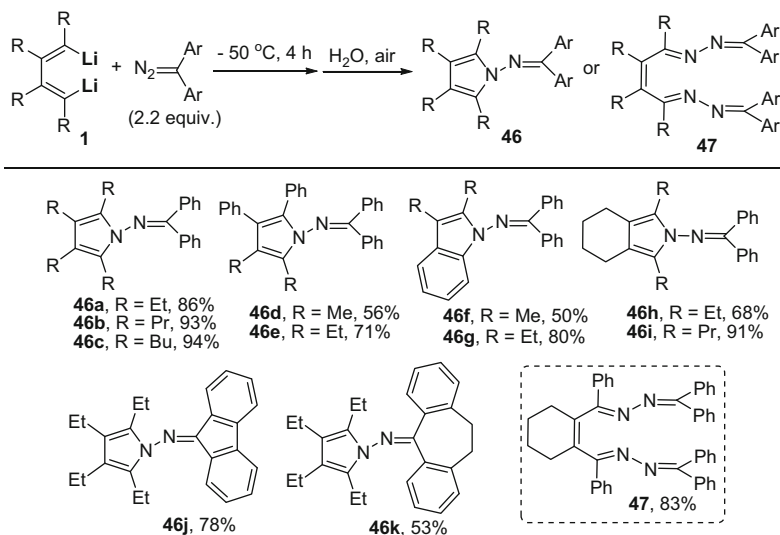
Scheme 26 Synthesis of 1-imino-pyrrole derivatives and bis(diazo) compounds via the reaction with diazo compounds
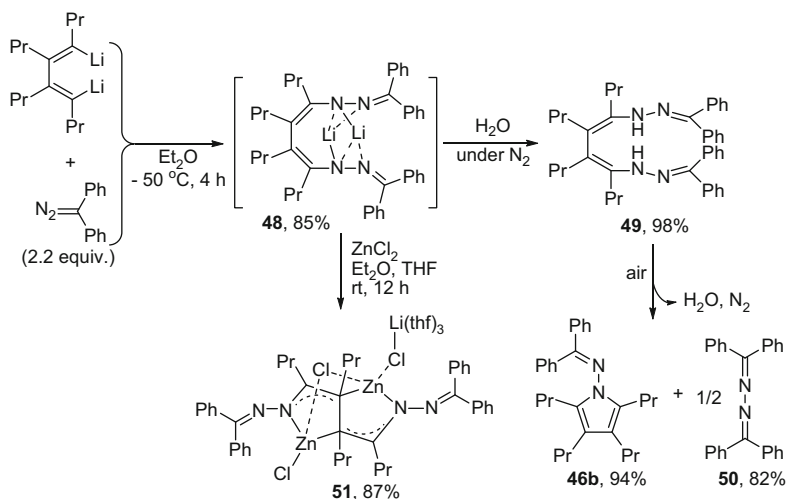
Scheme 27 Reaction mechanism and synthetic application of **48**

5.1 *Transmetallation with Aluminum*

Aluminacyclopentadiene as a metallole compound was not widely studied, and synthesis toward aluminacyclopentadiene via transmetallation of organolithium reagent and aluminum base compound was few. In 1977, Hoberg and

Krause-Going and others reported the formation of well-defined pentaphenylalu-minacyclopentadienes by the reaction of 1,2,3,4-tetraphenyl-1,4-dilithio-1,3-buta-diene with PhAlCl$_2$ in Et$_2$O [74]. However, their reaction chemistry as well as applications in organic synthesis had not been widely investigated. We prepared chloro-aluminacyclopentadienes **52** in situ from the transmetallation of AlCl$_3$ and 1,4-dilithio-1,3-butadienes **1** at room temperature (Scheme 28) [75]. **52** reacted with aldehydes at room temperature to afford multi-substituted cyclopentadienes **1** or tetrahydroindenes in good yields. Both aromatic and aliphatic aldehydes could be applied in this reaction.

So as to confirm whether the cyclopentadiene product was formed from the reaction of aldehydes with di-lithio compounds **1** or with aluminacyclopentadienes **52**, in situ NMR experiment was carried out and **52** was observed in the ^{13}C NMR spectrum. Besides, **52** did not react with ketones. However, in contrast, di-lithio reagents could react with ketones to form cyclopentadienes. When **52** was formed at room temperature, no 2,5-dihydrofuran derivatives were generated in the pres-ence of excess aldehydes. Moreover, the reactivity of aluminacyclopentadienes **52** with DMAD was further explored to give benzene derivatives **53** in moderate isolated yields.

5.2 Transmetallation to Copper

Transmetallation of 1,4-dilithio-1,3-butadienes with copper salt such as CuCl would lead to 1,4-dicopper-1,3-butadienes. Upon thermolysis or further treatment with other substrates, the organo-*di*-copper reagents could be transformed into a wide variety of compounds with interesting skeletons, which could be obtained by other methods or via the reactions of 1,4-dilithio-1,3-butadienes.

5.2.1 Cyclodimerization Leading to Semibullvalenes and Other Strained Ring Systems

As mentioned above, semibullvalene (SBV) and its nitrogen analog 2,6-diazasemibullvalene (NSBV) have attracted much attention both theoretically and experimentally [66–69]. As a valence isomer of cyclooctatetraene **56**, semibullvalene **55** has attracted much attention because of the strained ring systems as well as rapid *degenerate* Cope rearrangement. However, the synthesis and structural study of these highly strained ring systems have been a great challenge in organic chemistry. We found that 1,4-dilithio-1,3-butadienes **1** could react with stoichiometric amount of CuCl to give octa-substituted semibullvalenes **55** in high yields (Scheme 29) [76, 77]. This is the first example of metal-mediated synthesis of semibullvalenes via C–C bond forming process. We demonstrate that the reac-tion proceeds first via transmetallation from 1,4-dilithio-1,3-butadienes **1** to 1,4-dicopper-1,3-butadienes **54**, and toluene solvent played a key role in the
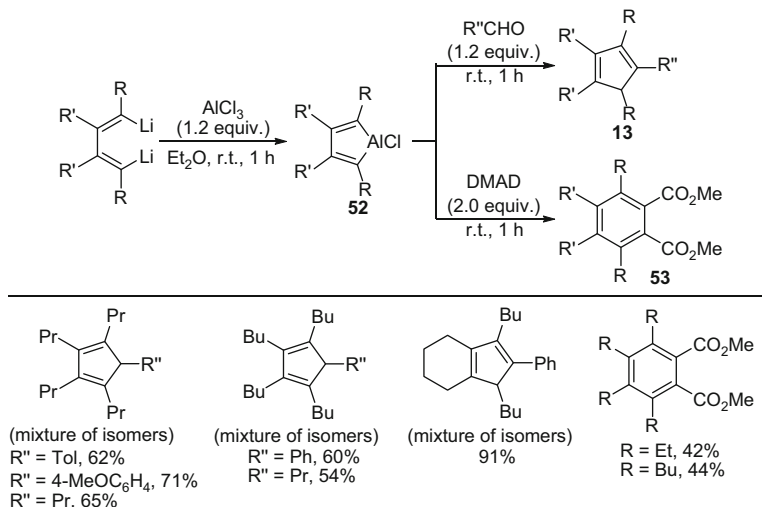
Scheme 28 Transmetallation of 1,4-dilithio-1,3-butadienes to aluminacyclopentadienes and their reactions with aldehydes or DMAD
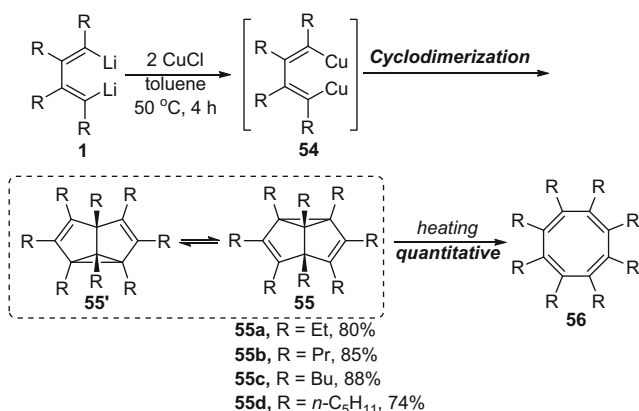
Scheme 29 CuCl-mediated cyclodimerization of di-lithio reagents affording semibullvalenes

cyclodimerization reaction of **54**. The thermo-induced homolysis of Cu–C bonds followed by cyclodimerization afforded the product semibullvalenes **55**. The semibullvalenes obtained here could be readily transformed to their corresponding COT derivatives **56** upon heating in quantitative yields.

As we demonstrated in the previous section, the structure and substitution patterns of organo-*di*-lithium reagents have great influence on their reactivity. We studied the transmetallation of benzo-fused di-lithio reagents with CuCl in ether or toluene, and dibenzotricycle[3.3.0.0^{2,6}]-1,2,5,6-tetraalkyloctanes **57** (twisted tricycles) were formed, which could be also quantitatively transformed into more stable

Scheme 30 CuCl-mediated cyclodimerization of di-lithio reagents affording twisted strained ring systems
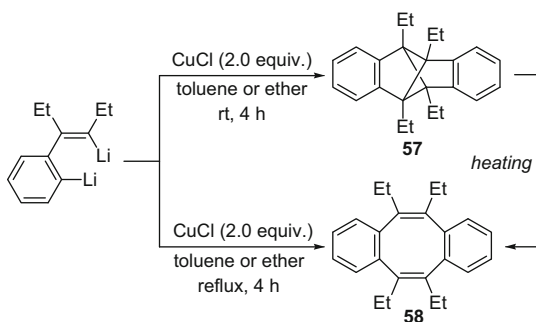
dibenzo-COT derivatives (Scheme 30) [78]. No semibullvalene derivatives were isolated. Besides, this is the first experimental evidence including X-ray analysis of compound **57**. **57** is also a significant member of COT valence isomers and has attracted much attention due to its special structure with highly strained ring system. It was proposed as skeletal rearrangement intermediate between two di-substituted dibenzo-COT [79].

5.2.2 Linear Dimerization Leading to All-*cis*-Octatetraenes

Conjugated polyenes have attracted much attention in recent decades because of their unique electronic structures and optoelectronic properties [80, 81]. Although many examples are known for the synthesis of *trans*-substituted octatetraenes, there are only few reports in the literature for the synthesis of fully substituted all-*cis* octatetraenes [82]. We found that 1,4-dicopper-1,3-butadienes **54**, generated in situ via transmetallation of **1** and CuCl, could undergo thermal decomposition-linear dimerization in the presence of additional LiI, yielding the corresponding octatetraenyl dicopper **59** (Scheme 31) [83]. Hydrolysis of **59** afforded octa-alkyl substituted all-*cis* octatetraene derivatives **60** in excellent yields (Scheme 31). The use of diethyl ether solvent and the addition of extra LiI were found to be key for this linear dimerization process, and the cyclodimerization was successfully depressed. If no extra LiI was added, the yield of **60** would be much lower, along with formation of cyclodimerization products. Subsequent Pd-catalyzed cross-coupling of **59** with organohalides constructed fully substituted all-*cis* octatetraene derivatives **61** (Scheme 32) [83]. Single-crystal X-ray structural analysis of **61** clearly show their all-*cis* and nonplanar skeleton structures.

5.2.3 Tandem CO Insertion and Intra- or Intermolecular Annulation of Organo-di-Copper Reagents

The further reaction patterns of 1,4-dicopper-1,3-butadienes **54** were expanded by investigation of the annulation of **54** with carbon monoxide. This reaction led to cycloaddition reaction and afforded expected cyclopentadienones **20** as well as the
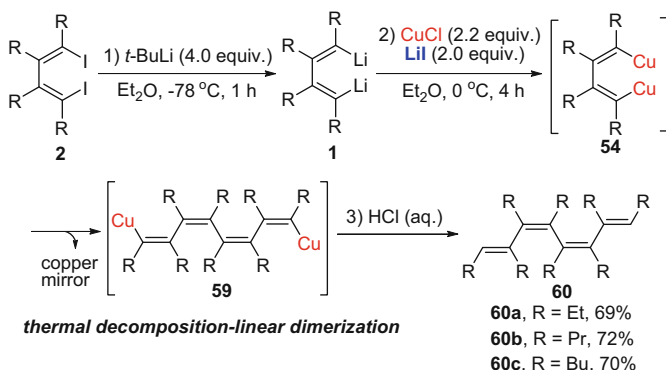
Scheme 31 CuCl/LiI-mediated dimerization of 1,4-dilithio-1,3-butadienes
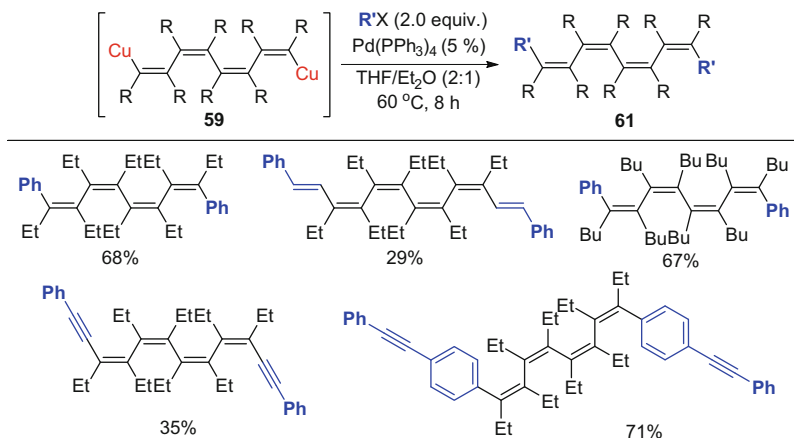
Scheme 32 Construction of fully substituted all-*cis* octatetraenes

head-to-head dimers **62** (Scheme 33) [84]. The substitution patterns again have a strong effect on the chemoselectivity to afford either cyclopentadienones **20** or their head-to-head dimers **62**. Compared with the annulation of 1,4-dilithio-1,3-butadienes **1** with CO, the reactions of transmetallated dicopper intermediates **59** showed different results.

5.3 Transmetallation to Iron

When Li–C bonds in di-lithio reagents **1** were transmetallated to Fe–C bonds by use of common and simple FeCl₃, the in situ generated organoiron intermediates showed different reactivity with that of di-lithio reagents **1**. For example, di-lithio reagents **1** did not react with unactivated alkynes such as 4-octyne. However, in the presence
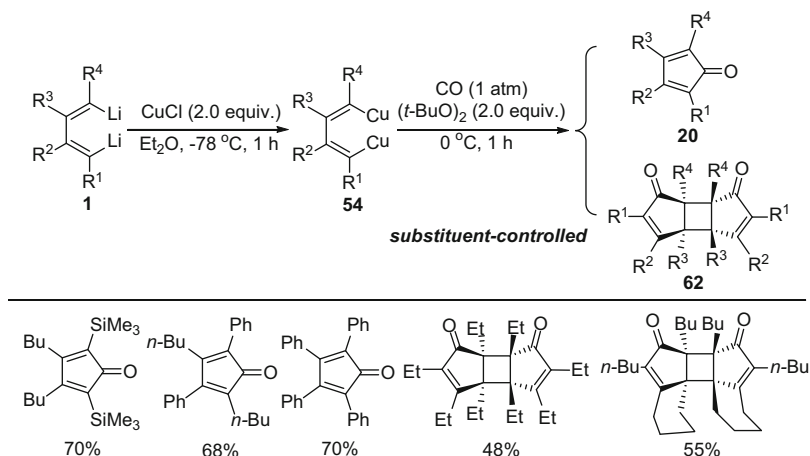
Scheme 33 Tandem CO insertion and annulation of organo-*di*-copper intermediates
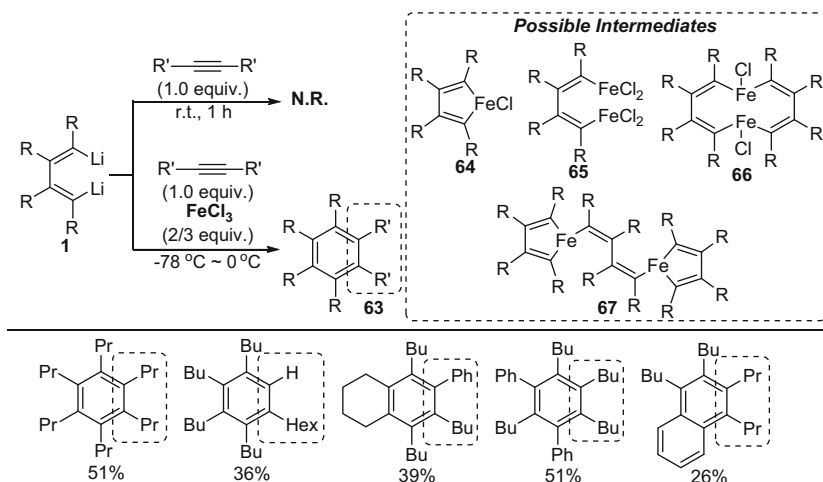
Scheme 34 Transmetallation of 1,4-dilithio-1,3-butadienes with FeCl$_3$ and further cycloaddition reactions with unactivated alkynes

of FeCl$_3$, the reaction occurred and afforded benzene derivatives **63** as formal [4+2] cycloaddition products (Scheme 34) [85]. The amount of the FeCl$_3$ used was found to have great impact on the results of the reaction. When three equivalents of FeCl$_3$ were used, the corresponding **63** was formed in low yield, with substrate **1** disappeared completely. Most of the di-lithio reagent **1** was polymerized. 1,4-Diiron-1,3-butadienes **65** or ferrole **64** was considered to be possible intermediates of transmetallation of **1** with FeCl$_3$. However, other kinds of intermediates such as **66** and **67** might be
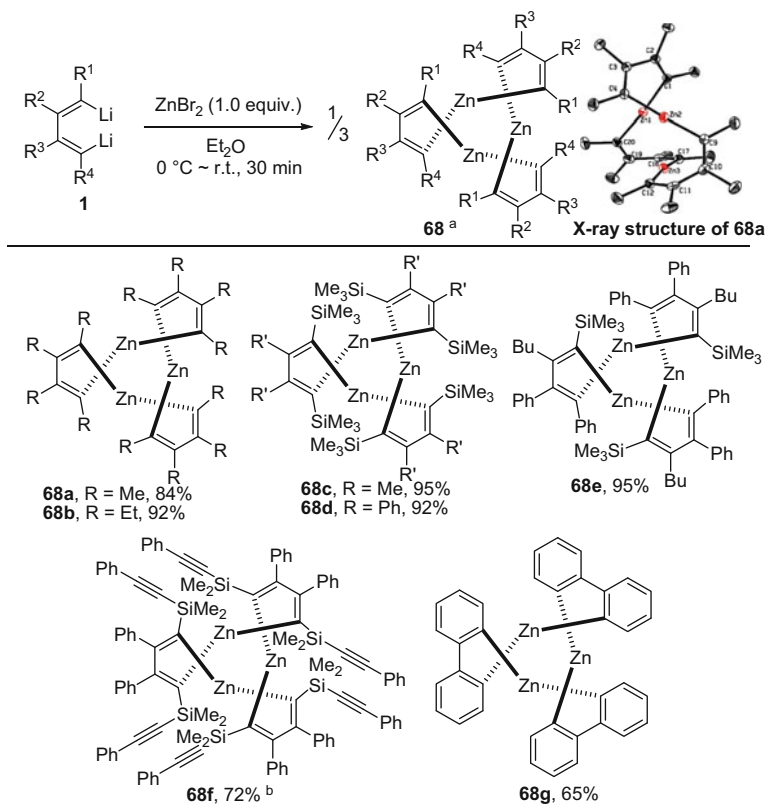
Scheme 35 Formation of 1,3-butadienylzinctrimers via transmetallation of 1,4-dilithio-1,3-buta-dienes with ZnBr₂

also involved. This illustration was based on the experimental results that 2/3 equivalents of FeCl₃ was used to give best yield of product **63**.

5.4 Transmetallation to Zinc

Organozinc compounds are useful synthetic reagents and readily available reactive organometallic intermediates [86]. There are many reports on their reactivities and synthetic applications; in contrast, much less investigation has been carried out on the synthesis and structures of new types of organozinc compounds [87]. When 1,2,3,4-tetra-substituted 1,4-dilithio-1,3-butadiene **1** were treated with one equiv of ZnBr₂ in Et₂O at room temperature, 1,3-butadienylzinctrimers **68** were formed in excellent isolated yields (Scheme 35) [88]. Treatment with excess ZnBr₂ still gave the same complexes **68** as sole products. X-ray single-crystal structural analyses of

Scheme 36 Pd-catalyzed Negishi cross-coupling of 1,3-butadienylzinctrimer with iodobenzenes
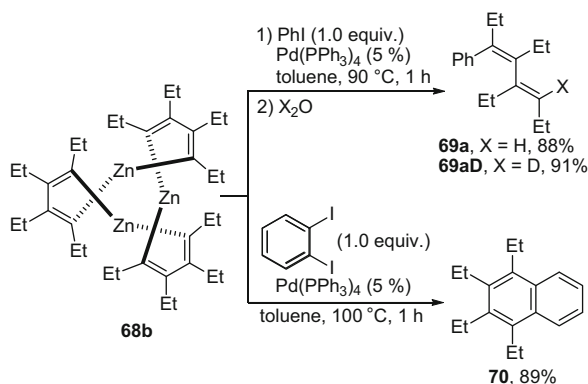
1,3-butadienylzinctrimers **68a**, **68b**, and **68c** all exhibit novel trimeric 1,3-butadienezinc pattern as fifteen-membered metallacycle in their solid state, independent on the substituents on 1,3-butadienyl skeleton (Scheme 35, **68a**). In contrast, the structures of their precursors 1,4-dilithio-1,3-butadienes are dependent on substituents. The distance between two zinc centers indicated the absence of Zn–Zn bonds [89].

The reaction chemistry of such macrocyclic organozinc compounds was demonstrated by the Pd-catalyzed Negishi cross-coupling with iodobenzenes [90]. As shown in Scheme 36, the reaction between **68b** and iodobenzene gave the monophenylated product **69a** upon hydrolysis instead of expected double-phenylated product [88]. The D-incorporated product **69aD** was isolated upon deuterolysis, indicating that one remaining Zn–C bond was inert toward a second cross-coupling with iodobenzene. Cross-coupling of **68b** with 1,2-diiodobenzene gave 1,2,3,4-tetraethyl naphthalene **70** in high yield, probably owing to the aromatization driving force that makes the second intramolecular Negishi cross-coupling take place (Fig. 6).

5.5 Transmetallation to Barium

We investigated the transmetallation of 1,4-dilithio-1,3-butadienes **1** with Ba[N(SiMe$_3$)$_2$]$_2$, expecting that novel reaction might occur because of the higher ionicity and reactivity of the resulted Ba–C(sp^2) bonds [91, 92]. Treatment of **1e** with 1 equivalent of Ba[N(SiMe$_3$)$_2$]$_2$ in hexane followed by recrystallization from THF at room temperature afforded the barium dibenzopentalenide **71a** in 61% isolated yield (Scheme 37) [33]. Hydrolysis of the isolated intermediate **71a** with H$_2$O afforded its corresponding dibenzopentalene derivatives **73a** in a quantitative yield. Moreover, the barium dibenzopentalenide **71a** could also be generated quantitatively by the reaction between **73a** and Ba[N(SiMe$_3$)$_2$]$_2$ (Scheme 37). The structure of **71a** was determined by single-crystal X-ray structural analysis. The single barium atom is coordinated to the parent pentalene

Fig. 6 The crystal structure
of barium
dibenzopentalenides **71a**
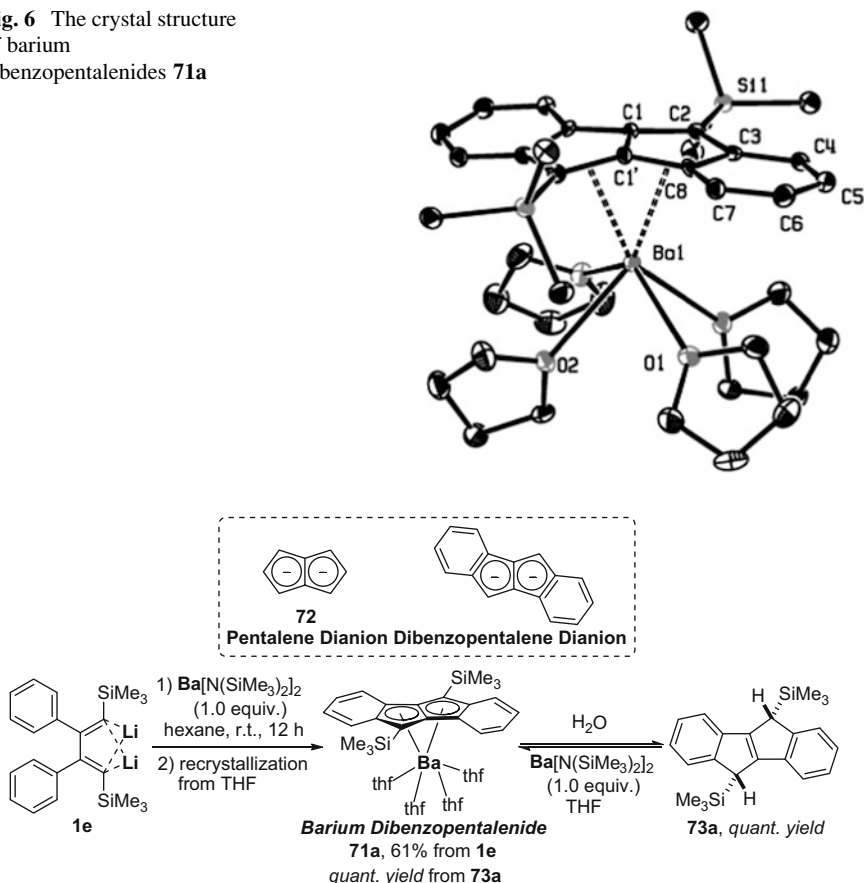
Scheme 37 Coordination modes of pentalene dianion and formation of barium dibenzopentalenides via transmetallation of 1,4-dilithio-1,3-butadienes with $Ba[N(SiMe_3)_2]_2$

in an η^8 fashion, which represents the first example binding to a main group metal with an η^8 mode among all pentalene and dibenzopentalene complexes.

Dibenzopentalene derivatives have attracted considerable recent attention because of their unique planar structures and antiaromatic characters [93]. We investigated the reaction chemistry of barium dibenzopentalenides (Scheme 38). When the in situ generated barium dibenzopentalenides **71** were quenched with H_2O, 5,10-dihydro-dibenzopentalenes **73a** and 73**b** were isolated in 63% and 61% yields, respectively (Scheme 38) [33]. In situ generated **71** was oxidized with $FeCl_3$ to give the dibenzopentalene derivative 7**4** in high yield. Treatment of the in situ generated barium dibenzopentalenides **71a** and **71b** with Br_2 in THF afforded their corresponding 5,10-dibromodibenzopentalene **75** in 52% and 55% isolated yields, respectively, which could be used for the synthesis of a series of functionalized dibenzopentalenes and dibenzopentalene oligomers.
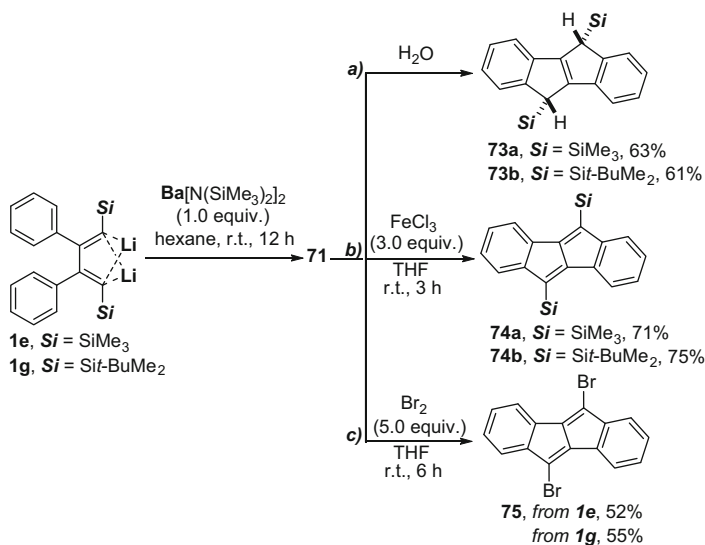
Scheme 38 Reactivity of barium dibenzopentalenides **71**

6   Summary, Conclusions, Outlook

In this review, we describe our systematic work on the structures, reactions, and synthetic application of 1,4-dilithio-1,3-butadienes (di-lithio reagents). The chemistry of the di-lithio reagents shows different reactivity from their corresponding mono-lithium reagents. These di-lithio reagents could be used to synthesize interesting and useful compounds that are not available by other means, such as *N*-, *O*-, and *Si*-containing heterocycles, strained ring systems, metal-containing macrocycles, and metal complexes bearing new types of ligand. The unique structure of the butadienyl dilithium compounds leads to exciting cooperative reactivity. Three major reaction patterns have been observed: (1) intramolecular reactions, (2) intermolecular reactions, and (3) transmetallation to form organo-*di*-metallic or metallacyclic compounds have been presented. The substituents on the butadienyl skeleton have remarkable effect on both the structures and reactions of di-lithio reagents. Currently we hope to develop new types of organo-*di*-metallic compounds and expect novel structures, interesting reactivities, and useful synthetic applications: (1) organo-*di*-metallic compounds bearing two different metallic centers and (2) organo-*di*-metallic compounds with other types of bridges instead of butadienyl skeleton, such as longer bridges with 5- or 6-carbon chains or with heteroatoms inserted in the bridge.

References

1. Rappoport Z, Marek I (2004) The chemistry of organolithium compounds. Wiley, Chichester
2. Clayden J (2002) Organolithiums: selectivity for synthesis. Pergamon, Oxford
3. Gessner VH, Däschlein C, Stohmann C (2009) Structure formation principles and reactivity of organolithium compounds. Chem Eur J 15:3320–3334
4. Lucht BL, Collum DB (1999) Lithium hexamethyldisilazide: a view of lithium ion solvation through a glass-bottom boat. Acc Chem Res 32:1035–1042
5. Hoppe D, Hense T (1997) Enantioselective synthesis with lithium/(−)-sparteine carbanion pairs. Angew Chem Int Ed Engl 36:2282–2316
6. Weiss E (1993) Structure of organo alkali metal complexes and related compounds. Angew Chem Int Ed Engl 32:1501–1523
7. Najera C, Sansano JM, Yus M (2003) Recent synthetic uses of functionalised aromatic and heteroaromatic organolithium reagents prepared by non-deprotonating methods. Tetrahedron 59:9255–9303
8. Langer P, Freiberg W (2004) Cyclization reactions of dianions in organic synthesis. Chem Rev 104:4125–4149
9. Foubelo F, Yus M (2005) Organodilithium intermediates as useful dianionic synthons: recent advances. Curr Org Chem 9:459–490
10. Wu W, Gu D, Wang S, Ning Y, Mao G (2011) Recent developments in homobimetallic reagents and catalysts for organic synthesis. Chin Sci Bull 56:1753–1769
11. Ananikov VP, Hazipov OV, Beletskaya IP (2011) 1,4-Diiodo-1,3-dienes: versatile reagents in organic synthesis. Chem Asian J 6:306–323
12. Xi Z (2004) Reaction chemistry of 1,4-Dilithio-1,3-diene and 1-lithio-1,3-diene derivatives. Eur J Org Chem 2773–2781
13. Xi Z (2010) 1,4-dilithio-1,3-dienes: reaction and synthetic applications. Acc Chem Res 43:1342–1351
14. Zhang WX, Xi Z (2008) Synthetic methods for multiply substituted butadiene-containing building blocks. Synlett 2557–2570
15. Barluenga J, Fananas FJ, Sanz R, Ignacio JM (2003) Synthesis of pyrrole derivatives through functionalization of 3,4-Bis(lithiomethyl)dihydropyrroles. Eur J Org Chem 771–783
16. Leng L, Xi C, Shi Y, Guo B (2003) Dianionic cycloaddition of decatetraenes with RCOX forming nine-membered carbocycles. Synlett 183–186
17. Maercker A, Flierdt J, Girreser U (2000) Polylithiumorganic compounds. Part 27: C, C-bond forming reactions of 3,4-dilithio-2,5-dimethyl-2,4-hexadiene. Tetrahedron 56:3373–3383
18. Lillo VJ, Gomez C, Yus M (2009) 2,2′-Dilithiobiphenyl by direct lithiation of biphenylene. Tetrahedron Lett 50:2266–2269
19. Yus M, Ramon DJ, Gomez I (2002) Lithiophenylalkyllithiums: new dilithium reagents having both sp(2)- and sp(3)-hybridised remote carbanionic centres. J Organomet Chem 663:21–31
20. Foubelo F, Saleh SA, Yus M (2000) 3-Chloropropyl and 4-chlorobutyl phenyl ethers as sources of 1,3-dilithiopropane and 1,4-dilithiobutane: sequential reaction with carbonyl compounds. J Org Chem 65:3478–3483
21. Strohmann C, Lehmen K, Dilsky SA (2006) Monolithiated and its related 1,3-dilithiated allylsilane: syntheses, crystal structures, and reactivity. J Am Chem Soc 128:8102–8103
22. Dubac J, Laporterie A, Manuel G (1990) Group 14 metalloles. 1. Synthesis, organic chemistry, and physicochemical data. Chem Rev 90:215–263
23. Schlenk W, Bergmann E (1928) The products of the addition of alkali metals on multiple carbon-carbon fusions. Liebigs Ann Chem 463:71
24. Smith LI, Hoehn HH (1941) The reaction between lithium and diphenylacetylene. J Am Chem Soc 63:1184–1187
25. Kos AJ, PvR S (1980) Cyclic 4 stabilization. Combined Moebius-Hueckel aromaticity in doubly lithium bridged $R_4C_4Li_2$ systems. J Am Chem Soc 102:7928–7929

26. Schubert U, Neugebauer W, Schleyer PvR (1982) Symmetrical double lithium bridging in 2,2′-di(lithium-tmeda)biphenyl (tmeda = MeNCH$_2$CH$_2$NMe$_2$): experimental confirmation of theoretical predictions. J Chem Soc Chem Commun 1184–1185

27. Ashe AJ III, Kampf JW, Savla PM (1993) The structure of (1Z,3Z)-1,4-Bis(trimethylsilyl)-1,4-bis(lithiotetramethylethylenediamine)-2,3-dimethyl-1,3-butadiene. A double bridged dilithium compound. Organometallics 12:3350–3353

28. Pauer F, Power PP (1994) 1,4-Dilithio-1,2,3,4-tetraphenyl-butadiene – crystal structure of the 1,2-dimethoxyethane adduct. J Organomet Chem 474:27–30

29. Saito M, Nakamura M, Tajima T, Yoshioka M (2007) Reduction of phenyl silyl acetylenes with lithium: unexpected formation of a dilithium dibenzopentalenide. Angew Chem Int Ed 46:1504–1507

30. Liu L, Zhang WX, Luo Q, Li H, Xi Z (2010) Isolation and X-ray structure of a trimeric 1,4-dilithio-1, 3-butadiene and a dimeric Me$_3$Si-substituted 1,4-dilithio-1,3-butadiene. Organometallics 29:278–281

31. Liu L, Zhang WX, Wang C, Wang CY, Xi Z (2009) Isolation, structural characterization and synthetic application of oxy-cyclopentadienyl dianions. Angew Chem Int Ed 48:8111–8114

32. Zhang S, Zhan M, Zhang WX, Xi Z (2013) 3-D brick-wall polymeric structure of TMEDA-supported 1,4-dilithio-1,3-butadiene. Organometallics 32:4020–4023

33. Li H, Wei B, Xu L, Zhang WX, Xi Z (2013) Barium dibenzopentalenide as a main-group metal η^8 complex: facile synthesis from 1,4-dilithio-1,3-butadienes and Ba[N(SiMe$_3$)$_2$]$_2$, structural characterization and reaction chemistry. Angew Chem Int Ed 52:10822–10825

34. Wang C, Luo Q, Sun H, Guo X, Xi Z (2007) Lithio siloles: facile synthesis and applications. J Am Chem Soc 129:3094–3095

35. Luo Q, Gu L, Wang C, Liu J, Zhang WX, Xi Z (2009) Synthesis of functionalized siloles from Si-Tethered diynes. Tetrahedron Lett 50:3213–3215

36. Luo Q, Wang C, Gu L, Zhang WX, Xi Z (2010) Formation of α-lithio siloles from silylated 1,4-dilithio-1,3-butadienes: mechanism and applications. Chem Asian J 5:1120–1128

37. Knorr R, von Roman TF (1984) Configurational stability of vinyllithium derivatives with 1-trimethylsilyl and 1-alkoxy substituents. Angew Chem Int Ed 23:366–368

38. Negishi E, Takahashi T (1986) The origin of the configurational instability of 1-silyl-1-alkenyllithiums and related alkenylmetals. J Am Chem Soc 108:3402–3408

39. Wang Z, Fang H, Xi Z (2005) Cleavage of C-Si bond by intramolecular nucleophilic attack: lithiation-promoted formation of siloles from 1-bromo-4-tetrasubstituted silyl-1,3-butadiene derivatives. Tetrahedron Lett 46:499–501

40. Hudrlik PF, Dai D, Hudrlik AM (2006) Reactions of dilithiobutadienes with monochlorosilanes: observation of facile loss of organic groups from silicon. J Organomet Chem 691:1257–1264

41. Yamaguchi S, Xu C, Okamoto T (2006) Ladder-conjugated materials with main group elements. Pure Appl Chem 78:721–730

42. Tamao K, Yamaguchi S, Shiro M (1994) Oligosiloles: first synthesis based on a novel endo-endo mode intramolecular reductive cyclization of diethynylsilanes. J Am Chem Soc 116:11715–11722

43. Xi Z, Song Q, Chen J, Guan H, Li P (2001) Dialkenylation of carbonyl groups by alkenyllithium compounds: formation of cyclopentadiene derivatives by the reaction of 1,4-dilithio-1,3-dienes with ketones and aldehydes. Angew Chem Int Ed 40:1913–1916

44. Fang H, Li G, Mao G, Xi Z (2004) Reactions of substituted (1,3-butadiene-1,4-diyl) magnesium, 1,4-bis(bromomagnesio) butadienes and 1,4-dilithiobutadienes with ketones, aldehydes and PhNO to yield cyclopentadiene derivatives and N-Ph pyrroles by cyclodialkenylation. Chem Eur J 10:3444–3450

45. Chen J, Song Q, Li P, Guan H, Jin X, Xi Z (2002) Stereoselective synthesis of polysubstituted 2,5-dihydrofurans from reaction of 1,4-dilithio-1,3-dienes with aldehydes. Org Lett 4:2269–2271

46. Gautam DR, Litinas KE, Fylaktakidou KC, Nicolaides DNJ (2003) Reactions of *o*-quinones with α-methyl- (or methylene) substituted phosphorus ylides. Synthesis of benzo[*b*]furan derivatives. Heterocycl Chem 40:399–404

47. Mandal S, Macikenas D, Protasiewicz JD, Sayre LM (2000) Novel *tert*-butyl migration in copper-mediated phenol *ortho*-oxygenation implicates a mechanism involving conversion of a 6-hydroperoxy-2,4-cyclohexadienone directly to an *o*-quinone. J Org Chem 65:4804–4809

48. Nguyen VH, Nishino H (2004) Novel synthesis of dihydropyrans and 2,8-dioxabicyclo[3.3.0] oct-3-enes using Mn(III)-based oxidative cyclization. Tetrahedron Lett 45:3373–3377

49. Mao G, Lu J, Xi Z (2004) Formation of 2,6-dioxabicyclo[3.3.0]-octa-3,7-dienes or multiply substituted o-benzoquinones from reactions of 1,4-dilithio-1,3-dienes with dimethyl oxalate. Tetrahedron Lett 45:8095–8098

50. Wakefield BS (1988) Organolithium methods. Academic, San Diego

51. Zadel G, Breitmaier E (1992) A one-pot synthesis of ketones and aldehydes from carbon dioxide and organolithium compounds. Angew Chem Int Ed Engl 31:1035–1036

52. Xi Z, Song Q (2000) Efficient synthesis of cyclopentadieneone derivatives by the reaction of carbon dioxide with 1,4-dilithio-1,3-dienes. J Org Chem 65:9157–9159

53. Wang C, Chen J, Song Q, Li Z, Xi Z (2003) Preparation of S-containing heterocycles via novel reaction patterns of carbon disulfide with 1-lithlobutadienes and 1,4-dilithiobutadienes. Arkivoc 155–164

54. Chen J, Song Q, Xi Z (2002) Novel reaction patterns of carbon disulfide with organolithium compounds via cleavage of C=S bonds or via cycloaddition reactions. Tetrahedron Lett 43:3533–3535

55. Wang CY, Song Q, Xi Z (2004) Reactions of 1,4-dilithiobutadienes with isothiocyanates: preparation of iminocyclopentadiene derivatives via cleavage of the C=S double bond of a RN=C=S molecule. Tetrahedron 60:5207–5214

56. Wang Z, Wang C, Xi Z (2006) Partially fluorinated naphthalene derivatives from 1,4-dilithio-1,3-dienes and C_6F_6. Tetrahedron Lett 47:4157–4160

57. Seyferth D, Weinstein RM (1982) High-yield acyl-anion trapping reactions: a synthesis of acyltrimethylsilanes. J Am Chem Soc 104:5534–5535

58. Murai S, Ryu I, Iriguchi J, Sonoda N (1984) Acyllithium to lithium enolate conversion by A 1,2-silicon shift. A shortcut to acylsilane enolates. J Am Chem Soc 106:2440–2442

59. Song Q, Chen J, Jin X, Xi Z (2001) Highly regio- and stereoselective 1,1-cycloaddition of carbon monoxide with 1,4-dilithio-1,3-dienes. Novel synthetic methods for 3-cyclopenten-1-one derivatives. J Am Chem Soc 123:10419–10420

60. Li H, Liu L, Wang Z, Zhao F, Zhang S, Zhang WX, Xi Z (2011) Iterative dianion relay along the ring: formation of gem-bis(trimethylsilyl) cyclopentenones from 2,5-bis(trimethylsilyl) oxy-cyclopentadienyl dianions and acid chlorides. Chem Eur J 17:7399–7403

61. Li H, Zhang WX, Xi Z (2013) Alkaline-earth metallocenes coordinated with ester pendants: synthesis, structural characterization, and application in metathesis reaction. Chem Eur J 19:12859–12866

62. Chen J, Song Q, Wang CY, Xi Z (2002) Novel cycloaddition of nitriles with monolithio- and dilithiobutadienes. J Am Chem Soc 124:6238–6239

63. Yu N, Wang CY, Zhao F, Zhang W-X, Xi Z (2008) Diversified reaction chemistry of 1,4-dilithio-1,3-dienes with nitriles: fine-tuning of reaction patterns by substituents on the butadienyl skeleton leading to multi-substituted pyridines and/or Δ^1-pyrrolines. Chem Eur J 14:5670–5679

64. Mangelinckx S, Giubellina N, De Kimpe N (2004) 1-azaallylic anions in heterocyclic chemistry. Chem Rev 104:2353–2399

65. Zhao F, Zhan M, Zhang WX, Xi Z (2013) DFT studies on the reaction mechanisms of 1,4-dilithio-1,3-dienes with nitriles affording pyridines and 1,3,5-triazines. Organometallics 32:2059–2068

66. Williams RV (2001) Semibullvalenes and related molecules: ever closer approaches to neutral homoaromaticity. Eur J Org Chem 227–235

67. Williams RV (2001) Homoaromaticity. Chem Rev 101:1185–1204
68. Dewar MJS, Náhlovská Z, Náhlovský BD (1971) Diazabullvalene; a "Nonclassical" molecule? Chem Commun 1377–1378
69. Schnieders C, Altenbach HJ, Müllen KA (1982) 2,6-diazasemibullvalene. Angew Chem Int Ed Engl 21:637–638
70. Zhang S, Wei J, Zhan M, Luo Q, Wang C, Zhang WX, Xi Z (2012) 2,6-Diazasemibullvalenes: synthesis, structural characterization, reaction chemistry and theoretical analysis. J Am Chem Soc 134:11964–11967
71. Zhang S, Zhan M, Luo Q, Zhang WX, Xi Z (2013) Oxidation of C–H bonds to C=O bonds by O_2 only or N-oxides and DMSO: synthesis of Δ^1-bipyrrolinones and pyrrolino[3,2-b] pyrrolinones from 2,6-diazasemibullvalenes. Chem Commun 49:6146–6148
72. Zhang S, Zhang WX, Xi Z (2013) Lewis acid-catalyzed site-selective cycloadditions of 2,6-diazasemibullvalenes with isocyanides, azides and diazo compounds for the synthesis of diaza- and triaza-brexadiene derivatives. Angew Chem Int Ed 52:3485–3489
73. Zhan M, Zhang S, Zhang WX, Xi Z (2013) Diazo compounds as electrophiles to react with 1,4-dilithio-1,3-dienes: efficient synthesis of 1-imino-pyrrole derivatives. Org Lett 15:4182–4185
74. Kruger C, Sekutowski JC, Hoberg H, Krause-Going R (1977) (Pentaphenyl)aluminacyclopentadiene as a complexing ligand. The molecular structure of (pentaphenyl)aluminacyclopentadiene and its complex with 1,5-cyclooctadienenickel. J Organomet Chem 141:141–148
75. Fang H, Zhao C, Li G, Xi Z (2003) Reaction of aluminacyclopentadienes with aldehydes affording cyclopentadiene derivatives. Tetrahedron 59:3779–3786
76. Wang C, Yuan J, Li G, Wang Z, Zhang S, Xi Z (2006) Metal-mediated efficient synthesis, structural characterization and skeletal rearrangement of octa-substituted semibullvalenes. J Am Chem Soc 128:4564–4565
77. Wang C, Xi Z (2007) Metal mediated synthesis of substituted cyclooctatetraenes. Chem Commun 5119–5133
78. Li G, Fan H, Zhang S, Xi Z (2004) Synthesis, structural characterization, and skeletal rearrangement of dibenzo tricyclo[3.3.0.0^{2,6}]-1,2,5,6-tetrasubstituted-octanes. Tetrahedron Lett 45:8399–8402
79. Stiles M, Burckhardt U (1964) Thermal and photochemical rearrangement of substituted dibenzo[a, e]cyclooctatetraenes. J Am Chem Soc 86:3396–3397
80. Müllen K, Wegner G (1998) Electronic materials: the oligomer approach. Wiley- VCH, Weinheim
81. Schwab PFH, Smith JR, Michl J (2005) Synthesis and properties of molecular rods. 2. Zig-Zag rods. Chem Rev 105:1197
82. Li G, Fang H, Xi Z (2003) Formation of stereodefined multiply substituted all-cis octatetraenes, tricycle-[4.2.0.0^{2,5}]octa-3,7-dienes and pentalenes via CuCl or FeCl$_3$-mediated dimerization of 1-lithiobutadienes and 1,4- dilithiobutadienes. Tetrahedron Lett 44:8705–8708
83. Wei J, Wang Z, Zhang WX, Xi Z (2013) Construction of octa-alkyl substituted and deca-substituted all-cis octatetraenes via linear dimerization of 1,4-dicopper-1,3-butadienes and subsequent cross-coupling with halides. Org Lett 15:1222–1225
84. Luo Q, Wang C, Zhang WX, Xi Z (2008) CuCl-mediated tandem CO insertion and annulation of 1,4-dilithio-1,3-dienes: formation of multiply substituted cyclopentadienones and/or their head-to-head dimers. Chem Commun 1593–1595
85. Li G, Fang H, Li Z, Xi Z (2003) FeCl$_3$-mediated reaction of 1,4-dilithio-1,3-dienes with alkynes affording benzene derivatives. Chin J Chem 21:219–221
86. Knochel P, Almena J, Jones P (1998) Organozinc mediated reactions. Tetrahedron 54:8275–8319
87. Wooten A, Carroll PJ, Maestri AG, Walsh PJ (2006) Unprecedented alkene complex of zinc (II): structures and bonding of divinylzinc complexes. J Am Chem Soc 128:4624–4631

88. Zhou Y, Zhang WX, Xi Z (2012) 1,3-Butadienylzinctrimer formed via transmetallation from 1,4-dilithio-1,3-butadienes: synthesis, structural characterization and application in negishi cross-coupling. Organometallics 31:5546–5550
89. Resa I, Carmona E, Gutierrez-Puebla E, Monge A (2004) Decamethyldizincocene, a stable compound of Zn(I) with a Zn-Zn bond. Science 305:1136–1138
90. Negishi E (2011) Magical power of transition metals: past, present, and future. Angew Chem Int Ed 50:6738–6764
91. Lambert C, PvR S (1994) Are polar organometallic compounds "carbanions"? The gegenion effect on structure and energies of alkali-metal compounds. Angew Chem Int Ed Engl 33:1129–1140
92. Westerhausen M, Digeser MH, Nöth H, Seifert T, Pfitzner A (1998) A unique barium−carbon bond: mechanism of formation and crystallographic characterization. J Am Chem Soc 120:6722–6725
93. Saito M (2010) Synthesis and reactions of dibenzo[a, e]pentalenes. Symmetry 2:950–969

Dynamics of the Lithium Amide/Alkyllithium Interactions: Mixed Dimers and Beyond

Anne Harrison-Marchand, Nicolas Duguet, Gabriella Barozzino-Consiglio, Hassan Oulyadi, and Jacques Maddaluno

Abstract This review summarizes detailed investigations on the enantioselective nucleophilic addition of organolithiums onto prochiral electrophilic substrates, one of the simplest reaction meant to create a C–C bond, using dipolar bimetallic systems. Interestingly, these very popular and useful chemical transformations, even if taught at the undergraduate level, have remained underdeveloped when it comes to their enantioselective versions. The systems we present consist of a nucleophilic organolithium (NuLi) in strong dipolar interaction with a second lithiated entity bearing the source of asymmetry, i.e., a chiral lithium amide (CLA) derived from a 3-aminopyrrolidine (3APLi). Several 1:1 3APLi/NuLi noncovalent mixed aggregates are described and their relevance to the enantioselective process is discussed. Since the Curtin–Hammett principle forbids to correlate the complexes to the final ee's of the products, we have run complementary experiments of which results led us to propose the participation of an ephemeral, but more reactive, triptych aggregate.

Keywords Chiral lithium amide (CLA) · Dipolar interactions · Mixed AggregAtes (MAA) · Structure–reactivity relationship · Synergy

Contents

A. Harrison-Marchand (✉), N. Duguet, G. Barozzino-Consiglio, H. Oulyadi, and
J. Maddaluno (✉)
IRCOF: Laboratoire COBRA, Université de Rouen, CNRS, INSA de Rouen,
UMR 6014 & FR 3038, 76821 Mont Saint Aignan Cedex, France
e-mail: anne.harrison@univ-rouen.fr; jmaddalu@crihan.fr

1   Introduction

Discussing the pivotal role played by lithium derivatives (RLi) in organic chemistry is most probably useless (see, for instance, reviews and books by [1–22]). These reactants have proved their efficiency in an endless list of synthetic applications in which they flourish as nucleophiles, bases, or ligands. Some of these reagents are so popular that the most generally employed lithium amides (LDA, LiTMP, LiHMDS) have even been nicknamed "essential utilities" by Mulvey in a recent review [22]. Expectedly, the number of studies dedicated to organolithiums, whether from the viewpoint of reactivity or structural identifications, continues to rise steadily as illustrated by the very topical papers by Reich or Williard [15–19]. In particular, the complete structural characterization of these reagents, both in the solid state and in solution, represents a long-lasting challenge that has been spectacularly revivified by the recent development or improvement of analytical techniques. One important domain of application that remains relatively little concerned by these progresses is that of asymmetric synthesis and particularly enantioselective processes, even if, for instance, recent structural findings on the role of sparteine or its surrogate have led to fundamental deductions on the organization into solution of several RLi–ligand complexes [23–27].

The main problem associated with organolithiums is their high reactivity, and thus sensitivity, that tends to limit success in enantioselective processes since they can easily react with their environment (as a base or a nucleophile if not through hydrolysis or solvolysis) before getting a chance to interact with the source of chirality. Skirting such a problem generally requires a deep understanding of the specific structure–reactivity relationship of organolithiums and, consequently, succeeding in characterizing the reaction intermediates in solution and mastering the dynamics of their interactions. In this context, our team has been interested, in the last twenty years, in the enantioselective version of one of the simplest reactions meant to create a C–C bond, viz. the nucleophilic addition of organolithiums onto prochiral electrophilic substrates. These chemical transformations, even if taught at the undergraduate level, have remained underdeveloped when it comes to enantioselective versions. Note that most of the works dedicated to the enantioselective nucleophilic 1,2 additions of organolithiums onto carbonyl or imine derivatives rely on alkyllithium species interacting with a chiral ligand (the chiral ligand is a σ-donor coordinating entity and the electrophile a carbonyl derivative: [28–35]; the chiral ligand is a dipolar lithium alkoxide and the electrophile a carbonyl derivative: [36–50]; the chiral ligand is a dipolar lithium amide and the electrophile a carbonyl derivative: [51–71]; the electrophile is an imine, see, for instance, [7, 72–95]) rather than on the activation of the electrophile by an exogenous chiral Lewis-acid catalyst. This is obviously related to the reactivity of alkyllithium nucleophiles, for which a preliminary interaction with the chiral inductor, necessary to set up an enantioselective process, is time-enabled. This limitation can be overpassed when working with poor electrophiles such as imines [7, 72–95], from which chiral amines could be prepared with ee's up to 94% and in excellent yields (81–99%) working in toluene at −78°C [95]. In contrast,

the literature suggests that obtaining comparable results with carbonyl substrates necessitates working at temperatures lower than $-115°C$ and in solvent mixtures for which the nature and the ratio vary for each case [35, 37, 38, 40, 51, 57, 65, 66, 70, 71]. Such drastic and restricted reaction conditions limit the interest for this chemistry. For our concern, we have tried to develop a methodology involving chiral ligands able to afford high induction levels in "classical" cryogenic conditions, that is to say, in one single solvent (THF, Et$_2$O, toluene) and not below $-78°C$ (Fressigné et al., unpublished results) [96–115]. For organometallic reactants, the ligand can be a σ-donor coordinating entity (chiral amines and polyamines, ethers, aminoethers, phosphines) [28–35] or a second dipolar species (chiral lithium or magnesium alkoxide, lithium or magnesium amide) [115]. The second strategy, which mixes two organometallics, takes advantage of the strong dipole–dipole interactions between the partners and leads to noncovalent Mixed AggregAtes (MAA) [20, 21]. These organo(bi)metallic reactants exhibit properties that can be distinct from those of the parent partners. The MAA's route revealing more efficient for organolithium reactants, we focused our efforts on reaching chiral lithium amides (CLA) derived from 3-aminopyrrolidines (3APLi) and showed that those species behave as good chiral ligands (ee's up to 86%) for nucleophilic alkyllithiums (NuLi) in the classical conditions defined earlier ($-78°C$, THF) [96, 100, 102–106, 109]. In a simultaneous work, we worked on interpreting the synthetic developments by a detailed understanding of the mechanisms of inductions, thanks to the characterization of the [3APLi/NuLi] MAA formed in solution, running NMR spectroscopy [98, 99, 103, 104, 106, 108, 110, 112, 114], and DFT calculations [97, 101, 103, 104, 106, 108, 111–114]. The hydroxyalkylation of nonenolizable aldehydes (ArCHO) was chosen as a simple prototypical reaction (Scheme 1).
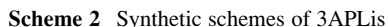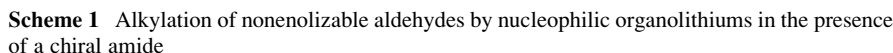
This article aims at (1) summarizing our approach in this field and (2) presenting new observations and their mechanistic interpretation which suggests that bimetallic species, and possibly higher aggregation states, play a key part in these model reactions.

2 Results and Discussion

2.1 State of the Art

Elaborating a versatile enantioselective process requires selecting efficient chiral ligands that are also cheap and easy to synthesize. Two short synthetic schemes based on affordable starting material have been developed in our laboratory to reach a wide range of 3APLi derivatives, among which are amides **1**, **2,** and **3** (Scheme 2) [96, 100, 103, 106, 109, 116, 117].

The optimization of the enantioselective nucleophilic 1,2 additions of methyllithium (MeLi) and *n*-butyllithium (*n*-BuLi), in the presence of 3APLis, started repeating a standard procedure originally described by Mukaiyama

Scheme 1 Alkylation of nonenolizable aldehydes by nucleophilic organolithiums in the presence of a chiral amide

Scheme 2 Synthetic schemes of 3APLis

(aldehyde = benzaldehyde, solvent = Et$_2$O, reaction time = 1 h, chiral ligand/ alkyllithium/aldehyde ratio = 4.0:6.0:1.0) [38]. Eighteen 3APLi structures [106] were synthesized, varying R^1, R^2, and R^3, and then tested independently. It appeared that (1) the substituent borne by the intracyclic nitrogen had very little, if any, influence, and (2) reaching an induction >20% at −78°C (instead of the −123°C in Mukaiyama's procedure) required working with an excess of 3APLi (1.5 equiv. compared with 1 equiv. of aldehyde), and the latter should present a hindered lateral amido chain (N(Li)R^{1}R^2), such as in amides **1** (N(Li)PhPh), **2,** and **3** (N(Li)MePh). The procedure was then optimized using **1** and varying the nature of the aldehyde (benzaldehyde, o-tolualdehyde, o-anisaldehyde, 1-naphthaldehyde, 2-naphthaldehyde, and pivalaldehyde), the solvent (toluene, DMM, DME, Et$_2$O, THF), the temperature (from −20 to −78°C), the time (from 30 min to 6 h), and the amide/alkyllithium/aldehyde ratio. Optimal 69–73% ee's (in favor of the formation of the (R) alcohol **4**), in addition to good yields (up to 79%), were finally reached reacting, for 2 h, the [**1**/n-BuLi] MAA with o-tolualdehyde at −78°C in THF. This highest levels of induction were attained for both 1.5:1.5:1.0 (Table 1, entry 1) and 1.5:2.5:1.0 (Table 1, entry 2) amide/alkyllithium/aldehyde ratios. Replacing n-BuLi by MeLi led, using the same ratios (Table 1, entries 3 and 4), to the main formation

Table 1 Enantioselective hydroxyalkylations of o-tolualdehyde reacting with the nucleophilic MeLi or n-BuLi in the presence of 3APLi **1**, **2**, and **3**

Entry	3APLi	NuLi	3APLi/NuLi/o-TolCHO	Yd (%)	Ee (%)	Alcohol
1	**1**	n-BuLi	1.5:1.5:1	79	69	**4** (R)
2	**1**		1.5:2.5:1	77	73	**4** (R)
3	**1**	MeLi	1.5:1.5:1	66	59	**5** (R)
4	**1**		1.5:2.5:1	46	61	**5** (R)
5	**2**	n-BuLi	1.5:1.5:1	83	83	**4** (R)
6	**2**		1.5:2.5:1	81	80	**4** (R)
7	**3**		1.5:1.5:1	84	56	**4** (S)
8	**3**		1.5:2.5:1	82	65	**4** (S)
9	**2**	MeLi	1.5:1.5:1	70	80	**5** (R)
10	**2**		1.5:2.5:1	78	82	**5** (R)

of the (R) alcohol **5**, however with lower inductions (up to 59–61%) and yields (up to 66%).

The above experimental conditions optimized with **1** (THF, $-78°$C, 2 h) were repeated in the presence of **2** and **3**. The results (Table 1, entries 5–10) evidenced higher yields and enantioselectivities for amide **2** (Table 1, entries 5, 6 and 9, 10). Indeed, yields and ee's were mostly reaching 80–83%. One can note that once more, working with a 1 equiv. excess of nucleophile with respect to the amide (amide/alkyllithium/aldehyde ratio 1.5:2.5:1.0 instead of 1.5:1.5:1.0) did not alter the enantioselectivities and had a variegated effect on the yields. From such an observation one can deduce that the faster reactive species in the reaction medium is an alkyllithium–lithium amide "complex" (whatever this term encompasses structurally speaking) and not free alkyllithium in excess. Note however that the induction began to decrease when the amide/alkyllithium/aldehyde ratio became superior to 1.5:3.0:1.0. Interestingly, the sense of the inductions appeared to depend on the configuration of the second stereogenic center. Amide **2** (3S, 8R) led to the formation of the mainly (R) alcohol, while the (S) enantiomer was formed preferentially introducing amide **3** (3S, 8S) (entries 5 and 6 compared with entries 7 and 8). This observation suggests that, in the presence of the second stereogenic center on C-8, the sense of induction is driven by this center, dimming the inductive effect brought by the one on C-3. The racemic analogs at C-3, i.e., 3S, 8R/3R, 8R and 3S, 8S/3R, 8S, were synthesized to clarify this point and the alkylations run with n-BuLi and these C-3 racemic amides led to ee's similar to those obtained with **2** and **3**, respectively [109].

NMR characterizations of the intermediates in solution were initiated at this point of the study, with the aim at better understanding the stereochemical outcomes of the reaction and then undertaking a fine-tuning of the 3APLi structures. Thus, ^{1}H, ^{13}C, and ^{6}Li mono- and bidimensional NMR spectra were first recorded
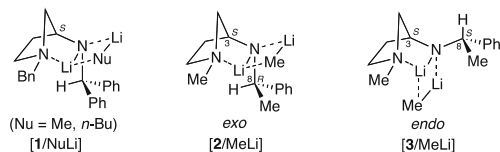
Fig. 1 Structures of [**1**/MeLi], [**1**/*n*-BuLi], [**2**/MeLi], and [**3**/MeLi] aggregates in solution

from [6]Li-labeled [**1**/NuLi] aggregates [98, 99]. These combined data, and particularly the homo-, and heteronuclear dipolar couplings (NOESY, HOESY), as well as the ^{13}C signal analysis of the *ipso*-carbon of the AlkLi, led us to propose structural arrangements for the [**1**/*n*-BuLi] and [**1**/MeLi] mixed complexes in THF at $-78°$C. Both consist in 1:1 noncovalent aggregates organized around a quadrilateral C_{Alk}–Li–N–Li core (Fig. 1, left). Noteworthy is the azanorbornyl folding observed for the 3APLi partner due to an intramolecular coordination between the lithium of the amide and the intracyclic nitrogen. A similar spectroscopic study was undertaken to examine the structural arrangements of [**2**/MeLi] and [**3**/MeLi] and understand the origin of the reversal of stereoselectivity imposed by the chiral lateral amido chain [103]. The formation of comparable 1:1 mixed complexes organized around C_{Alk}–Li–N–Li quadrilaterals was highlighted as well in THF at $-78°$C. However, the organization around this quadrilateral core showed to be dependent on the configuration of the C-8 stereogenic carbon since the benzylic proton tends to point toward the more crowded portion of the complex (Fig. 1, middle and right). Those two isomers were respectively given the name of *exo*- and *endo*-complex. Within the limits of the Curtin–Hammett principle, we reasonably assumed that these two complexes were, at least in part, responsible for the opposite sense of induction.

A complementary set of DFT computations was then launched to analyze the interaction between such dissymmetric bimetallic entities and the electrophile (*o*-tolualdehyde in the model reaction). Note that the docking of the aldehyde could not be examined spectroscopically, the reaction running too fast on the NMR time scale [13, 118, 119]. A primary but crucial question to be solved concerned the relative Lewis acidity of the two Li cations and therefore the regioselective docking of the oxygen of the carbonyl moiety. The computational results obtained on a realistic disolvated model of **2** revealed unambiguously that Li^2 (Fig. 2) exhibits a much stronger affinity for the aldehyde than its Li^1 competitor, which is buried at the heart of the dimer. Once the complex is formed, a description of the addition reaction itself, justifying the sense of the induction observed experimentally, remained to be proposed. This work was undertaken but never completed. However, a simple reasoning on the fully loaded 3APLi–2THF–TolCHO complex suggests that the aldehyde rotation, the key motion controlling the exposition of the *Si* vs. *Re* face of the aldehyde to the incoming nucleophile, can be determined by the bulkiness and location of the substituents (Fig. 2).
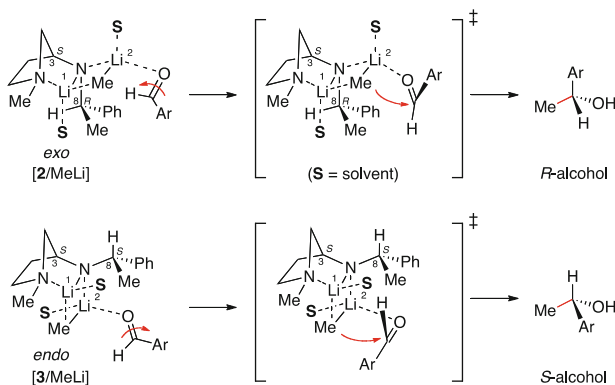
Fig. 2 Putative interpretation of the docking of the aldehyde onto the [**2**/MeLi] and [**3**/MeLi] complexes

With the above data in hand, we prepared a set of new 3-aminopyrrolydines, 3-aminothiophenes, and 3-aminotetrahydrofurans designed to introduce supplementary steric hindrances and additional chelating heteroatoms close to the C_{Alk}–Li–N–Li reactive core [109]. Disappointingly, the levels of induction returned by these new amines never exceeded those measured with **2** and **3** (80% ee).

We thus decided to address another important challenge that consisted in being able to work with substoichiometric amounts of chiral ligand. Unfortunately, all our attempts failed as well, with ee's plummeting when less than 1 equiv. of amide was involved. Such a failure prompted us to reconsider the whole reaction course and in particular the influence of the lithium alkoxide accumulating in the solution that was ignored in our static model. This primary product is also a dipolar entity able to interact with the amide and the alkyllithium and likely to interfere with the simple [3APLi/AlkLi] + ArCHO ideal microcosm. Thus, keeping in mind that the overall system involves three polar entities, namely the amide, the nucleophile, and the lithium alkoxide progressively produced in the medium, another series of DFT computations were undertaken to compare the stabilities of the aggregates that could form. The calculations were run considering amide **2**, MeLi, and *o*-TolCH (OLi)Me **5Li** and assuming that 1:1 mixed complexes would form (Fig. 3: the energy scale has been calibrated on complex [**2**/MeLi] for which $E = 0$ kcal/mol) [113, 115].

Both aggregates incorporating the alkoxide moiety ([MeLi/**5Li**] and [**2**/**5Li**]) revealed more stable than the assumed inductive complex [**2**/MeLi], which confirms the fact that the alkoxide cannot be ignored when trying to interpret the whole mechanism of the reaction. In particular, the cohesion energy related to the [**2**/**5Li**] aggregate exceeds that of [**2**/MeLi] by −6 kcal/mol, a result which suggests that the alkoxide will progressively trap the amide and this irreversibly. Such a result indicates that a stoichiometric amount of the chiral ligand becomes necessary to reach significant ee's. The same DFT results also show an even stronger affinity between the alkoxide and the nucleophile to give complex [MeLi/**5Li**] likely to

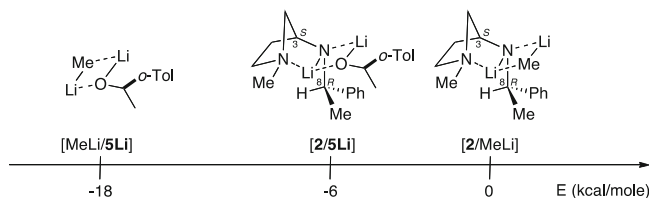**Fig. 3** Relative energies of [**2**/MeLi], [**2**/**5Li**], and [MeLi/**5Li**] 1:1 mixed aggregates

compete with the [**2**/MeLi] aggregate [42]. We actually checked that the former indeed converts the aldehyde into **5**, albeit as a racemic mixture. This latter result can explain the limitation of the induction at ~80% ee.

Improvement of the ee's and refinement of the reaction into its substoichiometric version was then carried out adding a fourth dipolar species, i.e., LiCl. This lithium salt, of which beneficial effect on inductions had already been proved in many cases (for enantioselective protonations, see [120–122]; for enantioselective deprotonations, see [123–129]), was introduced in the reaction medium at two different times of the optimized procedure. Adding LiCl onto the [**2**/MeLi] mixed aggregate and then reacting the resulting three-component mixture with the aldehyde led to a plunge of the induction (37% ee) [108]. By contrast, introducing the lithium halide in the same time than the aldehyde on the [**2**/MeLi] complex led to 86% ee [113]. Additional DFT calculations were then carried out to estimate the relative stabilities of the 1:1 mixed aggregates formed with the new dipolar partner in the reaction medium, i.e., [MeLi/LiCl], [**2**/LiCl], and [**5Li**/LiCl]. While the [MeLi/LiCl] heterodimer revealed by far the least stable aggregate possible (+21 kcal/mol compared with [**2**/MeLi] still calibrated at $E = 0$ kcal/mol), a result in line with parallel observations made when running NMR investigations on this species [130], the two other aggregates were found to be more stable than the reference [**2**/MeLi] heterodimer: [**2**/LiCl] by -12 kcal/mol and [**5Li**/LiCl] by -27 kcal/mol (Scheme 3). The first value explains why the induction plummeted when adding the lithium halide directly on the [**2**/MeLi]. This complex dissociates in the presence of LiCl to form irreversibly the [**2**/LiCl] dormant complex next to free methyllithium (Scheme 3, left). Such a conclusion could actually be verified by NMR spectroscopy: a THF solution of ^{6}LiCl was added to an equimolar amount of [**2**/Me^{6}Li], also in THF solution, and the resulting spectra clearly show the progressive replacement of the alkyllithium by the lithium halide to finally evidence the selective formation of [**2**/LiCl] next to free Me^{6}Li [108]. Addition of an excess of MeLi onto the latter solution did not change the final result. Otherwise, the stability of the [**5Li**/LiCl] complex, the more stable among all possible 1:1 aggregates optimized hitherto, suggests two conclusions: (1) the lithium halide should efficiently trap the alkoxide, provided that it interacts exclusively with **5Li** when it is introduced into the reaction medium (this is probably the case when LiCl is the cosolute of the substrate: Scheme 3, right); (2) in principle, such a procedure should allow running the model reaction with substoichiometric amounts of chiral
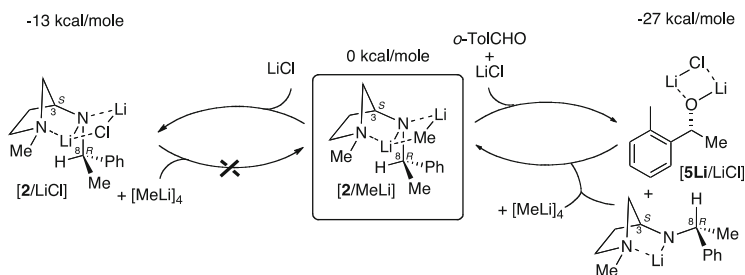
Scheme 3 Evolution of the [**2**/MeLi] complex upon addition of LiCl (**a**) directly on the [**2**/MeLi] aggregate before addition of ArCHO (*left*) and (**b**) as a cosolute of the substrate (*right*)

ligand. And indeed, an 80% ee could be maintained in the presence of 33% molar of 3APLi, and a 70% ee was returned when using only 10% molar of the chiral amide.[1]

These results show that all these noncovalent bimetallic entities undergo rapid exchanges suggesting that in situ competitions can be elicited between partners and open the door to a dynamic combinatorial chemistry of which principle has been exposed by Lehn some years ago [131].

2.2 Examining the Competitive Affinity of Different Alkyllithiums for a Given Amide

Knowing that methyllithium and *n*-butyllithium were independently and efficiently forming 1:1 complexes with the 3APLi **1**, **2**, or **3**, we wondered about the relative stability of these mixed aggregates. In other words, can two alkyllithiums compete to aggregate with a given amide in solution? To address this question, we preformed a 1:1 complex between **2** and a first alkyllithium (Alk^{1}Li) in THF at $-20°$C for 30 min (Scheme 4). The temperature was decreased at $-78°$C for another 30 min before an equimolar amount of a second alkyllithium (Alk^{2}Li) was introduced. The resulting solution was kept at $-78°$C for an aging stage (*x* min) before the aldehyde (0.67 equiv.) was introduced,[2] still at the same temperature. The reaction mixture was quenched after 2 h stirring at $-78°$C.

Starting with Alk^{1}Li=MeLi, we examined the possibility for *n*-BuLi (=Alk^{2}Li) to chase the MeLi off the [**2**/MeLi] aggregate. Applying the experimental sequence depicted on Scheme 4 and varying the aging time from 5 to 30, 40, and then 100 min led to the series of results reported Table 2.

---

[1] A result that was obtained after "cleansing" the methyllithium solution from traces (5–10%) of LiCl naturally present in commercial vials. See [113].

[2] The 1:1:1:0.67 3APLi/Alk^1/Alk^2/ArCHO ratio can also be read as 1.5:1.5:1.5:1.
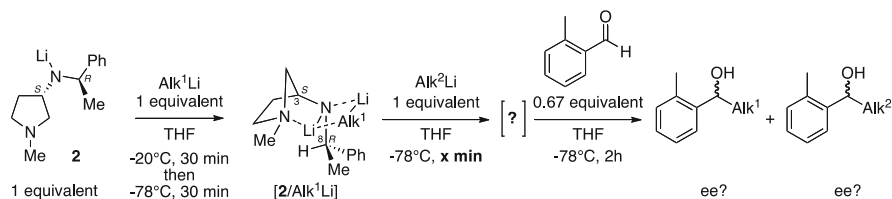
**Scheme 4** General sequence applied to examine the relative stability between aggregates

Table 2 Yields and ee's obtained running the hydroxyalkylation of *o*-tolualdehyde in the presence of the {[**2**/MeLi] + *n*-BuLi} mixture

	4		**5**	
x (min)	Conv (%)	Ee (%)	Conv (%)	Ee (%)
5	75	73	24	65
30	71	72	27	64
45	65	68	33	63
100	68	73	30	65

The two expected *R* alcohols formed with good ee's, however slightly lower than those measured when working with one single alkyllithium (63–73% instead of 80%). Regardless of the aging time following the introduction of the second alkyllithium, the **4/5** ratio remains more or less constant (≈70:30), suggesting, at first, a swift replacement of the MeLi by *n*-BuLi to reach a thermodynamic equilibrium between the two [**2**/MeLi] and [**2**/*n*-BuLi] complexes, in favor of the *n*-BuLi one (Scheme 5).

The reverse sequence was next carried out, i.e., 1 equiv. of MeLi was added onto the [**2**/*n*-BuLi] preformed aggregate. The above hypothesis was suggesting that alcohol **4** would be selectively obtained after 5 min aging, the **4/5** ratio being expected to plateau toward 70:30 upon longer maturing. However, the results gathered in Table 3 rebuff entirely these anticipations. Actually, the **4/5** ratio evolved from 0:100 after 5 min to 60:40 after 200 min aging.

These two sets of data suggested that the interaction between the various species in THF was not as simple as a thermodynamically controlled alkyllithium exchange between two 1:1 mixed aggregates. It rather seems that after a short aging time, the alcohol formed first derives from the alkyllithium introduced last in the reaction medium (Alk²Li). This observation parallels that by Andersson and Tanner who reacted MeLi with an aromatic aldimine (**7**) in the presence of a chiral tertiary
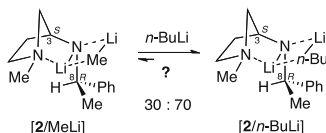
Scheme 5 Hypothetic thermodynamic equilibrium between the two [**2**/MeLi] and [**2**/*n*-BuLi] complexes

Table 3 Yields and ee's obtained running the hydroxyalkylation of *o*-tolualdehyde in the presence of the {[**2**/*n*-BuLi] + MeLi} mixture

x (min)	**4**			**5**	
	Conv (%)	Ee (%)		Conv (%)	Ee (%)
5	0	–		98	81
30	14	79		84	80
45	33	73		64	68
100	43	76		55	74
200	57	76		40	71

Table 4 Nucleophilic additions of {[**6**/MeLi] + CD_3Li} and then {[**6**/CD_3Li] + MeLi} mixtures onto aldimine **7** [3]

Alk^1	Alk^2	CH_3 adduct/CD_3 adduct
CH_3	CD_3	30:70
CD_3	CH_3	70:30

diamine (**6**, Table 4) [83, 132]. Because they had observed that higher inductions were obtained with 2 equiv. of alkyllithium, these authors reacted the same imine with the {[**6**/CH_3Li] + CD_3Li} system and then with the {[**6**/CD_3Li] + CH_3Li} one. The results showed that the nucleophile introduced last was always leading to the major product (Table 4). To our knowledge, this puzzling phenomenon was left unexplained.
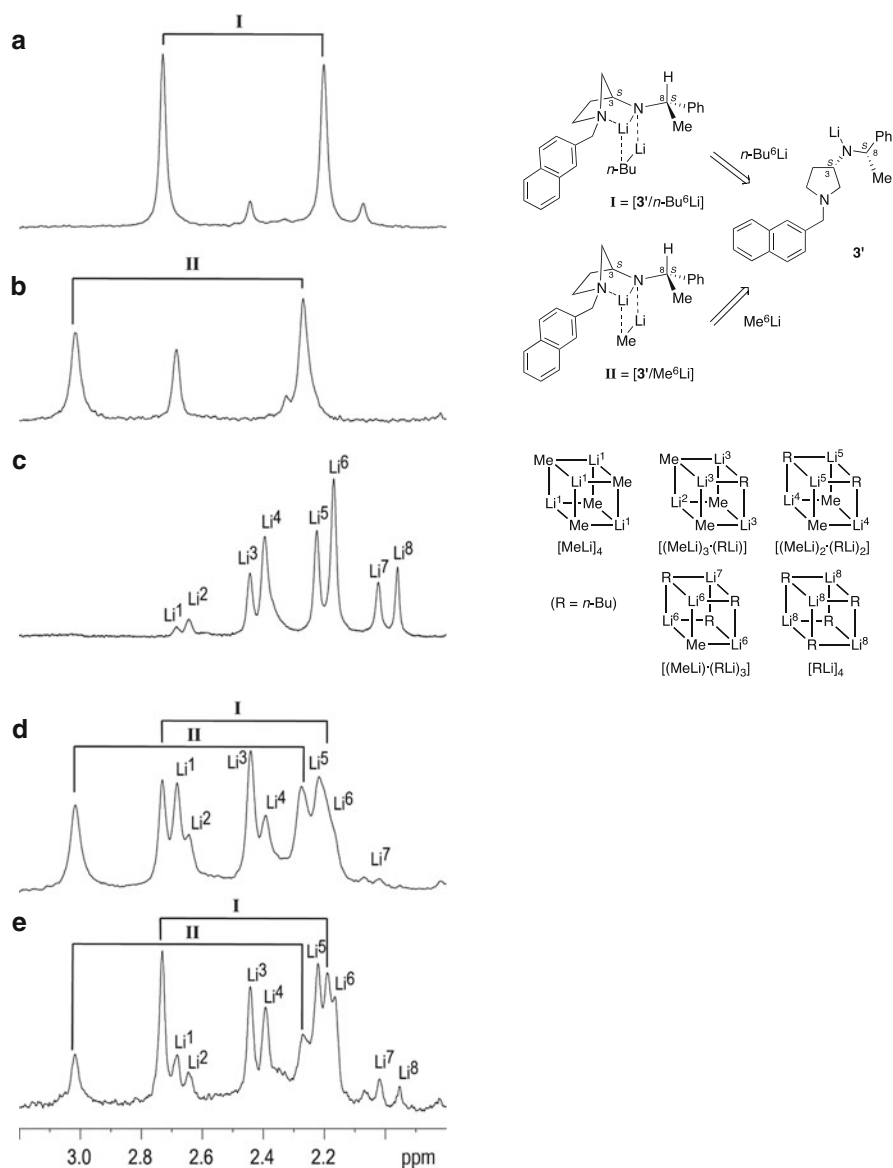
Fig. 4 ^{6}Li spectra in THF at 195 K of (**a**) [**3′**/n-BuLi]; (**b**) [**3′**/MeLi]; (**c**) [(Me^{6}Li)$_{4-n}$·(n-Bu^{6}Li)$_n$]; (**d**) a mixture resulting from the addition of MeLi on [**3′**/n-BuLi]; (**e**) a mixture resulting from the addition of n-BuLi on [**3′**/MeLi]

We tried to shine some light on our chemical results resorting to NMR spectroscopy. We examined mixtures of the three partners MeLi, n-BuLi, and 3APLi **3′** (Fig. 4). This amide, which led to a slightly lower ee than **3** in the hydroxyalkylation of o-TolCHO by n-BuLi (51% for **3′** vs. 65% for **3**, both in favor of alcohol **4** (S)),

was retained for simple practical reasons.[3] Thus, the 1:1 ^{6}Li-labeled [**3′**/n-BuLi] complex was prepared in THF-d$_8$ solution directly in an NMR tube at $-20°$C, and then, after cooling at $-78°$C, an equivalent of Me^{6}Li was introduced (Fig. 4, line d). The reverse sequence adding n-Bu^{6}Li onto a ^{6}Li-labeled [**3′**/MeLi] complex solution was also carried out (Fig. 4, line e) [110].

Whatever the sense of introduction of the alkyllithiums onto the preformed complex, the NMR spectra recorded after $\approx$60 min showed very similar profiles. Both the [**3′**/Me^{6}Li] and [**3′**/n-Bu^{6}Li] complexes could be identified, in addition to a series of cubic tetramers [(Me^{6}Li)$_{4-n}$·(n-Bu^{6}Li)$_n$] $(0 < n < 4)$. The juxtaposition of all of these aggregates did not allow to determine accurately the relative proportions of each [3APLi/AlkLi] mixed aggregate, so no preference for a given complex could be evidenced in these conditions.

To interpret the above chemical results, we propose the following hypothesis based on the formation of a putative triptych aggregate {[3APLi/Alk^{1}Li]/Alk^{2}Li}. This noncovalent supramolecular edifice would result, for instance, from the interaction between the original [3APLi/MeLi] mixed aggregate and [n-BuLi]$_n$, to form a transient trimer {[3APLi/MeLi]/[n-BuLi]$_n$} **A** that would be in equilibrium with its components on one side and its "swapped" isomer {[3APLi/n-BuLi]/ [MeLi]$_n$} **B** on the other (Scheme 6). Similarly, **B** would be in equilibrium with [3APLi/n-BuLi] plus [MeLi]$_n$. The two dimeric aggregates being probably the more stable species, the equilibria would be strongly shifted in their direction, explaining that no NMR signals could be detected for **A** and/or **B** on Fig. 4d, e.

Actually, we had already been pushed to assume that such ephemeral triptych aggregates could form, in particular to decipher the results of an exchange experiment in which a solution of ^{7}LiCl (considered as being dimeric in THF^{13}) was added to a [3AP^{6}Li/Me^{6}Li] dimer in THF. Indeed, a series of NMR spectra recorded during this reaction suggested a puzzling exchange of anions but not of cations, leading to the single formation of the [3AP^{6}Li/^{6}LiCl] mixed dimer plus the mixed dimer [Me^{7}Li/^{7}LiCl] [130]. A series of DFT computations led us to propose that this phenomenon could be understood if a triptych aggregate of the type {[3APLi/^{6}LiCl]/[^{7}LiCl]$_2$} was formed (Scheme 7) [111].

If systems such as **A** and **B** not only are intermediates allowing the 3APLi ligands exchange but also have an intrinsic reactivity, larger than that of the dimers toward tolualdehyde, then they could trigger the rapid addition of the "external" alkyllithium Alk^{2}Li and yield the Ar–CHOH–Alk^2 alcohol. Therefore, if one assumes that one of the two triptychs is more stable than the other and/or much more reactive, it will determine the chemoselectivity of the addition. The results in Tables 2 and 3 suggest that the {[3APLi/MeLi]/[n-BuLi]$_n$} complex **A** is more stable than **B**. The data of Table 3 being obtained from the [3APLi/n-BuLi] dimer, one can assume that the less stable triptych **B** is formed first and would progressively evolve toward **A**. During the time of this rearrangement (that corresponds to the settling of the thermodynamical equilibrium), **B** would react by itself and
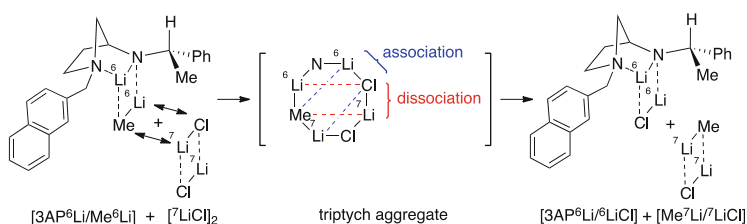
---

[3] Availability of the starting materials at the time of the study
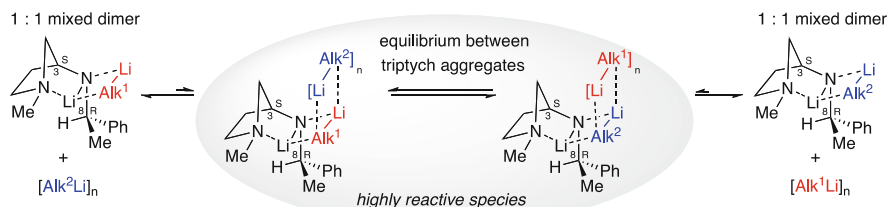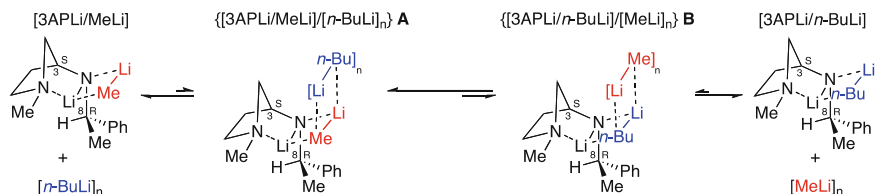
Scheme 6 Equilibria between triptych aggregates **A** and **B**, 1:1 mixed dimers [3APLi/MeLi] and [3APLi/*n*-BuLi], and free oligomers [*n*-BuLi]$_n$ and [MeLi]$_n$

Scheme 7 Edge-to-edge aggregation (then dissociation) of a 1:1 [3AP^{6}Li/Me^{6}Li] mixed aggregate and [^{7}LiCl]$_2$ proposed on the basis of Car–Parrinello molecular dynamic computations [111]

provide alcohol **5** almost exclusively at the beginning. The proportion of **5** with respect to **4** would then decrease with time, as **A** would become the predominant species. If this analysis were right, starting from [3APLi/MeLi] dimer should give directly the more stable triptych **A** and thus 100% alcohol **4** should be recovered for short aging time. However, Table 2 indicates that only 75% **4** is formed. We think that this difference can be assigned to the fact that the **4/5** ratio does not only reflect the **A/B** proportion but it also incorporates the differential between the kinetics of the reaction of each triptych toward the aldehyde. In other words, if **B** reacts faster than **A**, one can reasonably expect that **5** forms quicker than **4**, misrepresenting the theoretical **4/5 = A/B** equation.

Note that we have no clue about the structure of triptychs **A** and **B**. One can however suppose that a ladder-type organization, in which the supplementary alkyllithium would dock antiparallel to its congener (as presented on Scheme 6), offers a reasonable option. In this perspective, we reexamined the NMR spectra

Scheme 8 Formation of a
putative {[3APLi/AlkLi]/
[AlkLi]n} complex
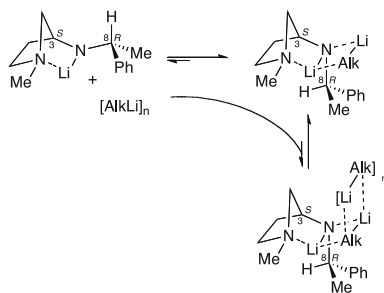
registered when mixing the amide with two different alkyllithiums (mixture **3′** +
MeLi + *n*-BuLi studied previously). If the EXSY experiments highlighted lithium
exchanges between the well-identified 1:1 dimers in the above mixture, the NMR
spectra displayed neither additional peaks assignable to the **A** and/or **B** triptych
complexes nor correlation on the NOESY or HOESY two-dimensional spectra
related to an interaction between the mixed aggregates and the "free" alkyllithiums.
Of course, the coexistence of all the species and their aggregates leads to untangled
signals and the presence of minor species such as **A** or **B** could easily be
overlooked.

At this stage, two additional series of works could be launched to buttress the
above hypotheses. First, complementary NMR experiments involving partners with
significantly different affinities for the 3APLi could be run such that a "stable"
dimer would form and undergo a dead-end interaction with the external partner,
increasing the concentration of only one triptych that could become observable.
If we consider that placing the smaller alkyllithium (MeLi) in close contact to the
3APLi leads to the most stable triptych, one can imagine that the above experiments
could be undertaken using MeLi and a bulkier complementary alkyllithium such as
i-PrLi, *s*-BuLi, or even *t*-BuLi. Second, a computational approach to the formation
of the triptych complexes could be launched. This endeavor is very likely to be
tedious since it will require taking into account a system including two entities of
which both aggregation and solvation levels are uncertain and expected to change
along the interaction.

To end up with, let us mention that the above hypothesis is not in contradiction
with our previous analyses on the origin of the enantioselectivity based on model
1:1 mixtures between 3APLi and an alkyllithium. In all our previous papers, we
always reminded the reader that the Curtin–Hammett principle forbids relating the
species observed in solution to the reacting ones. Actually, the triptych systems
we describe here may have also been at work in our previous investigations, albeit
we were not able to detect them. Even when equimolar amounts of 3APLi and
AlkLi were employed, the equilibrium between the observable dimeric [3APLi/
AlkLi] aggregate and its 3APLi plus AlkLi components can explain that some free
AlkLi in the medium will combine with [3APLi/AlkLi] and afford minute amounts
of a reactive {[3APLi/AlkLi]/[AlkLi]$_n$} trimeric structure (Scheme 8).

3 Conclusion

This paper condenses the conclusions of two decades of researches dedicated to bimetallic systems organized around N–Li–C–Li cores. In these noncovalent mixed aggregates, a chiral lithium amide plays the unusual role of chiral ligands for standard alkyllithiums, transforming the latter "ordinary" reagents into chiral nucleophiles (and possibly bases, most aspects of this reactivity remaining to be explored). The dimeric 3APLi–AlkLi structures are stable species that have been well characterized by NMR and DFT calculations. The unpublished results we present in the Sect. 2.2 suggest that their intrinsic nucleophilicity is low, while they could exhibit a coordinating potential toward a second alkyllithium unit to form much more reactive (but unstable) triptychs of which elusive structure remains to be determined.

Overall, the natural propensity of organolithium entities to aggregate into supramolecular structures in solution, a phenomenon that is often overlooked as being the cradle of fruitless problems, is also a stimulating source of inspiration, in particular in asymmetric synthesis. The lithiated systems studied here demonstrate that synergetic effects are to be expected from bimetallic organizations, even when they undergo strong dynamic effects.

References

1. Snieckus V (1990) Chem Rev 90:879–933
2. Williard PG (1991) Carbanions of alkali and alkaline earth cations: synthesis and structural characterization. In: Trost BM, Fleming I (eds) Comprehensive organic synthesis, vol 1. Pergamon, London, pp 1–47
3. Lucht BL, Collum DB (1999) Acc Chem Res 32:1035–1042
4. Clayden J (2002) Organolithiums: selectivity for synthesis. In: Baldwin JE, Williams RM (eds) Tetrahedron organic chemistry series, vol 23. Pergamon, Oxford, pp 1–377
5. Hodgson D (2003) Organolithiums in enantioselective synthesis. In: Brown J-M, Dixneuf P, Fürstner A, Hegedus LS, Hofmann P, Knochel P, Murai S, Reetz M, van Koten G (eds) Topics in organometallic chemistry, vol 5. Springer, New York, pp 1–324
6. Rappoport Z, Marek I (2004) The chemistry of organolithium compounds. In: Pataï series: the chemistry of functional groups. Wiley, pp 1–1363
7. Wu G, Huang M (2006) Chem Rev 106:2596–2616
8. Rappoport Z, Marek I (2006) The chemistry of organolithium compounds. In: Pataï series: the chemistry of functional groups. Wiley, pp 1–750
9. Collum DB, McNeil AJ, Ramirez A (2007) Angew Chem Int Ed 46:3002–3017
10. Luderer MR, Bailey WF, Luderer MR, Fair JD, Dancer RJ, Sommer MB (2009) Tetrahedron Asymmetry 20:981–998
11. Hoepker AC, Collum DB (2011) J Org Chem 76:7985–7993
12. Fyfe AA, Kennedy AR, Klett J, Mulvey RE (2011) Angew Chem Int Ed 50:7776–7780
13. Kolonko KJ, Wherritt DJ, Reich HJ (2011) J Am Chem Soc 133:16774–16777
14. Reich HJ (2012) J Org Chem 77:5471–5491
15. Su C, Hopson R, Williard PG (2013) J Am Chem Soc 135:12400–12406
16. Su C, Hopson R, Williard PG (2013) Eur J Inorg Chem 4136–4141

17. Su C, Hopson R, Williard PG (2013) J Org Chem 78:7288–7292
18. Su C, Hopson R, Williard PG (2013) J Am Chem Soc 135:14367–14379
19. Reich HJ (2013) Chem Rev 113:7130–7178
20. Harrison-Marchand A, Mongin F (2013) Chem Rev 113:7470–7562
21. Mongin F, Harrison-Marchand A (2013) Chem Rev 113:7563–7727
22. Mulvey RE, Robertson SD (2013) Angew Chem Int Ed 52:11470–11487
23. Gallagher DJ, Kerrick ST, Beak P (1992) J Am Chem Soc 114:5872–5873
24. Strohmann C, Seibel T, Strohfeldt K (2003) Angew Chem Int Ed 42:4531–4533
25. Strohmann C, Strohfeldt K, Schildbach D (2003) J Am Chem Soc 125:13672–13673
26. Strohmann C, Strohfeldt K, Schildbach D, McGrath MJ, O'Brien P (2004) Organometallics 23:5389–5391
27. Carbone G, O'Brien P, Hilmersson G (2010) J Am Chem Soc 132:15445–15450
28. Nozaki H, Aratani T, Toraya T (1968) Tetrahedron Lett 9:4097–4098
29. Nozaki H, Aratani T, Toraya T, Noyori R (1971) Tetrahedron 27:905–913
30. Seebach D, Kalinowski H-O, Bastani B, Crass G, Daum H, Dörr H, DuPreez NP, Ehrig V, Langer W, Nüssler C, Oei H-A, Schmidt M (1977) Helv Chim Acta 60:301–325
31. Seebach D, Crass G, Wilka E-M, Hilvert D, Brunner E (1979) Helv Chim Acta 62:2695–2698
32. Seebach D, Langer W (1979) Helv Chim Acta 62:1701–1709
33. Langer W, Seebach D (1979) Helv Chim Acta 62:1710–1722
34. Whitesell JK, Jaw B-R (1981) J Org Chem 46:2798–2799
35. Mazaleyrat J-P, Cram DJ (1981) J Am Chem Soc 103:4585–4586
36. Mukaiyama T, Soai K, Kobayashi S (1978) Chem Lett 219–222
37. Soai K, Mukaiyama T (1978) Chem Lett 491–492
38. Mukaiyama T, Soai K, Sato T, Shimizu H, Suzuki K (1979) J Am Chem Soc 101:1455–1460
39. Soai K, Mukaiyama T (1979) Bull Chem Soc Jpn 52:3371–3376
40. Mukaiyama T (1981) Tetrahedron 37:4111–4119
41. Colombo L, Gennari C, Poli G, Scolastico C (1982) Tetrahedron 38:2725–2727
42. Alberts AH, Wynberg H (1989) J Am Chem Soc 111:7265–7266
43. Ye M, Logaraj S, Jackman LM, Hillegass K, Hirsh KA, Bollinger AM, Grosz AL, Mani V (1994) Tetrahedron 50:6109–6116
44. Carlier PR, Lam WW-F, Wan NC, Williams ID (1998) Angew Chem Int Ed 37:2252–2254
45. Knollmüller M, Ferencic M, Gärtner P (1999) Tetrahedron Asymmetry 10:3969–3975
46. Schön M, Naef R (1999) Tetrahedron Asymmetry 10:169–176
47. Goldfuss B, Khan SI, Houk KN (1999) Organometallics 18:2927–2929
48. Goldfuss B, Steigelmann M, Rominger F (2000) Angew Chem Int Ed 39:4133–4136
49. Goldfuss B, Steigelmann M, Rominger F, Urtel H (2001) Chemistry 7:4456–4464
50. Sun X, Winemiller MD, Xiang B, Collum DB (2001) J Am Chem Soc 123:8039–8046
51. Eleveld MB, Hogeveen H (1984) Tetrahedron Lett 25:5187–5190
52. Muraoka M, Kawasaki H, Koga K (1988) Tetrahedron Lett 29:337–338
53. Hilmersson G, Davidsson Ö (1995) Organometallics 14:912–918
54. Hilmersson G, Davidsson Ö (1995) J Organomet Chem 489:175–179
55. Hilmersson G, Arvidsson PI, Davidsson Ö, Håkansson M (1997) Organometallics 16:3352–3362
56. Hilmersson G, Arvidsson PI, Davidsson Ö, Håkansson M (1998) J Am Chem Soc 120:8143–8149
57. Arvidsson PI, Davidsson Ö, Hilmersson G (1999) Tetrahedron Asymmetry 10:527–534
58. Arvidsson PI, Hilmersson G, Ahlberg P (1999) J Am Chem Soc 121:1883–1887
59. Arvidsson PI, Ahlberg P, Hilmersson G (1999) Chemistry 5:1348–1354
60. Arvidsson PI, Hilmersson G, Davidsson Ö (1999) Chemistry 5:2348–2355
61. Hilmersson G (2000) Chemistry 6:3069–3075
62. Hilmersson G, Malmros B (2001) Chemistry 7:337–341
63. Johansson A, Hilmersson G, Davidsson Ö (2002) Organometallics 21:2283–2292
64. Sott R, Granander J, Hilmersson G (2002) Chemistry 8:2081–2087
65. Granander J, Sott R, Hilmersson G (2002) Tetrahedron 58:4717–4725
66. Granander J, Sott R, Hilmersson G (2003) Tetrahedron Asymmetry 14:439–447

67. Sott R, Granander J, Dinér P, Hilmersson G (2004) Tetrahedron Asymmetry 15:267–274
68. Granander J, Sott R, Hilmersson G (2006) Chemistry 12:4191–4197
69. Sott R, Håkansson M, Hilmersson G (2006) Organometallics 25:6047–6053
70. Granander J, Eriksson J, Hilmersson G (2006) Tetrahedron Asymmetry 17:2021–2027
71. Rönnholm P, Södergren M, Himersson G (2007) Org Lett 9:3781–3783
72. Tomioka K, Inoue I, Shindo M, Koga K (1990) Tetrahedron Lett 31:6681–6684
73. Tomioka K, Inoue I, Shindo M, Koga K (1991) Tetrahedron Lett 32:3095–3098
74. Itsuno S, Yanaka H, Hachisuka C, Ito K (1991) J Chem Soc Perkin Trans 1 1341–1342
75. Inoue I, Shindo M, Koga K, Tomioka K (1993) Tetrahedron Asymmetry 4:1603–1606
76. Inoue I, Shindo M, Koga K, Tomioka K (1994) Tetrahedron 50:4429–4438
77. Inoue I, Shindo M, Koga K, Kanai M, Tomioka K (1995) Tetrahedron Asymmetry 6:2527–2533
78. Itsuno S, Sasaki M, Kuroda S, Ito K (1995) Tetrahedron Asymmetry 6:1507–1510
79. Gittins CA, North M (1997) Tetrahedron Asymmetry 8:3789–3799
80. Taniyama D, Kanai M, Iida A, Tomioka K (1997) Heterocycles 46:165–168
81. Jones CA, Jones IG, Mulla M, North M, Sartori L (1997) J Chem Soc Perkin Trans 1 2891–2896
82. Bloch R (1998) Chem Rev 98:1407–1438
83. Andersson PG, Johansson F, Tanner D (1998) Tetrahedron 54:11549–11566
84. Shindo M, Koga K, Tomioka K (1998) J Org Chem 63:9351–9357
85. Taniyama D, Hasegawa M, Tomioka K (1999) Tetrahedron Asymmetry 10:221–223
86. Brózda D, Chrzanowska M, Gluszynska A, Rozwadowska MD (1999) Tetrahedron Asymmetry 10:4791–4796
87. Taniyama D, Hasegawa M, Tomioka K (2000) Tetrahedron Lett 41:5533–5536
88. Hasegawa M, Taniyama D, Tomioka K (2000) Tetrahedron 56:10153–10158
89. Arrasate S, Lete E, Sotomayor N (2001) Tetrahedron Asymmetry 12:2077–2082
90. Derdau V, Snieckus V (2001) J Org Chem 66:1992–1998
91. Chrzanowska M (2002) Tetrahedron Asymmetry 13:2497–2500
92. Risberg E, Sommai P (2002) Tetrahedron Asymmetry 13:1957–1959
93. Wu GG, Huang M (2004) Top Organomet Chem 6:1–35
94. Cabello N, Kizirian J-C, Gille S, Alexakis A, Bernardinelli G, Pinchard L, Caille J-C (2005) Eur J Org Chem 4835–4842
95. Denmark SE, Nakajima N, Stiff CM, Nicaise OJ-C, Kranz M (2008) Adv Synth Catal 350:1023–1045
96. Corruble A, Valnot J-Y, Maddaluno J, Duhamel P (1997) Tetrahedron Asymmetry 8:1519–1523
97. Fressigné C, Corruble A, Valnot J-Y, Maddaluno J, Giessner-Prettre C (1997) J Organomet Chem 549:81–88
98. Prigent Y, Corruble A, Valnot J-Y, Maddaluno J, Duhamel P, Davoust D (1998) J Chim Phys 95:401–405
99. Corruble A, Valnot J-Y, Maddaluno J, Prigent Y, Davoust D, Duhamel P (1997) J Am Chem Soc 119:10042–10048
100. Corruble A, Valnot J-Y, Maddaluno J, Duhamel P (1998) J Org Chem 63:8266–8275
101. Fressigné C, Maddaluno J, Marquez A, Giessner-Prettre C (2000) J Org Chem 65:8899–8907
102. Flinois K, Yuan Y, Bastide C, Harrison-Marchand A, Maddaluno J (2002) Tetrahedron 58:4707–4716
103. Corruble A, Davoust D, Desjardins S, Fressigné C, Giessner-Prettre C, Harrison-Marchand A, Houte H, Lasne M-C, Maddaluno J, Oulyadi H, Valnot J-Y (2002) J Am Chem Soc 124:15267–15279
104. Yuan Y, Desjardins S, Harrison-Marchand A, Oulyadi H, Fressigné C, Giessner-Prettre C, Maddaluno J (2005) Tetrahedron 61:3325–3334
105. Yuan Y, Harrison-Marchand A, Maddaluno J (2005) Synlett 1555–1558
106. Harrison-Marchand A, Valnot J-Y, Corruble A, Duguet N, Oulyadi H, Desjardins S, Fressigné C, Maddaluno J (2006) Pure Appl Chem 78:321–331
107. Duguet N, Harrison-Marchand A, Maddaluno J, Tomioka K (2006) Org Lett 8:5745–5748

108. Paté F, Duguet N, Oulyadi H, Harrison-Marchand A, Fressigné C, Valnot J-Y, Lasne M-C, Maddaluno J (2007) J Org Chem 72:6982–6991
109. Duguet N, Petit SM, Marchand P, Harrison-Marchand A, Maddaluno J (2008) J Org Chem 73:5397–5409
110. Paté F, Oulyadi H, Harrison-Marchand A, Maddaluno J (2008) Organometallics 27:3564–3569
111. Paté F, Gérard H, Oulyadi H, de la Lande A, Harrison-Marchand A, Parisel O, Maddaluno J (2009) Chem Commun 319–321
112. Lecachey B, Duguet N, Oulyadi H, Fressigné C, Harrison-Marchand A, Yamamoto Y, Tomioka K, Maddaluno J (2009) Org Lett 11:1907–1910
113. Lecachey B, Fressigné C, Oulyadi H, Harrison-Marchand A, Maddaluno J (2011) Chem Commun 47:9915–9917
114. Oulyadi H, Fressigné C, Yuan Y, Maddaluno J, Harrison-Marchand A (2012) Organometallics 31:4801–4809
115. Harrison-Marchand A, Gérard H, Maddaluno J (2012) New J Chem 36:2441–2446
116. Dejaegher Y, Mangelinckx S, De Kimpe N (2002) Synlett 113–115
117. Houghton PG, Humphrey GR, Kennedy DJ, Roberts DC, Wright SHB (1993) J Chem Soc Perkin Trans 1 1421–1424
118. McGarrity JF, Ogle CA (1985) J Am Chem Soc 107:1805–1810
119. McGarrity JF, Ogle CA, Brich Z, Loosli H-R (1985) J Am Chem Soc 107:1810–1815
120. Yanagisawa A, Kikuchi T, Yamamoto H (1998) Synlett 174–176
121. Asensio G, Aleman PA, Gil J, Domingo LR, Medio-Simón M (1998) J Org Chem 63:9342–9347
122. Duhamel L, Duhamel P, Plaquevent J-C (2004) Tetrahedron Asymmetry 15:3653–3691
123. Bunn BJ, Simpkins NS (1993) J Org Chem 58:533–534
124. Toriyama M, Sugasawa K, Shindo M, Tokutake N, Koga K (1997) Tetrahedron Lett 38:567–570
125. O'Brien P (1998) J Chem Soc Perkin Trans 1 1439–1457
126. Simoni D, Roberti M, Rondanin R, Kozikowski AP (1999) Tetrahedron Lett 40:4425–4428
127. Laumer JM, Kim DD, Beak P (2002) J Org Chem 67:6797–6804
128. Butler B, Schultz T, Simpkins NS (2006) Chem Commun 3634–3636
129. Simpkins NS, Weller MD (2010) Top Stereochem 26:1–52
130. Lecachey B, Oulyadi H, Lameiras P, Harrison-Marchand A, Gérard H, Maddaluno J (2010) J Org Chem 75:5976–5983
131. Lehn J-M (1999) Chemistry 5:2455–2463
132. Tanner D, Harden A, Johansson F, Wyatt P, Andersson PG (1996) Acta Chem Scand 50:361–368

Stable Geminal Dianions as Precursors for Gem-Diorganometallic and Carbene Complexes

Marie Fustier-Boutignon and Nicolas Mézailles

Abstract In this chapter, recent advances in the use of stable gem-dilithio compounds for the synthesis of carbene complexes or bimetallic complexes of groups 1–4, lanthanides, actinides and groups 13–14 are presented. This chemistry is based on the precise understanding of the factors that govern the stabilization of the gem-dilithio species. It is particularly noticeable that at least one high valent phosphorus moiety is needed to isolate the desired precursor in high yield and purity. For each family of complexes, the question of the nature of the metal–ligand interaction is addressed as well as their general reactivity.

Keywords Carbene complexes · Gem-diorganometallic complexes · Geminal dianions · Hypervalent phosphorus

Contents

M. Fustier-Boutignon
Institute of Inorganic Chemistry, Karlsruhe Institute of Technology, Engesserstr.15,
76131 Karlsruhe, Germany

N. Mézailles (✉)
Université de Toulouse, UPS, CNRS, LHFA UMR 5069, 118 route de Narbonne,
31062 Toulouse, France
e-mail: mezailles@chimie.ups-tlse.fr

1   Introduction

Gem-dimetallic compounds, prepared by successive metalation of derivatives containing two acidic protons, possess great synthetic potential. Indeed, the two M–C bonds might react selectively in successive fashion and most desirably in a synergistic way. The simplest derivative of all, CH_2Li_2, was synthesized by Wittig, West, and Ziegler in pioneering works some 70 years ago [1–3]. However, this compound showed poor solubility and stability in inert solvents, consistent with oligomeric or even polymeric arrangement in the solid state. Computational studies were thus of great importance to probe the geometry at the carbon center, revealing only a slight preference (8 kcal/mol) for the tetrahedral vs. the planar geometry, for the monomeric CH_2Li_2 species [4, 5]. Modification of the substituents at the carbon was predicted to even lower this difference, and the related tBuCHLi$_2$ and TMSCHLi$_2$ species have been prepared, but their structure is still unknown [6, 7]. The only X-ray structure data of an α,α-dilithiated hydrocarbon, 9,9-dilithiofluorene **1**Li$_2$, was reported in 2002 [8]. This species was obtained by the dismutation of lithiofluorene in THF/benzene medium. The key questions in the use of geminal dianionic species are: (1) how to generate them efficiently, devoid of reactive by-products and (2) the true nature of the species.

The first point is classically linked to the acidities of the two H atoms to be deprotonated. In order both to increase the acidity and to stabilize the resulting
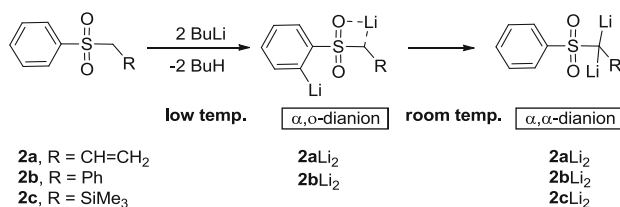
Scheme 1 Nature of the di-lithiated species in phenyl sulfone derivatives

anion, strongly electron-withdrawing substituents have been used. In this respect, the case of sulfone derivatives, developed in 1988 by Gais et al., is particularly informative [9]. Indeed, they showed that the nature of the species in solution depended on the temperature of the reaction as well as on the second substituent at C (Scheme 1).

For derivatives **2a** and **2b**, an α,o-dilithiated species was formed at low temperature, and only at room temperature was the expected α,α-dilithiated species isolated. On the other hand, only the α,α-dianion was formed from **2c**. Among other experimental conditions, the nature of the base was studied in detail and proved crucial. It was, for example, shown that the deprotonation of $PhCH_2CN$ with excess of lithium hexamethyldisilazide (LHDMS) did not lead to the formation of the dianion but rather of a heterodimer [10]. The heterodimer evolved to the desired dianion only when the more basic *n*-BuLi was used [11]. Nevertheless, a mixture of heterodimer and dianion was still observed with 2.2 equiv. of *n*-BuLi, and only when 2.7 equiv. of *n*-BuLi was used was the dianion formed quantitatively. Alkylation and deuteration studies on the dianions generated from $PhCH_2CN$ with variable amounts of *n*-Buli (2.0–2.7 equiv.) have been recently performed [12]. Interestingly, they showed that the yield of di-alkylation falls when an excess of BuLi is used, indicating the formation of other species. These results highlight both the difficulty and necessity to generate the gem-dimetallic species in the absence of any other by-product for further efficient use. This is achieved in two cases. Either the substituents at C allow for a quantitative double deprotonation under strict stoichiometric conditions, or the gem-dimetallic species can be separated from excess of base, typically by crystallization or precipitation. The paucity of X-ray structures of geminal dianions is a proof of the high sensitivity of these species, and thus, the first case is far from being general.

This review is mainly dedicated to derivatives containing at least one P(V) substituent at the α position to the carbon. It will be seen that, by addition of another strongly stabilizing moiety, P(V) or else, efficient generation of geminal dianion is achieved in a stoichiometric fashion. From these dianions, a very rich chemistry has been developed over the past 15 years, mainly directed toward the synthesis of metal complexes. Depending on the metal fragment of the type $[(L)_n(X)_yM(Hal)_2]$ used (route A, Scheme 2), either the carbene complex, featuring a formal M=C double bond, or the bimetallic complex, featuring two M–C single bonds, was obtained.

Alternatively, the same or related complexes may be obtained directly from the neutral species and the appropriate metal precursor, bearing two strongly basic
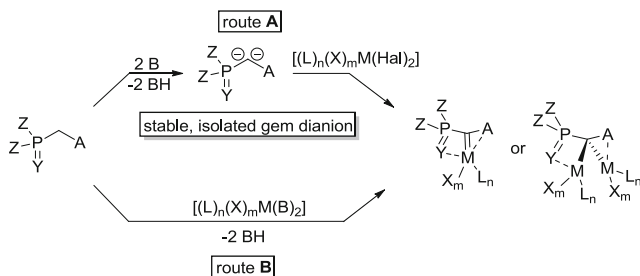
Scheme 2 Major synthetic routes to gem-diorganometallic and carbene complexes

ligands (route B, Scheme 2). This strategy is however limited to early transition metals and lanthanides and actinides, or group 13 and 14 metals. In this review, we are mainly interested with the reactivity of stable, isolated, structurally character-ized gem-dianions, thus following "route A," Scheme 2, as well as the reactivity of "route B" when it leads to bimetallic complexes. However, for the sake of com-pleteness, results dealing with the synthesis of carbene complexes following "route B" are also presented. The review is organized according to the group of the metal center(s) bound to the carbon atom.

2 Group 1: Alkali Metal Dianions

2.1 Synthesis

As mentioned above, the first example of an X-ray structure of a gem-dilithio derivative was obtained by Gais et al. in 1988 [9], with a sulfone derivative (Chart 1). The structure of the sparingly soluble $(SiMe_3)CLi_2SO_2Ph \cdot Li_2O \cdot (THF)_6$ **2c**Li_2 was obtained in the presence of Li_2O. In the absence of Li_2O, other crystals were obtained but the structure was not reported. However, this latter species was soluble in THF, and a beautiful NMR study, with ^{13}C- and ^6Li-labeled derivatives, was performed. Low temperature and 2D spectra allowed for a proposal of arrangements of aggregates of gem-dilithio species in solution. Shortly after, Boche et al. reported the double deprotonation of trimethylsilylacetonitrile with an excess of n-BuLi in hexane/ Et_2O mixture at $-78°C$ [13]. The dianionic species **3**Li_2 crystallized from solution as a dodecamer $[Li_2(SiMe_3CCN)_{12}(Et_2O)_6(C_6H_{14})]$, but the yield of the crystallized prod-uct was not given. In direct relation with the sulfone derivatives mentioned above, Müller et al. developed the first chiral substituted dilithiomethane derivative: the sulfoximine compound **4**Li_2 [14]. This dianion was obtained using an excess of n-BuLi (2.5 equiv.) together with a sub-stoichiometric amount of water, added to generate in situ Li_2O, crucial for the crystallization. In this derivative, bearing two Li–C bonds, the two Li atoms are diastereotopic, and the selective replacement of one Li atom should lead to the formation of a novel stereogenic C center. This could have
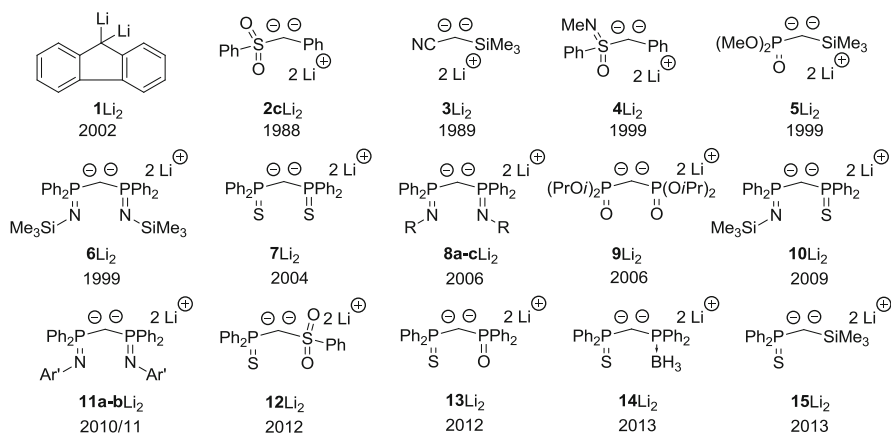
1Li$_2$ 2002 **2cLi$_2$** 1988 **3Li$_2$** 1989 **4Li$_2$** 1999 **5Li$_2$** 1999

6Li$_2$ 1999 **7Li$_2$** 2004 **8a–cLi$_2$** 2006 **9Li$_2$** 2006 **10Li$_2$** 2009

11a–bLi$_2$ 2010/11 **12Li$_2$** 2012 **13Li$_2$** 2012 **14Li$_2$** 2013 **15Li$_2$** 2013

Chart 1 Gem-dilithio compounds for which X-ray structures are known

interesting developments in organic synthesis, but unfortunately, the low yield of the crystallized gem-dianion (17%) has probably hampered the use of this chiral species. The same group has reported the same year the successful synthesis of the mixed phosphonate/trimethylsilyl derivative **5Li$_2$** [15]. The reaction was carried out in TMEDA which appeared important for several reasons. Indeed, in this case too an excess of base (2.5 equiv. of *n*-BuLi) had to be used to favor both the deprotonation and partial decomposition of TMEDA into a dimethylamido fragment. Both the dimethylamido and TMEDA were incorporated in the crystal. Although the yield of the crystallized dianion would have allowed further use (67%), it is reported to decompose after 24 h of storage.

Also in 1999, dianion **6Li$_2$** was synthesized independently by Cavell et al. [16] and Stephan et al. [17]. Most importantly, this species was obtained as the sole product under stoichiometric conditions (either 2 equiv. of MeLi or PhLi in toluene or benzene) and crystallized in more than 60% yield. The generation of this dianion devoid of additional base truly started a new field of investigation, namely the synthesis of metal carbene complexes using geminal dianions as precursors, as will be seen below. It occurred to us that unlike the other examples, neutral compound **6H$_2$** incorporated not one but two strongly electron-withdrawing substituents, and we then postulated that with two P(V) moieties at C, other examples of geminal dianions would be accessible in stoichiometric conditions. Thus, in 2004, we reported the quantitative synthesis and use of dianion **7Li$_2$** [18], which was crystallized in 2006 [19]. The good solubility of this compound allowed a ^{31}P NMR spectrometry monitoring that revealed that it was the single P containing species obtained from the reaction between **7H$_2$** and 2 equiv. of MeLi in toluene or diethyl ether within few hours. This clean reaction allowed its use without further purification. In 2006 also, we reported the novel dianions **8a–cLi$_2$** (**a–c**, R=*i*Pr, Ph, and (S)-MeCH(*i*-Pr), respectively) and **9Li$_2$** obtained, respectively, from bis-iminophosphorane and bisphosphonate derivatives [20]. The isolated yields of these species range from
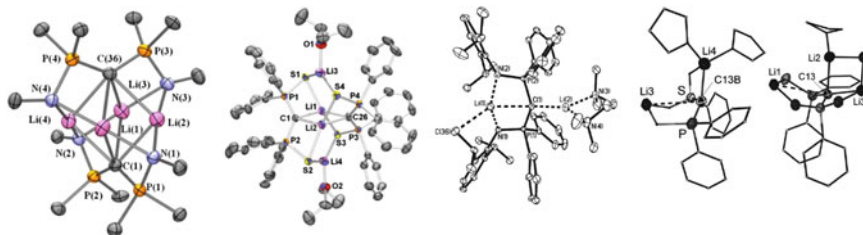
Fig. 1 X-ray structures of Li dianions **8c**Li$_2$, **7**Li$_2$, **11b**Li$_2$, and **12**Li$_2$

70 to 93%. Quite surprisingly, the kinetics of the second deprotonation proceeded in tremendously different fashions between bis-PS, bis-PN, and bis-PO derivatives. Indeed, if **7**Li$_2$ is obtained at room temperature within hours, compounds **6**Li$_2$ and **8**Li$_2$ are obtained in ca. 1 day, and **9**Li$_2$ in 10 days (3 days when TMEDA was added), and there seems to be no direct link between the electron-withdrawing capacity of the C substituent (thermodynamic effect) and the kinetics of double deprotonation. At this point in time, three classes of symmetrical gem-dilithio derivatives were thus accessible. Two directions were then taken by different groups. Firstly, the development of unsymmetrical dianions featuring at least one P(V) moiety was pursued, with the aim of being able to finely tune the electronic properties at C. In 2009, So et al. developed the first example of unsymmetrical bis-P(V)-stabilized gem-dianion, **10**Li$_2$ featuring P=S and P=N moieties [21], followed in 2012 by the group of Gessner (**12**Li$_2$, mixed P=S and sulfone) [22] and our own (**13**Li$_2$, mixed P=S and P=O, and **14**Li$_2$, mixed P=S and P-BH$_3$) [23, 24]. Finally, although we were able to crystallize compound **15**Li$_2$ recently [24], the stoichiometric reaction led to a mixture of compounds, which will likely preclude further use. The second goal was linked to the early theoretical prediction that planar arrangement at a CLi$_2$ fragment could be envisaged. In this sense, the X-ray structures of **6**Li$_2$ and **8a**Li$_2$ were important. They are unsolvated dimers of the dianionic species, and the coordination sphere of the Li cations is completed by the iminophosphorane moieties. The group of Liddle then modulated the steric bulk at the N atom to disfavor dimerization. Compound **11a**Li$_2$, featuring a mesityl (Ar$'$ = Mes = 2,4,6 trimethyl-Ph) group on the N, was synthesized but this compound was still dimeric [25]. In 2010, their strategy met success with the more bulky Dipp (Ar$'$ = Dipp = 2,6-diisopropyl-Ph) group [26]. Indeed, **11b**Li was obtained by deprotonation of **11b**H$_2$ with 2 equiv. of t-BuLi in the presence of 1 equiv. of TMEDA. Interestingly and quite surprisingly, the presence of TMEDA was required for the second deprotonation to be effected; otherwise, only the monoanion **11b**Li was observed. The X-ray structure (Fig. 1) showed the dianion to crystallize as a monomer and presents the unprecedented distorted *trans*-planar geometry at C. The authors ascribed this geometry to the close fit of the Li(TMEDA) unit into the pocket formed by the four P-Ph rings, as confirmed by the space filling model obtained from DFT calculation [26]. The planar vs. tetrahedral geometry at carbon was also probed recently with the mixed thiophosphinoyl/sulfone derivative **12** [27]. In fact, the crystal structure of **12**Li$_2$
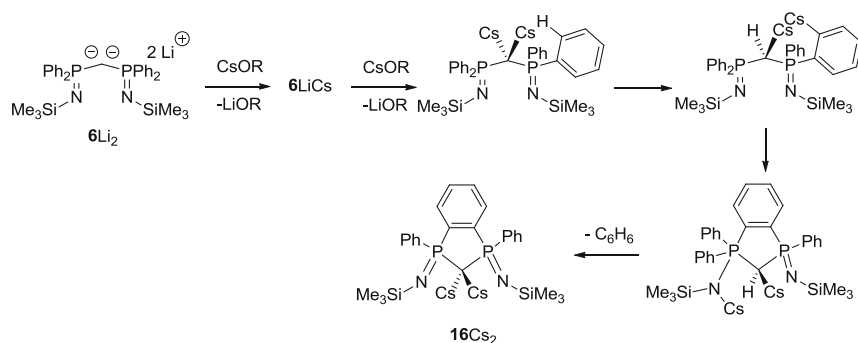
Scheme 3 Gem-dicesium synthesis from gem-dilithio derivative **6**Li$_2$

consisted of four methanediide and six THF molecules. Two different geometries were found for methanediide carbon atoms and differed strongly from the ideal tetrahedral (see Fig. 1).

Heavier analogues of gem-dilithio derivatives have been studied to a much lesser extent. In fact, such studies have been performed only with the bis-iminophosphorane derivative **6**H$_2$. The formal replacement of Li cations by heavier analogues appeared quite complex. Henderson et al. reported the synthesis of **6**Na$_2$ using the very strong base *n*-BuNa and the mixed derivative **6**LiNa in 2006 using sequential deprotonations [28]. In 2008, the same group reported a thorough study (solid state, solution behavior, mass spectrometry) on mixed species **6**LiK, **6**NaK, and **6**Na$_{3/2}$ K$_{1/2}$ which were obtained using different strategies, among which is cation exchange using the corresponding heavier analogue alkoxide [29]. They also performed calculations to determine the relative energies of the homo- and heterometallic complexes. Shortly thereafter, Harder et al. performed calculations to evaluate the efficiency of the reaction between the dilithio derivative and an M-alkoxide species [30]. They could show that although the first exchange is favorable for any element (M=Na, K, Rb, Cs), the second Li cation is not readily displaced (except for Na for which the second displacement is nearly thermodynamically neutral). They therefore devised the method using the benzyl-M (M=K, Rb, Cs), which is less reactive than the alkyl metal reagent but enough to successfully achieve the double deprotonation. The highly reactive **6**K$_2$ and **6**Rb$_2$ were thus isolated and crystallized, and **6**Cs$_2$ was synthesized but could not be structurally characterized. In the case of the larger cation Cs, an interesting, unforeseen, alternative path was discovered for the Li/Cs exchange. A rearranged geminal dianion **16**Cs$_2$ was isolated and crystallized, and a mechanism proposed (Scheme 3).

The mechanism of this transformation is interesting in the sense that it does point a competitive path to the desired deprotonation reaction, the nucleophilic substitution at the high-valent P center, promoted by an α,o-dianion.

In conclusion, although the two first structures of gem-dilithio derivatives were reported some 25 years ago, the main developments started in 1999. It is now apparent from the known examples that two strongly stabilizing substituents have

to be borne by the C atom in order to allow for a quantitative double deprotonation. Moreover, the presence of NMR probes (^{31}P, ^{6}Li) is a great asset for careful optimizations (nature of base, solvent) of the experimental conditions for the "quantitative" synthesis of the desired gem-dianion.

2.2 Electronic Structure of the Gem-Dianions

It is important here to discuss the electronic nature of these dianions for several reasons. Firstly, it is interesting to quantify the "stabilizing" power of the respective substituents at C. Secondly, since the gem-dianions are used in the synthesis of several complexes and in particular carbene complexes, the extent of electron transfer from the C atom to the M center in the complexes presented below is of interest. Therefore, an initial description of the electronic structure of these species would be a starting point for the understanding of bonding scheme in these complexes. DFT calculations on some of the dilithiated gem-dianions were performed (Table 1) [31]. The NBO analysis was particularly informative. It showed the positive charge at Li greater than 0.82 and Wiberg bond indexes between C–Li and X–Li (X=S, O or N) lower than 0.1, both indicative of an almost pure electrostatic interaction. The NBO analysis also showed single bonds between P–C and P–X bonds (Wiberg bond indexes of 1.13–1.21 for P–C and from 1.01 to 1.16 for P–X). As expected, the NPA charges at C were very (strongly) negative, ranging between −1.51 and −2.01 (Fig. 2). Accordingly, the charges at P too varied to a large extent (from 0.88 to 2.31). These variations are due to the substituents at P (and S in **12**Li$_2$).

It is interesting to note that the Kohn–Sham orbitals describing the two lone pairs at C presented numerous similarities in the five cases. Indeed, in each case, the HOMO described an almost pure p lone pair at C (LP2 in Table 1), whereas the second lone pair was lower in energy. This latter lone pair (LP1) was an sp^{n} hybrid. Overall, these data pointed to a Lewis structure which involved two lone pairs at C strongly stabilized by the low-lying empty orbitals at P [19]. As a consequence, the different groups have all proposed the best Lewis representation of the gem-dilithio derivatives presented as in Chart 2.

2.3 Reactivity of Gem-Dilithio Derivatives

Although heavy analogues of group 1 gem-dianions have been prepared, only the reactivity of gem-dilithio derivatives has been studied. The main focus was paid to the synthesis of metal complexes, as will be shown below in separate sections. In this section, we will only present the use of gem-dilithio derivatives in organic synthesis. The prototypical reactions to characterize the gem-dilithio derivatives are based on the high charge located at the C atom. Accordingly, a proof of the double deprotonation is

Table 1 NBO analysis of gem-dilithio derivatives

Compound (or model of compound)	qC	qP	qX	qLi	qS or qP	qO or qB	nP–C	nP–X	nS–O or nP–B	Lone pair at C: hybridization		References
										LP1	LP2	
6Li$_2$[a]	−1.79	1.18	−1.09	0.82								[31]
7Li$_2$[b]	−1.77	0.91	−0.80	0.82 av.			1.19	1.10		sp$^{2.17}$	p$^{1.00}$	[19]
7Li$_2$[b]	−1.88	0.88	−0.76	0.86			1.13	1.16		sp$^{2.11}$	p$^{1.00}$	[19]
9Li$_2$	−2.01	2.37	−1.23	0.93			1.15	1.03		sp$^{3.74}$	p$^{1.00}$	[19]
11bLi$_2$	−1.60	1.56	−1.14	0.89 av.			1.24	1.01		sp$^{3.21}$	sp$^{70.3}$	[26]
12Li$_2$	−1.51	1.37	−0.79		2.05	−1.07 av.	1.16	1.12	1.03 av.	sp$^{1.99}$	sp$^{99.9}$	[22]
14Li$_2$	−1.76	1.41	−0.8	0.87 av.	1.35	−0.7	1.21 av.	1.12	0.96	sp$^{2.75}$	p$^{1.00}$	[24]

[a]Monomer
[b]Dimer
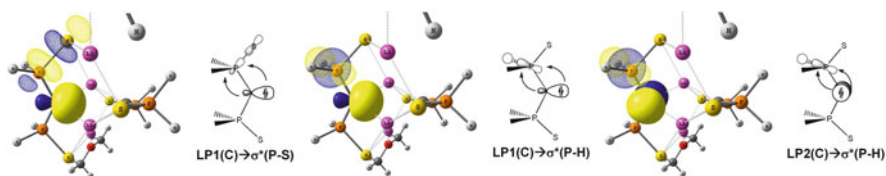
Fig. 2 NBO plots of principal donor–acceptor interactions in **7Li₂** (reproduced from [19])
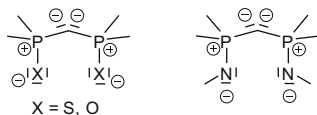
Chart 2 Consensus for the Lewis structure of gem-dilithio derivatives
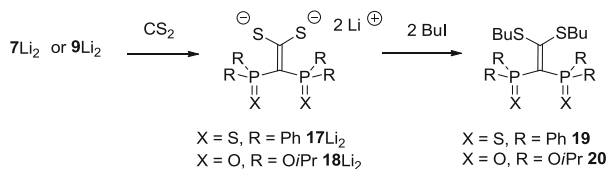
Scheme 4 Reactivity of gem-dilithio derivatives **7Li₂** and **9Li₂** toward CS₂

the deuteration reaction, as is the alkylation with MeI. Interestingly, although a high nucleophilic character could be envisaged, dianion **7Li₂** is reported not to react with benzophenone to yield the expected alkene derivative. The formation of Li_2O as the other product of the reaction appeared to be too poor a driving force. On the other hand, the reaction of **7Li₂** and **9Li₂** with more electrophilic substrates, such as CS₂, is reported to give the expected dianionic alkenes (**17Li₂** and **18Li₂**) which were subsequently trapped to form electron-rich alkenes **19** and **20**, respectively (Scheme 4) [19].

The existence of the intrinsically electron-rich gem-dianions led us to probe the redox properties of **7Li₂**, with an initial goal to generate novel types of stable carbene moieties (Scheme 5). The reaction with the mild oxidizing agent C_2Cl_6 generated instead the room temperature-stable carbenoid species **21** [32]. This compound is the most stable carbenoid species reported to date. A similar reaction with iodine was studied by Chivers et al., leading to a 75/25 mixture of carbenoid **22** and compound **23** [33]. Obviously, the LiI elimination was favored compared to the elimination of LiCl, and the authors proposed the intermediate formation of the free unstable carbene fragment, which dimerized.

Very recently, oxidation of dianion **14Li₂** was performed, allowing the isolation of yet another example of stable carbenoid (up to −30°C), **25** [34] (Scheme 5). The chemistry of carbenoid **21**, expected to be highly electrophilic, has been explored in two different directions. Firstly, it was used as a carbene precursor for the electron-rich
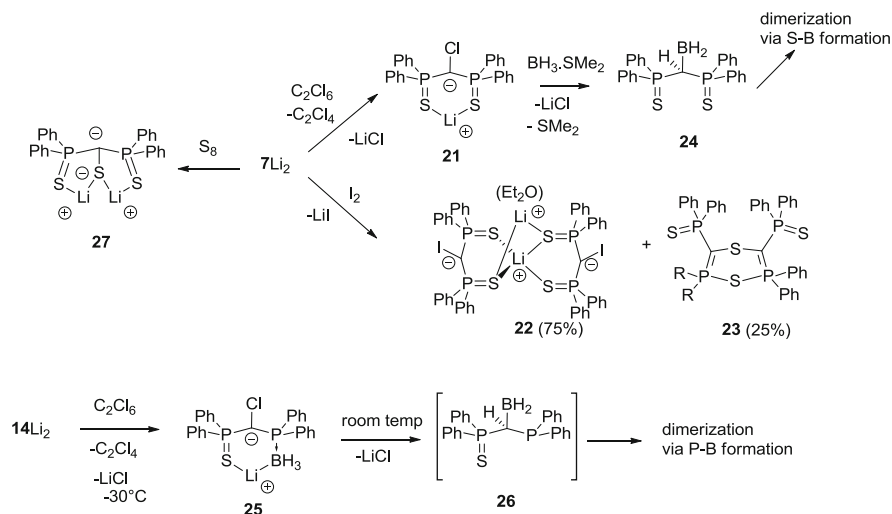
Scheme 5 Synthesis and reactivity of carbenoids from **7**Li$_2$ and **14**Li$_2$

transition metal fragment "Pd(PPh$_3$)" (vide infra) [32]. Secondly, it was shown to react with the strong Lewis acid BH$_3$ acting as a Lewis base via the B–H bond. Formation of compound **24** was observed, prior to its dimerization. A similar intramolecular reactivity was observed from compound **25**, at room temperature, leading to the formation of dimers, via **26**, as corroborated by DFT calculations. It is to be noted here that a related electrophilic carbenoid, although not obtained from the corresponding dianion but rather via a sequence "deprotonation–oxidation with C$_2$Cl$_6$ deprotonation," was shown to react with BH$_3$ to form a lithium borate compound [35].

Finally, oxidation of **7**Li$_2$ by sulfur and selenium was also reported [36]. It led to the formation of yet other dianionic species which have been used in coordination chemistry as a tridentate "SSS^{2-}" and "SSeS^{2-}" ligands.

3 Group 2: Alkaline Earth Metal Dianions

Transition metal carbene complexes, Schrock type (nucleophilic) and Fischer type (electrophilic), involve, at least formally, a metal–carbon double bond. In the bonding scheme, overlap between d orbitals and orbitals at the carbene fragment is preponderant. When the energies of valence orbitals at the metal become very high (i.e., for highly electropositive metals), which is typically the case for group 2 and group 3 metal centers, the following question arises: Would these complexes still be adequately called "carbene complexes," and what would be the nature of the metal–carbon interaction? The results in this domain will be treated in the following sections. It will be seen that subtle changes in the dianionic ligand can either lead to monometallic or bimetallic complexes.
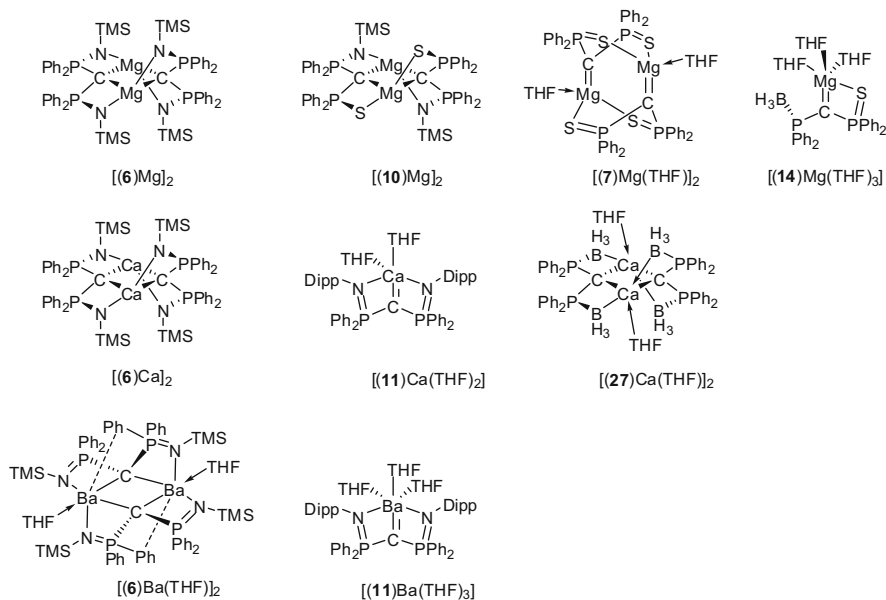
Chart 3 Representation of the different alkaline earth complexes featuring a gem-dianion as a ligand

3.1 Synthesis

A question prior to the one written above is "can a species featuring an alkaline earth (AE) metal–carbon formal double bond be synthesized?" In fact, this is no trivial matter and "AE=CH_2" species are likely polymeric. The first synthesis of such a molecular complex was only realized in 2006. Therefore, examples of structurally characterized alkaline earth metal complexes featuring a hypervalent phosphorus-stabilized geminal dianion as a ligand are scarce enough to be thoroughly reviewed here. While a few examples are found for magnesium [24, 37, 38], calcium [39–41], and even barium [30], there is to date no example of such complexes with strontium or beryllium. The full set of complexes is represented in Chart 3.

Despite the existence of corresponding gem-dilithiated species $6Li_2$, $7Li_2$, $10Li_2$, $11Li_2$, and $14Li_2$, all of the nine complexes presented in Chart 3 were synthesized following route B, i.e., by deprotonation of the neutral ligand in the coordination sphere of the metal which features strongly basic ligands. Harder et al. were the first to follow this route for alkaline earth metals in 2006. They showed that in the case of calcium and the neutral ligand $6H_2$, the use of [Ca(N(TMS)$_2$)$_2$] did not allow a double deprotonation, but rather stopped at the monodeprotonated stage. The more basic p-tert-butylbenzyl ligand was required for a successful twofold deprotonation to yield [(6)Ca]$_2$ [39]. The same route allowed for the synthesis of complex [(27)Ca (THF)]$_2$ [41], featuring a dianionic bis-(phosphinoboranyl)methanediide that has not been isolated as the gem-dilithio derivative to date (Scheme 6).
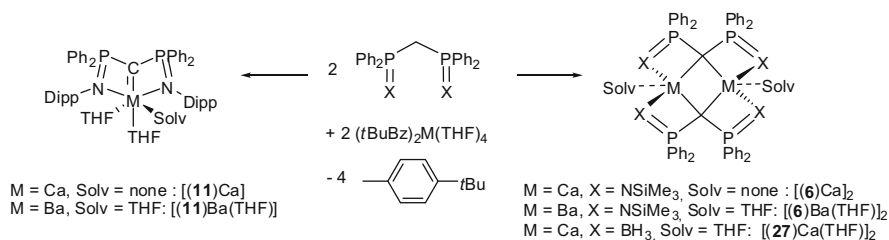
Scheme 6 Synthesis of calcium and barium methanediide complexes
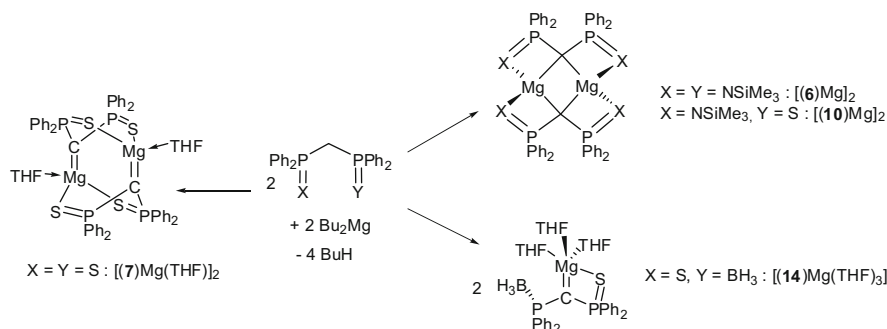
Scheme 7 Synthesis of magnesium methanediide complexes

Two main coordination schemes occur for calcium and barium, depending on the steric bulkiness of the phosphorus substituent [40, 42]. For the less hindered NTMS and BH_3 derivatives (complexes [(**6**)Ca]$_2$ [39], [(**6**)Ba(THF)]$_2$ [42], and [(**27**)Ca(THF)]$_2$ [41]), dimeric structures were obtained with two dianionic carbons bridging two different metallic centers. The difference in the ionic radii of Ca and Ba results in significantly different crystal structures for the dimers. Not only an additional THF molecule is coordinated, but also are Ph···Ba interactions observed. The same authors reported that with the much more bulky substituent 2,6-diisopropylphenyl, monomeric Ca and Ba complexes [(**11**)Ca] [40] and [(**11**)Ba (THF)] were synthesized, as expected [42]. NMR studies in coordinating solvents showed that the dimeric forms [(**6**)Ca]$_2$ and [(**6**)Ba(THF)]$_2$ are in equilibrium with monomeric forms [(**6**)Ca] and [(**6**)Ba] that could not be isolated.

Interestingly, Mg complexes were reported only recently, independently by So et al. and Leung et al. who used the same bis-*n*-butylmagnesium as precursor (Scheme 7) [24, 37, 38]. From a structural point of view, this alkaline earth features the most varied coordination scheme, which does not seem to depend on the size of the substituents at P. Indeed, with neutral ligand **6**H$_2$, a dimer [(**6**)Mg]$_2$, with a structure similar to the ones of Ca and Ba complexes, was observed. With the bis-thiophosphinoyl derivative **7**H$_2$, a head-to-tail dimer was formed. In this complex, the Mg center is only bound to one C atom, and the two S atoms are bound to the Mg center of the other molecular unit. Most recently, a monomeric Mg complex, [(**14**)Mg(THF)$_3$], was reported by So, Mézailles et al. (Fig. 3) [24].
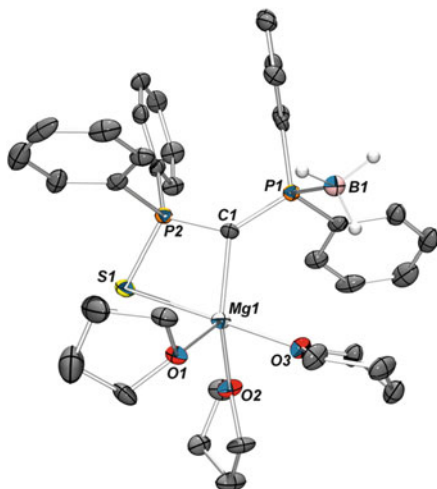
Fig. 3 X-ray structure of complex [(**14**)Mg(THF)$_3$]

In this complex, the BH$_3$ moiety is not bound to the Mg center, unlike in the Ca complex, and the coordination sphere is completed by three THF molecules. This structure is quite surprising in light of the lack of steric requirements which could have led to a dimeric structure. The M–C bond lengths in complexes [(**7**)Mg (THF)]$_2$ and [(**14**)Mg(THF)$_3$] at 2.156(5) Å and 2.113(4) Å, respectively, are significantly shorter than in the dimers [(**6**)Mg]$_2$ and [(**10**)Mg]$_2$ at 2.225(2) Å (av.) and 2.267(3) Å (av.).

Finally, one example of a different synthetic route is given for a gem-bis-magnesium methanediide [43] [(**28**){MgBr(THF)$_2$}$_2$] stabilized by two trimethylsilyl substituents instead of any hypervalent phosphorus (Eq. (1)). Complex [(**28**){MgBr (THF)$_2$}$_2$] is obtained by a double Grignard reaction on a gem-dibromomethane. In this case, the corresponding dilithiated species has not been isolated to date.

$$[(\mathbf{28})\{MgBr(THF)_2\}_2] \tag{1}$$
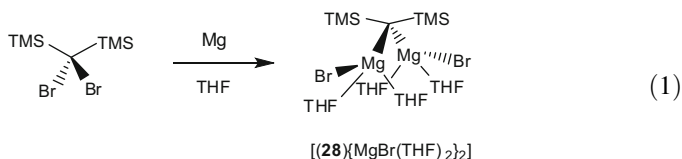
3.2 Electronic Structure

Now that it has been shown that carefully designed methanediide species may form monomeric complexes with AE, the question of the nature of the bond between the AE metal and C had to be asked. Harder et al. performed a DFT study first on
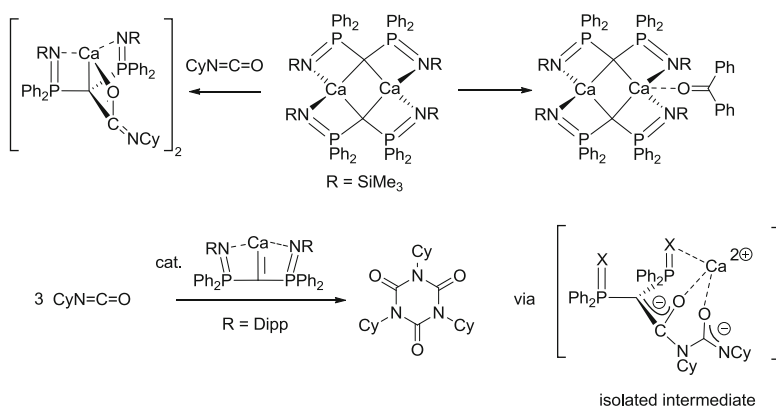
Scheme 8 Reactivity of calcium complexes toward ketone and isocyanate

models of [(**6**)Ca]$_2$ and [(**11**)Ca] where phenyl groups at P and groups (SiMe$_3$ and Ar, respectively) at N were replaced by H atoms. The monomeric (tricoordinated Ca center) and dimeric (tetracoordinated Ca center) forms were calculated, without taking into account the additional solvent molecules in the case of the monomer. The charges at Ca varied between +1.760 (monomer) and +1.821 (dimer), and the charges at C varied between −1.623 (monomer) and −1.847 (dimer). The Ca–C bond was thus described as highly ionic. The calculations with the full dimeric system were carried out, leading to a similar conclusion, with slightly reduced charge at C (−1.778). The authors thus proposed a Lewis structure in full accord with the one proposed for the gem-dilithio compounds (see Chart 2). They propose however that the stabilization of the high negative charge on the central carbon proceeds via electrostatic interactions with the Ph$_2$P$^+$ moieties, rather than via negative hyperconjugation proposed by Mézailles et al.

3.3   Reactivity of AE Complexes

The bonding situation described above and earlier results on related lanthanide complexes (vide infra) point to a high nucleophilic character. The prototypical reactions involving unsaturated species in [2+2] cycloaddition process to form the corresponding alkene derivative were attempted. The calcium dimer [(**6**)Ca]$_2$ did not react at room temperature with benzophenone or nitrile but rather formed adducts. Under more forcing conditions, partial reaction with benzophenone was observed as shown by hydrolysis (characterization of the tertiary alcohol). Despite a monomeric nature, complex [(**10**)Ca] did not prove more reactive. The much more reactive unsaturated substrate cyclohexyl isocyanate was then used, and [(**10**)Ca] appeared to be a catalyst in a trimerization process. Interestingly, the complex resulting from the double insertion of the isocyanate reagent was isolated and characterized by X-ray crystallography (Scheme 8).

Finally, the reactivity of the Mg dimeric complex was tested toward the same highly electrophilic isocyanate but without success, confirming the trend in reactivity in AE complexes increasing down the group. Accordingly, the Ba complex [(**11**)Ba (THF)] did also react with cyclohexyl isocyanate [42].

4 Rare Earth Elements: Group 3 and Lanthanides

Following a common usage, we gathered here group 3 metals and lanthanides in a same group. This is justified by the similarities of the main characteristics relevant to their coordination chemistry: quasi-exclusive prevalence of (+III) oxidation state, relatively important ionic radius that evolves smoothly amongst the group, and valence orbitals poorly accessible for metal–ligand interactions due to high energy level or shielding by 4d electrons in the case of lanthanides. One may note however that within these elements, scandium presents a number of particularities that make it an outsider. For all rare earth elements, interactions with any ligands are supposed to be mostly ionic in nature, even if some clues of involvement of 5d orbitals [44] and of 4f orbitals [45] in some case have been highlighted. In agreement with this, in any structurally characterized methylidene complex of rare earth, the methylidene ligand CH_2^{2-} is bridging between at least two rare earth ions or main group metals [46–49], highlighting the poor influence of d orbitals for its stabilization and the important ionic character of the involved interactions. This brings us back to the question of the existence and pertinent description of any multiple interactions between rare earth metals and a carbon atom as featured by geminal dianions.

One year only after his discovery of the stability of the geminal dianion **6**Li$_2$, Cavell was first to report a rare earth metal complex featuring a geminal dianion as ancillary ligand [50]. In fact, he used route B with bis(trimethylsilyliminophosphoranyl)methane **6**H$_2$ as a ligand precursor and [Sm(NTMS$_2$)$_3$] and obtained a monomeric, monometallic complex of samarium (III). Since this groundbreaking example, the use of geminal dianion in coordination chemistry of rare earths has seen important developments, and a few reviews have already appeared [51–54]. Most strikingly, as will be shown below, bis(thiophosphinoyl)methanediide **7**Li$_2$ and bis (iminophosphoranyl)methanediide **6**Li$_2$ have been widely used and shown to be the only ligands allowing for the synthesis of complexes in which the C atom is bound to a single metal center. Our aim is here to give an overview of characterized complexes of rare earths bearing a geminal dianionic ligand, paying more attention to more recent results, and on the reactivity of these complexes.

4.1 Synthesis

Both routes A and B have been used. Route A was mostly used for bis (thiophosphinoyl)methanediide complexes (ligand **7**$^{2-}$), whereas route B was
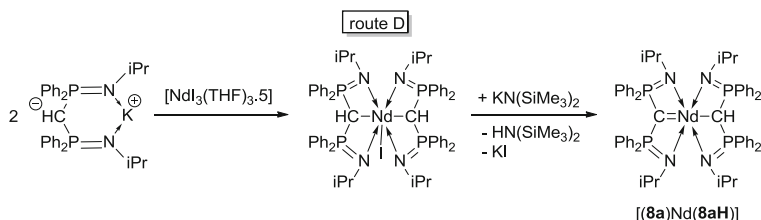
Scheme 9 Alternative route for the synthesis of methanediide rare-earth complexes starting from a coordinated monoanion


[A] :

[(**6**)Sm(**6H**)]
[(**6**)La(**6H**)]
[(**6**)Ce(**6H**)]
[(**6**)Pr(**6H**)]
[(**6**)Nd(**6H**)]
[(**6**)Gd(**6H**)]

E = NTMS: **6H₂**
E = NMes : **11aH₂**

[A] :

[(**6**)Sm(NCy₂)(THF)]
[(**6**)Y(CH₂TMS)]
[(**6**)Y(CH₂Ph)]
[(**6**)Y(OC(Ph)₂CH₂Ph)]
[(**6**)Y(I)]
[(**6**)CeI(DME)]
[(**6**)Y(Ga{(NDippCH)₂})]
[(**6**)Er(I)]
[(**6**)Er(CH₂Ph)(THF)]
[(**6**)Dy(CH₂Ph)(THF)]
[(**11a**)La(I)(THF)₃]
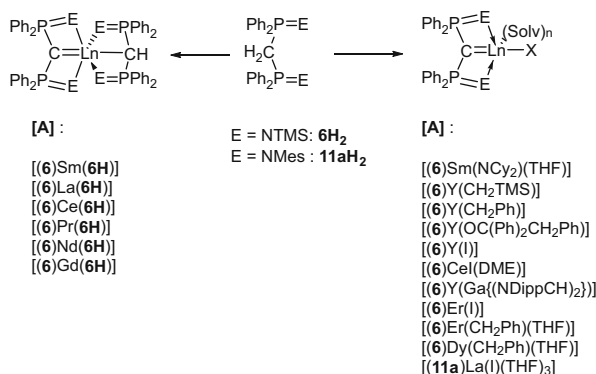
Scheme 10 Synthesis of rare-earth bis-iminophosphorane carbene complexes

usually preferred for bis(iminophosphoranyl)methanediide (ligand 6^{2-}, 8^{2-}, 11^{2-}) complexes. An intermediate route D, starting from a coordinated monoanion, was also used. The methanediide fragment was generated upon further deprotonation (Scheme 9) [55, 56].

Following one route or the other, various complexes can be obtained: a mono-meric, monometallic, and monocarbenic structure [**A**] (Scheme 10); a dimeric one in which each metallic center bears one dianionic carbon [**B**]; or a biscarbenic, anionic, monometallic structure [**C**] (Scheme 11). To date, this last structure could only be obtained following route A. Other complexes, such as the alkoxide-coordinated yttrium complex [(**6**)Y(OCPh₂CH₂Ph)] [57], can be obtained by trans-formation of the coordination sphere of these primary complexes (see Sect. 4.2). Independently of the substitution on the phosphorus atoms, the dianionic carbon usually coordinates a single rare earth metal, i.e., examples of a geminal dianion bridging two rare earth metals are extremely scarce (Table 2). The only two examples were recently obtained with lanthanum [56] and yttrium [57].

As shown in Scheme 10, different structures were obtained depending on the ionic radii of the metal following route B with tribenzyl rare earth complexes and bis(iminophosphoranyl)methane as a ligand precursor. Thus for the bigger ions, despite a 1:1 stoichiometry between ligand and metal precursors, the sole isolated
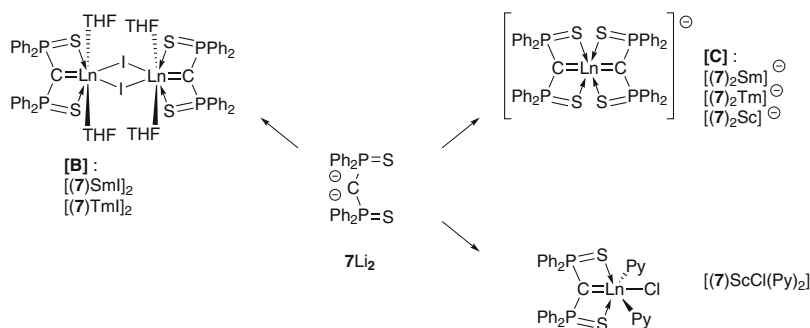
Scheme 11 Synthesis of rare-earth bis-thiophosphinoyl carbene complexes

Table 2 List of different rare earth complexes featuring a geminal dianion as a ligand and the corresponding reference

Name	Ln	E	X	(Solv)n	Reference
[(**6**)Sm(NCy$_2$)]	Sm	N(SiMe$_3$)	Cy$_2$N$^-$	(THF)	[50]
[(**7**)SmI]$_2$	Sm	S	I$^-$	THF	[58]
[(**7**)$_2$Sm]$^-$	Sm	S	–	–	[58]
[(**7**)TmI]$_2$	Tm	S	I$^-$	THF	[59]
[(**7**)$_2$Tm]$^-$	Tm	S	–	–	[59]
[(**6**)Y(CH$_2$SiMe$_3$)]	Y	N(SiMe$_3$)	Me$_3$SiCH$_2$$^-$	THF	[60]
[(**6**)Y(CH$_2$Ph)]	Y	N(SiMe$_3$)	PhCH$_2$$^-$	THF	[57]
[(**6**)Y(OCPh$_2$CH$_2$Ph)]	Y	N(SiMe$_3$)	(PhCH$_2$)Ph$_2$CO$^-$	THF	[57]
[(**8**)Nd]	Nd	N(*i*Pr)	**8aH**$^-$	–	[55]
[(**6**)YI]	Y	N(SiMe$_3$)	I$^-$	(THF)$_2$	[61]
[(**6**)CeI]	Ce	N(SiMe$_3$)	I	DME	[62]
[(**6**)ErI]	Er	N(SiMe$_3$)	I$^-$	(THF)$_2$	[61]
[(**6**)Y(Ga{(NDippCH$_2$)$_2$}]]	Y	N(SiMe$_3$)	[:Ga{(NDippCH$_2$)$_2$}]$^-$	(THF)$_2$	[63]
[(**6**)$_2$Y$_2$(OCPh$_2$CH$_2$Ph)$_2$]	Y	N(SiMe$_3$)	(CH$_2$Ph)Ph$_2$CO$^-$	–	[57]
[(**11a**)LaI]	La	NMes	I$^-$	(THF)$_3$	[56]
[(**11a**)La$_2$I$_2$][LiI]$_2$	La	NMes	2 I$^-$	ILi(THF)$_2$, THF	[56]
[(**6**)Er(CH$_2$Ph)]	Er	N(SiMe$_3$)	PhCH$_2$$^-$	THF	[64]
[(**6**)Dy(CH$_2$Ph)]	Dy	N(SiMe$_3$)	PhCH$_2$$^-$	THF	[64]
[(**6**)La(**6H**)]	La	N(SiMe$_3$)	**6H**$^-$	–	[64]
[(**6**)Ce(**6H**)]	Ce	N(SiMe$_3$)	**6H**$^-$	–	[64]
[(**6**)Pr(**6H**)]	Pr	N(SiMe$_3$)	**6H**$^-$	–	[64]
[(**6**)Nd(**6H**)]	Nd	N(SiMe$_3$)	**6H**$^-$	–	[64]
[(**6**)Sm(**6H**)]	Sm	N(SiMe$_3$)	**6H**$^-$	–	[64]
[(**6**)Gd(**6H**)]	Gd	N(SiMe$_3$)	**6H**$^-$	–	[64]
[(**7**)ScCl]	Sc	S	Cl$^-$	(Py)$_2$	[65]

lanthanide complexes featured both bis(iminophosphoranyl)methanide and – methanediide ligands ([(**6**)M(**6H**)], M=La, Ce, Pr, Nd, Sm, Gd) [64]. On the contrary, with erbium, yttrium [57], and dysprosium, in decreasing ionic radii

order, the alkyl-methanediide complex was obtained. These observations support the idea that, for bigger lanthanide ions and bis(iminophosphoranyl)methanide and benzyl ligands, disproportionation equilibrium may easily occur, despite the steric bulkiness of the ligand.

Structurally speaking, it seems that coordination of the dianionic carbon is influenced by the nature of the second, anionic ligand. Indeed, from halogenated complexes to alkylated ones in a set of complexes featuring the same dianionic ligand and same metal, an increase of the dianionic carbon–metal bond length and a bending of the MNPCPN ring from a flat geometry to a boat configuration are observed as shown by a decrease of the PCP angle (Table 3). An exception to this trend is however found with benzyl ligand, which presents an η^2 coordination to yttrium in complex [(**6**)Y(CH$_2$Ph)] [57]. Complexes of structure [**C**] [58, 59] are particularly interesting; their low-temperature structure revealed two different conformation for the coordination of the geminal dianion, one being bent and the other being flat, both with bond length similar to the one observed in the related complex of structure [**B**]. In any case, a decrease of the Lewis acidity of the rare earth metal center by coordination of a strongly donor ligand is invoked to explain this trend in bond lengths. More generally speaking, the boat conformation, for which the geometry at carbon is closer to a sp^3 hybridization than in complexes featuring a T-shaped planar geometry at carbon [61], is supposed to be less in favor of a double σ and π interaction between the geminal dianionic carbon and the metal.

Other parameters important for the understanding of the electronic structure of hypervalent phosphorus-stabilized methanediide complexes are the P(E) (E = N or S) and P–C bond lengths (see Sect. 2). Comparing the evolution of these parameters upon coordination shows no variation of the P(E) bond length in all structures. Slight shortening of the P–C bond upon coordination of a single metal center could be observed and an elongation for bridging geminal dianions. The small amplitude of these variations reflect the remaining stabilization of the double negative charge at carbon by the two hypervalent phosphorus atoms, already present in free, lithiated geminal dianions. A better understanding on how the electronic charge at carbon is shared between this intra-ligand stabilization and the interaction with the metal required the use of modeling.

4.2   Description of the Bonding Scheme

Theoretical studies have been made on yttrium and lanthanum complexes with bis (iminophosphoranyl)methanediide ligand and a scandium complex with bis (thiophosphinoyl)methanediide ligand. Indeed, the closed-shell configuration of these rare earth ions renders their modeling more straightforward. However, comparison between these different studies is hampered by the inhomogeneity of methods, bases, and even different choices of bonding or charge distribution models. We will thus focus on complexes [(**6**)Y(CH$_2$SiMe$_3$)], [(**6**)YI], [(**6**)Y(Ga{(NDippCH$_2$)$_2$})], and comparison with the dianion **6**$^{2-}$, which have been studied and characterized by NBO

Table 3 Significant bond lengths and angles for a set of yttrium complexes bearing ligand 6^{2-} and various complexes of thulium and samarium bearing ligand 7^{2-}

Complex	[(6)Y(CH₂SiMe₃)]	[(6)Y(OCPh₂CH₂Ph)]	[(6)Y(CH₂Ph)]	[(6)Y(Ga{(NDippCH₂)₂})]	[(6)YI]	6Li₂[17]
C–M bond length (Å)	2.406(3)	2.393	2.357(3)	2.348(3)	2.356(3)	–
P–N bond length (Å)	1.627(3) 1.629(3)	1,626(2) 1,632(2)	1.627(2)	1.629(2) 1.630(2)	1.620(3) 1.623(3)	1.630(3) (av.)
P–C bond length (Å)	1.672(3) 1.662(3)	1.671(2) 1.660(2)	1.6521(12)	1.637(3) 1.643(3)	1.641(3) 1.640(3)	1.687(3) 1.694(3)
P–C–P angle (°)	138.4(2)	137.58(16)	147.6(2)	171.2(2)	172.5(2)	132.3(2)

Complex	[(7)SmI]₂	[(7)₂Sm]	[(7)TmI]₂	[(7)₂Tm]	[(7)ScCl(py)₂]	7Li₂
C–M bond length (Å)	2.371(6) 2.352(6)	2.491(5) 2.507(5)	2.325(5)	2.378(9) 2.423(9)	2.2072(1)	–
P–S bond length (Å)		2.042(2) 2.034(2)			2.046(1) 2.052(1)	2.037(1) 2.040(1)
P–C bond length (Å)	1.675(2) 1.667(2)	1.660(6) 1.635(6)	1.6652(5) 1.668(4)		1.660(3) 1.657(3)	1.672(3) 1.678(3)
P–C–P angle (°)	146.2(4) 145.4(4)	156.4(4) 136.5(4)	150.8(3)	158.0(6) 134.6(6)	159.3(2)	131.6(2)

Table 4 NBO charges, Wiberg bond indices, and percentage of atomic character for the relevant frontier orbitals for various yttrium complexes bearing ligand **6** and comparison with the corresponding dilithiated species

	q_C	q_P	q_N	I(PC)	I(PN)	I(CM)		%C	%P	%M
(**6**)Y(CH$_2$SiMe$_3$)	−1.49	+1.59	−1.61	1.31–1.24	1.07–1.08	0.6	LP1	53	4	0
							LP2	49	n.a.	3.7
(**6**)Y(Ga {(NDipp CH$_2$)$_2$})	−1.58	+1.58	−1.56	1.19	0.99	0.29	LP1	53	6	2
							LP2	58	2	3
(**6**)YI	−1.58	+1.58	−1.56	1.19	0.99	0.30	LP1	52	n.a.	2
							LP2	34	n.a.	0
								25	n.a.	9
6Li$_2$[17]	−1.37	+1.61	−1.48	1.29	1.04	–	LP1	60	12	n.a.
							LP2	56	13	n.a.

analysis, using NBO charges and Wiberg bond orders and/or for which a description of the Kohn–Sham frontier orbitals was given.

For most of complexes of this set, the Kohn–Sham orbitals reflect a strong reminiscence of the dianionic ligand, with HOMO and HOMO-1 frontier orbitals with respectively almost pure p orbital and sp^n hybrid orbital characters, and thus feature important contributions from carbon. Two exceptions to this clear scheme are given by the benzyl complex, for which the main contribution to the HOMO is almost exclusively of alkyl carbon nature, and the gallium–yttrium complex, for which the second lone pair at carbon is involved in a four-electron, three-center interaction with yttrium and gallium, resulting in its important contribution in two occupied molecular orbitals (HOMO-2 and HOMO-4). This ordering of the frontier orbitals is in agreement with reactivity studies that have been conducted for complexes [(**6**)Y (CH$_2$SiMe$_3$)] and [(**6**)Y(Ga{(NDippCH$_2$)$_2$})] (see below).

Considering NBO charges distribution for these complexes, the dipolar resonance form of the bis(iminophosphoranyl)methanediide that was described for the free ligand is still underlying and even emphasized under coordination, with an increase of all the charge values borne by the NPCPN pattern. This increase of the ionic character by interaction with an electro-deficient yttrium center also appears in the simultaneous decrease of all bond orders. It is quite interesting to note that the decrease of the P–C bond length observed earlier correlates well with an increase of the difference of charges between the dianionic carbon and phosphorus atoms. A decrease of the involvement of the phosphorus orbital in carbon-centered Kohn–Sham orbital from the free dianion to its coordinated form can also be noticed. Stabilization by negative hyperconjugation seems thus to be diminished upon coordination in favor of an increase of ionic interactions (Table 4).

Stabilization of the double charge at carbon is known to occur by negative hyperconjugation in bis(diphenylthiophosphinoyl)methanediide [19]. For the only rare earth metal complex featuring this ligand and for which a theoretical study was made, namely [(**7**)ScCl(py)$_2$], a quite different approach was used. A second-order perturbation analysis was used to quantify and compare the two different stabilization

processes (hyperconjugation vs. donation toward the metallic center) in each σ and π symmetry. It appeared that in σ symmetry, donation toward the metal overpasses clearly the hyperconjugation process (98.4 vs. 56.4 kcal/mol), whereas it is the opposite in π symmetry (39.2 vs. 55.4 kcal/mol). However, this last stabilization of the electronic density at carbon by donation toward metal remains in a same order of magnitude as what occurs by hyperconjugation. Despite this highlight of a slight covalent character, moderate C–M bond order of 0.6 emphasizes the high polarity of this scandium–carbon interaction.

4.3   Reactivity

Most of reactivity studies firstly aimed at emphasizing cooperativity and double-bond character between the carbenic carbon and the metal interaction in those complexes. Species containing unsaturated, polarized bond were thus chosen as substrate. Benzophenone was firstly used as a seminal reagent, for its unambiguous electrophilic reactivity. Indeed, examples of ortho-metalation of this reagent are scarce. However, a particularly interesting example was given by Z. Hou recently (Scheme 12). The addition of 1 equiv. of benzophenone to a tris-thulium tetramethyl methylidene complex resulted in the nucleophilic addition of the methylidene ligand to the carbonyl and subsequent double deprotonation of the phenyl rings in ortho-position by the newly generated alkyl ligand and a methyl. The same substrate added to a similar lutetium complex, featuring amidinate ancillary ligands instead of Cp derivatives, resulted in a total conversion of the ketone into the corresponding olefin, in a Wittig-like reaction. This difference in the reactivity of the methylidene ligand in these two strongly related systems empha-sizes the role of steric pressure in determining the reactivity of such species.

As far as a comparison can be made between a methylidene ligand bridging between three rare earth centers and a hypervalent phosphorus-stabilized geminal dianion coordinated to one single metallic center, it appeared that the addition of benzophenone to complexes [(**7**)SmI]$_2$ [58], [(**7**)TmI]$_2$ [59], [(**7**)$_2$Sm]$^-$, and [(**7**)$_2$Tm]$^-$ afforded the Wittig-like product Ph$_2$C=C(PPh$_2$(S))$_2$ as single product (Scheme 13), within 1 h for the first two and within 12 h for the second two. For those last, two isostructural intermediates could be isolated after 1 h of reaction. They correspond to the product of [2+2] cycloaddition of benzophenone to the C=M bond, with breaking of the remaining C–M interaction, as is observed when the monoanionic ligand is coordinated to a metal center.

With scandium complex [(**7**)ScCl(Py)$_2$] [65], the same reactivity toward benzo-phenone is observed but required heating or longer reaction time. Another interme-diate could be isolated, corresponding to the trapping of the resulting (Sc$_2$O$_2$Cl$_2$) by-product by two more equivalents of starting complex [(**7**)ScCl(Py)$_2$] (Scheme 14). The determining step in this reaction thus seems to be the oligomerization of the resulting oxo-salts, which may be improved by the presence of a halogen ligand on the metal, an important ionic radius and a dimeric structure of the complex.
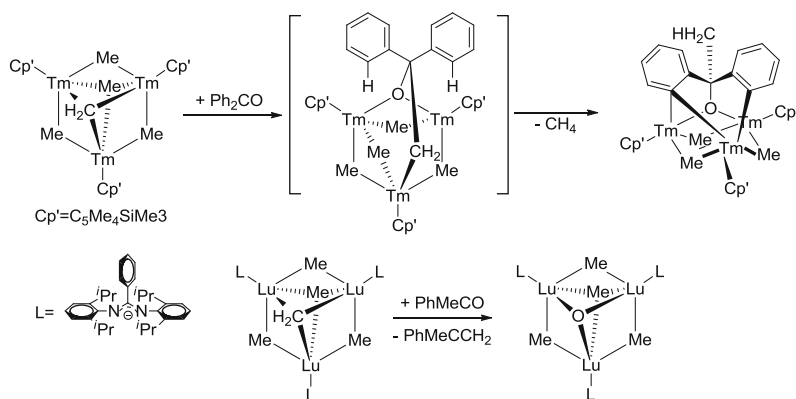
Scheme 12 Reactivities of tris-thulium and tris-lutetium tetramethyl μ3-methylene complexes toward benzophenone
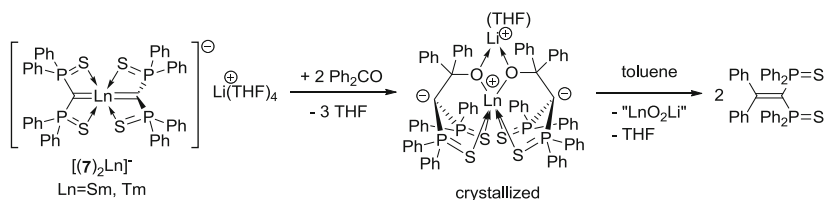
Scheme 13 Reaction of lanthanide bis(thiophosphinoyl)methanediide complexes toward benzophenone
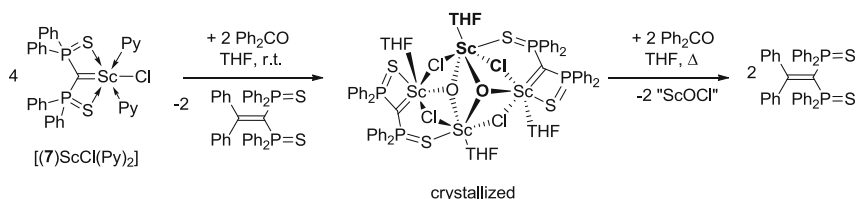
Scheme 14 Reactivity of complex [(**7**)ScCl(Py)₂] toward benzophenone

This same test of benzophenone reactivity proved to bring totally different results in the case of yttrium complex of the kind "(**6**)YX," where the pendant ligand X is an alkyl [57] or a halogen [66] (Scheme 15). In the case of an alkyl or any strong nucleophile, this last ligand is the primary reacting site, and the geminal dianion adopts the behavior of an ancillary ligand in a first step. On the contrary, when the pendant ligand is a halogen, the dianionic carbon behaves either as a base or as a nucleophile, depending on the substrate. In the case of benzophenone, deprotonation in ortho-position occurs, followed by subsequent nucleophilic attack of the newly formed carbanion on another equivalent of benzophenone. Increasing the steric

Scheme 15 Reactivities of bis(iminophosphoranyl)methanediide yttrium complexes toward benzophenone: alkyl vs. carbene based reactivity

pressure by coordination of a bulky ligand resulted in the cyclization of the oxymethylbenzophenone to substituted benzofurane.

During the reaction on a ketone featuring an electron-attracting group like a fluorine or a leaving group as an ester, a second nucleophilic attack of the initially dianionic carbon on the substrate could be observed with loss of fluoride salts or further coordination of the alkoxide derived from the ester function. In no case, a splitting of the C–O bond and formation of oxo-yttrium salts were observed. Changing the substrate to less energetic unsaturated polarized bonds as isothiocyanates gave access to a simili-Wittig reaction, in which a ketenimine is formed instead of an enolate (Scheme 16) [67]. However, when this same reagent is added to the alkyl analogue complex [68], a totally different reaction is observed, resulting in a dimeric yttrium complex in which the two metallic centers are linked by a tridentate ligand resulting from the addition of a sulfide on the isothiocyanate moiety (Scheme 16). Even if the reaction mechanism was not elucidated to date, it was supposed that the protonation of the geminal dianion was a clue of its involvement as a base in the

Scheme 16 Reactivities of [(**6**)YI] and [(**6**)Y(CH₂Ph)] toward a isothiocyanate compound
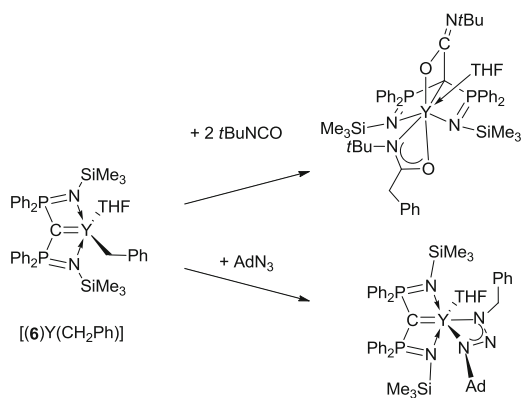
Scheme 17 Reactivities of complex [(6)Y(CH₂Ph)] toward isocyanate and azide derivatives

reaction mechanism, the first step being postulated to be a nucleophilic attack of the benzyl ligand on the isothiocyanate.

With substrates featuring a more energetic, multiply unsaturated polarized bonding scheme, like carbodiimides or isocyanides, a [2+2] cycloaddition reaction to the C=Y bond subsequent to the preliminary nucleophilic attack of the benzyl ligand could be observed [68] (Scheme 17). The same cycloaddition was also observed with those substrates and the corresponding iodinated yttrium complex, which also reacted with tert-butyl phosphaalkyne [67]. However, no subsequent [2+2] cycloaddition was observed with pivalonitrile or adamantly azide on the benzylated complex.

Reactivity studies on other rare earth methanediide complexes are scarce. Complex [(**8a**)Nd(**8aH**)] showed some activity in ring-opening polymerization of *rac*-lactide [69]. Scandium carbene complex [(**7**)ScCl(Py)₂] has been used as a ligand transfer reagent for the synthesis of a new dimeric, dimetallic iron complex featuring two bridging methanediide ligands (Scheme 18) [70].

Very recently, a metal-centered reactivity was probed by Liddle et al. They showed that an oxidation of Ce(III) to Ce(IV) by silver salts was possible starting
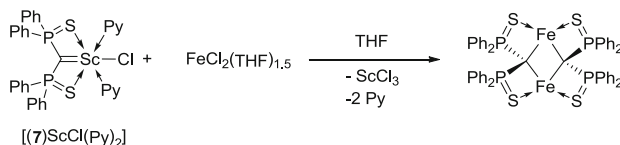
Scheme 18 Transmetalation reaction of the bis(thiophosphinoyl)methanediide ligand from scandium to iron II
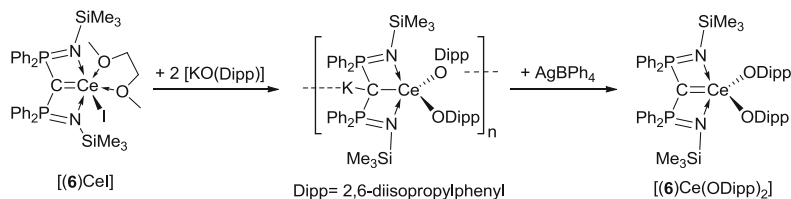
Scheme 19 Synthesis of the first Ce(IV) carbene complex

from complex [(**6**)CeI] through an electron-rich "ate" complex to insure a better control of the oxidation (Scheme 19) [62].

Although the carbon bond to the cerium is pyramidal, the resulting Ce(IV) complex [(**6**)Ce(ODipp)$_2$] presented many characteristics that sustain comparison with more classical transition metal–carbene complexes: a highly downfield-shifted signal for the PCP carbon in ^{13}C-NMR (324.6 ppm), a quite short carbon–cerium bond of 2.441 (5) Å. An absorption band in the visible spectra resulting from LMCT from C=Ce to 4f orbitals was also observed. Complex [(**6**)Ce(ODipp)$_2$] was also engaged in a metalla-Wittig reaction with aldehydes. A theoretical study described the carbon–cerium bond as mostly electrostatic with modest covalent character. However, 4f orbitals are clearly involved in this covalent part, which also present some twofold σ and π character according to QTAIM calculation.

5 Actinide Complexes

5.1 *Synthesis*

The chemistry of actinides is quite rich, and unlike for Ln centers, not only several oxidation states are accessible, but the metal–ligand bonding has also more covalent character, with a potential implication of f orbitals. In this domain, the range of isolated carbene complexes of actinides (mainly uranium with a small number of Th complexes) is still underdeveloped. The first example of U carbene complex was reported by Gilge in 1981 [71]. The synthetic strategy is somewhat related to the use of geminal dianion (route B) as they used the anionic ylids (CH$_2$)P(Me)(R)(CH$_2$)Li (R=Me and Ph) as precursors. Upon reaction with [Cp$_3$UCl], an internal rearrangement was observed, with a proton migration to the second CH$_2$ moiety,
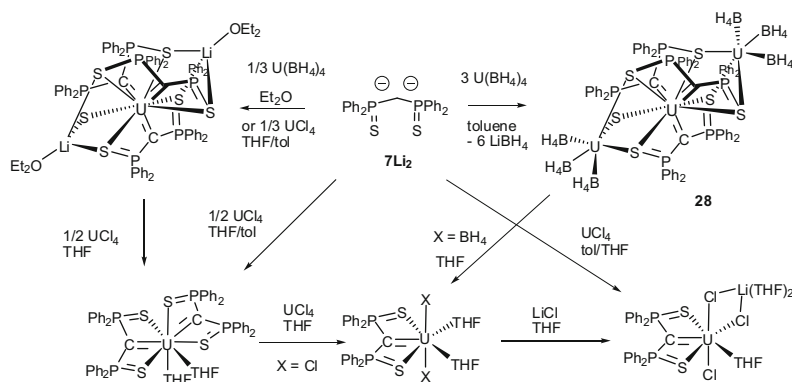
Scheme 20 Synthesis of uranium carbene complexes with gem-dilithio compound **7Li₂**

thereby forming the corresponding [Cp₃U=CHP(R)Me₂] complexes. Although the chemistry of these complexes was very rich (vide infra), almost 30 years went by without any other examples of such U carbene complexes. The access to geminal dilithio derivatives appeared to us as well as to Liddle and Cavell as very promising candidates to further expand this chemistry. The results that have been gathered in the past 5 years are quite impressive, as will be shown below. Thus, in 2009, we reported the synthesis of two triscarbene complexes of U(IV) **28** from the U(BH₄)₄ precursor and **7Li₂** [72]. Quite interestingly, the triscarbene slowly rearranged into a monocarbene complex when dissolved in THF. It is worth noticing that the dianion **7Li₂** reacts rapidly with THF, which implies that this rearrangement occurs in the coordination sphere of U. In 2010, Liddle et al. reported the formation of the first biscarbene of U(IV) from the reaction of UI₃(THF)₄ with the dianion **11aLi₂** [73]. This complex obviously results from an unwanted oxidation of the precursor. Key in this chemistry is the choice of the uranium precursor, and the use of both U(BH₄)₄ and UI₃ did not appear optimal as they are, respectively, tedious to make and easily oxidized. We thus extended the chemistry of U(IV) carbene complexes using the more readily available precursor (Scheme 20) [74]. Careful optimization of the experimental conditions was needed. In particular, the use of a small amount of THF was used to solubilize the U(IV) precursor so that the reaction was fast enough to prevent the side reaction between THF and **7Li₂**.

Route **B** could also be used, starting from the uranium amide complex [U(NEt₃)₄] in particular [75]. This route gave access to mixed carbene/amide complexes. Liddle et al. also used the tetrachloride precursor to generate the monocarbene U ate complex, **29**, featuring ligand **6** (Scheme 21) [78]. In parallel of the work by Liddle et al., the group of Cavell also developed the chemistry of ligand **6Li₂** toward actinides. They reported a similar dichloride U(IV) but also the only examples of Th(IV) carbene complexes, which were subsequently used for the synthesis of the bis-Cp [(**6**)UCp₂] and tris-pyrazolylborate [(**6**)UClTp] complexes [76].

Also in 2011, the first carbene complexes of higher oxidation states of U were obtained, using two different approaches (Scheme 22). Firstly, coordination to the uranyl ion UO₂²⁺ was attempted, and secondly, chemical oxidation of
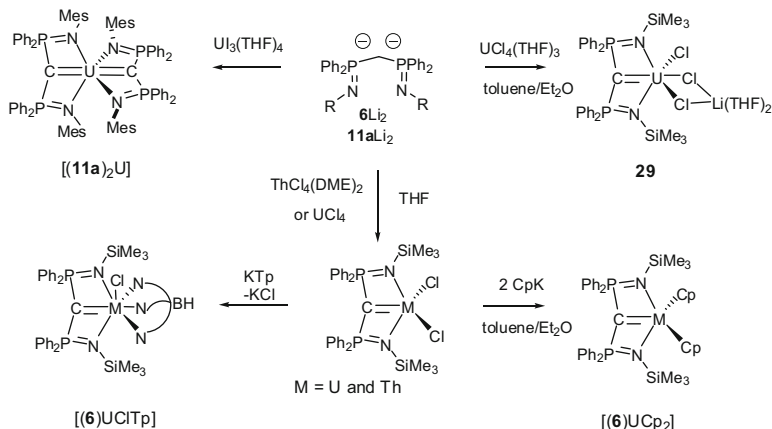
Scheme 21 Synthesis of uranium and thorium carbene complexes with gem-dilithio compounds **6**Li$_2$ and **11a**Li$_2$
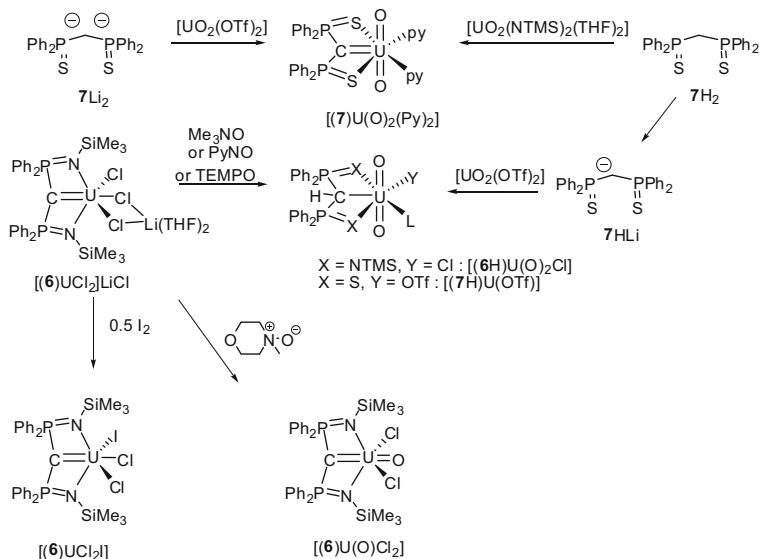
Scheme 22 Synthesis of uranium V and uranium VI carbene complexes

U(IV) precursors was studied. The first approach was quite a challenge as alkyl derivatives had always led to reduction of the U(VI) starting compound into U(V) with concomitant coupling of the alkyl species. In preliminary experiments, it was shown that the reaction of monoanionic species **7**HLi with U(VI) did not reduce it, opening the way for the reaction with **7**Li$_2$ which was equally successful [77]. Alternatively, the complex could be synthesized using the neutral **7**H$_2$ and the appropriate bis-amido complex [U(O)$_2$(NTMS$_2$)(THF)$_2$].
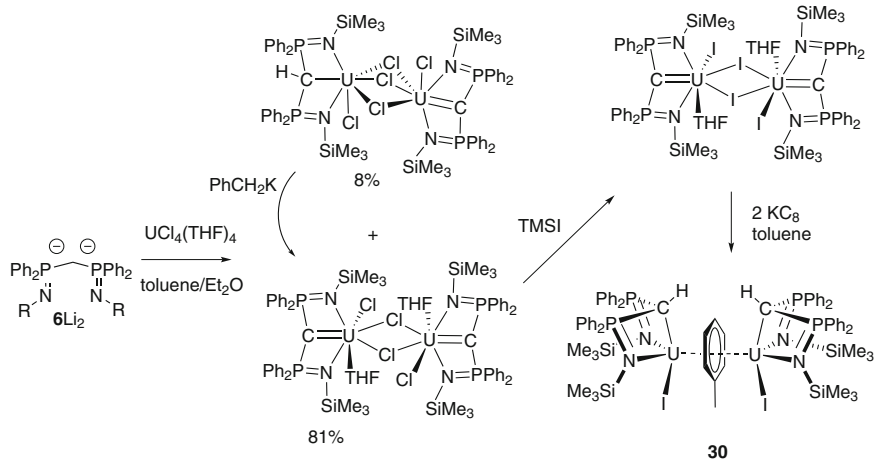
Scheme 23 Synthesis and reduction of a bis(iminophosphoranyl)methanediide U(IV) complex

The second strategy was pursued by Liddle et al. building on the convenient access of U(IV) carbene complexes. This approach proved very rewarding as they could obtain not only U(VI) carbene complexes but also U(V) [78]. Indeed, in 2011, they reported the oxidation of the U(IV) carbene/LiCl ate complex using the mild oxidant I_2. It provided the first example of U(V) carbene complex as proven by magnetic measurements as well as electronic absorption spectra (UV/Vis/NIR) and corroborated by DFT calculations (vide infra). With the same U(IV)/LiCl ate complex, oxidation with several "O" atom donors was then studied. The kinetics of the oxidation appeared crucial. When Me_3NO, PyNO, or TEMPO was used, an unwanted side reaction occurred, resulting in a formal protonation at the carbene center and leading to the uranyl complex of monoanion **6H**, previously reported by Sarsfield in 2003 [79]. On the other hand, the reaction with 4-morpholine-N-oxide led to the expected mono-oxygen transfer and the formation of C=U=O arrangement, analogous to the ubiquitous O=U=O arrangement found in U(VI) chemistry [80].

The extreme importance of the U precursor was once again exemplified by Liddle et al. in yet another recent study, dealing with reduction of a U(IV) carbene complex. When non-solvated UCl_4 was used in toluene/Et$_2$O mixture, a complex was obtained in very low yield (4%). In this complex, quantitative protonation of the dianion **6Li$_2$** had occurred prior to coordination. On the other hand, when solvated [$UCl_4(THF)_4$] was used in the same mixture of solvents, the desired carbene complex was synthesized in excellent 81% yield, as a chloro-bridged dimer, together with a minor species in 8% yield (Scheme 23). This latter species is also a dimer but features a monoprotonated fragment **6H** on one U center and the expected carbene fragment on the other. The carbene chloro-bridged dimer was quantitatively transformed into the iodo-bridged dimer in which reduction was studied. Most interestingly, it resulted in the formation of a dimer featuring a monoprotonated ligand **6H** but also a bridging
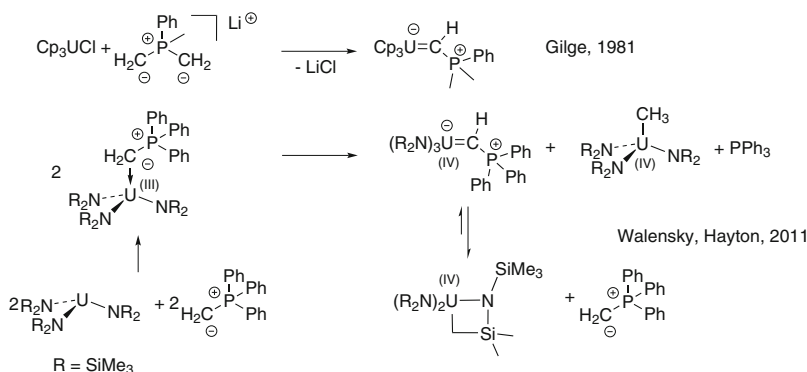
Scheme 24 Synthesis of uranium IV complexes from phosphorus ylides

toluene molecule. As such this complex is no longer a carbene complex and its properties appeared very unusual. Indeed, in the UV/Vis/NIR spectrum, the absorptions were both more intense and more complex than in other U(III) or U (IV) complexes. The DFT analysis (Mulliken charges, spin densities, and orbital composition) is consistent with complex **30** being formulated as two U(III) centers linked by an arene^{2-} moiety through covalent δ backbonding. Finally, the magnetic properties of this complex were studied and revealed a "single-molecule magnet" (SMM) behavior [81].

Walensky, Hayton et al. reported in 2011 on the oxidation of a U(III)-ylide adduct to generate the corresponding U(IV)–carbene complex (Scheme 24) [82]. This complex is an analogue of the carbene complex developed early on by Gilge. The formal replacement of the three Cp rings by three N(TMS)$_2$ ligands at the U center results in the ortho-metalation of one NTMS group and the transfer of one H to the carbene, regenerating the neutral, free ylid. Interestingly, these complexes are in equilibrium in solution, which is highly dependent on the solvent and temperature. The intermediate carbene is the major product in Et$_2$O at low temperature, whereas the metallacycle is favored in toluene at room temperature.

5.2 Electronic Structure

As shown above, dianions **6**Li$_2$ and **7**Li$_2$ appeared ideal for the synthesis of U carbene complexes of various oxidation states (IV, V, and VI), yet not for the stabilization of U(III) carbene (as of today). It is to be noted that this stabilization of different oxidation states by these kinds of ligands has not been observed so far for any other metal center. The nature of the interaction between the carbon center and the U center was therefore of high importance. This characterization was done by different experimental techniques (X-ray, UV/Vis/NIR, magnetism) as well as by DFT calculations. The U=C bond distances vary to a great extent in the reported complexes,

linked to the coordination numbers at U, the oxidation state, as well as the steric requirements of the ligands. Thus, in the early examples by Gilge, the distances were measured at 2.29(3) Å for R=Ph (X-ray diffraction) and 2.293(1) Å for R=Me (neutron diffraction) [71]. Similar bond distances were measured in SCS U(IV) monomeric complexes (2.327(3) Å in [U(**7**)(BH$_4$)$_2$(THF)$_2$] to 2.396(4) Å in [Cp*$_2$U(**7**)]) and in NCN U(IV) complexes (2.351(2) Å for [Cp$_2$U(**6**)]). It is interesting to note that the U–C bond distance is similar in the SCS and NCN complexes despite a strong geometrical difference within the ligand. Indeed, the SCS ligand is planar in the complexes, whereas the NCN ligand adopts an "open book" conformation, due to both the much longer P–S and U–S bonds compared to the P–N and U–N bonds. These C–U bond distances are shorter than the σ alkyl–U bond distances in U(IV) complexes (between 2.4 and 2.6 Å). In the triscarbene, dianionic SCS complexes of U(IV), much longer bond distances of 2.46(2) Å (av.), were measured, in line with greater coordination number. Liddle et al. showed that the U=C bond was almost not affected upon oxidation (2.268(10) Å in the U(V) vs. 2.310(4) Å in the U(IV) complex), reflecting that an electron of essentially nonbonding f character was removed upon oxidation. In the U(VI) complex [(**7**)UO$_2$(Py)$_2$], the U–C bond distance is greatly increased to 2.430(6) Å, although the ionic radius of U(VI) is smaller than the U(IV) radius by ca. 0.2 Å. It is interesting to note in this complex that the O=U=O trans arrangement is greatly affected, as shown by an angle of 171.8(2)°. This severe bending likely results from the repulsion between the negatively charged oxo ligands and the dianionic SCS ligand, which may also be responsible for the C=U bond increase. On the other hand, in the [(**6**)U(O)Cl$_2$] complex, also featuring a U(VI) center, but in which the carbene is *trans* to the oxo, the bond distance is shortened to 2.183(3) Å and ascribed to the inverse trans influence (ITI).

DFT calculations were performed on many of the abovementioned complexes, which provided further important information on the nature of the bonding. The first calculations were performed on the U(IV) complex featuring the SCS system, [(**7**)U(BH$_4$)$_2$(THF)$_2$], and revealed the presence of 2.15 unpaired electrons on the uranium center, consistent with a U^{IV} metal center (high spin 6d^0 5f^2 configuration). Correspondingly, the HOMO and HOMO-1 are almost pure 5f AOs (%5f > 78%), with a small antibonding interaction with the S atoms. It is interesting to note that interactions between lone pairs at C and S in the ligand lead to strong mixing of their contributions to the ligand MOs (Fig. 4).

The NBO analysis then revealed that both the σ and the π U–C interactions are mainly developed on the C atom (80.7% C and 19.3% U in the interaction of σ symmetry, 82.9% C and 17.1% U in the π interaction). It is however interesting to note that the U contribution is done via hybrid 5f/6d orbitals and that the lower energy of the 5f orbitals results in a major contribution of them in the hybrid (52.6% 5f, 37.0% 6d in the contribution to the σ bond, and 59.0% 5f and 40.9% 6d in the contribution to the π bond), despite their smaller radial expansion compared to the 6d. The bonding scheme points a U=C double bond polarized toward the carbon atom (NBO calculated charges: $q_C = -1.52$ and $q_U = 0.98$). DFT calculations were then performed by the groups of Liddle and Cavell on their U(IV) complexes, featuring
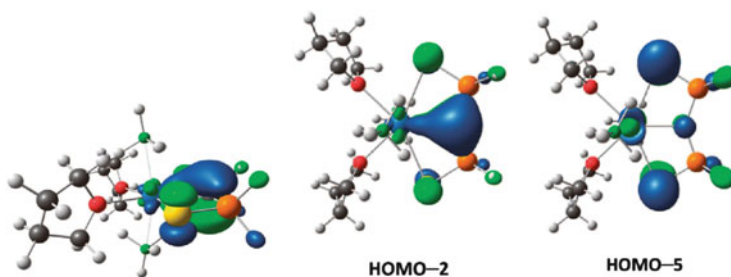
Fig. 4 Representation of Kohn–Sham orbitals HOMO-2 and HOMO-5 for complex U(SCS)
$(BH_4)_2$. Taken from [72]

NCN ligands. As stated by Cavell the "NCN carbene has the same central coordination properties as SCS^{2-}, and the ligand belongs to the same methanediide family, so it is not surprising to see very similar actinide M=C double bond bonding structures in both complexes" [76]. Accordingly, the NBO analysis, performed on complex [(**6**) UCl_2] (Scheme 22), reveals almost identical involvement of C and U in the polarized U=C bonds (82.4% C, 17.6% U in the σ bond and 82.2% C, 17.8% U in the π bond).

Interestingly enough, Walensky, Hayton et al. have performed DFT calculations on their $[(NR_2)_3U=CH(PPh_3)]$ complex but also on Gilge's complex $[Cp_3U=CHPMe_2Ph]$ (see Scheme 24, L = NR_2 and Cp). In these two cases, the formal dianionic C center in "$CH(PR_3)^-$" is much less stabilized compared to the methanediide systems (such as **6**Li_2 or **7**Li_2), as evidenced by the fact that it is not stable in the isolated form. Therefore, much like in the Schrock-type carbene complexes, the stabilization of the fragment has to be brought by its interaction with the metal fragment. A strong donation from the "$CH(PR_3)^-$" fragment would have been expected. In fact, the Mulliken population analysis of the $[(NR_2)_3U=CH(PPh_3)]$ complex showed that the HOMO and HOMO-6, which describe the π and σ interactions, are mostly C centered. The π interaction possesses 22% U character, which is stated as "only slightly more" than in the abovementioned complexes. Furthermore, the NBO analysis, which provides a more localized picture, revealed that the U–C σ bond in the complex includes 12% U character (with 40% contribution from 5f vs. 35% for 6d) and only 8% U character in the π bond (with 17% contribution from 5f vs. 54% for 6d). The respective contribution from the C center is 88 and 92%, respectively. A very similar picture was obtained for Gilge's complex which features 12% and 7% U character (and thus 88 and 93% C character) in the U–C σ and π bonds, respectively. Thus, the NBO analysis points to a strongly polarized U–C with a modest π character. Overall, comparing the NBO analysis with the ones performed on methanediide systems points striking and quite unexpected differences. Indeed, as shown by the involvement of the U center in the corresponding NBOs, the π character appears weaker than in the methanediide cases. Therefore, despite a more efficient stabilization of the two charges in the methanediides by PPh_2N or PPh_2S moieties, compared to the

formal "CH(PPh$_3$)$^-$" moiety, the donation to the metal center is also more efficient, likely because of the additional charge in the methanediide.

The U(V) complex [(**6**)UCl$_2$I] synthesized by Liddle et al. was also subjected to DFT calculations. The comparison with the U(IV) was made. The U(V) possesses a single unpaired electron, localized in an essentially pure f-orbital (HOMO). The U–C bond index (Nalewajski–Mrozek) is slightly increased compared to the U(IV) complex (1.54 vs. 1.43), showing a significant multiple bond character. The NBO analysis again presents almost identical involvement of C and U in the polarized U=C bonds (74.2% C, 25.8% U in the σ bond and 74.3% C, 25.7% U in the π bond). The involvement of the 5f orbitals is much more important than the 6d orbitals (ca. 90:10) and increased compared to the U(IV) complex (ca. 18:82 on average). Finally, the only two known U(VI) carbene complexes were also studied by means of DFT. They presented very significant differences, which are directly linked to the presence (and number) of O atoms, as well as on their relative position compared to the carbene fragment (*cis* or *trans*). Complex [(**7**)U(O)$_2$(Py)$_2$], featuring the *cis* arrangement, presents a high charge at C (−1.46 vs. −1.52 in the U(IV) complex), again showing the dianionic character of the C center. This was confirmed by the NBO analysis which supports the polarized U=C bond. Indeed, the U–C σ bond is described by the donation from the C lone pair (80.6%, sp$^{2.3}$) to a U hybrid orbital (19.4%, with 24.0% 6d and 30.2% 5f). The U–C π bond is described by the donation from the second C lone pair (87.3%, pure p) to a U hybrid orbital (12.7%, with 23.3% 6d and 68.1% 5f). Most interestingly, this polarized U=C bond is marginally affected by the oxidation state of the U center, despite a significant modification of the electrophilicity of the U center [U(VI) that is more electrophilic than the U(IV)]. It appears that the two oxo ligands compensate the increased electrophilicity. The other known U(VI) carbene complex, [(**6**)UOCl$_2$], presents the lowest C character in the U–C σ bond (68.0%), and the U contribution represents the largest involvement of a 5f orbital (94.4% 5f and 5.2% 6d). On the other hand, the U–C π bond is almost unchanged compared to the related U(V) complex (see Table 5).

Overall, these DFT calculations all point a strongly polarized U=C double bond with significant covalent character. As such, these complexes are predicted to be strongly nucleophilic, as confirmed by reactivity.

5.3 Reactivity of Actinide Complexes

It is quite obvious from the very recent results presented above that the challenge resided more in the synthesis of carbene complexes of actinides (mainly U) with different oxidation states than in studying their reactivity. Nevertheless, Gilge et al. presented early on several examples of the nucleophilic behavior of the U(IV) [Cp$_3$U(CHP(Ph)$_2$Me)] carbene complex (Scheme 25). Indeed, the first

Table 5 Bond indices, charges, and percentage of atomic character for the U=C bonds in U carbene complexes

Complex	Bond lengths and indices			Atomic charges		U=C σ-component			U=C π-component		
	U–C exp	U–C calc	BI	qU	qC	C%	U%	U 6d:5f	C%	U%	U 6d:5f
7U(BH$_4$)$_2$	2.327(3)	2.32		−1.52[c]	0.98[c]	80.7	19.3	37.0:52.6	82.9	17.1	40.9:59.0
6U(Cp)$_2$	2.351(2)		0.66[a]						88.0	12.0	
6UCl$_2$	2.310(4)	2.313	1.43[b]	2.53[d]	−2.00[d]	82.4	17.6	20.0:79.4	82.2	17.8	15.8:84.2
U(CHPR$_3$)Cp$_3$		2.284				88	12		93	7	
U(CHPR$_3$)(NR$_2$)$_3$	2.278(8)	2.267				88	12	35:40	92	8	54:17
6UClI	2.268(10)	2.223	1.54[b]	2.53[d]	−1.85[d]	74.2	25.8	10.3:89.4	74.3	25.7	9.8:90.0
6UCl$_2$O	2.183(3)		1.50[b]	3.64[d]	−2.01[d]	68.0	32.0	5.2:94.4	75.8	24.2	8.1:91.8
7UO$_2$	2.430(6)	2.41	0.91[a]	0.91[c]	−1.46[c]	80.6	19.4	24.0:30.2	87.3	12.7	23.3:68.1

[a] Wiberg bond index
[b] Nalewajski–Mrozek bond index
[c] NBO charge
[d] MDQ charge
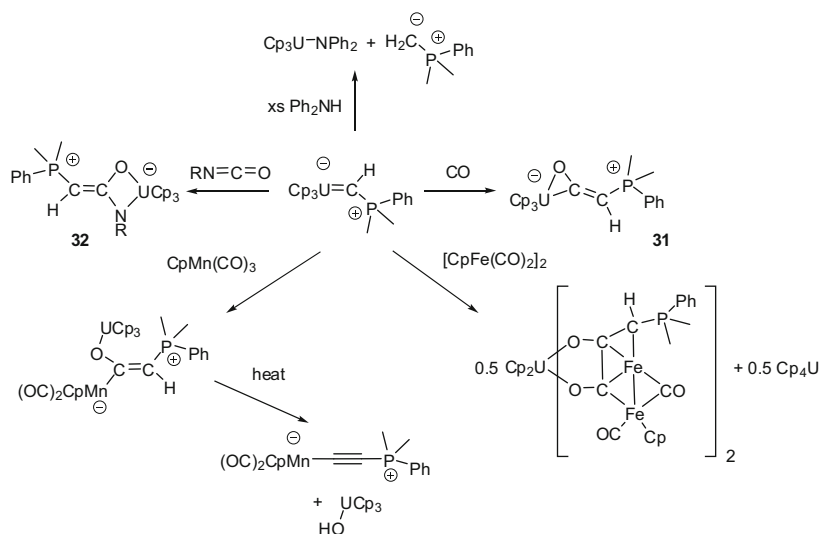
Scheme 25 Reactivity studies performed on complex [Cp$_3$U(CHP(Ph)$_2$Me)]

reaction involved CO, which inserted in the U=C bond to form complex **31** [83]. They also reported the coupling of the carbene moiety with strong electrophiles such as isocyanates to form **32** [84]. They extended the chemistry of carbonyl compounds to carbonyl complexes (both terminal and bridging) [85, 86]. This chemistry is driven by both the C–C bond formation and the strong U–O (and U–N) bond. Not surprisingly, the carbene fragment, being formally anionic, is also basic enough to deprotonate diphenyl amine, to generate the corresponding uranium amide complex [87]. Note that this reactivity was successful whereas the analogous reaction from [Cp$_3$U(Me)] complex did not produce the expected amide.

With the complexes featuring ligand **7**, we studied the reaction with other carbonyl compounds (ketones and aldehydes). The reaction was very fast and proceeded in a Wittig-like fashion to yield the corresponding alkene in excellent to quantitative yields [72, 77]. These results are identical to the ones obtained with group 3 complexes, but the kinetics is much faster in the case of uranium complexes. This reaction was also studied with the systems featuring ligand **6** and led to the corresponding alkene, although in lower yield [80]. It was noted that this reactivity was different than the one observed for Y complexes of the same ligand, for which CH bond activation of one phenyl ring was observed rather than coupling. Cavell et al. studied the reactivity with nitriles and showed that the expected [2+2] reaction with the U=C bond stopped at 50% conversion (Scheme 26) [76].

These examples clearly prove the nucleophilic carbene character of the U complexes.
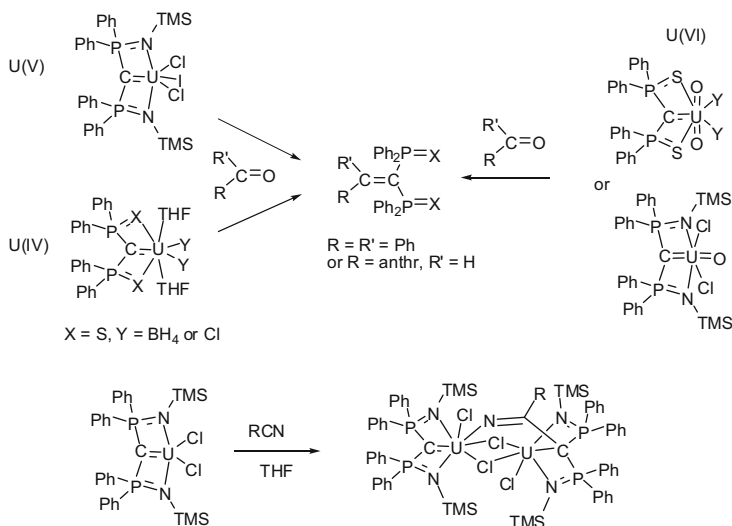
Scheme 26 Reactivity studies performed on bis(iminophosphoranyl)methanediide and bis (thiophosphinoyl)methanediide complexes of U(IV), U(V), and U(VI)

6 Group 4 Complexes

6.1 Synthesis

The group of Cavell developed in 1999 the first complexes featuring ligand **6** as a formal dianion. In fact, as stated by R.G. Cavell, this discovery "was unexpected and serendipitous" as they had wished for TMS-Cl elimination from the reaction of [TiCl$_4$] with **6**H$_2$. The simple adduct was obtained instead. Using the more reactive [Zr(NTMS$_2$)$_2$(Cl)$_2$] precursor under forcing conditions (toluene, reflux), the clean formation of the corresponding carbene complex was observed (Eq. (2)) [88, 89].

$$\tag{2}$$

M = Zr; R = SiMe$_3$, Adamantyl; X = CH$_2$Ph
M = Zr; R = SiMe$_3$; X = Cl
M = Hf; R = SiMe$_3$; X = Cl
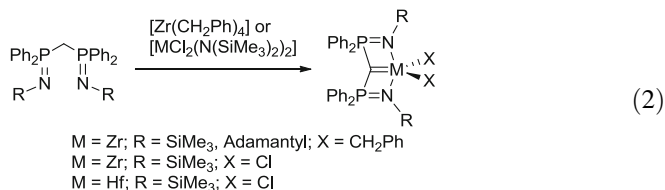
At the same time, they found out that the dilithio derivative was stable and isolable and realized that it could be used advantageously to generate the same complexes or others in very mild conditions. Indeed, route A, involving salt metathesis, readily occurred at room temperature from the MCl$_4$·THF$_2$ precursors (M=Ti, Zr) [90], providing the first stable carbene complexes of group 4 metals which do not
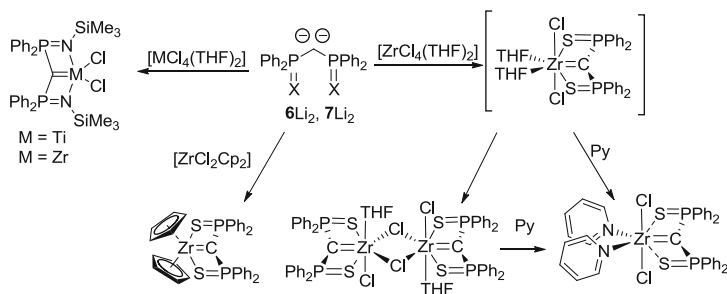
Scheme 27 Group 4 metal complexes synthesized following route A and the influence of a strongly coordinating solvent
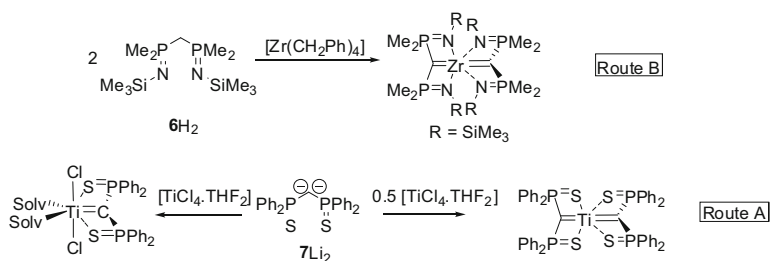
Scheme 28 Group 4 metal complexes synthesized following route B and various titanium bis (thiophosphinoyl)methanediide complexes obtained following route A

incorporate Cp ligands. We used this route with **7**Li$_2$ few years after to obtain the related Zr complexes (Scheme 27) [91]. The reaction goes through an intermediate, [(**7**)ZrCl$_2$(THF)$_2$], which is converted within 2 h into a chloro-bridged dimer. Upon addition of excess of pyridine, both the intermediate and the chloro-bridged dimer formed the mono-Zr complex. The bis-Cp complex [(**7**)ZrCp$_2$] was obtained following the same method starting from commercially available zirconocene dichloride.

Interestingly, in the case of the bis-iminophosphorane, the bulkiness at the nitrogen atom seems to prevent further coordination of solvent molecules at the metal center, leading to pentacoordinated complexes (distorted trigonal bipyramid). On the other hand, in the case of the bis-thiophosphinoyl, the lack of steric bulkiness at S results either in the formation of a dimer (weak solvent) or a monomer in which two molecules of solvent are bound to the Zr center, leading to heptacoordination. In these cases, the homoleptic [M(**6**)$_2$] (M=Ti, Zr, Hf) or [Zr(**7**)$_2$] were never observed. Cavell et al. were able to synthesize one example of such species, but only when the substituents at P were methyl groups, and failed with either Ph or even Cy [92]. It is interesting to note that the corresponding dianionic dilithio derivative has not been reported (Scheme 28). This complex was thus obtained via route B, starting from [Zr(CH$_2$Ph)$_4$], under very mild conditions (room temperature).
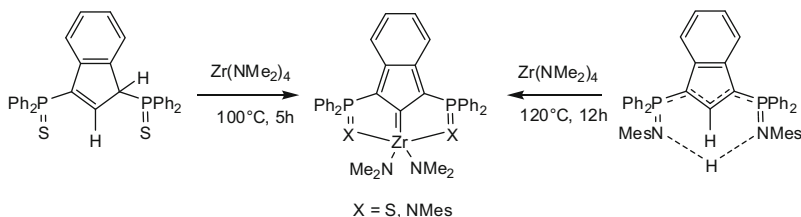
Scheme 29 First examples of indenilydene complex of zirconium, synthesized following route B
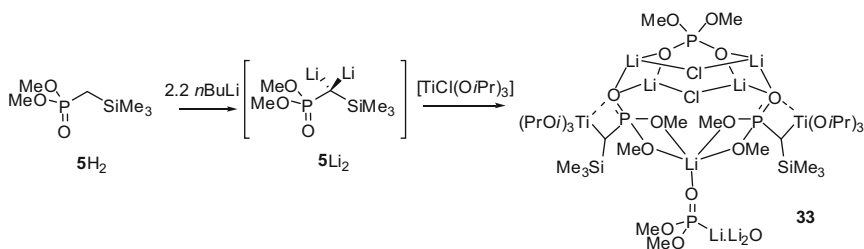
Scheme 30 Synthesis of a Ti/Li cluster featuring a phosphonate-stabilized geminal dianion

This example shows the extreme influence of the nature of each of the substituents at P on the stabilization of the gem-dianion as well as on the formation of carbene complexes. Most recently, we were able to synthesize either the monocarbene or the homoleptic biscarbene of titanium using dianion **7**Li$_2$ (route A) [93]. In 2009, a related class of pincer ligand was developed by Martin-Vaca, Bourissou et al. who used route B to obtain the first example of indenylidene complexes of Zr (Scheme 29) [94]. Here also, the corresponding isolable dianionic ligands are not accessible. It is to be noted here that the in situ coordination/deprotonation required forcing conditions (ca. 100°C for several hours).

First results pertaining to the coordination of phosphonate-stabilized dianions appeared in 1999. Although they have shown that gem-dilithio phosphonate/silyl derivative **5**Li$_2$ is stable, Müller et al. did not use the isolated species but rather a species generated in situ (by deprotonation of **5**H$_2$ with a slight excess of *n*-BuLi) to study the coordination of the Ti(IV) precursor [TiCl(O*i*Pr)$_3$] [95]. It resulted in the formation of the mixed Ti/Li cluster **33** crystallized in 48% yield. Among the notable features of the structure, one can note that both the P=O and the P–OMe moieties coordinate the Li atoms, the P=O moiety being the bridge between one Ti and two Li centers (Scheme 30). Also notable is the partial "destruction" of the ligand as a lithiated methylphosphonate moiety is present in the crystal (as well as Li$_2$O).

In 2010, we reported on the coordination behavior of the bisphosphonate derivative **9**Li$_2$ toward Zr(IV) [96]. The stoichiometric reaction led to the formation of the first triscarbene complex as a kinetic product, isolated in a low yield of 20%, as well as a thermodynamic species, likely more aggregated "Zr(**9**)Cl$_2$" fragments, as
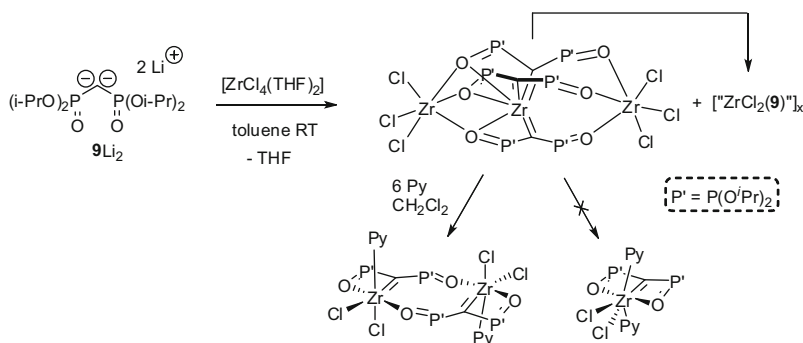
Scheme 31 Synthesis of a zirconium triscarbene complex and its rearrangement to a monocarbenic, dimeric complex

shown by reactivity (vide infra). Despite the presence of strongly coordinating phosphonate moieties, LiCl is not retained in the complexes. The phosphonate is likely responsible for the facile kinetic/thermodynamic product rearrangement via ligand redistribution at room temperature in non-coordinating solvent. Indeed, as mentioned above, the chloro-bridged Zr dimer complex $[(\mathbf{7})\text{ZrCl}_2(\text{THF})]_2$ bearing ligand **7** could be cleaved but only with stoichiometric amounts of strongly coordinating pyridine ligand, and the trinuclear U(IV) complex $[(\mathbf{7})\text{U}(\text{BH}_4)_2(\text{THF})_2]$ also rearranged to mononuclear species but only in THF. Here, the addition of a stoichiometric amount of pyridine resulted in the formation of a novel bimetallic complex, in which one P=O fragment coordinates to the second Zr center (Scheme 31), instead of the monometallic complex similar to the ones obtained with bis-iminophosphorane and bis-thiophosphinoyl substituents most likely because of the shorter P=X bond distance.

6.2 Electronic Structure

As was presented above, the nature of the interaction between the carbon center and the metal(s) for groups 1–3 and actinides has been probed by DFT calculations. Because of the energies of the orbitals involved, it can be expected that the orbital overlap, and thus the covalency of the M=C bond, would be better with group 4 metals. Müller et al. have focused on the rotation barrier about the P–C bond in the mixed Ti/Li silyl-phosphonate system (see Scheme 30) in order to compare it to the barrier found in phosphoryl-stabilized carbanions. They obtained a very similar barrier of rotation, meaning that the presence of the Ti center did not enhance the configurational stability at the C center [95].

Compounds of Chart 4 were also studied [91, 96]. Importantly, in each case, the charge calculated at C is greatly reduced compared to the gem-dilithio derivatives (e.g., -2.01 in $\mathbf{9}\text{Li}_2$ to -1.67 in $[(\mathbf{9})\text{Zr(OMe}_2)_2\text{Cl}_2]$), which translates a significant
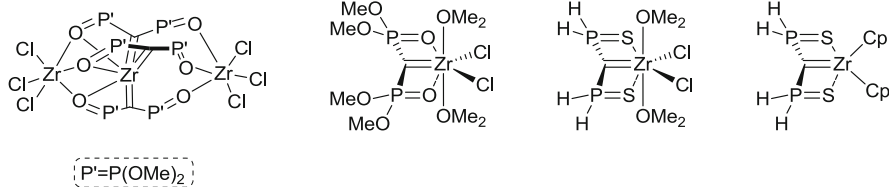
Chart 4 Representation of model complexes used for DFT calculations
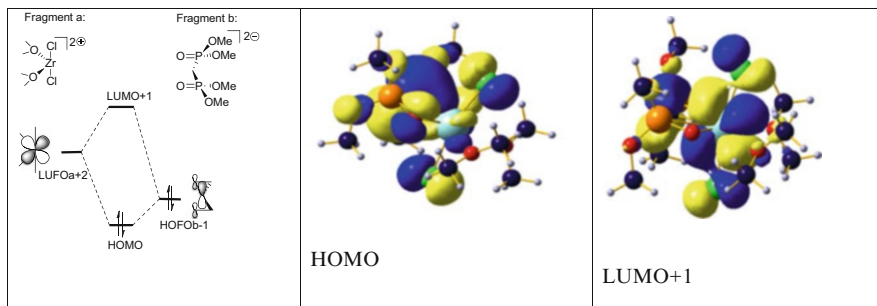
Fig. 5 MO diagram for the π interaction in complex [(**9**)Zr(OMe$_2$)$_2$Cl$_2$], reproduced from [96]

electronic donation to the Zr center. The Zr carbene complexes were then analyzed with the aim to clarify or quantify the Zr=C double-bond character. As a representative example, the analysis of complex [(**9**)Zr(OMe$_2$)$_2$Cl$_2$] is summarized here. An MO diagram describing the π interaction was built by decomposing the complex into two fragments, the [Cl$_2$(OMe$_2$)$_2$Zr^{2+}] fragment (fragment a) and the dianionic ligand **9**$^{2-}$ (fragment b) (Fig. 5). Interactions between the two fragments were analyzed using the AOMIX program. The carbon–zirconium interactions of π symmetry mainly result from the combination of two fragment orbitals (FO) of same symmetry to form the HOMO and the LUMO + 1 of the complex. The HOMO features an important contribution from the ligand-centered fragment orbital (77.2% of HOFOb-1) and to a lesser extent from the metal-centered one (10.5% of LUFOa-2). These percentages are quite comparable to the ones obtained for the analogous complex containing/featuring ligand **7**. They show that an important electron density remains on the carbon center, consistent with the NBO charge. Overall, as expected, going to group 4 metal centers, the orbital overlap increases compared to group 1, 2, and 3 metals and the metal–carbon interaction gains in covalency, although the bond stays strongly polarized.

The case of the indenylidene complexes (see Scheme 29) revealed a different picture. For both complexes, it is stated that "no significant π interaction between C and Zr was identified" [94]. The HOMO-1 in the two complexes (with P=S or P=NR arms) shows that the π lone pair at C is delocalized toward the carbon backbone of the indenyl.

6.3 Reactivity of Group 4 Metal Complexes

The reactivity of these group 4 metal complexes has been studied to some extent. Starting from complex [(**6**)MCl$_2$], the reaction with nucleophiles such as alkyllithium led to the classical reactivity at M–Cl (Scheme 32) [89]. The reactions with strong electrophiles such as isocyanates, carbon dioxide, or carbodiimide did not show the expected insertion into the M=C bond, but rather a [2+2] cycloaddition. The basicity and nucleophilicity of the C center was proved by reactions with aromatic amines, phenols, aliphatic alcohols, or methyl iodide leading to the 1,2 addition product.
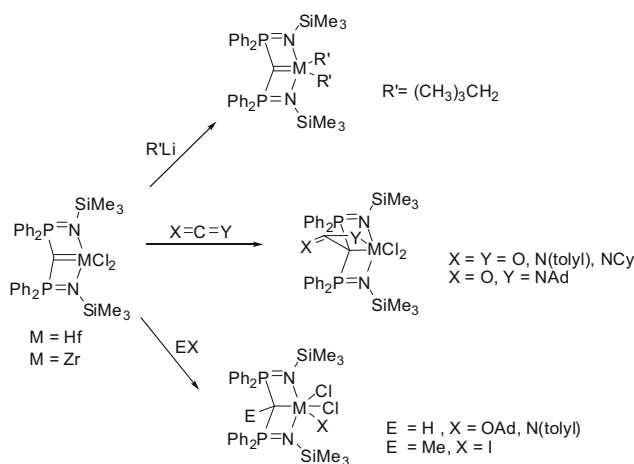
Scheme 32 Reactivity of bis(iminophosphoranyl)methanediide group 4 metal complexes

Our group studied the reactivity of (SCS) carbene complexes [(**7**)ZrCp$_2$], [(**7**) ZrCl$_2$(THF)]$_2$, and [(**7**)ZrCl$_2$(Py)$_2$] [91]. Despite being electron rich, complex [(**7**) ZrCp$_2$] proved to be unreactive because of its electronic saturation. On the other hand, the dichloro bis(thiophosphinoyl)methanediide complexes were found to be more reactive than the iminophosphorane derivatives, and reaction with weaker electrophiles (aldehydes and ketones) afforded the corresponding geminal bis (diphenylthiophosphinoyl)olefins (Scheme 33). Zr complexes featuring the bisphosphonate ligand **9** were reported to react with aldehydes but not with ketones [96]. It is to be noted that related titanocene and zirconocene complexes featuring a phosphorus analogue of Arduengo carbene exhibited similar nucleophilic reactivity leading to 1,3-diphosphafulvenes [97]. It was then shown that these electron-rich alkenes could be reduced by one electron to generate stable radical species [98, 99].

Finally, Zr carbene complex $[(\mathbf{7})ZrCl_2(THF)]_2$ was tested as a carbene transfer agent, in a reaction similar to this observed with the Sc carbene complex $[(\mathbf{7})ScCl(THF)_2]$. Not surprisingly and because of the stronger Zr=C bond, its reactivity was lower. Nevertheless, transmetalation to Ru(II), Co(II), and Pd(II) was successful [70].

R=Ph,   X=S, R_1=H, R_2=9-anthracenyl, 2-furyl
R=Ph,   X=S, R_1=R_2=Ph, 2-pyridyl, 2-thienyl
R=Oi-Pr, X=O, R_1=H, R_2=9-anthracenyl
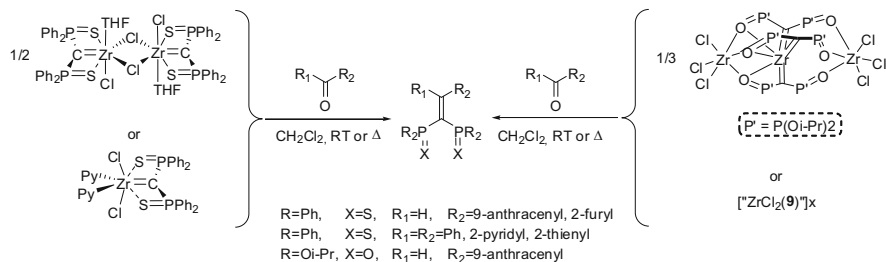
Scheme 33 Reactivity of bis(thiophosphinoyl)methanediide and bisphosphonate dianion complexes of zirconium

7 Group 13 Complexes

Although structurally characterized methylidene-bridged bis-aluminum species are known for more than 20 years [100], group 13 complexes featuring a hypervalent phosphorus-stabilized methanediide moiety are scarce. The known syntheses rely almost exclusively on route B, from the neutral ligand and an alkyl complex. Their structures depend to a great extent on the nature of the phosphorus substituents, with dimetallic structures with bis(iminophosphoranyl) methanediide ligand or thiophosphinoylphosphinomethanediide and monometallic, dimeric structures for the softer bis(thiophosphinoyl)methanediide and dissymmetrical thiophosphinoyliminophosphoranylmethanediide. Very little is known about their reactivity yet.

7.1 Synthesis

Three synthetic paths have proved to be fruitful in the synthesis of group 13 complexes bearing a hypervalent phosphorus-stabilized methanediide ligand. C–H/Al–Me bond cleavage (corresponding to route B) is the most commonly used synthetic path for aluminum complexes. The first examples of such species were given by Robinson et al. in 1988 following route B [101, 102]. Using C–H/Al–Me bond cleavage with concomitant elimination of methane, they obtained the dimeric complex $[Al(CH_3)][Ph_2P(O)CP(O)Ph_2]_2[Al(CH_3)_2]$ [101] ([Al1], Scheme 34) from the addition of an excess of trimethylaluminum to the neutral bidentate ligand bis(diphenylphosphinoyl)methane $Ph_2P(O)CH_2P(O)Ph_2$ in chlorobenzene at 100°C. The crystallographic structure reveals two $AlMe_2$ moieties, each one

Ph$_2$P PPh$_2$
X   X'

X=X'=O   7: X=X'=S   6: X=X'=N-TMS   10: X=N-TMS; X'=S

xs AlMe$_3$ 2.5 eq ^{i}Bu$_2$AlH   2 AlR$_3$ R=Me, ^{t}Bu   AlR$_3$ AlMe$_3$
chlorobenzene   Tol/Hex   -2 CH$_4$ -CH$_4$ Toluene
100°C   160°C   Toluene   Toluene   120°C
- 4 CH$_4$ -H$_2$S, - ^{t}BuH   120°C   r. t.

[Al$_1$]   [Al$_2$]   [(6)(AlR$_2$)$_2$]   [(6H)AlR$_2$]   [(10)AlMe]$_2$

AlMe$_3$
Toluene, 120°C.
-CH$_4$
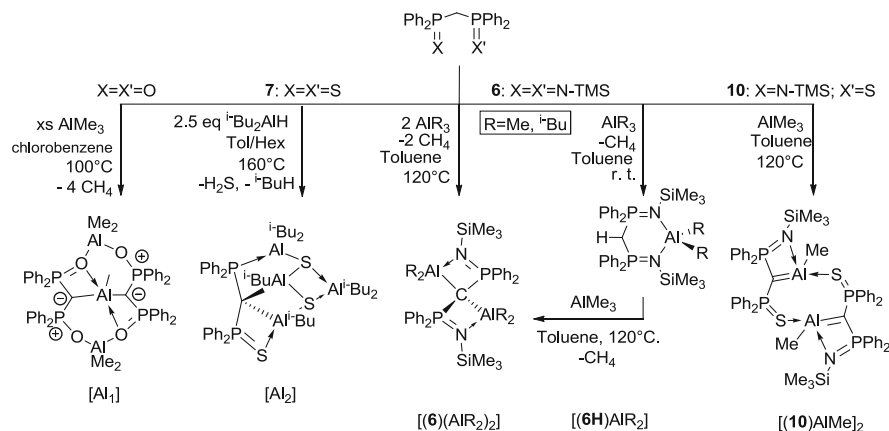
Scheme 34 Synthesis of group 13 complexes

bridging two oxygen atoms of the two ligands, and one central AlMe moiety linked to the two central carbons and the two remaining oxygen of each ligand.

The reaction of analogous bis(diphenylthiophosphinoyl)methane with 2.5 equiv. of di(isobutyl)aluminum hydride in a mixture of toluene and hexane afforded after heating at 160°C a complex of molecular formula [iBuAl]$_2$[(Ph$_2$P(S)CPPh$_2$(S)$_2$] [iBu$_2$Al]$_2$ ([Al$_2$], Scheme 34) resulting from the partial reduction of the ligand via postulated H$_2$S elimination as well as alkane elimination [102]. One can note the rather drastic conditions for this reaction to proceed.

The first well-defined monomeric aluminum complex featuring a methanediide ligand stabilized by hypervalent phosphorus was reported by Cavell in 1999 [103]. The reaction, analogous to this of Robinson et al., was performed in toluene at 100°C with the more bulky ligand **6**. It afforded a spirocyclic bis-dialkylaluminum complex, [(**6**)(AlMe$_2$)$_2$]. An intermediate was observed during the course of the reaction and was synthesized quantitatively at room temperature using only 1 equiv. of trimethylaluminum in toluene.

More recently, the dissymmetrical ligand **10** has been used to obtain a rare monometallic aluminum complex [37] following a procedure similar to Cavell's. In fact, the addition of 1 equiv. of trimethylaluminum to a solution of ligand **10** in refluxed toluene afforded complex [(**10**)AlMe]$_2$ featuring the first formal C=Al bond. This complex is dimeric via further coordination of the thiophosphinoyl moiety to a second aluminum atom doubly bonded to another dianionic ligand. Comparing with the related spiro complex [(**6**)(AlMe$_2$)$_2$] [103], Al–N and Al–C bond distances are shortened from 1.933(3) Å to 1.915(1) Å and from 2.121(3) Å to 1.976(1) Å in [(**6**)(AlMe$_2$)$_2$] and [(**10**)AlMe]$_2$, respectively. P–C bonds are shortened, from 1.769(6) in [Al$_1$] and 1.751(3)/1.746(3) Å in [Al$_1$] to 1.710(1) Å and 1.686(1) Å in [(**10**)AlMe]$_2$. This increase of strength of PC bond is consistent with the increase of the electronic density on C due to the monometallic structure of the latter complex and the subsequent increase of hyperconjugative interactions.

Fig. 6 Crystallographic structure of compound $[\{(Ph_2PS)_2C\}InCl]_2$, reproduced with the permission from ACS [38]
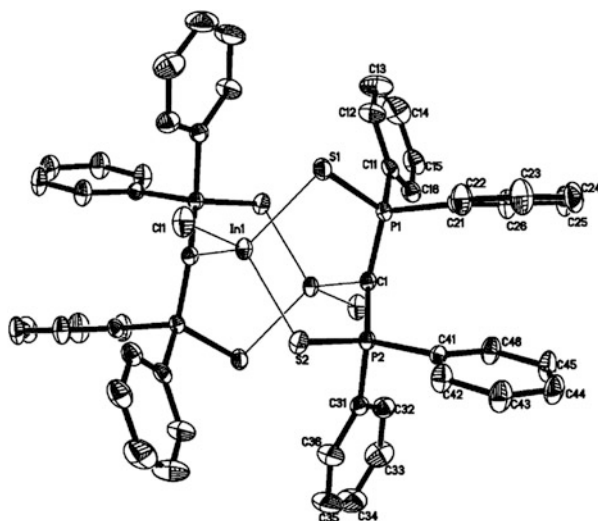
A milder route toward methanediide aluminum complexes has been explored recently by Leung et al. [38], expanding the field of methanediide complexes to other elements of the group 13 elements. Starting from the readily available MCl_3 (M=Al, Ga, In) and using the monoanionic **7HLi** both as a ligand transfer reagent and as a base, they obtained a set of homologous group 13 complexes (Eq. (3)).

$$(3)$$
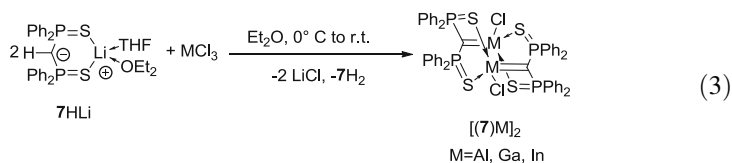
All three complexes are isostructural (Fig. 6) and similar to the related magnesium species [38] $[(\mathbf{7})Mg]_2$ (cf. Sect. 3.1). The measured values of the P–C–P angles (116.8(1)° for $[(\mathbf{7})Al]_2$, 117.8(3)° for $[(\mathbf{7})Ga]_2$, and 121.1(2)° for $[(\mathbf{7})In]_2$) are in agreement with a sp^2-hybridized methanediide carbon. Similarly elongated P–S and shortened P–C bond lengths (between, respectively, 1.710(5) Å and 1.724(2) Å and 2.051(2) Å and 2.062(1) Å in the whole set), compared with the neutral ligand $(S=PPh_2)_2CH_2$ (respectively, 1.95 Å and 1.83 Å), suggest a similar delocalization of the electronic density from the carbon to the stabilizing $Ph_2P=S$ substituents. An increase of the S–M and Cl–M bond distances is naturally observed along this set of complexes, as expected for this range of metals of similar electronic configuration,

Chart 5 Two gem-dialuminum methanediide complexes obtained from the reaction of diphenyl(N-tert-butyl) iminophosphorano-(8-quinolyl)methane with one or two equivalents of trimethylaluminum

[8QN(AlMe₂)₂]   [Al₃]
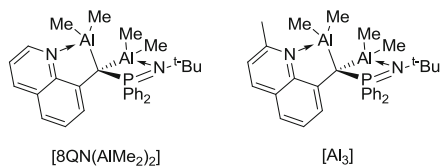
with a more important increase for indium. On the contrary, In–C bond distance of 2.173(3) Å is much more important in the indium complex than in the very similar gallium and aluminum one (respectively, 1.972(4) and 1.975(2) Å) and close to the one in the magnesium analogue complex (2.156(5) Å).

It is worth to notice that those complexes are the first group 13 methanediide complex featuring a dianionic carbon interacting with one sole metal atom and the first indium and gallium methanediide complexes.

It is also worth to cite a set of complexes of dissymmetrical, hypervalent phosphorus-substituted methanediide for which a dilithiated form has not been isolated to date, but which present interesting structures and reactivity. Complex [8QN (AlMe₂)₂] was obtained by stepwise reaction of diphenyl(N-tert-butyl)iminophosphorano-(8-quinolyl)methane with 1 equiv. of trimethylaluminum in toluene at 60°C and subsequent reaction of a second equivalent of trimethylaluminum at 120°C [104]. When 2 equiv. of trimethylaluminum is directly added and heated, complex [Al₃] is formed, for which the quinolyl substituent was methylated in position 2. A catalytic role of excess trialkylaluminum was highlighted (Chart 5).

Those two complexes have very similar structures, and characteristic bond lengths and angles concerning the iminophosphoranyl moiety are very close to those in spirocyclic complex [(**6**)(AlMe₂)₂]. For example, ($^{t-}$BuN)Ph₂PC–Al bond is 2.126(4) Å long in complex [Al₃] vs. 2.121(3) Å and 2.117(3) Å in complex [(**6**)(AlMe₂)₂].

7.2 Electronic Structure

Theoretical studies of group 13 complexes remain scarce. So et al. [37] have presented a description of the methanediide–aluminum bond in complex [(**10**)Al]₂ using various methods, from NBO analysis to QTAIM. Indeed, this species featuring one single aluminum atom bonded to one single methanediide is of particular interest, with the question of its belonging to the group of alkylidene complexes. In this species, the two lone pairs on the methanediide are described as sp$^{1.6}$ hybridized and pure p orbitals in, respectively, σ and π symmetries by NBO analysis. These two

lone pairs interact with $sp^{2.2}$ aluminum-centered hybrid orbital in σ symmetry and $p^3d^{1.1}$ aluminum-centered hybrid with almost no s character in π symmetry. In this model, aluminum–carbon interactions of σ and π symmetries are described as highly polarized toward carbon, with, respectively, 85 and 98% of carbon character. The overall carbon–aluminum interaction is thus described as strongly polarized and having little covalent character. The comparison between QTAIM values for a model of complex [(**7**)Al$_2$] and for the two related models, $H_2C=Al-CH_3$ and $H_3C-Al(CH_3)(SH)$ highlights similarities between both methanediide–aluminum interaction and methyl–aluminum interaction.

7.3   Reactivity

Two kinds of reactivity have been explored to date, essentially by Cavell on spirocyclic dimetallic bis(diphenyliminophosphoranyl)methanediide complexes [(**6**)(AlR$_2$)$_2$]. Bimetallic compound [(**6**)(AlMe$_2$)$_2$] was proved to react stoechiometrically with heteroallenes to afford the bimetallic bicyclic compounds [Al$_4$] and [Al$_5$] [105] (Eq. (4)).

$$[(\mathbf{6})(AlMe_2)_2]\qquad\begin{array}{l}X=N\text{-}Ad, Y=O: [Al_4]\\X=Y=N\text{-}Cy\ :\ [Al_5]\end{array}\tag{4}$$
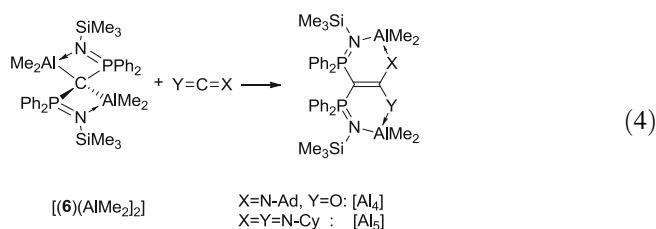
Complexes [(**6H**)AlR$_2$] and [(**6**)(AlR$_2$)$_2$], R=Me, ^{i}Pr (Scheme 34), have also proved to be efficient as polymerization catalysts [106], but the bimetallic [(**6**)(AlR$_2$)$_2$] species featured higher activities. Experiments using either aluminoxanes or trityl borates as activator suggested that reactivity relies on the functionality of the aluminum itself. Comparison between methyl and isobutyl bis-aluminum methanediide showed an increase of the molecular weight of the polymer and a decrease of the activity with the bulkiness of the ligand pendant to the aluminum atom. Copolymerization of ethylene and 1-octene was also performed with spirocyclic complex [(**6**)(AlMe$_2$)$_2$].

8   Group 14 Complexes

The synthesis and study of species containing a carbon-heavier group 14 element double bonds have known a growing interest since the first challenging isolation of a silene in 1981 [107]. Their very rich chemistry [108] is strongly related to their

peculiar electronic structure [109, 110]. The synthesis of such species usually requires bulky substituents to preclude dimerization process. Even more challenging is the synthesis of a terminal group 14 metallavinylidene $R_2C=M$, for which both steric protection around the group 14 metal and stability of its electronic configuration are intrinsically lowered. Hypervalent phosphorus-stabilized methanediides proved to be particularly appropriate precursors for the synthesis of such species and gave rise to a wide set of group 14 complexes of various structures, reflecting the complexity of any control on the structure and stability of multiple bonds between carbon and low-valent heavier group 14 metals.

8.1 Synthesis

Most classical hypervalent phosphorus-stabilized methanediide complexes of germanium [111, 112], tin, and lead [113] in their (+II) oxidation state are usually synthesized following either route B or intermediate route C. Most of the tin and lead complexes resulting from either route are dimeric, cyclic dimetalacyclobutanes, regardless of the steric bulkiness of the ligand (Scheme 35).

In 2001, Leung obtained the first non-dimetalacyclobutane structure for germanium [112]. Following route C with the well-known bis(trimethylsilyliminophosphoranyl)methane **6H$_2$**, complex [(**6**)Ge]$_2$ is obtained, resulting from a head-to-head dimerization of two germavinylidenes (Fig. 7). The Ge–Ge bonding was described as a donor–acceptor interaction. Both carbon–germanium bond lengths of 1.908(7) Å and 1.905(8) Å are shorter than the usual germanium–alkyl or aryl bonds. Multinuclear NMR spectroscopy showed one single signal for each nucleus, suggesting a fluxional coordination of amido groups to the two germanium centers at 25°C. Reactivity of this species has also been well studied and will be described in Sect. 8.3.

Using the dissymmetrical (thiophosphinoyl)(iminophosphoranyl)methane **10H$_2$** $CH_2(Ph_2P = S)(Ph_2 P=N-SiMe_3)$ as a neutral precursor of the ligand and following route B, Guo et al. [114] obtained the first stable monomeric stannavinylidene in solution. This last undergoes dimerization in the solid state (Eq. (5)). In this structure, the carbon–tin bond length of 2.2094(9) Å is much shorter than this in the corresponding monoanionic complex [{Ph$_2$P(S)}{Ph$_2$PN(SiMe$_3$)}CHSnN (SiMe$_3$)$_2$] of 2.384(4) Å, which suggests an increased C–Sn bond order. Interestingly, the same route with the symmetrical bis-iminophosphoranyl ligand **6H$_2$** gave a spirocyclic structure [112] (Scheme 35) with a longer C–Sn bond length of 2.376 Å in average. ^{119}Sn NMR spectra of compound [(**10**)Sn]$_2$ showed that no oligomer was present in solution. This dimeric structure in the solid state is very similar to this of analogous aluminum complex [(**10**)AlMe]$_2$.
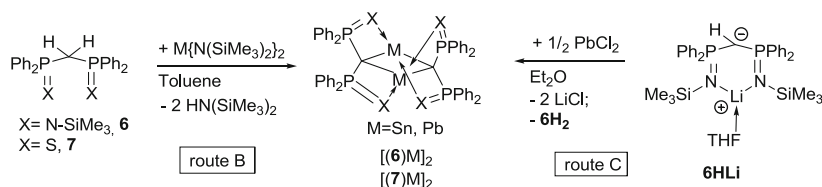
Scheme 35 Synthesis of dimeric, dimetallic, bis(iminophosphoranyl)methanediide and bis(thiophosphinoyl)methanediide group 14 metal complexes following route B or C
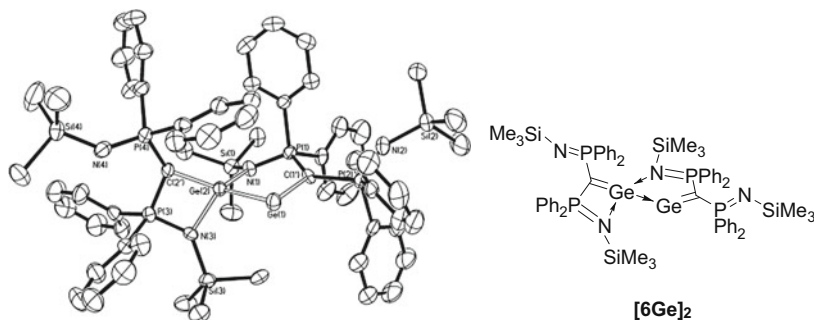
Fig. 7 ORTEP drawing and representation of [(**6**)Ge]$_2$; hydrogen atoms are omitted for clarity. Reproduced with permission from Wiley [112]

$$\text{(5)}$$
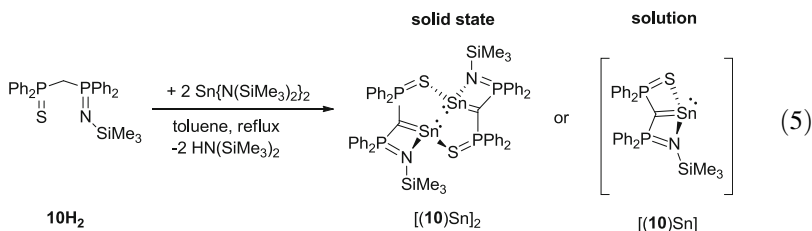
Another important advantage of both route B and C cited earlier is their reliability with precursors that are not available in an isolable dilithiated form. An impressive number of such precursors have been used in the chemistry of heavier group 14 metals, highlighting the pertinence of this synthetic approach for this group. In fact, most of the hypervalent phosphorus-stabilized methanediide complexes of group 14 metals belong to this set (Chart 6). Interestingly, all these mono-phosphorus-substituted ligands except one, namely, [(PhosN)Ge]$_3$, gave dimetalacyclobutane-type structures. In most cases too, the coordination number of each metallic center is brought to 3 for germanium and tin and to 4 for tin and lead by coordination of the more nucleophilic substituent amongst those available: iminophosphoranyl, pyridyl, and/or thiophosphinoyl moieties in decreasing nucleophilic order.
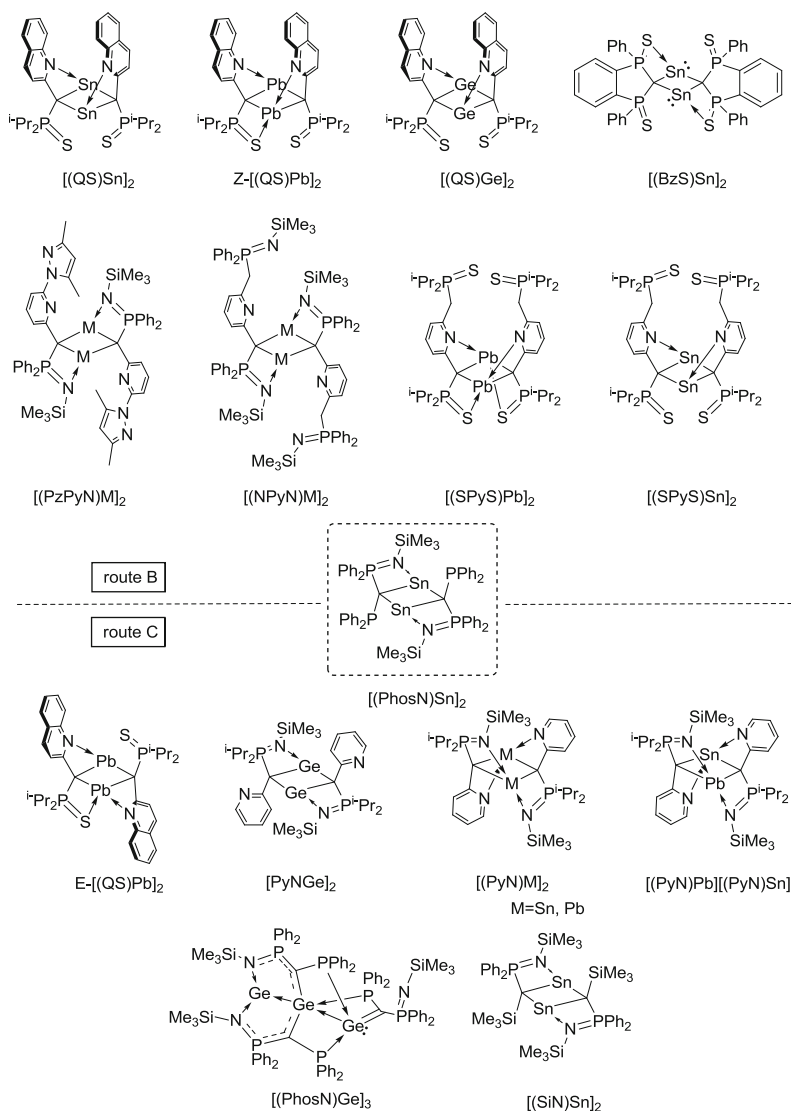
Chart 6 Representation of group 14 metal complexes featuring a non-usual hypervalent phosphorus-stabilized geminal dianion as a ligand, ordered according to their synthetic path. [**PyNM**]$_2$, M=Ge, Sn, Pb, and [**PyNPb**][**PyNSn**] [115]; [**QSSn**]$_2$, **E-[QSPb]**$_2$ [116]; [**PzPyNM**]$_2$, [**NPyNM**]$_2$ [117]; [**SiNSn**]$_2$ [118]; [**PhosNSn**]$_2$; [**PhosNGe**]$_3$ [115]; [**SPySM**]$_2$, M=Sn, Pb [119]; [**BzSSn**]$_2$ [120]. The complex in dashed frame could be synthesized by both routes

By the addition of diiron nonacarbonyl, complex [(PhosN)Sn]$_2$ is transformed to an iron tetracarbonyl adduct in which two stannavinylidenes arranged in a head-to-tail manner are subtended, one of which being coordinated to the iron atom by the mean of its lone pair (Eq. (6)).

$$[(PhosN)Sn]_2 \qquad \{[(PhosN)Sn]_2[Fe(CO)_4]\} \tag{6}$$
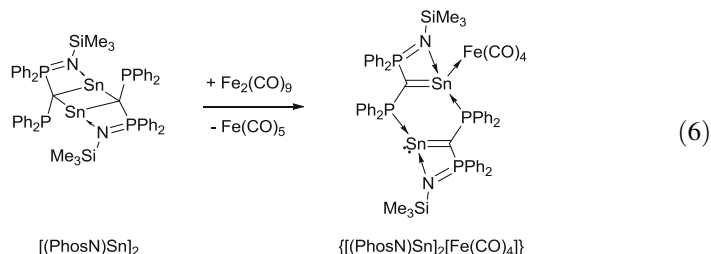
Despite potential undesired redox reactivity, route A was used for the successful synthesis of the first 2-germaallene or bis-methanediide complex by So et al. [121] starting from the high-valent $GeCl_4$ precursor and **7Li$_2$**, generated in situ (Eq. (7)).

$$\tag{7}$$
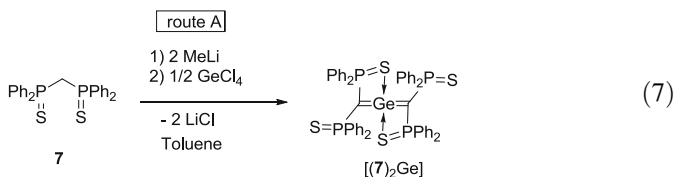
^{31}P NMR characterization of [(**7**)$_2$Ge] showed a single signal for phosphorus in solution even at low temperature, and two signals obtained in the solid state by ^{31}P CP/MAS-NMR. These observations suggest a coordination of the four sulfur atoms to the germanium center in solution. The germanium carbon bond lengths of 1.882(2) Å are slightly shorter than the one observed in Ge(II) complex [**6Ge**]$_2$ (1.908(7) Å and 1.905(8) Å). This shortening was attributed to the higher oxidation state of the metallic center.

Finally, one example of transmetalation from magnesium to tin was given by Leung in 2011 [122], resulting in the bis-methanediide complex [(**7**)$_2$Sn] analogue to the 2-germaallene [(**7**)$_2$Ge] (Eq. (8)).

$$[(7)Mg]_2 \qquad\qquad [(7)_2Sn] \tag{8}$$
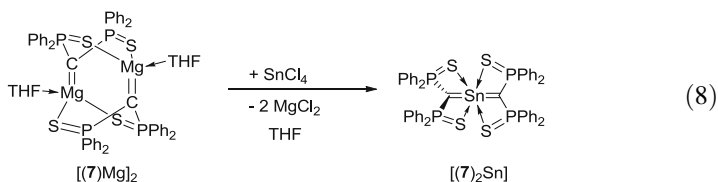
Contrarily to complex [(**7**)$_2$Ge], the crystallographic structure of [(**7**)$_2$Sn] showed a coordination of all of the four sulfur atoms to the metallic center. However, a fluxional decoordination of one thiophosphinoyl arm was observed to occur in solution, as highlighted by low-temperature NMR measurement.

8.2 Electronic Structure

Theoretical studies of group 14 hypervalent phosphorus-stabilized methanediide complexes are still relatively scarce. In most case, the bonding scheme between the carbon and the metal is evaluated from the observation of the evolution of bond lengths in crystallographic structures and comparison with previously described complexes (Table 6). Thus, in [(**7**)$_2$Ge] [121], the carbon–germanium bond distance of 1.882(2) Å is relatively long compared to other Ge(IV) germavinylidene (Table 6, entry 2,3,4). This observation together with the abnormal values of C–P and P–S bond lengths leads to the hypothesis of a π-electron delocalization around the Ge–C–P–S cycle by conjugation of P=S and C=Ge bonds. This results in a lowering of the bond order between carbon and germanium. This explanation was confirmed by theoretical calculation (see below) and was also verified for tin complex [(**7**)$_2$Sn] [122]. In a similar way, the shortening of the carbon–tin bond distance going from the stannacyclobutane [**6Sn**]$_2$ to the stannavinylidene [**10Sn**]$_2$ was attributed to an increase of the carbon–tin bond order, which was confirmed by DFT calculation [113] (Table 6, entry 5,6).

The first theoretical modeling of group 14 complexes was introduced in 2009 by So et al. [121] with a description of germanium bis-methanediide complex [(**7**)$_2$Ge]. From the crystallographic structure, one could already notice that the carbon–germanium interaction is weaker than the predicted interaction in the 2-germaallene $H_2C=Ge=CH_2$ [127] with a Ge–C bond length of 1.882(2) Å in [(**7**)$_2$Ge] vs. 1.745 Å predicted for $H_2C=Ge=CH_2$. A DFT calculation on the whole system, consisting in a geometric optimization, and an NBO analysis sustained the description of the germanium–carbon bond as an interaction between an $sp^{2.2}$-hybridized carbon-centered orbital and an $sp^{1.8}$-hybridized germanium-centered orbital. This interaction was described as having 71% carbon character. A study of the impact of sulfur atom coordination to the metallic center on the overall stability and evolution of carbon–germanium bond length was performed on a simplified model. It was showed that when this interaction was removed, the carbon–germanium bond lengths decreased to 1.789 Å and thus became close to this predicted for $H_2C=Ge=CH_2$, but it also resulted in a destabilization of ca. 54 kcal/mol compared to the similar system with two coordinated sulfur atoms. A topological analysis of the electronic density using Bader's Quantum Theory of Atoms in Molecules allowed the description of the carbon–germanium bond as being intermediate between an alkyl–germanium bond and a 2-germaallene.

The same group presented a similar study for the stannavinylidene [**10Sn**]$_2$ using a simplified model for which all substituents on phosphorus and nitrogen atoms have been replaced by hydrogen atoms [114]. An NBO analysis described the carbon–tin bond as resulting from two carbon–tin interactions of different symmetries: (1) an interaction of σ symmetry between an almost pure p, tin-centered orbital ($s^{0.25}p^{2.00}$ hybridized) and an $sp^{2.00}$-hybridized, carbon-centered orbital featuring 85% C character and (2) an interaction of π symmetry between two pure p, carbon- and tin-centered orbitals with 97% C character. The overall

Table 6 Carbon–metal bond distances for most significant metallavinylidenes or 2-metallaallenes of germanium and tin

M	Complex	d(C–M) (Å)	References
Ge(II)	[(**6**)Ge]$_2$	1.905(8)–1.908(7)	[112]
Ge(IV)	[(**7**)$_2$Ge]	1.882(2)	[121]
	[{(Me$_3$Si)$_2$ N}$_2$-Ge=C(Bt-Bu)$_2$C(SiMe$_3$)$_2$]	1.827(4)	[123]
	[Mes$_2$Ge=C$_{fluor}$]	1.803(4)	[124]
Sn(II)	[(**6**)Sn]$_2$	2.376 av.	[112]
	[(**10**)Sn]$_2$	2.2094(9)	[114]
Sn(IV)	[(**7**)$_2$Sn]	2.063(2)	[122]
	[(Tbt)(Mes)Sn=CR$_2$]	2.016(5)	[125]
	[{(Me$_3$Si)$_2$CH}$_2$Sn=C{(BtBu)$_2$C(SiMe$_3$)$_2$}]	2.025(4)	[126]

interaction is thus described as highly polarized toward carbon. Of interest are the second-order stabilizing interactions. It was shown that one lone pair on nitrogen interacts with a vacant, tin-centered p-rich hybrid, which represents a second-order stabilization energy of 80 kcal/mol. In a similar way, a sulfur-centered lone pair afforded 42 kcal/mol second-order stabilization energy by donation in the carbon–tin π* orbital. A topological analysis of the carbon–tin bond gave similar results as those obtained for [(**7**)$_2$Ge], i.e., a covalent but polar bond which is intermediate between what is calculated for tin alkyl and tin vinylidene.

Although some dimetalacyclobutane featured metal–metal bond distances short enough to ask the question of a metal–metal interaction [119], no theoretical studies were performed on these systems.

8.3 Reactivity

The very rich reactivity of bisgermavinylidene complex [(**6**)Ge]$_2$ was reviewed in 2007 by Leung et al. [111, 128]. This variety results both from the presence of two relatively available germanium- and carbon-centered lone pairs and a possible redox behavior of the low-valent germanium center (Scheme 36). Complex [(**6**)Ge]$_2$ was thus engaged in various reactions, showing its utility as follows: (1) a two-electron donor ligand toward Ni, Pd, Au [129], and Mn [130] (germanium lone pair-centered reactivity); (2) a reducing agent [129]; (3) a germaketene >C=Ge=E precursor (E = S, Se, Te) [131]; (4) a carbene transfer reagent [132]; (5) a germene precursor [128]; (6) a [2+2] cycloaddition, 1,2 addition [133], and [2+3] cycloaddition [134] reagent; and (7) a precursor of geminal heterodimetallic complexes of rhodium [130], iron, and manganese [134] (carbon lone pair-centered reactivity).

In gem-heterodimetallic structures featuring iron and manganese, the distance between germanium and the second metal is too long to sustain a germanium–metal interaction; the metal–carbon bond length is also longer than expected for a metal–
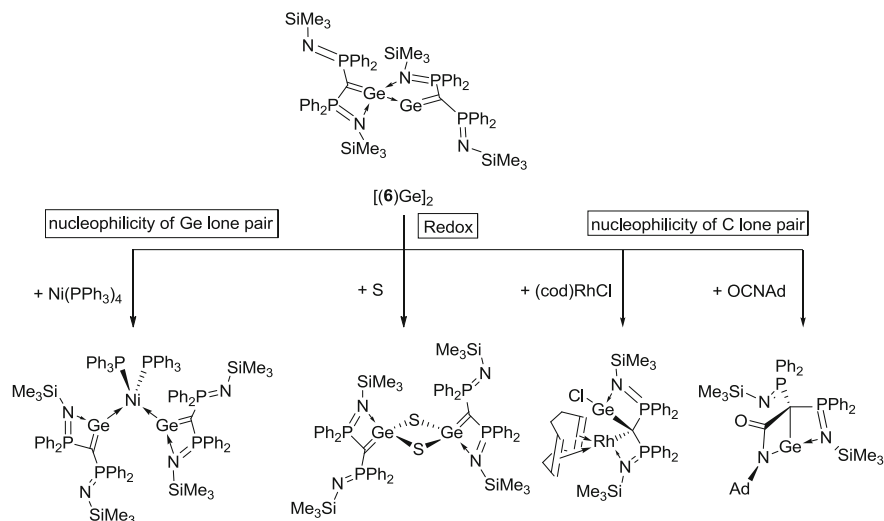
Scheme 36 Different kinds of reactivity featured by bisgermavinylidene complex [(**6**)Ge]₂

alkyl interaction, which was attributed to an important steric pressure. The reactivity of these species was not explored further to date.

In a similar way, the analogous tin complex [(**10**)Sn]₂ proved to undergo [2+2] cyclization reaction with various isocyanides and to coordinate rhodium (I) center by means of its carbon atom [135]. However, reaction with elemental sulfur [136] resulted in the formation of a mixed valence complex in which three complexes of tin (IV) sulfide condensed to a metallacyclohexane structure that stabilize a fourth tin atom in its second oxidation state. This structure was described as resulting from the oxidation of [(**10**)Sn]₂to a stannathiomethene which then decomposed partially to generate a bis(iminophosphoranyl)methene and SnS. This last by-product is further stabilized by 3 equiv. of the remaining stannathiomethene (Scheme 37). This complex was modeled by means of DFT, and an NBO analysis was performed. The apical tin–sulfur interaction was described as a single σ bond between a pure p, tin-centered orbitals and an sp$^{1.8}$-hybridized, sulfur-centered orbital. Interaction with the other sulfur atoms resulted in an overlap between almost pure p orbitals from the tin atom and sp-hybridized orbital of high p character from the adjacent sulfur atoms. An almost pure s occupied orbital remained on the tin atom. Each carbon connected to a tin atom was described as σ-bonded to each corresponding tin atom. The remaining lone pair of p character on each carbon was stabilized by hyperconjugation in adjacent σ*C=P, σ*P=S, and σ*Sn=S orbitals. The carbon–tin bonds were described as highly polarized toward carbon and with high ionic character.

In contrast, until recently, the only reported reaction for stanna- and plumbacyclobutanes [(**7**)Pb]₂ (Eq. (9)) was their oxidation by elementary chalcogen to afford chalcogenate species resulting from the chalcogen insertion into the C–M bond [113].
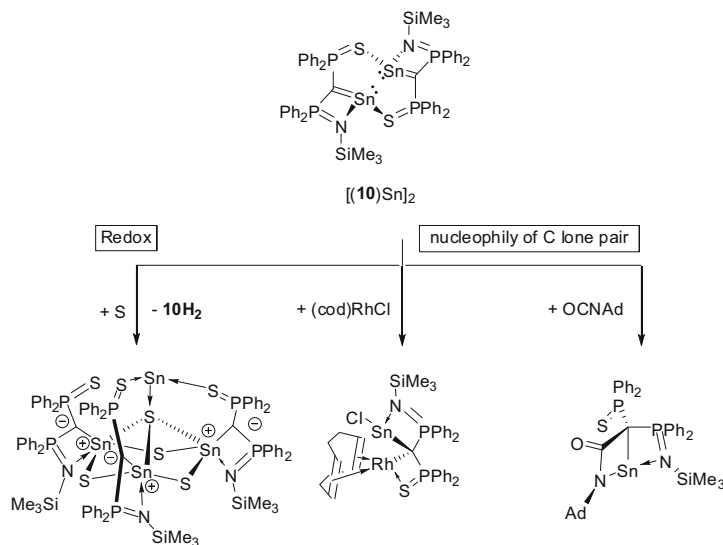
$[(\mathbf{10})Sn]_2$

Scheme 37 Different kinds of reactivity featured by bisstannavinylidene complex $[(\mathbf{10})Sn]_2$

$[(\mathbf{7})Pb]_2$ (9)
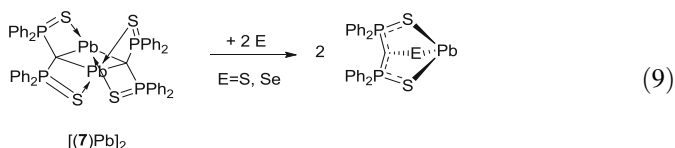
In 2012, So et al. probed the reactivity of tin complex $[(BzS)Sn]_2$ toward group 12, 13 and 14 species (Scheme 38) [120]. It was shown that despite the presence of a free lone pair on the tin atom, trichloroaluminum coordinates preferentially to the carbon atom, resulting in the formation of a heterodimetallic aluminum/tin complex that was isolated in its monomeric form. A same trend is observed with trichlorogallium and trichlorogermanium [137] (Scheme 38). A transmetalation reaction between trimethylaluminum and $[(BzS)Sn]_2$ allowed the isolation of the dimeric, zwitterionic aluminum complex $[(BzS)Al]_2$.

A very different reactivity was observed with diethylzinc. Instead of a simple electrophilic addition to the carbon or tin lone pairs, the tin atom is oxidized to Sn (IV) and one half equivalent of the ligand is desulfurized (Eq. (10)). The resulting product is isolated as a dimeric, dimetallic structure in which the freed sulfur atom is trapped as a μ^3-thio ligand bridging between two zinc atoms and a tin atom. This latter is in (+IV) oxidation state and is also coordinated to the dianionic carbon of the benzodithiophosphonylmethanediide ligand. The desulfurized, transient carbene $C_6H_4(PhPS)(PhP)C$: was supposed to be an intermediate product of this reaction, isolated as its two-time protonated form after proton abstraction from the solvent.
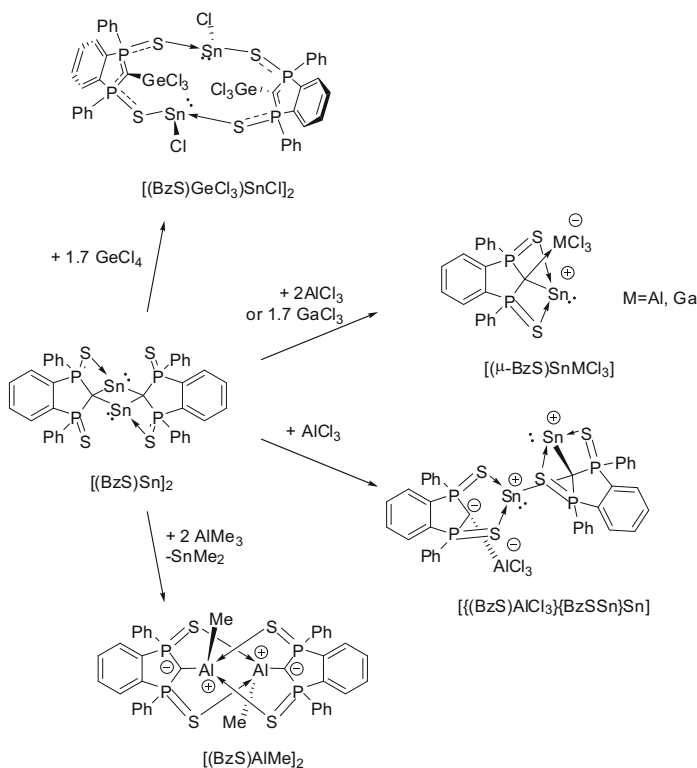
Scheme 38 Reactivity of dimeric tin 1,3-benzobis(thiophosphinoyl)methanediide complex toward group 12, 13, and 14 compounds

(10)
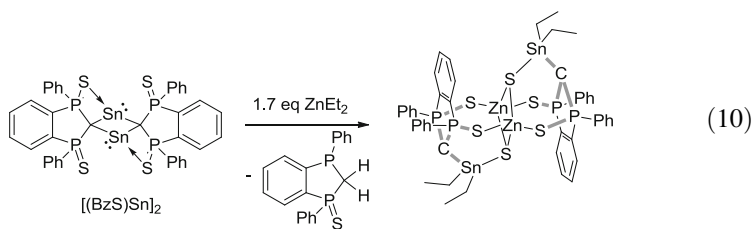
9 Conclusion

In conclusion, the chemistry based on isolable geminal dianions has gained momentum in the past 15 years. This can be traced back to the independent synthesis by Cavell et al. and Stephan et al. of the bis-iminophosphorane derivative **6Li$_2$**, in very satisfactory yield, which truly allowed novel directions to be pursued. Indeed, compared to earlier examples of geminal dianions, this species possesses two very important features: (1) two strongly electron-accepting phosphorus

π lone pair interactions

| stabilization via negative hyperconjugation into σ* P-R | donation into orbitals of appropriate symmetry at the metal | electrostatic interaction |
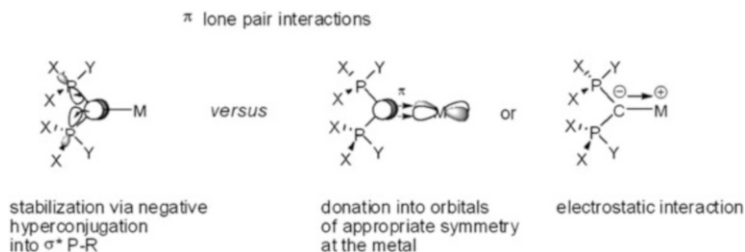
Scheme 39 Stabilization of the π lone pair on dianionic carbon within a complex

substituents which allow the desired efficient stabilization of the two charges at the same C atom to the point that the geminal dianion is generated with *stoichiometric* amounts of base (to be carefully chosen) and (2) a very convenient NMR probe (^{31}P) which allows a careful following of the reactions involving these highly sensitive species. Combined, these two features were the key to the development of other examples of geminal dianions in which both electronics and sterics could be tuned. We have focused this review on the complexes of early transition metals (groups 3–4 and actinides) as well as main group metals (groups 1–2 and 13–14) because of the intrinsic difference of the nature of the C–M interaction in these species, and with late transition metals. Indeed, the presence of the two lone pairs at C provides unique opportunity to generate species featuring an M=C double-bond interaction (at least formally) between C and strongly electropositive metals. Three facets of this chemistry have been developed so far for each group of metals. The first important facet dealt with the synthesis of the complexes themselves, featuring a single M=C interaction rather than bimetallic C bridging complexes. The second facet of this chemistry focused on the electronic nature of the M–C interaction, and the third facet concerned the reactivity of these complexes. The three facets have been extensively studied with groups 2–4. Overall, the nature of the M–C interaction in these species can be tuned to a large extent by playing on several parameters: nature of all phosphorus substituents, nature of the metal, and nature of the other ligands at the metal. Indeed, in a geminal dianion, the moieties at the phosphorus center strongly stabilize the two carbon lone pairs by hyperconjugation. The same stabilizing interaction will also exist in the metal complexes. Then, the precise electronic character of "M=C" double bond will depend on the relative proportion between stabilization and donation into orbitals of appropriate symmetry and energy at the metal (Scheme 39).

Because of these peculiar features, several directions can be foreseen in this domain. For example, analogies could be drawn between the recently developed chemistry with "non-innocent" ligands which allow H–L (typically H$_2$) addition at metal/ligand without oxidation of the metal center and the "dianion/metal" complexes presented in this review (Scheme 40). We believe that H–L additions to the C=M bond could be a first step in catalyzed additions on polar or nonpolar A=B systems. Such bond activation would provide an alternative to the sigma bond metathesis operating with early transition metals.
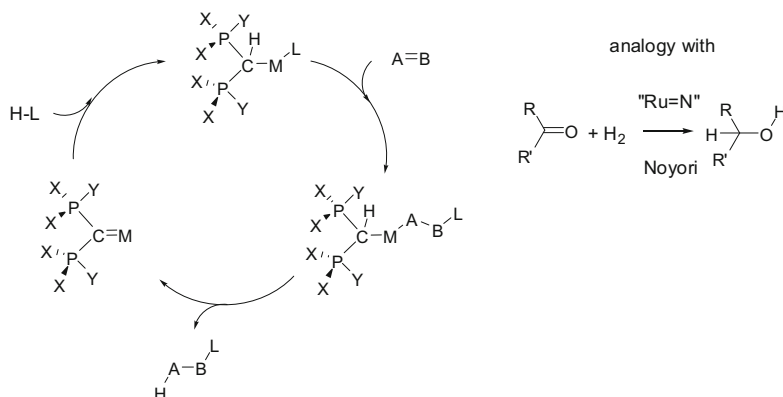
Scheme 40 Reaction scheme of an expected catalytic cycle for addition reactions on unsaturated molecule driven by a coordinated geminal dianion

References

1. Wittig G, Harborth G (1944) Über das Verhalten nichtaromatischer Halogenide und Äther gegenüber Phenyl-lithium. Chem Ber 77:306. doi:10.1002/cber.19440770505
2. West R, Rochow EG (1953) Reactions of dibromoalkanes with lithium metal. J Org Chem 18:1739. doi:10.1021/jo50018a018
3. Ziegler K, Nagel K, Patheiger M (1955) Metallorganische verbindungen. XX. Lithium- und magnesium-methylen. Z Anorg Allg Chem 282:345–351. doi:10.1002/zaac.19552820136
4. Laidig WD, Schaefer HF (1978) Structures and energetics of planar and tetrahedral dilithiomethane. A near degeneracy of singlet and triplet electronic states. J Am Chem Soc 100:5972–5973. doi:10.1021/ja00486a075
5. Jemmis ED, Von Schleyer Ragué P, Pople JA (1978) Structure and bonding of CH_2Li_2 dimers. J Organomet Chem 154:327–335. doi:10.1016/S0022-328X(00)90872-6
6. Kawa H, Manley BC, Lagow RJ (1985) Synthesis of 1,1-dilithio-2,2,3,3-tetramethylcyclopropane. J Am Chem Soc 107:5313–5314. doi:10.1021/ja00304a069
7. Kawa H, Manley BC, Lagow RJ (1988) Polylithium compounds: a new general high yield synthesis for 1,1-dilithio compounds. Polyhedron 7:2023–2025. doi:10.1016/S0277-5387(00)80718-4
8. Linti G, Rodig A, Pritzkow H (2002) 9,9-Dilithiofluorene: the first crystal-structure analysis of an alpha, alpha-dilithiated hydrocarbon. Angew Chem Int Ed 41:4503–4506. doi:10.1002/1521-3773(20021202)41:23<4503::AID-ANIE4503>3.0.CO;2-5
9. Gais HJ, Vollhardt J, Guenther H, Moskau D, Lindner HJ, Braun S (1988) Solid-state and solution structure of dilithium trimethyl[(phenylsulfonyl)methyl]silane, a true dilithiomethane derivative. J Am Chem Soc 110:978–980. doi:10.1021/ja00211a054
10. Zarges W, Marsch M, Harms K, Boche G (1989) X-ray structure analysis of alpha-lithiophenylacetonitrile. Lithium diisopropyl amide. 2 Tetramethylethylenediamine. A quasi-dianion complex. Angew Chem Int Ed 28:1392–1394. doi:10.1002/anie.198913921
11. Corset J, Castellà-Ventura M, Froment F, Strzalko T, Wartski L (2003) Study of the lithiated phenylacetonitrile monoanions and dianions formed according to the lithiated base used (LHMDS, LDA, or n-BuLi). 1. Evidence of heterodimer ("Quadac") or dianion formation by vibrational spectroscopy. J Org Chem 68:3902–3911. doi:10.1021/jo020492t

12. Strzalko T, Wartski L, Corset J, Castellà-Ventura M, Froment F (2012) Study of the lithiated phenylacetonitrile monoanions and dianions formed according to the lithiated base used (LHMDS, LDA, or n-BuLi). 2. Alkylation and deuteration mechanism study by vibrational and NMR spectroscopy and quantum chemistry calculations. J Org Chem 77:6431–6442. doi:10.1021/jo300758g

13. Zarges W, Marsch M, Harms K, Boche G (1989) [{Li$_2$(Me$_3$SiCCN)}$_{12}$(Et$_2$O)$_6$(C$_6$H$_{14}$)], Kristallstruktur mit dem trimethylsilylacetonitril-dianion. Chem Ber 122:1307–1311. doi:10.1002/cber.19891220714

14. Müller J, Neuburger M, Springer B (1999) X-Ray structure of a heterochiral, sulfoximine-stabilized dilithiomethane derivative. Angew Chem Int Ed 38:3549–3552. doi:10.1002/(SICI)1521-3773(19991203)38:23<3549::AID-ANIE3549>3.0.CO;2-D

15. Müller JFK, Neuburger M, Springer B (1999) Structural investigation of a dilithiated phosphonate in the solid state. Angew Chem Int Ed 38:92–94. doi:10.1002/(SICI)1521-3773(19990115)38:1/2<92::AID-ANIE92>3.0.CO;2-U

16. Kasani A, Babu RPK, Mcdonald R, Cavell RG (1999) [Ph$_2$P(NSiMe$_3$)]$_2$CLi$_2$: a dilithium dianionic methanide salt with an unusual Li$_4$C$_2$ cluster structure. Angew Chem Int Ed 38:1483–1484. doi:10.1002/(SICI)1521-3773(19990517)38:10<1483::AID-ANIE1483>3.0.CO;2-D

17. Ong CM, Stephan DW (1999) Lithiations of Bis-diphenyl-N-trimethylsilylphosphinimi-nomethane: an X-ray structure of a 1,1-dilithiomethane derivative. J Am Chem Soc 121:2939–2940. doi:10.1021/ja9839421

18. Cantat T, Mézailles N, Ricard L, Jean Y, Le Floch P (2004) A bis(thiophosphinoyl) methanediide palladium complex: coordinated dianion or nucleophilic carbene complex? Angew Chem Int Ed 43:6382–6385. doi:10.1002/anie.200461392

19. Cantat T, Ricard L, Le Floch P, Me N (2006) Phosphorus-stabilized geminal dianions. Organometallics 25:4965–4976. doi:10.1021/om060450l

20. Demange M, Boubekeur L, Auffrant A, Mézailles N, Ricard L, Le Goff X, Le Floch P (2006) A new and convenient approach towards bis(iminophosphoranyl)methane ligands and their dicationic, cationic, anionic and dianionic derivatives. New J Chem 30:1745. doi:10.1039/b610049j

21. Chen J-H, Guo J, Li Y, So C-W (2009) Synthesis and structure of [Li$_2$C(PPh$_2$=NSiMe$_3$)(PPh$_2$=S)]: a geminal dianionic ligand. Organometallics 28:4617–4620. doi:10.1021/om900364j

22. Schröter P, Gessner VH (2012) Tetrahedral versus planar four-coordinate carbon: a sulfonyl-substituted methandiide. Chemistry 18:11223–11227. doi:10.1002/chem.201201369

23. Heuclin H, Le Goff XF, Mézailles N (2012) Mixed (P=S/P=O)-stabilized geminal dianion: facile diastereoselective intramolecular C–H activations by a related ruthenium-carbene complex. Chem Eur J 18:16136–16144. doi:10.1002/chem.201202680

24. Heuclin H, Fustier-Boutignon M, Ho SY, Le Goff X-F, Carenco S, So C, Mézailles N (2013) Synthesis of phosphorus(V)-stabilized geminal dianions. The cases of mixed P=X/P → BH$_3$ (X=S, O) and P=S/SiMe$_3$ derivatives. Organometallics 32:498–508. doi:10.1021/om300954a

25. Cooper OJ, McMaster J, Lewis W, Blake AJ, Liddle ST (2010) Synthesis and structure of [U{C(PPh(2)NMes)(2)}(2)] (Mes=2,4,6-Me(3)C(6)H(2)): a homoleptic uranium bis (carbene) complex with two formal U[double bond, length as m-dash]C double bonds. Dalton Trans 39:5074–5076. doi:10.1021/om300954a

26. Cooper OJ, Wooles AJ, McMaster J, Lewis W, Blake AJ, Liddle ST (2010) A monomeric dilithio methandiide with a distorted trans-planar four-coordinate carbon. Angew Chem Int Ed 49:5570–5573. doi:10.1002/anie.201002483

27. Schröter P, Gessner VH (2012) Tetrahedral versus planar four-coordinate carbon: a sulfonyl-substituted methandiide. Chemistry 18:11223–11227

28. Hull KL, Noll BC, Henderson KW (2006) Structural characterization and dynamic solution behavior of the disodio and lithio–sodio geminal organodimetallics [{{Ph$_2$P(Me$_3$Si)N}$_2$ CNa 2–2] and [{{Ph$_2$P(Me$_3$Si)N}$_2$ CLiNa}$_2$]. Organometallics 25:4072–4074

29. Hull KL, Carmichael I, Noll BC, Henderson KW (2008) Homo- and heterodimetallic geminal dianions derived from the bis(phosphinimine) {Ph$_2$P(NSiMe$_3$)}2CH$_2$ and the alkali metals Li, Na, and K. Chem Eur J 14:3939–3953. doi:10.1002/chem.200701976

30. Orzechowski L, Jansen G, Harder S (2009) Methandiide complexes (R$_2$CM$_2$) of the heavier alkali metals (M=potassium, rubidium, cesium): reaching the limit? Angew Chem Int Ed 48:3825–3829. doi:10.1002/anie.200900830

31. Klobukowski M, Decker S, Lovallo C, Cavell R (2001) Structure and bonding in an octahedral Li$_4$C$_2$ cluster, the dilithium bis {dihydrido(silylimino)phosphorano}methanide dimer. A combined DFT–AIM analysis. J Mol Struct (THEOCHEM) 536:189–194. doi:10.1016/S0166-1280(00)00626-6

32. Cantat T, Jacques X, Ricard L, Le Goff XF, Mézailles N, Le Floch P (2007) From a stable dianion to a stable carbenoid. Angew Chem Int Ed 46:5947–5950. doi:10.1002/anie.200701588

33. Konu J, Chivers T (2008) Formation of a stable dicarbenoid and an unsaturated C$_2$P$_2$S$_2$ ring from two-electron oxidation of the [C(PPh$_2$S)$_2$]$^{2-}$ dianion. Chem Commun 4995–4997. doi:10.1039/B810796C

34. Heuclin H, Ho SY-F, Le Goff XF, So C-W, Mézailles N (2013) Facile B–H bond activation of borane by stable carbenoid species. J Am Chem Soc 135:8774–8777. doi:10.1021/ja401763c

35. Molitor S, Gessner VH (2013) Reactivity of stabilized Li/Cl carbenoids towards Lewis base adducts of BH$_3$: B–H bond activation versus carbene dimerization. Chem Eur J 19:11858–11862. doi:10.1002/chem.201302612

36. Konu J, Chivers T, Tuononen HM (2010) Synthesis and redox behaviour of the chalcogen-ocarbonyl dianions [(E)C(PPh(2)S)(2)](2-): formation and structures of chalcogen-chalcogen bonded dimers and a novel selone. Chem Eur J 16:12977–12987. doi:10.1002/chem.201001699

37. Guo J, Lee J-S, Foo M-C, Lau K-C, Xi H-W, Lim KH, So C-W (2010) Synthesis and characterization of magnesium and aluminum bis(phosphoranyl)methanediide complexes. Organometallics 29:944. doi:10.1021/om900985f

38. Leung W-P, Wan C-L, Mak TCW (2010) Synthesis and structure of magnesium and group 13 metal bis(thiophosphinoyl)methanediide complexes. Organometallics 29:1622–1628. doi:10.1021/om100019c

39. Orzechowski L, Jansen G, Harder S (2006) Synthesis, structure, and reactivity of a stabilized calcium carbene: R$_2$CCa. J Am Chem Soc 128:14676–14684. doi:10.1021/ja065000z

40. Orzechowski L, Harder S (2007) Isolation of an intermediate in the catalytic trimerization of isocyanates by a monomeric calcium carbene with chelating iminophosphorane substituents. Organometallics 26:2144–2148. doi:10.1021/om070023n

41. Orzechowski L, Jansen G, Lutz M, Harder S (2009) Calcium carbene complexes with boranophosphorano side-arms: CaC[P(Ph)$_2$BH$_3$]$_2$. Dalton Trans 2958–2964. doi:10.1039/B823224E

42. Orzechowski L, Harder S (2007) Syntheses, structures, and reactivity of barium carbene complexes with chelating bis-iminophosphorano arms. Organometallics 26:5501–5506. doi:10.1021/om700640c

43. Hogenbirk M, Schat G, Akkerman OS, Bickelhaupt F, Smeets WJJ, Spek AL (1992) The first X-ray structure of a 1,1-di-Grignard compound: bis(bromomagnesio)bis(trimethylsilyl)methane. J Am Chem Soc 114:7302–7303. doi:10.1021/ja00044a056

44. Giesbrecht GR, Gordon JC (2004) Lanthanide alkylidene and imido complexes. Dalton Trans 2387–2393. doi:10.1039/b407173e

45. Clark DL, Gordon JC, Hay PJ, Poli R (2005) Existence and stability of lanthanide − main group element multiple bonds. New paradigms in the bonding of the 4f elements. A DFT

study of Cp_2CeZ ($Z=F^+$, O, NH, CH^-, CH_2) and the ligand adduct $Cp_2Ce(CH_2)(NH_3)$. Organometallics 24:5747–5758. doi:10.1021/om050693y

46. Hong J, Zhang L, Yu X, Li M, Zhang Z, Zheng P, Nishiura M, Hou Z, Zhou X (2011) Syntheses, structures, and reactivities of homometallic rare-earth-metal multimethyl methylidene and oxo complexes. Chem Eur J 17:2130–2137. doi:10.1002/chem.201002670

47. Zhang W, Wang Z, Nishiura M, Xi Z, Hou Z (2011) $Ln_4(CH_2)_4$ cubane-type rare-earth methylidene complexes consisting of "$(C_5Me_4SiMe_3)LnCH_2$" units (Ln=Tm, Lu). J Am Chem Soc 133:5712–5715. doi:10.1021/ja200540b

48. Dietrich HM, Törnroos KW, Anwander R (2006) "Ionic carbenes": synthesis, structural characterization, and reactivity of rare-Earth metal methylidene complexes. J Am Chem Soc 128:9298–9299. doi:10.1021/ja062523y

49. Scott J, Fan H, Wicker BF, Fout AR, Baik M-H, Mindiola DJ (2008) Lewis acid stabilized methylidene and oxoscandium complexes. J Am Chem Soc 130:14438–14439. doi:10.1021/ja806635x

50. Aparna K, Ferguson M, Cavell RG (2000) A monomeric samarium bis (iminophosphorano) chelate complex with a Sm=C bond. J Am Chem Soc 122:726–727. doi:10.1021/ja9936114

51. Liddle ST, Mills DP, Wooles AJ (2010) Bis(phosphorus-stabilised)methanide and methandiide derivatives of group 1–5 and f-element metals. Organomet Chem 36:29–55. doi:10.1039/9781847559616-00029

52. Panda TK, Roesky PW (2009) Main-group and transition-metal complexes of bis (phosphinimino)methanides. Chem Soc Rev 38:2782–2804. doi:10.1039/b903651b

53. Heuclin H, Fustier M, Auffrant A, Mézailles N (2010) Bis-phosphorus(V) stabilized carbene complexes. Lett Org Chem 7:596–611. doi:10.2174/157017810793811740

54. Liddle ST, Mills DP, Wooles AJ (2011) Early metal bis(phosphorus-stabilised)carbene chemistry. Chem Soc Rev 40:2164–2176. doi:10.1039/c0cs00135j

55. Buchard A, Auffrant A, Ricard L, Le Goff XF, Platel RH, Williams CK, Le Floch P (2009) First neodymium(III) alkyl-carbene complex based on bis(iminophosphoranyl) ligands. Dalton Trans 10219–10222. doi:10.1039/B918971H

56. Wooles AJ, Cooper OJ, Mcmaster J, Lewis W, Blake AJ, Liddle ST (2010) Synthesis and characterization of dysprosium and lanthanum bis (iminophosphorano) methanide and -methanediide complexes. Organometallics 29:2315–2321. doi:10.1021/om100104s

57. Mills DP, Cooper OJ, McMaster J, Lewis W, Liddle ST (2009) Synthesis and reactivity of the yttrium-alkyl-carbene complex $[Y(BIPM)(CH_2C_6H_5)(THF)]$ (BIPM=$\{C(PPh_2NSiMe_3)_2\}$). Dalton Trans 4547–4555. doi:10.1039/b902079a

58. Cantat T, Jaroschik F, Nief F, Ricard L, Mézailles N, Le Floch P (2005) New mono- and bis-carbene samarium complexes: synthesis, X-ray crystal structures and reactivity. Chem Commun 5178–5180. doi:10.1039/b510327d

59. Cantat T, Jaroschik F, Ricard L, Le Floch P, Nief F, Mézailles N (2006) Thulium alkylidene complexes: synthesis, X-ray structures, and reactivity. Organometallics 25:1329–1332. doi:10.1021/om050877c

60. Liddle ST, McMaster J, Green JC, Arnold PL (2008) Synthesis and structural characterisation of an yttrium-alkyl-alkylidene. Chem Commun 78:1747–1749. doi:10.1039/b719633d

61. Mills DP, Wooles AJ, McMaster J, Lewis W, Blake AJ, Liddle ST (2009) Heteroleptic $[M(CH_2C_6H_5)2(I)(THF)_3]$ complexes (M=Y or Er): remarkably stable precursors to yttrium and erbium t-shaped carbenes. Organometallics 28:6771–6776. doi:10.1021/om9007949

62. Gregson M, Lu E, McMaster J, Lewis W, Blake AJ, Liddle ST (2013) A cerium(IV)-carbon multiple bond. Angew Chem Int Ed 52:13016–13019. doi:10.1002/anie.201306984

63. Liddle ST, Mills DP, Gardner BM, McMaster J, Jones C, Woodul WD (2009) A heterobimetallic gallyl complex containing an unsupported Ga–Y bond. Inorg Chem 48:3520–3522. doi:10.1021/ic900278t

64. Wooles AJ, Mills DP, Lewis W, Blake AJ, Liddle ST (2010) Lanthanide tri-benzyl complexes: structural variations and useful precursors to phosphorus-stabilised lanthanide carbenes. Dalton Trans 39:500–510. doi:10.1039/b911717b

65. Fustier M, Le Goff XF, Le Floch P, Mézailles N (2010) Nucleophilic scandium carbene complexes. J Am Chem Soc 132:13108–13110. doi:10.1021/ja103220s

66. Mills DP, Soutar L, Lewis W, Blake AJ, Liddle ST (2010) Regioselective C–H activation and sequential C–C and C–O bond formation reactions of aryl ketones promoted by an yttrium carbene. J Am Chem Soc 132:14379–14381. doi:10.1021/ja107958u

67. Mills DP, Lewis W, Blake AJ, Liddle ST (2013) Reactivity studies of a T-shaped yttrium carbene: C–F and C–O bond activation and C=C bond formation promoted by [Y(BIPM)(I)(THF)$_2$] (BIPM=C(PPh$_2$NSiMe$_3$)$_2$). Organometallics 32:1239–1250. doi:10.1021/om301016j

68. Mills DP, Soutar L, Cooper OJ, Lewis W, Blake AJ, Liddle ST (2013) Reactivity of the yttrium alkyl carbene complex [Y(BIPM)(CH$_2$C$_6$H$_5$)(THF)] (BIPM={C(PPh$_2$NSiMe$_3$)$_2$})$^{2-}$: from insertions, substitutions, and additions to nontypical transformations. Organometallics 32:1251–1264. doi:10.1021/om3010178

69. Buchard A, Platel RH, Auffrant A, Le Goff XF, Le Floch P, Williams CK (2010) Iminophosphorane neodymium(III) complexes as efficient initiators for lactide polymerization. Organometallics 29:2892–2900. doi:10.1021/om1001233

70. Fustier-Boutignon M, Heuclin H, Le Goff XF, Mézailles N (2012) Transmetalation of a nucleophilic carbene fragment: from early to late transition metals. Chem Commun 48:3306–3308. doi:10.1039/c2cc17934b

71. Cramer RE, Maynard RB, Paw JC, Gilje JW (1981) A uranium-carbon multiple bond. Crystal and molecular structure of (.eta.5-C$_5$H$_5$)3UCHP(CH$_3$)$_2$(C$_6$H$_5$). J Am Chem Soc 103:3589–3590. doi:10.1021/ja00402a065

72. Cantat T, Arliguie T, Noël A, Thuéry P, Ephritikhine M, Le Floch P, Mézailles N (2009) The U=C double bond: synthesis and study of uranium nucleophilic carbene complexes. J Am Chem Soc 131:963–972. doi:10.1021/ja807282s

73. Cooper OJ, McMaster J, Lewis W, Blake AJ, Liddle ST (2010) Synthesis and structure of [U{C(PPh$_2$NMes)$_2$}$_2$] (Mes = 2,4,6-Me(3)C(6)H(2)): a homoleptic uranium bis(carbene) complex with two formal U=C double bonds. Dalton Trans 5074–5076. doi:10.1039/c0dt00152j

74. Tourneux J-C, Berthet J-C, Thuéry P, Mézailles N, Le Floch P, Ephritikhine M (2010) Easy access to uranium nucleophilic carbene complexes. Dalton Trans 39:2494–2496. doi:10.1039/b926718m

75. Tourneux J-C, Berthet J-C, Cantat T, Thuéry P, Mézailles N, Le Floch P, Ephritikhine M (2011) Uranium(IV) nucleophilic carbene complexes. Organometallics 30:2957–2971. doi:10.1021/om200006g

76. Ma G, Ferguson MJ, McDonald R, Cavell RG (2011) Actinide metals with multiple bonds to carbon: synthesis, characterization, and reactivity of U(IV) and Th(IV) bis(iminophosphorano)methandiide pincer carbene complexes. Inorg Chem 50:6500–6508. doi:10.1021/ic102537q

77. Tourneux J-C, Berthet J-C, Cantat T, Thuéry P, Mézailles N, Ephritikhine M (2011) Exploring the uranyl organometallic chemistry: from single to double uranium-carbon bonds. J Am Chem Soc 133:6162–6165. doi:10.1021/ja201276h

78. Cooper OJ, Mills DP, McMaster J, Moro F, Davies ES, Lewis W, Blake AJ, Liddle ST (2011) Uranium-carbon multiple bonding: facile access to the pentavalent uranium carbene [U{C(PPh$_2$NSiMe$_3$)$_2$}(Cl)2(I)] and comparison of U(V)=C and U(IV)=C bonds. Angew Chem Int Ed 50:2383–2386. doi:10.1002/anie.201007675

79. Sarsfield MJ, Steele H, Teat SJ (2003) Uranyl bis-iminophosphorane complexes with in- and out-of-plane equatorial coordination. Dalton Trans 3443–3449. doi:10.1039/B304602H

80. Mills DP, Cooper OJ, Tuna F, McInnes EJL, Davies ES, McMaster J, Moro F, Lewis W, Blake AJ, Liddle ST (2012) Synthesis of a uranium(VI)-carbene: reductive formation of

uranyl(V)-methanides, oxidative preparation of a $[R2C=U=O]^{2+}$ analogue of the $[O=U=O]^{2+}$ uranyl ion (R=Ph$_2$PNSiMe$_3$), and comparison of the nature of U(IV)=C, U(V)=C, and U(VI)=C double bonds. J Am Chem Soc 134:10047–10054. doi:10.1021/ja301333f

81. Mills DP, Moro F, McMaster J, Van Slageren J, Lewis W, Blake AJ, Liddle ST (2011) A delocalized arene-bridged diuranium single-molecule magnet. Nat Chem 3:454–460. doi:10.1038/nchem.1028

82. Fortier S, Walensky JR, Wu G, Hayton TW (2011) Synthesis of a phosphorano-stabilized U(IV)-carbene via one-electron oxidation of a U(III)-ylide adduct. J Am Chem Soc 133:6894–6897. doi:10.1021/ja2001133

83. Cramer RE, Maynard RB, Paw JC, Gllje JW (1982) Carbon monoxide insertion into a U–C double bond. Organometallics 1:869–871. doi:10.1021/om00066a020

84. Cramer RE, Jeong JH, Gilje JW (1987) Uranium–carbon multiple bond chemistry. 9. The insertion of phenyl isocyanate into the uranium-carbon bond of Cp3U:CHP(Ph)(R)(Me) to form Cp3U[(NPh)(O)CCHP(Ph)(R)(Me)]. Organometallics 6:2010–2012. doi:10.1021/om00152a040

85. Cramer RE, Higa KT, Gilje JW (1984) U–C multiple bonds. 4. Addition of coordinated carbon monoxide across a uranium-carbon multiple bond. J Am Chem Soc 106:7245–7247. doi:10.1021/ja00335a065

86. Cramer RE, Higa KT, Pruskin SL, Gilje JW (1983) U–C multiple bond chemistry. 2. Coupling of bridging and terminal carbonyls in the formation of an iron .eta.1:.eta.3-allyl complex. J Am Chem Soc 105:6749–6750. doi:10.1021/ja00360a052

87. Cramer RE, Engelhardt U, Higa KT, Gilje JW (1987) U–C multiple bond chemistry. The reaction of Cp3UCHP (CH$_3$) (C$_6$H$_6$)$_2$ with diphenylamine and the structure of Cp$_3$UN (C$_6$H$_5$)$_2$. Organometallics 6:41–45. doi:10.1021/om00144a010

88. Babu RPK, Mcdonald R, Decker SA, Klobukowski M, Cavell RG (1999) New zirconium hydrocarbyl bis (phosphoranimino) " pincer " carbene complexes. Organometallics 18:4226–4229. doi:10.1021/om9901473

89. Kamalesh Babu RP, McDonald R, Cavell RG (2000) Nucleophilic reactivity of the multiply bonded carbon center in group 4 − pincer bis(iminophosphorano)methanediide complexes. Organometallics 19:3462–3465. doi:10.1021/om000181d

90. Cavell RG, Kamalesh Babu RP, Kasani A, McDonald R (1999) Novel metal − carbon multiply bonded twelve-electron complexes of Ti and Zr supported by a bis(phosphoranimine) chelate. J Am Chem Soc 121:5805–5806. doi:10.1021/ja984087o

91. Cantat T, Ricard L, Mézailles N, Le Floch P (2006) Synthesis, reactivity, and DFT studies of S − C − S zirconium(IV) complexes. Organometallics 25:6030–6038. doi:10.1021/om060665v

92. Aparna K, Babu RPK, Mcdonald R, Cavell RG (2001) The first biscarbene complex of a group 4. Angew Chem Int Ed 40:4400–4402. doi:10.1002/1521-3773(20011203)40:23<4400::AID-ANIE4400>3.0.CO;2-W

93. Lafage M, Heuclin H, Mézailles N (manuscript under preparation)

94. Oulié P, Nebra N, Saffon N, Maron L, Martin-Vaca B, Bourissou D (2009) 2-indenylidene pincer complexes of zirconium and palladium. J Am Chem Soc 131:3493–3498. doi:10.1021/ja809892a

95. Müller JFK, Kulicke KJ, Neuburger M, Spichty M (2001) Carbanions substituted by transition metals: synthesis, structure, and configurational restrictions of a lithium titanium phosphonate. Angew Chem Int Ed 12:2890–2893. doi:10.1002/1521-3773(20010803)40:15<2890::AID-ANIE2890>3.0.CO;2-T

96. Heuclin H, Grünstein D, Le Goff X-F, Le Floch P, Mézailles N (2010) Phosphorus stabilized carbene complexes: bisphosphonate dianion synthesis, reactivity and DFT studies of O~C~O zirconium(IV) complexes. Dalton Trans 492–499. doi:10.1039/b915468j

97. Cantat T, Mézailles N, Maigrot N, Ricard L, Le Floch P (2004) Titanocene and zirconocene complexes of a phosphorus analog of an Arduengo's carbene: application in the synthesis of 1,3-diphosphafulvenes. Chem Commun 1274–1275. doi:10.1039/b403436h
98. Biaso F, Cantat T, Mézailles N, Ricard L, Le Floch P, Geoffroy M (2006) Formation and structure of a stable monoradical cation by reduction of a diphosphafulvenium salt. Angew Chem Int Ed 45:7036–7039. doi:10.1002/anie.200603009
99. Cantat T, Biaso F, Momin A, Ricard L, Geoffroy M, Mézailles N, Le Floch P (2008) Synthesis of a stable radical anion via the one electron reduction of a 1,1-bis-phosphinosulfide alkene derivative. Chem Commun 874–876. doi:10.1039/b715380e
100. Layh M, Uhl W (1990) Synthesis and molecular structure of a bis[di(alkyl)alanyl]methane; R_2AL-CH_2-AIR_2 [R=CH($SiMe_3$)$_2$]. Polyhedron 9:277–282. doi:10.1016/S0277-5387(00)80580-X
101. Robinson GH, Lee B, Pennington WT, Sangokoya SA (1988) Facile cleavage of C-H bonds. Reaction of trimethylaluminum with bis(diphenylphosphinoyl)methane. Synthesis and molecular structure of [Al(CH_3)][(C_6H_5)$_2$P(O)CP(O)(C_6H_5)$_2$]$_2$[Al(CH_3)$_2$]$_2$. J Am Chem Soc 110:6260–6261. doi:10.1021/ja00226a059
102. Robinson GH, Self MF, Pennington WT, Sangokoya SA (1988) Organoaluminum chemistry of bidentate phosphine ligands. Reaction of diisobutylaluminum hydride with bis(diphenylthiophosphinoyl)methane: synthesis and molecular structure of [Al(C_4H_9)]$_2$[(C_6H_5)$_2$P(S)CP(C_6H_5)$_2$(S)$_2$][Al(C_4H_9)$_2$]$_2$. Organometallics 7:2424–2426. doi:10.1021/om00101a030
103. Aparna K, Mcdonald R, Ferguson M, Cavell RG (1999) Novel dialkyl aluminum bis (iminophosphorano) methanide and methanediide complexes. Organometallics 18:4241–4243. doi:10.1021/om990486w
104. Wang Z, Li Y (2003) Reactions of iminophosphorano(8-quinolyl)methane with AlMe 3: unexpected formation of aluminum iminophosphorano(2-methyl-8-quinolyl)methandiide complex. Organometallics 22:4900–4904. doi:10.1021/om034045v
105. Aparna K, McDonald R, Cavell RG (2000) Carbon–carbon double bond formation reactions of the unique spirocyclic aluminum bis(iminophosphorano) methandiide complex: insertion of heteroallenes into aluminum–carbon bonds. J Am Chem Soc 122:9314–9315. doi:10.1021/ja001445q
106. Cavell RG, Aparna K, Kamalesh Babu RP, Wang Q (2002) Aluminum bis(iminophosphorano)methanide and methandiide complexes: transition metal-free ethylene polymerization cationic catalyst precursors. J Mol Catal A Chem 189:137–143. doi:10.1016/S1381-1169(02)00205-4
107. Brook AG, Abdesaken F, Gutekunst B, Gutekunst G, Kallury RK (1981) A solid silaethene: isolation and characterization. J Chem Soc Chem Commun 191. doi:10.1039/c39810000191
108. Ottosson H, Steel PG (2006) Silylenes, silenes, and disilenes: novel silicon-based reagents for organic synthesis? Chemistry 12:1576–1585. doi:10.1002/chem.200500429
109. Ottosson H, Eklöf AM (2008) Silenes: connectors between classical alkenes and nonclassical heavy alkenes. Coord Chem Rev 252:1287–1314. doi:10.1016/j.ccr.2007.07.005
110. Fischer RC, Power PP (2010) Pi-bonding and the lone pair effect in multiple bonds involving heavier main group elements: developments in the new millennium. Chem Rev 110:3877–3923. doi:10.1021/cr100133q
111. Leung W, Kan K, Chong K (2007) Reactions of some organogermanium(II) chlorides. Coord Chem Rev 251:2253–2265. doi:10.1016/j.ccr.2006.12.012
112. Leung W-P, Wang Z-X, Li H-W, Mak TCW (2001) Bis(germavinylidene) [(Me_3SiN=PPh_2)$_2$C = Ge → Ge = C(Ph_2P = $NSiMe_3$)] and 1,3-Dimetallacyclobutanes [M{μ^2-C(Ph_2P=$NSiMe_3$)$_2$}]$_2$ (M = Sn, Pb). Angew Chem Int Ed 40:2501–2503. doi:10.1002/1521-3773(20010702)40:13<2501::AID-ANIE2501>3.0.CO;2-Q
113. Leung W-P, Wan C-L, Kan K-W, Mak TCW (2010) Synthesis, structure, and reactivity of group 14 bis(thiophosphinoyl) metal complexes. Organometallics 29:814–820. doi:10.1021/om9008923

114. Guo J, Lau K-C, Xi H-W, Lim KH, So C-W (2010) Synthesis and characterization of a tin (II) bis(phosphinoyl)methanediide complex: a stannavinylidene derivative. Chem Commun 46:1929–1931. doi:10.1039/b922377k

115. Leung W-P, Chiu W-K, Mak TCW (2013) Synthesis and structural characterization of base-stabilized oligomeric heterovinylidenes. Inorg Chem 52:9479–9486. doi:10.1021/ic4011345

116. Leung W-P, Chan Y-C, Mak TCW (2013) Synthesis and structural characterization of lithium, potassium, magnesium, and heavier group 14 metal complexes derived from 2-quinolyl-linked (thiophosphorano)methane. Organometallics 32:2584–2592. doi:10.1021/om400062e

117. Chai Z-Y, Wang Z-X (2009) Synthesis and characterization of Sn(II), Pb(II) and Yb (II) complexes supported by $[C(Ph(2)P=NSiMe_3)\{6-(2-RC_5H_3N)\}]^{2-}$ or $[CH(Ph_2P=NSiMe_3)\{6-(2-RC_5H_3N)\}]^-$ (R = 3,5-dimethyl-1-pyrazolyl or iminophosphoranyl) ligands. Dalton Trans 8005–8012. doi:10.1039/b906266a

118. Hitchcock PB, Lappert MF, Linnolahti M, Severn JR, Uiterweerd PGH, Wang Z-X (2009) Synthesis and structures of the dinuclear tin(II) complexes [R=Ph, X(Z)=CPh; R=SiMe_3, X(Z)=PPh_2] and of related compounds. J Organomet Chem 694:3487–3499. doi:10.1016/j.jorganchem.2009.06.025

119. Leung W-P, Kan K-W, Mak TCW (2010) Synthesis of heavier group 14 metal compounds from 2,6-lutidylbis(phosphoranosulfide). Organometallics 29:1890–1896. doi:10.1021/om1001167

120. Yang Y-F, Foo C, Ganguly R, Li Y, So C-W (2012) Synthesis of a tin(II) 1,3-benzobis (thiophosphinoyl)methanediide complex and its reactions with aluminum compounds. Organometallics 31:6538–6546. doi:10.1021/om300345u

121. Foo C, Lau K-C, Yang Y-F, So C-W (2009) Synthesis and characterization of a germanium bismethanediide complex. Chem Commun 6816–6818. doi:10.1039/b911384c

122. Leung W-P, Chan Y-C, Mak TCW (2011) Synthesis and structural characterization of a tin analogue of allene. Inorg Chem 50:10517–10518. doi:10.1021/ic201888d

123. Meyer H, Baum G, Massa W, Berndt A (1987) Stable germaethenes. Angew Chem Int Ed 26:798–799. doi:10.1002/anie.198707981

124. Lazraq M, Escudié J, Couret C, Satgé J, Dräger M, Dammel R (1988) (Mesityl)2Ge (fluorenylidene)-stabilization of a Ge–C double bond by charge transfer into an aromatic system. Angew Chem Int Ed 27:828–829. doi:10.1002/anie.198808281

125. Mizuhata Y, Takeda N, Sasamori T, Tokitoh N (2005) Synthesis and properties of a stable 6-stannapentafulvene. Chem Commun 5876–5878. doi:10.1039/b512097g

126. Meyer H, Baum G, Massa W, Berger S, Berndt A (1987) A stable stannaethene. Angew Chem Int Ed 26:546–548. doi:10.1002/anie.198705461

127. Sigal N, Apeloig Y (2002) Theoretical study of heavier group 14 analogues of allene. Organometallics 21:5486–5493. doi:10.1021/om020304p

128. Leung W, Kan K, So C, Mak TCW (2007) Formation of germenes from bis (germavinylidene). Organometallics 26:3802–3806. doi:10.1021/om7002706

129. Leung W, So C, Kan K, Chan H, Mak TCW (2005) Synthesis of novel metal–germavinylidene complexes from bisgermavinylidene. Organometallics 24:5033–5037. doi:10.1021/om0503085

130. Leung W-P, So C-W, Kan K-W, Chan H-S, Mak TCW (2005) Synthesis of a manganese germavinylidene complex from bis(germavinylidene). Inorg Chem 44:7286–7288. doi:10.1021/ic050969u

131. Leung W-P, So C-W, Wang Z-X, Wang J-Z, Mak TCW (2003) Synthesis of bisgermavinylidene and its reaction with chalcogens. Organometallics 22:4305–4311. doi:10.1021/om034071t

132. Leung W-P, So C-W, Wang J-Z, Mak TCW (2003) A novel synthesis of metallogermacy-clopropane and molybdenum bis(iminophosphorano)carbene complexes from bisgermavinylidene. Chem Commun 13:248–249. doi:10.1039/b210598e
133. Leung W, Kan K, So C, Mak TCW (2007) Some addition reactions of bisgermavinylidene. Appl Organomet Chem 21:814–818. doi:10.1002/aoc.1293
134. Leung W-P, Kan K-W, Chan Y-C, Mak TCW (2013) Synthesis of hetero-binuclear complexes from bisgermavinylidene. Inorg Chem 52:4571–4577. doi:10.1021/ic400056f
135. Guo J-Y, Li Y, Ganguly R, So C-W (2012) Reactivity of a Tin(II) (iminophosphinoyl) (thiophosphinoyl)methanediide complex toward isocyanates and rhodium(I) chloride. Organometallics 31:3888–3893. doi:10.1021/om300062n
136. Guo J-Y, Xi H-W, Nowik I, Herber RH, Li Y, Lim KH, So C-W (2012) Reactivity of a tin (II) (iminophosphinoyl)(thiophosphinoyl)methanediide complex toward sulfur: synthesis and ^{119}Sn Mössbauer spectroscopic studies of $[\{(\mu\text{-}S)SnC(PPh_2=NSiMe_3)(PPh_2=S)\}^3Sn(\mu^3\text{-}S)]$. Inorg Chem 51:3996–4001. doi:10.1021/ic2019633
137. Yang Y-F, Ganguly R, Li Y, So C-W (2013) Reactivity of a Tin(II) 1,3-Benzodi (thiophosphinoyl)methanediide complex toward gallium, germanium, and zinc compounds. Organometallics 32:2643–2648. doi:10.1021/om400141j

FascinATES: Mixed-Metal Ate Compounds That Function Synergistically

Robert E. Mulvey and Stuart D. Robertson

Abstract Ate complexes are generally thought of as having a cationic and an anionic moiety, each containing a metal atom, though these moieties can be contacted or separated depending on the system. They have been known for over 150 years but yet only recently has it dawned on synthetic chemists that ates can bring about lots of improvements to the metalation reaction. Alkali-metal magnesiates, zincates and aluminates in particular have been successfully utilized in metal-hydrogen exchange reactions of challenging weakly acidic aromatic substrates. The fascination of these mixed-metal reagents lies in their ability to effect unique deprotonations at ambient temperatures without attacking functional groups on the aromatic scaffold where conventional organolithium reagents would require subambient temperatures to reduce such attacks, to direct metalation to the *meta* position of certain substrates where *ortho* or lateral deprotonation is more common and to strip more than one hydrogen atom from multi-C-H bonded compounds where lithiation methods would generally fail. Furthermore some of these superficially simple ate-metal-induced deprotonation reactions produce complex but beautiful host-guest macrocyclic architectures referred to as inverse crowns. Since magnesium, zinc and aluminium organic compounds cannot replicate these metalation reactions, these alkali-metal-mediated reactions are synergistic in origin. This article is not intended to be comprehensive but provides a representative selection of these fascinates in action, with emphasis on their synergistic nature. Reactions of the heteroleptic alkyl-amido magnesiate TMEDA·Na(TMP)(*n*Bu)Mg (TMP) and zincate TMEDA·Na(TMP)(*t*Bu)Zn(*t*Bu) are featured prominently (TMP is 2,2,6,6-tetramethylpiperidide).

Keywords Ate compounds · Bimetallic · Metalation · Organometallic · Structure

R.E. Mulvey (✉) and S.D. Robertson
Department of Pure and Applied Chemistry, WestCHEM, University of Strathclyde, Glasgow
G1 1XL, UK
e-mail: r.e.mulvey@strath.ac.uk

Contents

1 Introduction

1.1 Historical Aspects of the Metalation Reaction

The metalation reaction, that is, the conversion of a relatively unuseful carbon–hydrogen bond to a synthetically advantageous carbon–metal bond, is one of the most important and widespread chemical transformations practiced today. A key intermediary tool for the preparation of pharmaceuticals, agrochemicals, perfumes/cosmetics and fine chemicals, amongst other everyday commodities, the metalation reaction has typically been the domain of the highly polar alkali metals, nearly always lithium. Indeed, Collum emphasized this domination in 1993 stating that 'it would appear that well over 95% of natural products syntheses rely upon lithium based reagents in one form or another' [1].

Lithium reagents can trace their roots back almost 100 years to the pioneering work of Wilhelm Schlenk [2, 3], who initially prepared ethyllithium, propyllithium and phenyllithium from the corresponding alkyl/aryl mercury compound and lithium metal (Fig. 1.) [4].

The first glimpse of their synthetic utility was realized just over a decade later when EtLi was used by Schlenk and Bergmann to metalate fluorene at the most acidic position to give fluorenyl lithium [5]. Although undoubtedly the forefather of alkyllithium chemistry, Schlenk is perhaps better known for two other reasons, namely, the development of his eponymous glassware required for the safe handling of such air-sensitive compounds and his discovery of the solution equilibrium of Grignard reagents (R-Mg-X) into their homoleptic components (R_2Mg and MgX_2), now commonly called the 'Schlenk equilibrium' [6].

The two most common families of lithium reagent employed for the metalation reaction are alkyllithiums (R-Li) [7] and sterically encumbered lithium secondary amides (R_2N-Li) [8, 9]. As the former reagents can also be highly nucleophilic,

Fig. 1 The advent of
organolithium chemistry

$$R_2Hg + xs\ Li \xrightarrow[]{\begin{array}{c}C_6H_6\\65^oC\end{array}} RLi + Li/Hg\ amalgam$$

R = Et, Pr, Ph
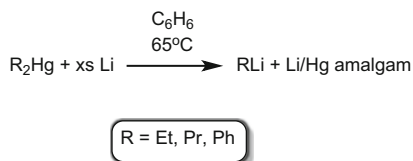
especially if relatively small in size, their chemistry with substrates bearing unsaturated linkages can be complicated by undesirable side reactions such as addition. Their high polarity and molecular constitutions endow lithium-centred reagents with high reactivity, often too high as they regularly have to be utilized at low temperature (typically -78°C) to avoid side reactions. Running reactions at -78°C is easy on the small scale in academic laboratories (surrounding a Schlenk tube with a jacket of dry ice generally suffices), but on a larger scale, especially in an industrial setting, it has major cost implications. Poor functional group tolerance and poor selectivity of reaction site are also common drawbacks of these popular reagents. An alternative to these lithium reagents are organo compounds of lower-polarity metals, with magnesium, zinc and aluminium being examples particularly germane to this chapter on synergistic effects. Possessing greater electronegativity than the Group 1 alkali metals, these Group 2/Group 12/Group 13 metals form more covalent bonds to their organo-moieties and as such they are by comparison decidedly diminished in reactivity. A consequence of this lower reactivity is that they often require to be encouraged to react through the application of heat, which can induce decomposition processes. This sluggishness of reactivity is however tempered with a functional group tolerance and selectivity which is generally superior to that of the polar metals of Group 1. What is certainly clear is that both sets of organo reagent (polar alkali metal or polar-covalent multivalent metal) have both strengths and weaknesses which must be carefully considered when choosing an appropriate reagent for any particular reaction. In the specific case where metalation of an aromatic (C-H) substrate is concerned, conventional organomagnesium, organozinc or organoaluminium reagents are almost never reactive enough to be considered.

That is the situation when these different classes of organometallic reagent are considered separately. However, since the turn of the century, we and others have focused our attention on the unique chemistry which can be obtained by pairing one metal from each of the classes mentioned above into a single complex, which more often than not could be designated an 'ate complex'. While this chemistry is hardly new, indeed Wanklyn synthesized the first zincate, NaZnEt$_3$, as long ago as 1858 [10, 11]; a deeper understanding of the useful reactivity of these complexes has only really come to light recently. It is appropriate therefore that this chapter looks briefly at some of the key historical events in the chemistry of ate complexes before turning to the most recent advances.
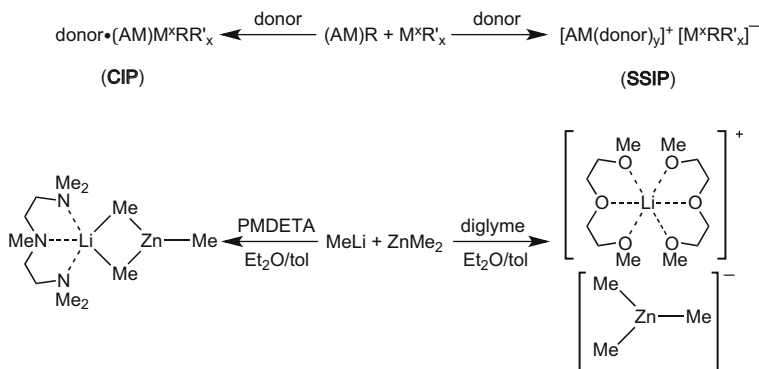
Fig. 2 Empirical general types of ate complex prepared via co-complexation (*top*) and an example of donor dependence on structural make-up (*bottom*) [13]. PMDETA=N,N,N',N'',N''-pentamethyldiethylenetriamine

1.2 Classification and Preparation of Ates

An ate (short for metal*ate*) complex can in the broadest terms be defined as a salt formed from the stoichiometric reaction of a Lewis base and a Lewis acid in which the acidic moiety formally increases its valency and becomes anionic [12]. Such a complex can generally be subdivided into two distinct categories: the contacted ion pair (CIP), in which some of the anions bridge between the two metals, or the solvent-separated ion pair (SSIP, Fig. 2).

The amount of donor employed is one factor which can dictate the preparation of a CIP or SSIP, with, in general, stoichiometric amounts favouring the contacted ion pair and excess amounts favouring the solvent-separated ion pair, although other factors such as the Lewis donating strength and denticity of the donor, the steric profile of the donor plus electronic and steric effects of the ligands (R) can also influence the compositional make-up of an ate. While the example given in Fig. 2 shows a homoleptic ate complex, it is also possible to prepare heteroleptic ate complexes. Ate complexes are typically prepared either by a co-complexation strategy (simple mixing of its Lewis acidic and Lewis basic component parts, Fig. 2) or through salt metathesis of a metal halide with an organo-alkali-metal reagent (Fig. 3). The former is the route of choice for the preparation of heteroleptic ate complexes (by simply using starting materials which contain different organoanions, R ≠ R') while the latter route is regularly employed for the preparation of homoleptic ate complexes.

The salt metathesis protocol can result in an alternative outcome whereby the generated alkali-metal halide salt co-complexes in preference to (or in competition with) the organo-alkali-metal unit with the low-polarity metal. This results in a formally heteroleptic ate complex of general formula $M^x R_x \cdot AMCl$. Of course, the presence of an alkali-metal halide salt in conjunction with a low-polarity metalator can be deliberate, as Knochel and co-workers have cleverly exploited [14]. The

Fig. 3 Preparation of an ate complex via co-complexation (*top*) and salt metathesis (*bottom*)

$$x+1 \, (AM)R + M^xCl_x \longrightarrow (AM)M(R)_{x+1} + x \, (AM)Cl$$
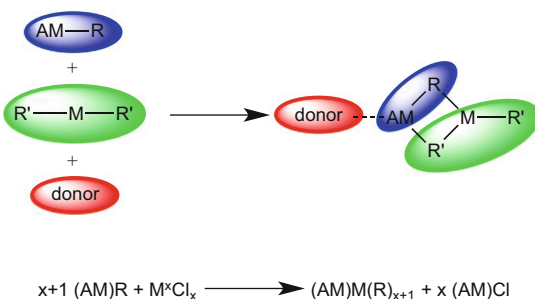
presence of the alkali-metal halide salt in their reagents is generally credited with increasing the solubility of the low-polarity metal reagent, for example, as in iPrMgCl·LiCl or (TMP)MgCl·LiCl (TMP = 2,2,6,6-tetramethylpiperidide), boosting its reactivity with recent studies demonstrating that a solvent-separated ion pair ate is the likely active species [15, 16]. Though relatively rare, these multicomponent bases can incorporate more than two metals as demonstrated by the examples (TMP)$_2$Fe·2MgCl$_2$·4LiCl [17] or (TMP)$_4$Zr·4MgCl$_2$·6LiCl [18], both of which are potent metalators that display high functional group tolerance. Recent progress in this area has resulted in the formation of salt-supported multicomponent bimetallic reagents of general formula RZnOPiv·MgOPiv (Cl)·2LiCl (OPiv = pivalate, tBuCO$_2^-$) which exhibit superior air stability and are ideal starting materials for carbon–carbon bond-forming reactions (R = aryl) [19, 20] or metalation reactions themselves (R = TMP) [21].

Thus far only ate complexes with a unity ratio of alkali metal to low-polarity metal have been considered; however, it is also possible to vary the stoichiometry such that this ratio is greater. The former class are considered to be 'lower-order' ates [that is corresponding to the empirical formula (AM)MR$_3$] and the latter class as 'higher-order' ates [that is corresponding to the empirical formula (AM)$_2$MR$_4$].

As alluded to earlier, Wanklyn first prepared an ate complex, NaZnEt$_3$, in 1858 by the redox reaction of sodium metal with the dialkylzinc compound Et$_2$Zn. It was almost a century later however before another giant of organometallic chemistry, Nobel laureate Georg Wittig, caught a glimpse of the synthetic potential of such a heterobimetallic complex when he reported fluorene deprotonation and addition to benzophenone with the tris-aryl ate complex LiZnPh$_3$ [22] (Fig. 4).

The realization of this special reactivity prompted Wittig to coin the term 'ate complex', with the awareness that the mixed-metal complex could show a different reactivity to that of its monometallic components [23, 24]. Despite this important clue to the vast potential of ates, surprisingly little progress was forthcoming in the deprotonative power of ate chemistry for a considerable period of time following Wittig's discoveries. One notable contribution around this time however was the discovery that the hetero-alkali-metallic mixture of nBuLi and KOtBu was a potent metalator (known as the Lochmann–Schlosser [LiCKOR] superbase, after the two independent discoverers of this reactivity) [25, 26]. It is still not entirely clear if this operates via an ate complex, although what is known is that some
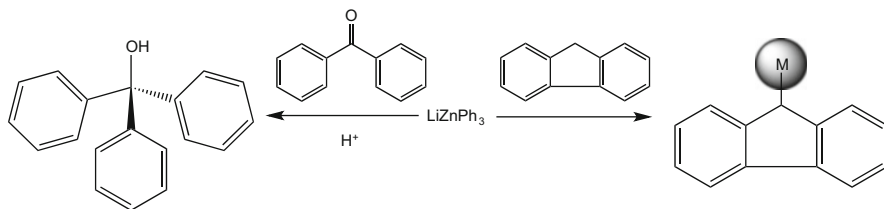
Fig. 4 Wittig begins ate-induced metalation chemistry. M denotes the position of metalation and is used when the metal is not explicitly identified

form of metal-ligand-metal' cooperativity is in operation since neither of the individual components can individually deprotonate toluene at the methyl group under equivalent conditions (although nBuLi can deprotonate the methyl arm of toluene in the presence of a Lewis basic heteroatom containing deaggregating reagent such as TMEDA, N,N,N',N'-tetramethylethylenediamine [27]), a benchmark metalation reaction of the LiCKOR superbase. Insight into the make-up of such a superbase has been provided by Mulvey [28] and Strohmann [29]. The former uses a primary amido ligand in place of the alkyl ligands and is formulated as $[(t\text{BuNH})_4(Ot\text{Bu})_4\text{Li}_4\text{K}_4(\text{C}_6\text{H}_6)_4]$ containing essentially perpendicular Li_2N_2 and K_2O_2 rings with potassium solvated by π-coordinated benzene molecules. The latter recently reported the molecular structure of $[(\text{PhK})_4(\text{PhLi})(t\text{BuOLi})$ $(\text{THF})_6(\text{C}_6\text{H}_6)_2]$ which is essentially the intermediate complex obtained 'post-metalation' when benzene is deprotonated using such a base. While this complex contains all the components of a LiCKOR superbase, the hydrocarbon constituent is in the form of the phenyl anion rather than the nBu present at the beginning and thus this structure can be considered as an intermediate on the pathway to preparing PhK from benzene and a superbasic mixture. The molecular structure can be best described as an 8-membered $[\text{KC}_{\text{Ph}}]_4$ ring with a 4-membered [LiCLiO] cyclic moiety captured inside the cavity (Fig. 5).

Of course the heteroleptic nature of this multicomponent system must contribute to the increased reactivity of this mixed alkyl-alkoxy system, an aspect which is supported by the excellent work of Caubère who utilized the unimetallic, heteroleptic mixture nBuLi/LiDMAE (DMAE = dimethylaminoethoxide, Me_2-$\text{NCH}_2\text{CH}_2\text{O}^-$) [30] in regioselective deprotonation reactions to great effect [31]. A new aspect of hetero-alkali-metallic metalation chemistry has recently come to light, thanks to O'Shea and co-workers who have discovered component-dependent selectivity when introducing the secondary amide TMP into a LiCKOR-based metalating reagent (cleverly denoted as LiNK chemistry), with metalation of *ortho*-directing group substituted toluenes occurring *ortho* to the directing group in the absence of TMP but switching to the methyl group in its presence (Fig. 6) [32].

The characterization of the active species responsible for this reactivity has been thus far limited and no definite structural knowledge has been thus far obtained. That said, the practical usage of this bimetallic approach has been evidenced, as
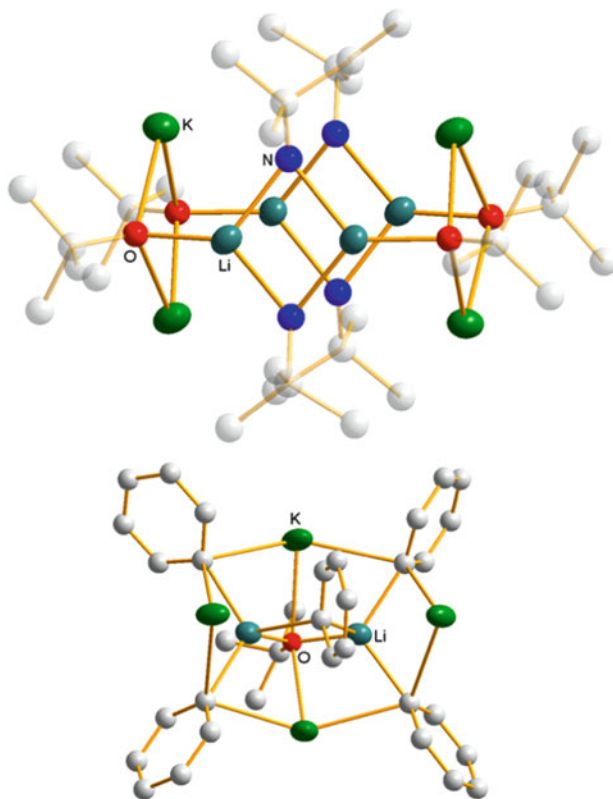
Fig. 5 Molecular structures of central cores of superbase-like complexes [(tBuNH)$_4$(OtBu)$_4$Li$_4$K$_4$(C$_6$H$_6$)$_4$] (*top*) and [(PhK)$_4$(PhLi)(tBuOLi)(THF)$_6$(C$_6$H$_6$)$_2$] (*bottom*). Neutral coordinating ligands have been omitted for clarity
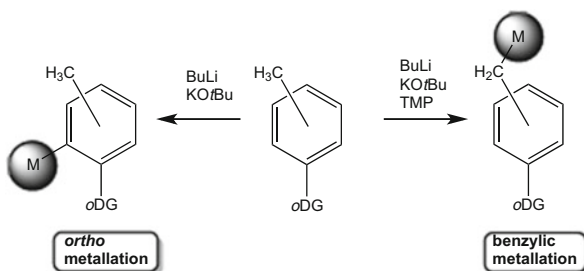
Fig. 6 Component-dependent selectivity of metalation; oDG = −OCH$_2$OMe, −OMe, −NMe$_2$, −CONiPr$_2$

metalation coupled with oxidative C–C bond formation has allowed the facile preparation of [2.2] metacyclophanes (Fig. 7) [33, 34].

Weiss and co-workers were instrumental in the early determination of the molecular structures of a plethora of ate complexes, revealing a variety of both
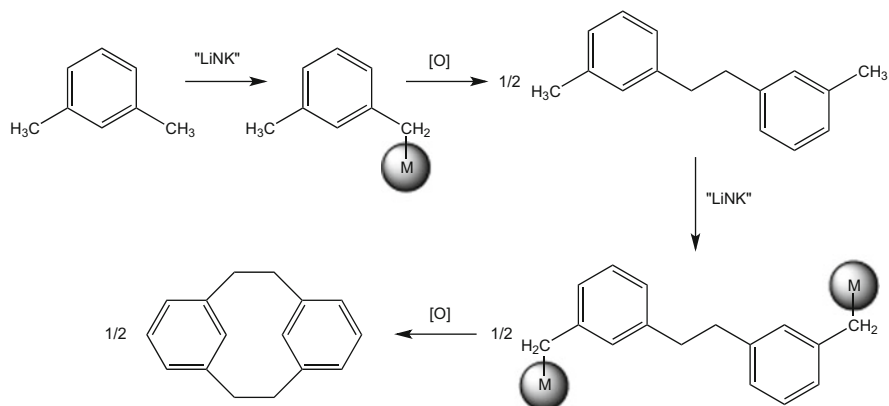
Fig. 7 Stepwise preparation of [2.2] metacyclophanes by sequential metalation/oxidation steps using LiNK conditions at $-78°C$ in THF
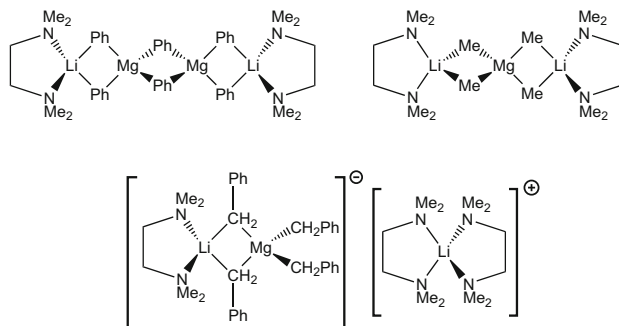
Fig. 8 Common *Weiss motifs* – lower-order (*top left*) [36], higher-order (*top right*) [37] and solvent-separated higher-order (*bottom*) [38] lithium magnesiate complexes

higher-order and lower-order examples [35]. Although no synthetic advances were attempted, this work was seminal in showing the exact make-up of such complexes, which we regularly refer to as *Weiss motifs* (Fig. 8).

There is a clear structural basis to the enhanced reactivity of a contacted ion pair ate complex, particularly when a nonpolar, non-donating solvent such as hexane is the reaction medium and when only a stoichiometric amount of Lewis donor solvent is present. Firstly the Lewis acidic alkali metal activates the substrate towards metalation by binding to it (by either dative donor-acceptor contact or π-arene interactions) and secondly the Lewis basic anionic MR_3^- unit activates the base ligands (R) by the extra negative charge available over the corresponding neutral R_2M species.

As mentioned previously, recent research in this area has been conducted in an effort to gain a deeper understanding of the cooperative effects of the two metals which govern the metalation reactions. The evidence points to the metalation reaction being executed by the less electropositive, less reactive metal as without

Fig. 9 Basis for coining cooperative reactions of this type as alkali-metal-mediated metalations (AMM*M*)
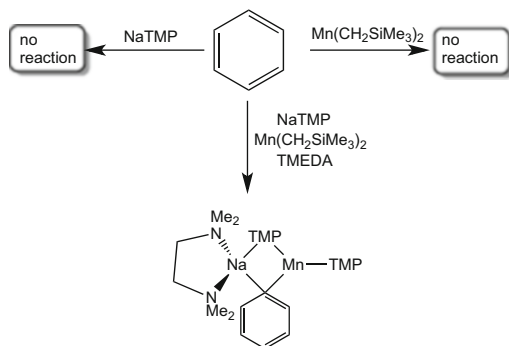
cooperative effects its metal–carbon bonds are generally less polar than analogous lithium–carbon bonds. Thus the site within the organic substrate formerly occupied by the abstracted hydrogen atom is now occupied by the non-alkali metal, although the presence of the alkali-metal reagent is essential for the hydrogen-new metal interchange reaction to proceed. This is clearly illustrated through the example in Fig. 9 which shows that benzene is unreactive to either metallic reagent Na(TMP) or Mn(CH$_2$SiMe$_3$)$_2$ on their own but reacts when they are mixed (co-complexed) together [39]. Consequently, this chemistry can be interpreted as alkali-metal-mediated metalation, with the acronym AMM*M*, where *M* represents the activated polyvalent non-alkali metal.

A key strategy for trying to unravel the complexities behind AMM*M* is to attempt to isolate and crystallographically characterize the intermediate species on the path between starting organic substrate and its functionalized derivative. This information is critically important when heteroleptic ate complexes are being used since there exists more than one possibility for the identity of the active base ligand and can also provide a structural foundation from which to study these reactions from a computational or theoretical perspective. This approach also helps shed light on any 'unexpected' results which are perhaps more complicated than a straightforward deprotonation, for example, a poly-deprotonation or functionalization at a typically unreactive site. That said it is even more important that solution studies, primarily NMR spectroscopic studies, are carried out in conjunction with solid state studies since it is in solution that ate complexes operate as synthetic intermediates for bond-forming reactions. Such solution studies can help deduce for example any equilibria as evidenced by the Weiss higher-order complex Li$_2$ZnMe$_4$ [40], which Mobley and Berger showed via isotopic labelling to be in equilibrium with the lower-order relative LiZnMe$_3$ and LiMe, with the position of equilibrium strongly favouring the lower-order trialkylzincate (Fig. 10) [41].

Similarly, Hevia and co-workers have investigated homoleptic alkali-metal magnesiates showing a higher-/lower-order dependence upon donor solvent ligation. Specifically, using the trimethylsilylmethyl anion (Me$_3$SiCH$_2$$^-$), the lithium magnesiate has the lower-order empirical formula LiMg(CH$_2$SiMe$_3$)$_3$. Introducing

$$LiZnMe_3 + LiMe \rightleftharpoons Li_2ZnMe_4$$

favoured in solution   favoured in solid state

Fig. 10 Equilibrium between lower-order and higher-order lithium zincate

Fig. 11 Donor-dependent disproportionation reactions of the homoleptic lithium alkylmagnesiate $LiMg(CH_2SiMe_3)_3$

the trifunctional amine PMDETA to break up the polymer affords the lower-order monomer, $PMDETA \cdot Li(CH_2SiMe_3)Mg(CH_2SiMe_3)_2$. However on changing to the less sterically imposing difunctional amine donor TMEDA a disproportionation into the higher-order tetraalkylmagnesiate $TMEDA \cdot Li(CH_2SiMe_3)_2Mg$ $(CH_2SiMe_3)_2Li \cdot TMEDA$ along with homometallic $Mg(CH_2SiMe_3)_2$ occurs (Fig. 11) [42]. The related sodium congener $NaMg(CH_2SiMe_3)_3$, which adopts a two-dimensional infinite network motif in the solid state, fails to produce a similar higher-order derivative upon addition of a further equivalent of Na (CH_2SiMe_3) [43].

2 Ate Complexes in Metalation

2.1 *Directed* Ortho-*Metalation*

Directed *ortho*-metalation (D*o*M) is one of the principal pathways by which an aromatic [44, 45] or related [46] substrate is metalated and subsequently functionalized. First recognized independently by Gilman and Bebb [47] and Wittig and Fuhrmann [48], this regiospecific deprotonative metalation process requires the presence of a Lewis basic functional group on the aromatic ring which potentially performs a dual role of inductively acidifying the *ortho* hydrogen atom and also acting as an anchor point for the incoming metalating agent by binding to it via its Lewis basic heteroatom, in a process known as the complex-induced proximity effect (CIPE) [49]. Such a mechanism is typically used to describe a lithiation reaction although the principles can be broadly applied when bimetallic ate complexes are being used also. Unhelpfully, homo-alkali-metallic reagents can often undergo undesirable side reactions with the *ortho*-directing group, depending on its

Fig. 12 Contrasting reactivity of a variety of metalating agents towards N,N-diethylbenzamide

identity. The fact that ate complexes typically tolerate such functionality, even at ambient temperature, is what makes them synthetically so attractive. This can be demonstrated via Fig. 12 where N,N-diethylbenzamide is the substrate. A typical alkyllithium reagent such as nBuLi reacts with the functional group, even at −78°C, to produce valerophenone (reaction a) [50]. However, the addition of TMEDA (this time using sBuLi) results in clean *ortho*-metalation (reaction b), although the trade-off is that cryogenic temperatures and a polar solvent are again required [51]. Moving to the hindered weakly nucleophilic secondary amide LiTMP, *ortho* deprotonation does occur, but this reaction is slower than the consequent reaction between the lithiated product and the starting benzamide resulting in *o*-benzoyl-N, N-diethylbenzamide (reaction c) [52]. Finally, moving to a bimetallic Na/Zn base, the synergy between the two metals results in *ortho* zincation occurring cleanly at room temperature in the nonpolar solvent hexane (reaction d) [53].

Another example of the desirable properties of certain ate complexes, particularly aluminates, is halogen tolerance as first reported by Uchiyama and co-workers [54]. As shown in Fig. 13, *ortho*-bromoanisole undergoes metal-halogen exchange when subjected to nBuLi [55]; however the bimetallic base formed from the co-complexation of LiTMP, iBu₂Al(TMP) and THF in bulk hexane solution leaves the halogen functionality untouched and rather executes an aluminium-hydrogen exchange at the position *ortho* to the directing methoxy group [56, 57].

Fig. 13 Contrasting reactivity of *n*BuLi and lithium aluminate base towards *ortho*-bromoanisole

2.2 *The Challenge of Directed* **Meta-***Metalation*

A colossal challenge to synthetic chemists is to develop a general methodology of metalating aromatic C–H bonds remote from the substituted site. There are a number of specific examples which have been accomplished using either a mono-metallic or bimetallic approach. Snieckus has introduced the term Directed remote Metalation (DreM) [49] to describe the metalation of a functionalized biaryl compound where the site of metalation occurs regioselectively on the ring which does not have the directing group directly attached to it (Fig. 14). By implication this means that the coordinating effect of the Lewis basic arm to the metalating agent overrides the inductive effect of the arm towards acidifying the position *ortho* to it on the same ring.

This can in fact be considered as an extension of D*o*M with the (*o*-CONEt$_2$)C$_6$H$_4$ group itself acting as the *ortho*-directing group.

These intriguing opening examples of directed *meta*-metalation (D*m*M) have been observed upon performing AMMZn on *N*,*N*-dimethylaniline substrates with the well-defined sodium zincate base TMEDA·Na(μ-TMP)(μ-*t*Bu)Zn(*t*Bu) (Fig. 15) [59]. This result highlights the synergy at play between the two metals since conventional monometallic (lithium) metalation of *N*,*N*-dimethylaniline occurs in the more common *ortho* position when using phenyllithium [60] or *n*-butyllithium [61] (the former occurs in only poor yield, while the latter requires harsh conditions in order to obtain good yields). The NMe$_2$ amino group has a diminished effective-ness as an *ortho*-directing group for although it still inductively acidifies the *ortho* position, it does not contribute well to the complex-induced proximity effect as its lone pair of electrons are occupied through delocalization into the π-system of the aromatic ring.

Studying these reactions in solution by quenching with electrophilic iodine revealed that while the *meta*-metalated product was the major product (73%), a small amount of *ortho-metalation* (6%) and *para-metalation* (21%) had also occurred [62]. The *meta*-metalation of toluene can also be accomplished using the heteroleptic sodium magnesiate TMEDA·Na(TMP)(*n*Bu)Mg(TMP) (Fig. 16) [63]. This base operates synergically via overall alkyl basicity to yield a discrete molecular framework containing a bridging molecule of toluene, metalated at the *meta* position [64].

Progress in directed *meta*-metalation appears set to continue using both the bimetallic ate approach described herein and other specific case transition metal

Fig. 14 Regioselectivity of deprotonation reaction of a substituted bisaryl compound using lithium diisopropylamide as base [58]

Fig. 15 Examples of directed *meta*-metalation executed by a sodium zincate base

Fig. 16 Contrasting regioselectivity of monometallic (Li) [65] and bimetallic (Na/Mg) [64] bases towards toluene

approaches such as the copper- or palladium-catalysed methodologies reported by Phipps and Gaunt [66] and Leow et al. [67], respectively, though a general approach may prove elusive for some time to come.

2.3 Mechanistic Insights

When a heteroleptic ate complex is employed in a metalation application, then, depending on the anions involved, there may exist more than one possibility for the identity of the reactive base component within it. Generally, the deprotonation reaction will follow a single-step mechanism whereby the substrate will simply take the place of the departing anion. This is particularly true when the departing anion (the Brønsted base) is an alkyl group, since the alkane (RH) co-product generated

Fig. 17 Two-step
mechanism for
deprotonation by a
heteroleptic sodium zincate

upon substrate metalation will simply be lost to the system in gaseous form. However, if the departing anion is for example a secondary amide, a less volatile (normally a liquid due to the steric bulk of R_2N) secondary amine (R_2NH) will be produced, which will remain within the solution and may then react with any reaction intermediate simultaneously generated. This situation is demonstrated in the example in Fig. 17 where the aforementioned heteroleptic (alkyl-amido) sodium zincate TMEDA·Na(TMP)(tBu)Zn(tBu) is used. The first step involves deprotonation of the aromatic substrate via amido basicity to generate an intermediate bimetallic triorganoate complex alongside TMP(H) which remains alive in the system. This intermediate is in turn able to deprotonate the TMP(H) via alkyl basicity to give the final heterotrileptic product. No retro-reaction can then occur as the alkane leaves the system through the inert gas stream needed to protect the air-sensitive organometallics.

This type of base was initially introduced as the lithium derivative [with THF as the donor; THF·Li(μ-TMP)(μ-tBu)Zn(tBu)] by Kondo and co-workers [68]. This base proved to be an excellent deprotonating agent with considerable tolerance of sensitive functional groups such as ester, cyano and halide [69]. Although never confirmed experimentally, in these cases TMP was implicated as being the active kinetic base in the reaction. Furthermore, the steric bulk of the *tert*-butyl ligands allowed aromatic deprotonation adjacent to a halide to occur without concomitant metal–halogen bond formation and benzyne generation [70]. Mulvey then provided crystallographic evidence that the final product when using the TMEDA-solvated sodium zincate still contained TMP and that overall alkyl basicity had occurred [71]. The role of bulk solvent appeared critical, with Uchiyama reporting amido basicity for the reaction of Li(μ-TMP)(μ-tBu)Zn(tBu) with anisole in polar THF [72] and Mulvey reporting alkyl basicity for the corresponding reaction in nonpolar hexane (Fig. 18) [73].

A variety of theoretical [74, 75] and experimental [76] studies then confirmed the two-step mechanism, with Hevia and co-workers devising a rational synthesis of the alkyl-rich intermediate via co-complexation of *ortho*-lithiated anisole with di-t-butylzinc and showing its reactivity with TMP(H) results in the final heteroanionic product (Fig. 19).

Fig. 18 Solvent dependence on basicity of lithium zincate reagent

Fig. 19 Rational synthesis of an alkyl-rich intermediate and its reactivity towards TMP(H)

A similar situation was witnessed in the metalation of anisole with the magnesiate base PMDETA·K(μ-TMP)(μ-CH$_2$SiMe$_3$)Mg(TMP) [77]. The kinetic and thermodynamic products obtained via overall amido and alkyl basicity, respectively, could be trapped in crystalline form simply by varying the reaction time (Fig. 20) while the conversion of the base to the kinetic and then the thermodynamic product was easily monitored by ^{1}H NMR spectroscopy since the reaction was relatively slow and all three products are soluble in cyclohexane. Specifically, the generation of TMP(H) in the preparation of the kinetic product was evident via the growth of its characteristic resonances followed later by a loss of such resonances and the growth of one representing SiMe$_4$ as the final thermodynamic product was generated.

2.4 Active Ate or Homometalation/Transmetalation

An alternative method of metalation using a bimetallic but homoleptic mixture has recently been postulated. Ate complexes of general formula 'LiM(TMP)$_3$' (M = Zn, Cd) have been used by Mongin and co-workers to great effect for a variety of deprotonative reactions (Fig. 21) [78–80].

The active base is accessed simply through mixing Li(TMP) with the appropriate metal salt MCl$_2$ in a 3:1 stoichiometric ratio in THF solution. However, 2-dimensional DOSY NMR studies (diffusion-ordered NMR spectroscopy, Fig. 22) suggested that the 'black box' THF solution mixtures are actually more complicated in practice, hinting that ate formation had not taken place to any

Fig. 20 Kinetic and thermodynamic products obtained upon *ortho*-metalation of anisole with PMDETA·K(μ-TMP)(μ-CH$_2$SiMe$_3$)Mg(TMP)

Fig. 21 Representative examples of *ortho*-metalation using the homoleptic bases LiM(TMP)$_3$ (M = Zn, Cd)

measurable extent but instead the products appear to be the homometallic compounds Li(TMP)·2LiCl and M(TMP)$_2$ (M = Zn [81], Cd [82]).

Utilizing the NMR activity of cadmium, an alternative mechanism for the aforementioned 'ate' deprotonation reactions was proposed whereby Li(TMP) executes the deprotonation in a small yield and then a transmetalation occurs to regenerate Li(TMP), with carbophilic cadmium accepting the sensitive carbanion, resulting in a more covalent (Cd–C) bond (Fig. 23).

2.5 Unconventional Metalations and Polymetalations

One of the most advantageous uses of ate complexes, which sets this class of compound apart from most homometallic metalating agents, is in their ability to effect poly-deprotonation (cleaving two or more C–H bonds) of selected substrates and/or the deprotonation of poorly acidic sites not normally accessible to

Fig. 22 DOSY NMR spectrum of CdCl$_2$+3 LiTMP in THF showing different diffusion for TMP components. Tetramethylsilane, 1-phenylnaphthalene and 1,2,3,4-tetraphenylnaphthalene are included as inert internal standards in order to prepare a calibration graph to predict molecular weights [83]

Fig. 23 Proposed alternative metalation pathways for homoleptic lithium zincates and cadmates

conventional organolithium bases. Deprotonating a substrate in more than one site is typically difficult in conventional organometallic chemistry because of the high reactivity of the resulting polyanion, plus instability caused by the repulsive forces of nearby negatively charges. However, this is more of a possibility with ate complexes since the carbon–metal bonds formed are normally more covalent in nature (since it is the weaker less electropositive metalator which takes the place of the hydrogen) than carbon–lithium bonds and the additional presence of the alkali metal can help stabilize the build-up of electron density. As is to be expected, the outcome of a reaction between an ate complex and an organic substrate is heavily

Fig. 24 Base-dependent regioselective metalation patterns of toluene

dependent on the original component parts of the ate. An excellent example of this is the ring dideprotonation of toluene by the sodium magnesiate complex NaMg (TMP)$_2$$n$Bu, generated from nBuNa, nBu$_2$Mg and TMP(H). Toluene is typically metalated at the most acidic lateral (CH$_3$) position to yield the resonance-stabilized benzyl anion (PhCH$_2$$^-$) [84]; however, reaction with the sodium magnesiate base leaves the methyl arm intact while the 2 (*ortho*) and 5 (*meta'*) positions are magnesiated (Fig. 24) [85].

What seems like a simple dideprotonation [two C–H bonds converted to two C–Mg(-TMP) bonds] reaction is in actuality manifested through a remarkable eye-catching macrocyclic host-guest architecture. The twofold deprotonated molecule of toluene [C$_6$H$_3$(Me)]$^{2-}$ is encapsulated within a sodium-rich 12-atom [NaNMgNNaN]$_2$ ring as shown in the molecular structure (Fig. 25).

This arrangement can be considered an 'inverse crown' molecule, so named as it is essentially antithetical with respect to traditional crown ethers such as 18-crown-6 [(CH$_2$CH$_2$O)$_6$] which involve a Lewis basic ring which can encapsulate a Lewis acidic cation such as K$^+$. A similar product is obtained upon substituting the substrate toluene with benzene, that is, a 12-atom inverse crown containing a *para*-dimetalated benzenediide host (C$_6$H$_4$$^{2-}$). Naphthalene can likewise be doubly deprotonated at the 1 and 4 positions [86].

The identity of the basic units plays an important role in the metalation pattern as shown by slightly modifying the above base. By replacing the nBu$_2$Mg starting material with the bulkier (Me$_3$SiCH$_2$)$_2$Mg, the toluene substrate is again dideprotonated, but this time the regioselectivity has changed from a 2,5 to a 3,5 (*meta*, *meta'*; Fig. 24) orientation [87].

Remarkably, upon moving to the congeneric potassium magnesiate, 'KMg (TMP)$_2$$n$Bu', O'Hara has identified three different polymorphic forms, each with a highly distinct structural motif. One is a helical chain polymer [MgNKN]$_\infty$, whereas the other two are cyclotetrameric or cyclohexameric containing a [MgNKN]$_4$ or [MgNKN]$_6$ ring, respectively [86]. Interestingly the 24-membered
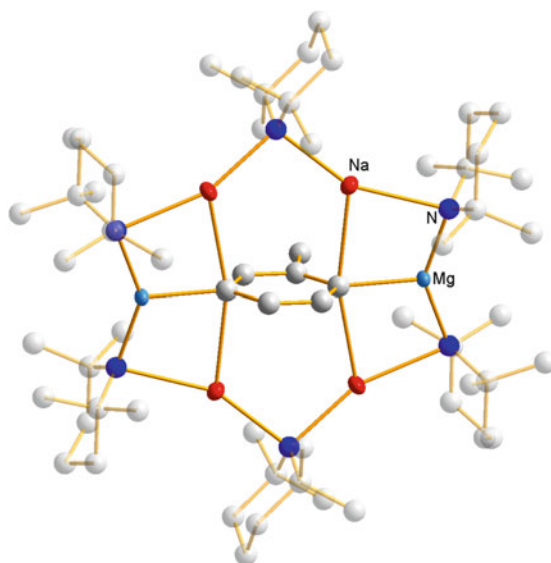
Fig. 25 Molecular structure of Na/Mg inverse crown containing the $C_6H_3CH_3$ dianion in its core
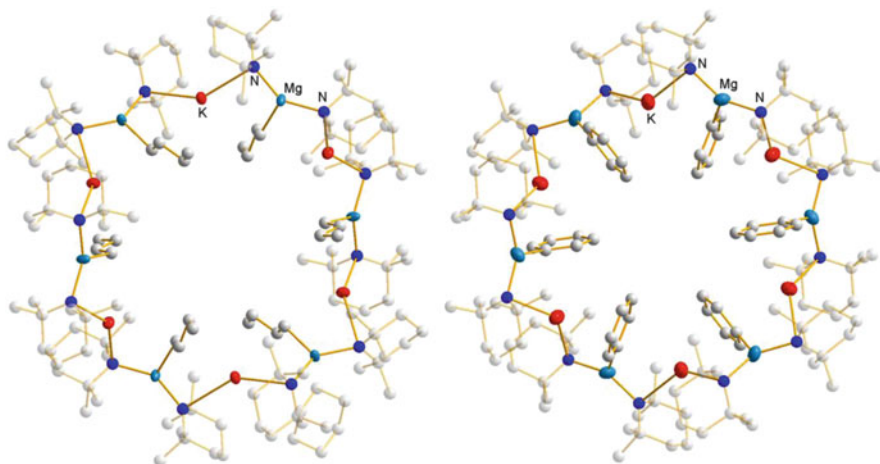
Fig. 26 Potassium magnesiate pre-inverse crown (*left*) and the inverse crown formed upon reaction with benzene (*right*)

hexameric ring can be described as a 'pre-inverse crown' with the active *n*Bu base units all pointing inwards to the centre of the ring appearing primed for deprotonating incoming arene molecules to give the final inverse crown structure with six singly deprotonated aryl anions within the core (Fig. 26) [88].

A slight modification of the sodium magnesiate has a profound effect on how the metalation of benzene is manifested. Specifically, the heteroleptic ate with a Lewis
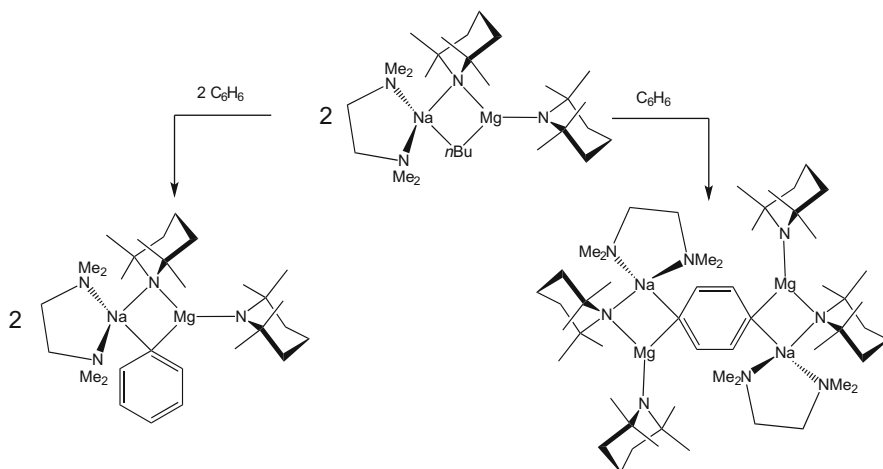
Fig. 27 Stoichiometric dependence of benzene deprotonation by magnesiate TMEDA·Na(TMP)(nBu)Mg(TMP)

donor capping the alkali metal, TMEDA·Na(TMP)(nBu)Mg(TMP) [63], still yields a product which contains a *para*-dimetalated benzene dianion, but there is no closed 'inverse crown' component due to its steric and electronic disruption by TMEDA (Fig. 27) [89]. However, by halving the reaction stoichiometry from two moles to one of ate base per substrate, the monodeprotonated complex conforming to the previously mentioned template motif (see Fig. 3) can be isolated. It is of note here that the heteroleptic base acts through alkyl (nBu) basicity as opposed to amido (TMP) basicity overall though it is possible that TMP reacts first as in the aforementioned two-step process discussed in Sect. 2.3.

The critical role played by the anionic ligand is emphasized in the contrasting products obtained upon reacting ferrocene with homoleptic NaMg(amide)$_3$ (where amide = TMP or diisopropylamide). With the former, a precedented dideprotonation of ferrocene takes place [90], whereas with the latter the unprecedented tetra-deprotonation of ferrocene occurs [91]. The resulting complex of the latter reaction is a sixteen-membered [NaNMgN]$_4$ inverse crown ring with an electron-abundant [Fe(C$_5$H$_3$)$_2$]$^{4-}$ molecule encapsulated within it (Fig. 28). The synergic effect of the two metals working in unison is clear here since neither of the homometallic NaNiPr$_2$ and Mg(NiPr$_2$)$_2$ component parts of the ate can achieve this on their own. The generality of this tetra-deprotonation was shown when the same outcome was achieved with the heavier group 8 congeners ruthenocene and osmocene [92]. This direct magnesiation was particularly eye-opening since no Grignard reagent or dialkylmagnesium reagent can metalate ferrocene, let alone tetrametalate it, although since the publication of this work Knochel has achieved monomagnesiations with (TMP)MgCl·LiCl [93]. By using a sequential magnesiation/electrophilic quenching protocol, carboethoxyferrocene could be converted into a 1,2 di-, 1,2,3 tri- and finally 1,2,3,4-tetra substituted ferrocene.
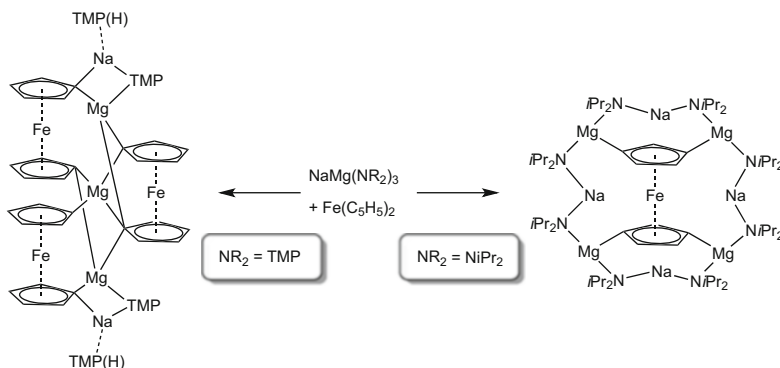
Fig. 28 Amide dependence of magnesiation of ferrocene with sodium magnesiate
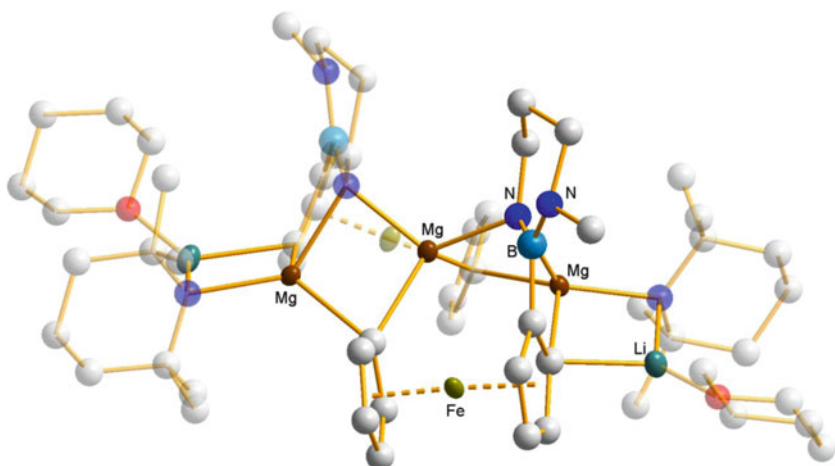
Fig. 29 Molecular structure of a polymetalated diaminoboryl substituted ferrocene

Meanwhile, Wagner, Lerner and co-workers have prepared magnesiated and zincated ferrocenophanes by transmetalation of lithiated ferrocene with MCl_2 (M = Mg, Zn) [94] and have recently directly magnesiated a diaminoboryl substituted ferrocene using a 1:2 mixture of Li(TMP) and $Mg(TMP)_2$ in tetrahydropyran (THP) [95]. This product ($[Li_2(THP)_2Mg_3(TMP)_2(C_5\text{-}H_4FeC_5H_3BN(Me)CH_2CH_2CH_2B)_2]$, Fig. 29) contains lithium in the *ortho* position and magnesium in the *ortho*, N and *1'* positions.

The sodium zincate base TMEDA·Na(TMP)(tBu)Zn(tBu) has also been shown to effect dideprotonation of a 2-substituted thiophene substrate at the 3 and 5 positions [96]. Rather than adopting an inverse crown with a central anion, this reaction produces a highly unusual supramolecular product {Na[μ-3,5-[2-C(O)NEt_2]-C_4H_1S]Zn(tBu)}_4 which can be considered as the cyclotetrameric derivative of the dizincated product (Fig. 30).

Fig. 30 Molecular
structure of supramolecular
complex obtained upon
dideprotonation of *N,
N*-diethyl-thiophene-2-
carboxamide. Sodium
atoms bound to carbonyl
group and donor solvent
molecules are omitted for
clarity
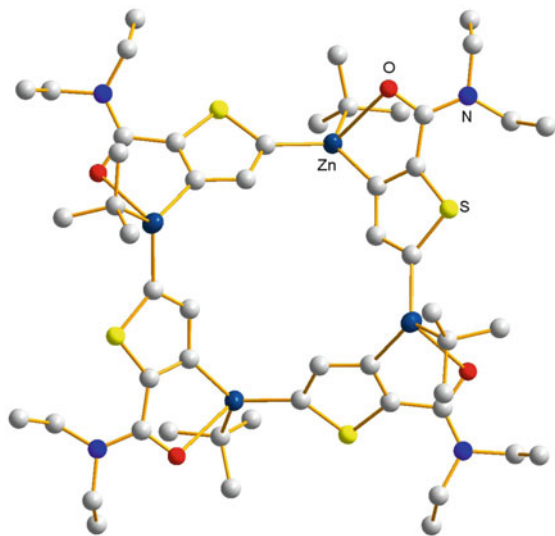
2.6   Deprotonation of Non-aromatic or Weakly Acidic
Substrates

Until now the majority of substrates discussed have been aromatic, many
containing functional groups which play a dual role of inductive acidification of
the *ortho* position as well as providing an anchoring point to coordinate the Lewis
acidic metalating agent. However, the synergic power of ate complexes has also
proven to be sufficient to deprotonate non-aromatic complexes at poorly acidic
sites. A pertinent example is that of the common cycloether THF which, when
metalated adjacent to the oxygen atom by a more conventional homometallic
approach, commonly spontaneously fragments into ethene and a metal enolate of
acetaldehyde by a 3+2 cycloreversion reaction (Fig. 31) [97], attributable to the
repulsive forces of the negative charge lying adjacent to Lewis basic oxygen.
However, the mild sodium zincate reagent TMEDA·Na(TMP)(CH$_2$SiMe$_3$)Zn
(CH$_2$SiMe$_3$) can execute such a deprotonation (C-H to C-ZnR exchange) and
then stabilize and keep intact the resulting cyclic anion [98]. Stabilization is
synergistic in execution too with Zn bonded to the α-C atom via a σ bond while
Na binds datively to one of the oxygen lone pairs.

   While this reaction requires the substrate THF to be in a vast excess (it actually
doubles up as the reaction solvent) and typically takes 2 weeks to obtain acceptable
yields, the lithium aluminate base LiAl(TMP)$_2$*i*Bu$_2$ can carry out a similar trans-
formation on stoichiometric THF in a considerably shorter time span [99].
The origin of the activity of this lithium aluminate is its bis-amido/bis-alkyl
composition, as the very similar lithium aluminate LiAl(TMP)*i*Bu$_3$ is an effective
metalating agent for aromatic substrates but does not metalate THF and is fre-
quently employed in such a medium [100]. Indeed, these two ate complexes have
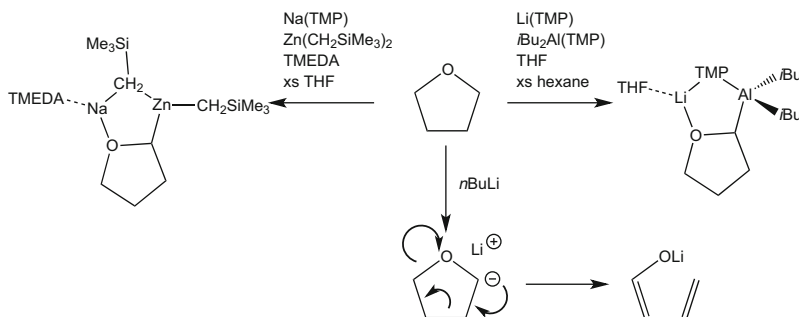
Fig. 31 Controlled deprotonation of THF and stabilization of the resulting carbanion by a sodium zincate and a lithium aluminate

been systematically examined in the presence of a variety of polydentate non-aromatic O or N/O donor molecules with the amido-rich aluminate deprotonating them and the alkyl-rich aluminate only producing a donor-acceptor adduct in most cases [101]. Surprisingly, an inverse of reactivity is seen with poly-N donors such as TMEDA or PMDETA, with the normally less reactive LiAl(TMP)iBu$_3$ deprotonating two equivalents via dual alkyl-amido basicity to give complexes of generic formula (donor - H)$^-_2$LiAliBu$_2$, while LiAl(TMP)$_2i$Bu$_2$ deprotonates only a single molar equivalent via amido basicity to yield (donor - H)$^-$Li(TMP)AliBu$_2$ (Fig. 32) [102].

A particularly attractive feature of lithium aluminates is their halogen tolerance, opening up a wider range of substrates since no metal-halogen exchange occurs. This is exemplified by the synthesis of 2,4,6-heterohaloanisoles starting from a 4-halogenated substrate. The first reaction is a DoM occurring at the 2 position, which when quenched provides a new substrate which can be resubjected to another equivalent of the base, this time being deprotonated at the 6 position. This second deprotonation is also a DoM reaction, occurring selectively adjacent to the strongest directing group. A final electrophilic quench provides after purification the tetrasubstituted triheterohalogenated aromatic species (Fig. 33) [57].

On moving to the potassium derivative, highly unusual reactivity is observed. Attempts to make the putative base TMEDA·K(TMP)$_2$AliBu$_2$ by the co-complexation of K(TMP) with iBu$_2$Al(TMP) in the presence of TMEDA saw a 'self-deprotonation' whereby one of the TMP anions effectively deprotonated a flanking methyl group of the other TMP molecule, producing an unprecedented TMP dianion in the complex TMEDA·K(TMP*)(iBu)AliBu (Fig. 34) [103]. What has occurred here is the highly unusual conversion of one of the TMP anions from a Brønsted base to a Brønsted acid.

Another interesting example of unusual reactivity with a bimetallic ate is found in the reaction between zincate THF·Li(TMP)(tBu)Zn(tBu) and trimethyl(phenoxy)silane. At first glance one might expect this molecule to undergo directed *ortho*-metalation (see Sect. 2.1) in a similar manner to that witnessed with anisole for example. However, a potent nucleophilic alkali-metal reagent such as tBuLi rather
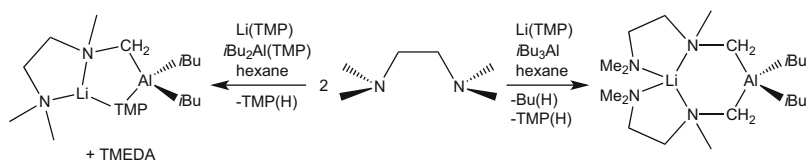
Fig. 32 Contrasting reactivity of lithium TMP aluminate bases towards TMEDA
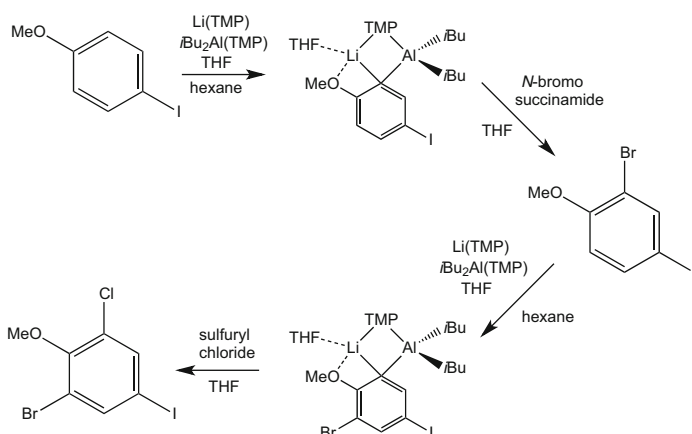
Fig. 33 Sequential deprotonation and halogenation steps to give a heterohalogenated aromatic molecule using a lithium aluminate base
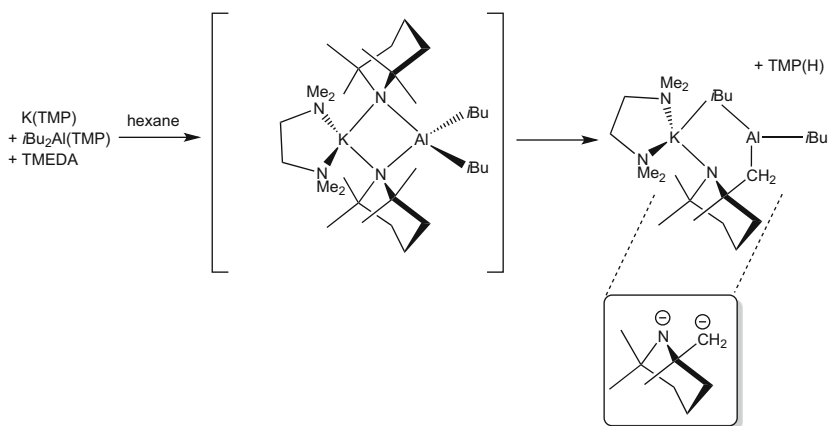
Fig. 34 Self-deprotonation of TMP in a potassium aluminate with TMP dianion emphasized (*inset*)
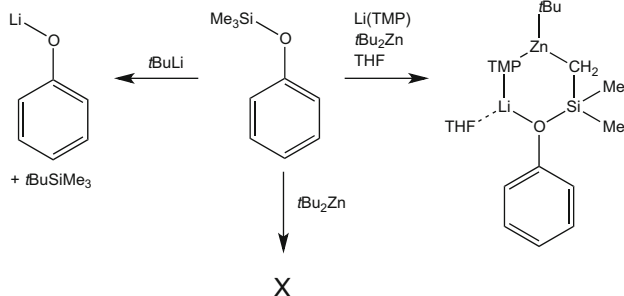
Fig. 35 Contrasting reactions of trimethyl(phenoxy)silane with homometallic and ate metalating reagents

effects O–Si bond cleavage, forming lithium phenoxide and a tertiary silane (tBuSiMe$_3$), while the lithium zincate deprotonates at a silicon-bound methyl arm leaving the resulting anion intact (Fig. 35) [104]. Corroborating the synergic nature of this reaction, a control reaction between the substrate and homometallic ZntBu$_2$ revealed no reaction.

2.7 Cleave and Capture

Although ate complexes are adept at sedating sensitive anions within their molecular framework, they can also, depending on their constitution, follow a different path of reactivity whereby the substrate in question is broken up into multiple components which are subsequently trapped within the framework. Designated as 'cleave and capture' chemistry [105], a reaction of THF with the reactive magnesiate TMEDA·Na(TMP)(CH$_2$SiMe$_3$)Mg(TMP), depicted in Fig. 36, shows an exemplar of this type [106].

Specifically this reaction involves the breaking of six THF bonds (note that THF only contains 13 bonds to begin with) resulting in an O^{2-} and a *trans*-1,3-butadienide (CH=CH–CH=CH) dianion being captured, the former within an eight-membered (MgNNaN)$_2$ inverse crown and the latter within a bimetallic TMEDA-solvated framework. The former structure represents somewhat of a common motif in inverse crown chemistry with other examples including [Li$_2$Mn$_2$(TMP)$_4$O] and [Na$_2$Mn$_2$(HMDS)$_4$O] [107]. The trapped butadiene structure has the 4-membered hydrocarbon chain bound terminal to magnesium via σ bonds while the Na component of the ate fragment stabilizes the structure via π interactions to the electron-rich olefinic region.
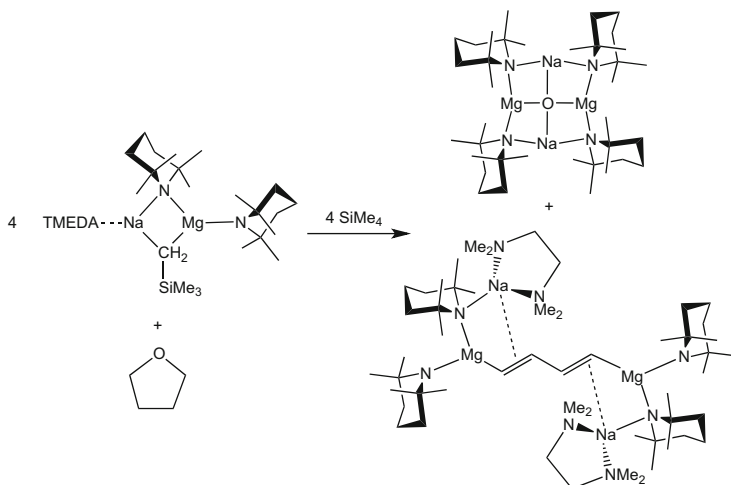
Fig. 36 Cleave and capture of THF by a sodium magnesiate

3 Conclusions and Outlook

Approaching nearly a century since the first reported reaction in this classification, metalation remains one of the most important tools in the synthetic chemist's toolbox today. From the highlights presented in this article, it is clear that the past decade or so has seen seminal progress in these C–H to C-metal exchange reactions with other organometallics, in particular those of magnesium and zinc now finding employment in reactions previously the near exclusive domain of lithium. These new practitioners of metalation cannot metalate on their own due to their weak electropositive nature; hence, they require activation which can often come about by incorporating them within an ate (anionic) composition in partnership with an alkali metal. In the most special cases, these alkali-metal-mediated metalations, for example, magnesiations and zincations, can effect *meta*-metalation or regioselective polymetalations of certain aromatic substrates where individually their component homometallic species fail altogether or produce a different outcome. Thus, these ate metalations can be thought of as metal-metal'-induced synergistic chemistry. Such chemistry is not limited to pairing an alkali metal with a less electropositive metal as it has been known for over half a century that mixing *n*-butyllithium with potassium *t*-butoxide will show reactivity patterns in metalation applications distinct from those of the individual components. Though perhaps not couched often in language of synergistic chemistry, reactions of this popular superbase and related systems can be interpreted as examples of mixed-metal mixed-ligand synergistic systems. The structural studies mentioned in this article show that ates and their metalated products retain the attributes of conventional alkali-metal systems in exhibiting a bewildering assortment of aggregation and solvation phenomena, most spectacularly demonstrated in the inverse crown

macrocycles with some host rings as large as 24 atoms in hexameric motifs. With modular permutations of ates and related polymetallic systems possible (systematically changing the metals, ligands and donor supports) it looks certain that synergistic chemistry will continue to advance metalation for years to come. Synergistic chemistry will also develop beyond the confines of metalation to other types of reaction. Petrukhina's beautiful mixed lithium-potassium corannulene 'clamshells' show that mixing s-block metals can also be beneficial to polyaromatic reduction chemistry [108]. At present the mixed-metal synergistic field lacks the rigour of the physical-organic chemistry studies that have been so critically important to the development of classical organolithium chemistry. Applying physical-organic studies to this field will help realize a more complete understanding of how these cooperative effects between pairs of metals and ligands operate and how we can best tune them for forthcoming synthetic campaigns. It is hoped that the many fascinating reactions described in this article may well inspire future studies of this type.

References

1. Collum DB (1993) Acc Chem Res 26:227
2. Tidwell TT (2001) Angew Chem Int Ed 40:331
3. Mulvey RE, Robertson SD (2013) Top Organomet Chem 45:103
4. Schlenk W, Holtz J (1917) Ber Dtsch Chem Ges 50:262
5. Schlenk W, Bergmann E (1928) Liebigs Ann 463:98
6. Schlenk W, Schlenk W Jr (1928) Chem Ber 62:920
7. Clayden J (2002) Organolithiums: selectivity for synthesis. Elsevier, Oxford
8. Lappert M, Power P, Protchenko A, Seeber A (2009) Metal amide chemistry. Wiley, Chichester
9. Mulvey RE, Robertson SD (2013) Angew Chem Int Ed 52:11470
10. Wanklyn JA (1858) Liebigs Ann 108:67
11. Wanklyn JA (1858) Proc R Soc London 9:341
12. Smith MB (2013) March's advanced organic chemistry. Wiley, New York
13. Merkel S, Stern D, Henn J, Stalke D (2009) Angew Chem Int Ed 48:6350
14. Haag B, Mosrin M, Ila H, Malakhov V, Knochel P (2011) Angew Chem Int Ed 50:9794
15. García-Álvarez P, Graham DV, Hevia E, Kennedy AR, Klett J, Mulvey RE, O'Hara CT, Weatherstone S (2008) Angew Chem Int Ed 47:8079

16. Armstrong DR, García-Álvarez P, Kennedy AR, Mulvey RE, Parkinson JA (2010) Angew Chem Int Ed 49:3185
17. Wunderlich SH, Knochel P (2009) Angew Chem Int Ed 48:9717
18. Jeganmohan M, Knochel P (2010) Angew Chem Int Ed 49:8520
19. Bernhardt S, Manolikakes G, Kunz T, Knochel P (2011) Angew Chem Int Ed 50:9205
20. Stathakis CI, Bernhardt S, Quint V, Knochel P (2012) Angew Chem Int Ed 51:9428
21. Stathakis CI, Manolikakes SM, Knochel P (2013) Org Lett 15:1302
22. Wittig G, Meyer FJ, Lange G (1951) Justus Liebigs Ann Chem 571:167
23. Wittig G (1958) Angew Chem 70:65
24. Wittig G (1966) Q Rev Chem Soc 20:191
25. Lochmann L, Pospíšil J, Vodňanský J, Trekoval J, Lím D (1967) Collect Czech Chem Commun 30:2187
26. Schlosser M (1967) J Organomet Chem 8:9
27. Broaddus CD (1970) J Org Chem 35:10
28. Kennedy AR, MacLellan JG, Mulvey RE (2001) Angew Chem Int Ed 40:3245
29. Unkelbach C, O'Shea DF, Strohmann C (2014) Angew Chem Int Ed 53:553
30. Gros P, Fort Y, Queguiner G, Caubère P (1995) Tetrahedron Lett 36:4791
31. Caubère P (1993) Chem Rev 93:2317
32. Fleming P, O'Shea DF (2011) J Am Chem Soc 133:1698
33. Blangetti M, Fleming P, O'Shea DF (2011) Beilstein J Org Chem 7:1249
34. Blangetti M, Fleming P, O'Shea DF (2012) J Org Chem 77:2870
35. Weiss E (1993) Angew Chem Int Ed 32:1501
36. Thoennes D, Weiss E (1978) Chem Ber 111:3726
37. Greiser T, Kopf J, Thoennes D, Weiss E (1981) Chem Ber 114:209
38. Schubert B, Weiss E (1984) Chem Ber 117:366
39. Carrella LM, Clegg W, Graham DV, Hogg LM, Kennedy AR, Klett J, Mulvey RE, Rentschler E, Russo L (2007) Angew Chem Int Ed 46:4662
40. Weiss E, Wolfrum R (1968) Chem Ber 101:35
41. Mobley TA, Berger S (1999) Angew Chem Int Ed 38:3070
42. Baillie SE, Clegg W, García-Álvarez P, Hevia E, Kennedy AR, Klett J, Russo L (2012) Organometallics 31:5131
43. Baillie SE, Clegg W, García-Álvarez P, Hevia E, Kennedy AR, Klett J, Russo L (2011) Chem Commun 47:388
44. Snieckus V (1990) Chem Rev 90:879
45. Schlosser M (2005) Angew Chem Int Ed 44:376
46. Campos KR (2007) Chem Soc Rev 36:1069
47. Gilman H, Bebb RL (1939) J Am Chem Soc 61:109
48. Wittig G, Fuhrmann G (1940) Ber Dtsch Chem Ges B 73:1197
49. Whisler MC, MacNeil S, Snieckus V, Beak P (2004) Angew Chem Int Ed 43:2206
50. Beak P, Brown RA (1982) J Org Chem 47:34
51. Beak P, Brown RA (1977) J Org Chem 42:1823
52. Beak P, Brubaker GR, Farney RF (1975) J Am Chem Soc 98:3621
53. Balloch L, Kennedy AR, Mulvey RE, Rantanen T, Robertson SD, Snieckus V (2011) Organometallics 30:145
54. Uchiyama M, Naka H, Matsumoto Y, Ohwada T (2004) J Am Chem Soc 126:10526
55. Harder S, Boersma J, Brandsma L, van Mier GPM, Kanters JA (1989) J Organomet Chem 364:1
56. Mulvey RE, Armstrong DR, Conway B, Crosbie E, Kennedy AR, Robertson SD (2011) Inorg Chem 50:12241
57. Conway B, Crosbie E, Kennedy AR, Mulvey RE, Robertson SD (2012) Chem Commun 48:4674
58. Fu J-m, Zhao B-p, Sharp MJ, Snieckus V (1991) J Org Chem 56:1683

59. Armstrong DR, Clegg W, Dale SH, Hevia E, Hogg LM, Honeyman GW, Mulvey RE (2006) Angew Chem Int Ed 45:3775
60. Wittig G, Merkle H (1942) Ber Dtsch Chem Ges B B75:1491
61. Lepley AR, Khan WA, Giumanini AB, Giumanini AG (1966) J Org Chem 31:2047
62. Armstrong DR, Balloch L, Hevia E, Kennedy AR, Mulvey RE, O'Hara CT, Robertson SD (2011) Beilstein J Org Chem 7:1234
63. Hevia E, Gallagher DJ, Kennedy AR, Mulvey RE, O'Hara CT, Talmard C (2004) Chem Commun 2422
64. Andrikopoulos PC, Armstrong DR, Graham DV, Hevia E, Kennedy AR, Mulvey RE, O'Hara CT, Talmard C (2005) Angew Chem Int Ed 44:3459
65. Eberhardt GG, Butte WA (1964) J Org Chem 29:2928
66. Phipps RJ, Gaunt MJ (2009) Science 323:1593
67. Leow D, Li G, Mei T-S, Yu J-Q (2012) Nature 486:518
68. Kondo Y, Shilai M, Uchiyama M, Sakamoto T (1999) J Am Chem Soc 121:3539
69. Imahori T, Uchiyama M, Sakamoto T, Kondo Y (2001) Chem Commun 2450
70. Uchiyama M, Miyoshi T, Kajihara Y, Sakamoto T, Otani Y, Ohwada T, Kondo Y (2002) J Am Chem Soc 124:8514
71. Andrikopoulos PC, Armstrong DR, Barley HRL, Clegg W, Dale SH, Hevia E, Honeyman GW, Kennedy AR, Mulvey RE (2005) J Am Chem Soc 127:6184
72. Uchiyama M, Matsumoto Y, Nobuto D, Furuyama T, Yamaguchi K, Morokuma K (2006) J Am Chem Soc 128:8748
73. Clegg W, Dale SH, Drummond AM, Hevia E, Honeyman GW, Mulvey RE (2006) J Am Chem Soc 128:7434
74. Uchiyama M, Matsumoto Y, Usui S, Hashimoto Y, Morokuma K (2007) Angew Chem Int Ed 46:926
75. Kondo Y, Morey JV, Morgan JC, Naka H, Nobuto D, Raithby PR, Uchiyama M, Wheatley AEH (2007) J Am Chem Soc 129:12734
76. Clegg W, Conway B, Hevia E, McCall MD, Russo L, Mulvey RE (2009) J Am Chem Soc 131:2375
77. Clegg W, Conway B, García-Álvarez P, Kennedy AR, Mulvey RE, Russo L, Sassmannshausen J, Tuttle T (2009) Chem Eur J 15:10702
78. Mongin F, Uchiyama M (2011) Curr Org Chem 15:2340
79. Kadiyala RR, Tilly D, Nagaradja E, Roisnel T, Matulis VE, Ivashkevich OA, Halauko YS, Chevallier F, Gros PC, Mongin F (2013) Chem Eur J 19:7944
80. Snégaroff K, Komagawa S, Chevallier F, Gros P, Golhen S, Roisnel T, Uchiyama M, Mongin F (2010) Chem Eur J 16:8191
81. García-Álvarez P, Mulvey RE, Parkinson JA (2011) Angew Chem Int Ed 50:9668
82. Armstrong DR, Kennedy AR, Mulvey RE, Parkinson JA, Robertson SD (2012) Chem Sci 3:2700
83. Li D, Keresztes I, Hopson R, Williard PG (2009) Acc Chem Res 42:270
84. Broaddus CD (1966) J Am Chem Soc 88:4174
85. Armstrong DR, Kennedy AR, Mulvey RE, Rowlings RB (1999) Angew Chem Int Ed 38:131
86. Martinez-Martinez AJ, Armstrong DR, Conway B, Fleming BJ, Klett J, Kennedy AR, Mulvey RE, Robertson SD, O'Hara CT (2014) Chem Sci 5:771
87. Blair VL, Carrella LM, Clegg W, Conway B, Harrington RW, Hogg LM, Klett J, Mulvey RE, Rentschler E, Russo L (2008) Angew Chem Int Ed 47:6208
88. Andrews PC, Kennedy AR, Mulvey RE, Raston CL, Roberts BA, Rowlings RB (2000) Angew Chem Int Ed 39:1960
89. Armstrong DR, Clegg W, Dale SH, Graham DV, Hevia E, Hogg LM, Honeyman GW, Kennedy AR, Mulvey RE (2007) Chem Commun 598
90. Henderson KW, Kennedy AR, Mulvey RE, O'Hara CT, Rowlings RB (2001) Chem Commun 1678

91. Clegg W, Henderson KW, Kennedy AR, Mulvey RE, O'Hara CT, Rowlings RB, Tooke DM (2001) Angew Chem Int Ed 40:3902
92. Andrikopoulos PC, Armstrong DR, Clegg W, Gilfillan CJ, Hevia E, Kennedy AR, Mulvey RE, O'Hara CT, Parkinson JA, Tooke DM (2004) J Am Chem Soc 126:11612
93. Stoll AH, Mayer P, Knochel P (2007) Organometallics 26:6694
94. Sánchez Perucha A, Heilmann-Brohl J, Bolte M, Lerner H-W, Wagner M (2008) Organometallics 27:6170
95. Reichert A, Schmidt J, Bolte M, Wagner M, Lerner H-W (2013) Z Anorg Allg Chem 639:1083
96. Balloch L, Garden JA, Kennedy AR, Mulvey RE, Rantanen T, Robertson SD, Snieckus V (2012) Angew Chem Int Ed 51:6934
97. Bates RB, Kroposki LM, Potter DE (1972) J Org Chem 37:560
98. Kennedy AR, Klett J, Mulvey RE, Wright DS (2009) Science 326:706
99. Crosbie E, García-Álvarez P, Kennedy AR, Klett J, Mulvey RE, Robertson SD (2010) Angew Chem Int Ed 49:9388
100. Naka H, Uchiyama M, Matsumoto Y, Wheatley AEH, McPartlin M, Morey JV, Kondo Y (2007) J Am Chem Soc 129:1921
101. Campbell R, Crosbie E, Kennedy AR, Mulvey RE, Naismith RA, Robertson SD (2013) Aust J Chem 66:1189
102. Conway B, García-Álvarez J, Hevia E, Kennedy AR, Mulvey RE, Robertson SD (2009) Organometallics 28:6462
103. Conway B, Kennedy AR, Mulvey RE, Robertson SD, García-Álvarez J (2010) Angew Chem Int Ed 49:3182
104. Hevia E, Kennedy AR, Klett J, McCall MD (2009) Chem Commun 3240
105. Mulvey RE (2013) Dalton Trans 42:6676
106. Mulvey RE, Blair VL, Clegg W, Kennedy AR, Klett J, Russo L (2010) Nature Chem 2:588
107. Kennedy AR, Klett J, Mulvey RE, Newton S, Wright DS (2008) Chem Commun 308
108. Filatov AS, Zabula AV, Spisak SN, Rogachev AY, Petrukhina MA (2013) Angew Chem Int Ed 52:5033

New Formulas for Zincate Chemistry: Synergistic Effect and Synthetic Applications of Hetero-bimetal Ate Complexes

Masanobu Uchiyama and Chao Wang

Abstract Organozincates are the oldest class of organometallic ate compounds in the history of chemistry. Their special molecular structures lead to synergetic operations which contribute to unique chemical properties. Therefore, these compounds have attracted considerable attention from organometallic chemists nowadays and also have been widely employed as an efficient synthetic tool towards various functional molecules. As a representative example, lithium zincates present many advantages such as easy preparation, adjustable reactivity/selectivity as well as diversified applicability. This chapter provides an overview of the research advances on lithium zincate, including observation history, general characterization, preparative methods, synthetic utilities as well as further applications.

Keywords Ate complex · Cross-coupling · Deprotonation · Exchange reaction · Organometallics · Polymerization · Silylzincation · Synergy · Synthetic method · Zincate

Contents

M. Uchiyama (✉) and C. Wang
Graduate School of Pharmaceutical Sciences, The University of Tokyo, 7-3-1 Hongo, Bunkyo-ku, Tokyo-to 113-0033, Japan

Advanced Elements Chemistry Research Team, Center for Sustainable Resource Science, and Elements Chemistry Laboratory, RIKEN, 2-1 Hirosawa, Wako-shi, Saitama-ken 351-0198, Japan
e-mail: uchiyama@mol.f.u-tokyo.ac.jp; uchi_yama@riken.jp

1   Introduction

In July 1849, Edward Frankland, a young chemist in England, investigated the reaction between zinc granules and iodoethane in a sealed tube under a hydrogen atmosphere. The reaction generated a mixture of diethylzinc ($ZnEt_2$) and ethylzinc iodide (EtZnI) (Eq. 1) [1, 2]. This experiment is now regarded as a key event in organic and organometallic chemistry, because it opened a door into a new field: the product of Frankland's reaction, diethylzinc, was not only the first observed organozinc compound but also the first main-group organometallic compound (IIB metals are considered as main group due to their similar electronic structure and reactivity). Nowadays, organozinc compounds are widely used. In organic chemistry, for example, organozinc compounds are employed in several famous reactions: the Barbier reaction (zinc), the Reformatsky reaction, the Simmons–Smith reaction, the Rieke metal protocol (zinc), and the Negishi coupling reaction, which was recognized by the award of the Nobel Prize in 2010:

$$Zn + EtI \xrightarrow{\text{heating under } H_2 \text{ in sealed tube}} R_2Zn + RZnI \tag{1}$$
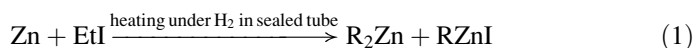
Nine years after the discovery of $ZnEt_2$, in 1858, James A. Wanklyn, who had been one of Frankland's assistants, discovered another category of organozinc: the zincate [2, 3]. When treating $ZnEt_2$ with sodium, Wanklyn found that part of the Zn(II) was reduced to zinc metal, while the rest combined with sodium to afford a new ate species, $Na^+[ZnEt_3]^-$ (Eq. 2). This zincate was also the first in the class of organometallic ate compounds:

$$Na + ZnEt_2 \xrightarrow{\text{Heating}} Na[ZnEt_3] + Zn \tag{2}$$
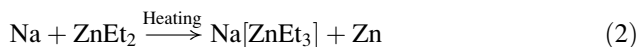
At that time, however, the development of zincate chemistry was somewhat limited compared with that of other branches of organometallic chemistry. For example, although sodium zincate had been reported in 1858, the lithium analog was discovered much later. In 1948, Dallas T. Hurd successfully obtained Li_2ZnMe_4 as the first tetra-coordinated dianion type of zincate (zincate-*da* for short), by treating dimethylzinc with 2 equiv. of methyllithium (Eq. 3) [4]. Three years later, in 1951, Georg Wittig synthesized $LiZnPh_3$ as the first tri-coordinated *mono*-anion type of lithium zincate (zincate-*ma* for short) via a similar route [5]. In those days, such ate complexes were usually called "complex metal alkyls" or

Table 1 ^{1}H-NMR signals of various methylmetal compounds

Entry	Methylmetal compound	δ (Me)/ppm
1	MeLi	-1.96
2	MeMgBr	-1.62
3	Me$_2$Zn	-0.84
4	Me$_3$ZnLi	-1.08
5	Me$_4$ZnLi$_2$	-1.44

Fig. 1 Electronic structures of different types of organozinc reagents

di-coordinated neutral organozinc
$3d^{10}\,4s^2\,4p^2$
14 electrons

tri-coordinated *mono*-anionic organozincate
$3d^{10}\,4s^2\,4p^4$
16 electrons

tetra-coordinated *di*-anionic organozincate
$3d^{10}\,4s^2\,4p^6$
18 electrons
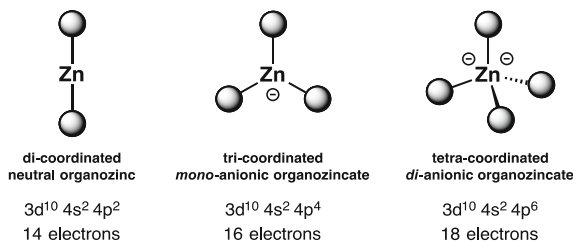
"complex anions"; until in 1958, a century after Wanklyn's observation, Wittig introduced the concept of the "ate complex." [6] This concept/name was widely accepted and is still used today:

$$\text{ZnMe}_2 + 2 \times \text{MeLi} \xrightarrow[\text{Et}_2\text{O, 0}^\circ\text{C or lower temperature}]{} \text{Li}_2\text{ZnMe}_4 \qquad (3)$$
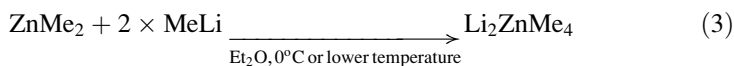
In the last three decades, zincates have attracted increasing attention from chemists, because of their special structure, unique reactivity, and high selectivity [7–9]. Neutral organozinc compounds, including organozinc halide (RZnX) and diorganozinc (ZnR$_2$), often show poor reactivity, especially for transferring the anionic R group, while zincates are much more reactive. As can be seen in the NMR data (Table 1), a more anionic ligand (Me$^-$) causes a dramatic shift in the signal of the methyl protons to much higher field [10–12]. The ^{1}H chemical shift of Li$_2$ZnMe$_4$ (-1.44 ppm) is close to that of the Grignard reagent, MeMgBr (-1.62 ppm). Therefore, carefully tuning of the zinc coordination could allow these ate complexes to act specifically as metalating reagents, bases, or nucleophiles in reactions that would be difficult for neutral organozinc compounds.

These differences can be explained in terms of the electronic structures (Fig. 1). In neutral organozinc compounds, the outer shell of zinc is 14e-form. Such an electron-deficient nature makes RZnX or R$_2$Zn able to act as a Lewis acid to accept electrons instead of donating the R anion. Coordination of an additional anionic ligand to the vacant orbital of zinc forms a favorable 16- or even 18-electron state, which makes the zincate species more stable (enhancing thermodynamic stability and reducing the Lewis acidity). On the other hand, with more anionic ligands, the whole molecule becomes more electronegative, facilitating anion transfer (promoting kinetic activity). In comparison, alkyllithium has rather high reactivity (low thermodynamic stability), which may also cause side reactions, potentially resulting in poor selectivity, while alkylzinc RZnX or R$_2$Zn usually shows quite low reactivity compared with RLi (poor kinetic activity). In short, synergy between the metals in zincates greatly modifies the reactivity, resulting in high selectivity (due to the
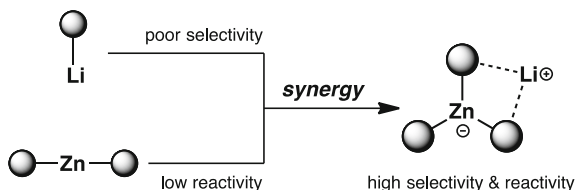
thermodynamic stability) and high reactivity (due to the kinetic activity) compared to those of monometallic reagents RLi and RZnX or R_2Zn (Fig. 2) [10–12].

In recent years, several groups, including those of Hevia, Knochel, Kondo, Koszinowski, Mongin, Mulvey, Organ, Wheatley, and others, have contributed to the evolution of zincate chemistry through structural characterization, new reactions, and synthetic applications, as well as theoretical investigations. Our group has long been interested in the chemistry of ate complexes and has successfully developed a series of novel complexes, reactions, and synthetic methods. In this chapter, we summarize our studies on lithium zincate, together with related results from other groups.

2 Hurd's Protocol for Preparation of Alkyllithium Zincates and Hybrid Zincates

As mentioned above, Hurd reported the first synthesis of Li_2ZnMe_4 by adding methyllithium to dimethylzinc in ether solution (Eq. 3) [4]. This method was used for synthesis of various zincates, including both dianionic Li_2ZnR_4 ("zincates-*da*") and monoanionic $LiZnR_3$ ("zincates-*ma*") types.

In 1977, Isobe and co-workers reported an equivalent procedure to prepare various zincates-*ma*, which were generated from zinc halide (instead of diorganozinc) and organolithium in 1:3 ratio [13]. Later, our group extended the $RLi/ZnCl_2$ procedure for the synthesis of several types of zincates-*da*, such as Li_2ZnMe_4, $Li_2Zn^nBu_4$, $Li_2Zn^tBu_4$, and so on (Eq. 4) [10–12, 14, 15]:

$$\begin{array}{c} ZnCl_2 + RLi_{(n \text{ equiv.})} \\ R = 1^\circ, 2^\circ, \text{ and } 3^\circ\text{-alkyl} \\ \text{aryl, alkenyl, alkynyl, } \textit{etc.} \end{array} \xrightarrow[\text{Et}_2\text{O, 0°C or lower temperature}]{} \begin{array}{cc} LiZnR_3 & Li_2ZnR_4 \\ (n = 3) & \text{or} & (n = 4) \end{array} \quad (4)$$
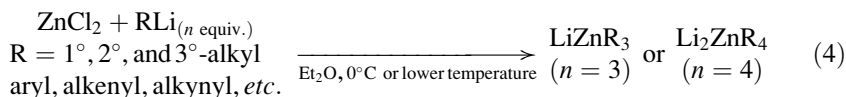
This method was also employed for synthesis of hybrid-type zincates (symbolized as *E*-zincate, *E*: heteroelement groups linked to Zn). So far, several hybrid-type zincates have been well investigated, including *H*-, *O*-, *N*-, *Si*-, *Sn*-, and *(pseudo-) halogen*-zincates.

2.1 H-Zincates

Complexes between $RZnX/ZnR_2$ and alkali-metal hydrides (MH), that is, *H*-zincates, were known considerably earlier [16, 17]. In 1970, Kubas and Shriver reported the synthesis of various kinds of new *H*-zincates from ZnR_2 and MH

(M=Li or Na) [18]. The reactivity of such *H*-zincates, LiZnHMe$_2$, and NaZnHMe$_2$ as reducing agents was subsequently investigated systematically [19]. Synthesis of *H*-zincates is still attracting interests from the viewpoint of synthetic and organo-metallic chemistry [19–25] and cluster chemistry [26, 27]. An interesting and noteworthy synthetic route was reported in 2007, when Håkansson and co-workers were reexamining Wanklyn's 1858 method [22]. They found that mild heating of NaZnEt$_3$ could trigger β-elimination of an ethyl group to give a new *H*-zincate, NaZnHEt$_2$, forming a *H*-bridged dimer, with release of ethylene gas (Eq. 5). Very recently, Mulvey and co-worker also reported an elimination protocol leading to tetra-coordinated lithium *H*-zincate-*da* [25]. Precursor **1** could be prepared via different routes, and elimination occurred soon after zincate **1** was formed, with release of isobutene to give *H*-zincate **2** as the final product (Eq. 6):
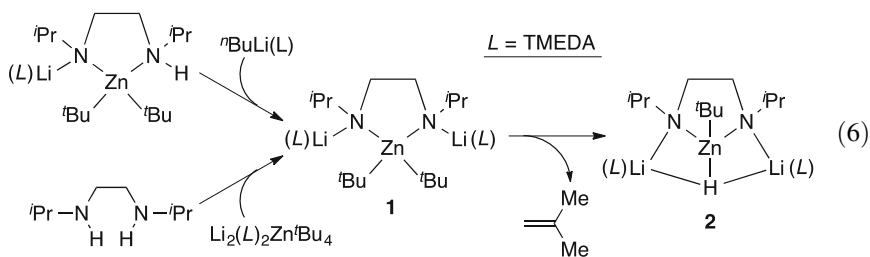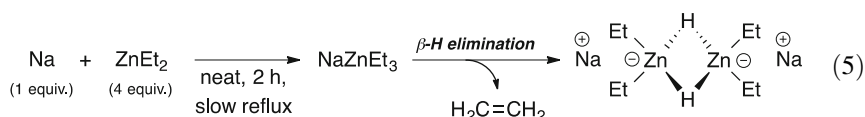
2.2 *N*-Zincates

In 1999, our group designed and synthesized a new category of 2,2,6,6-tetramethyl-piperidino-zincate, LiZn(TMP)^{t}Bu$_2$, simply by mixing Zn^{t}Bu$_2$ and LiTMP (Eq. 7) [28]. Several analogs such as diisopropylamino-zincates LiZn(DA)^{t}Bu$_2$ and LiZn(DA)Me$_2$ were obtained later similarly [29]. These *N*-zincates possess excellent reactivity for directed *ortho*-metalation (DoM) of arenes: [9]
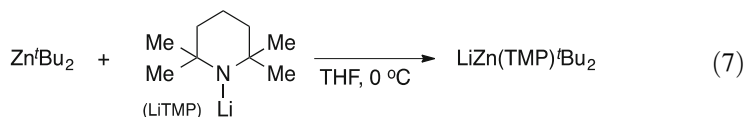
2.3 *O*-Zincates

In 1991, Richey reported that addition of KO^{t}Bu to ZnR$_2$ afforded *O*-zincate KZn(O^{t}Bu)R$_2$ [30]. In 1993, Harada and co-workers applied the lithium version of this protocol to promote alkyl migration in the reaction of *gem*-dibromocyclopropane and organozinc compounds (Fig. 3) [31]. Diorganozinc **3**, prepared from the

ROLi (equiv.)	yield of 3	cis : trans
PhCH$_2$OLi (3.0)	49%	43 : 1
LiOCH$_2$CH$_2$OLi (1.0)	70%	10 : 1
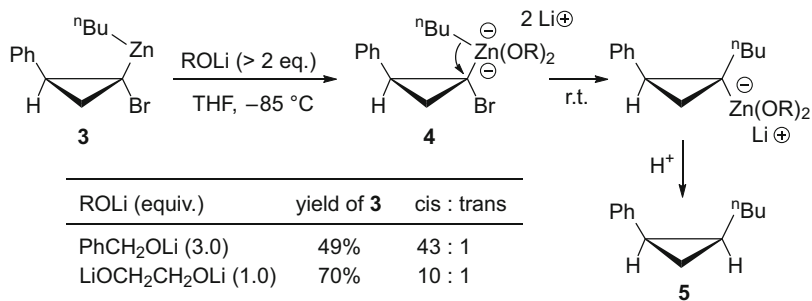
Fig. 3 1,2-Alkyl-migration promoted by in situ generated O-zincates
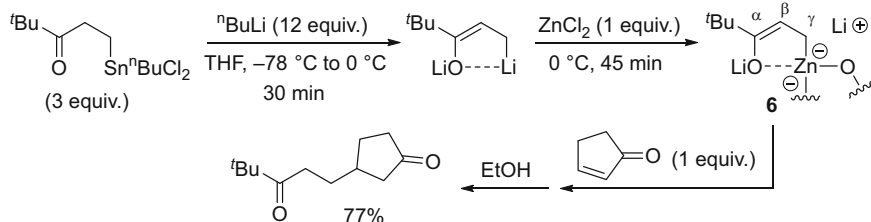
Fig. 4 *Enol*-zincate with C–O-bidentate structure

corresponding 1,1-dibromocyclopropane, was rather stable and could not launch 1,2-alkyl migration [8, 32], due to the low nucleophilicity of neutral Zn species. However, introduction of lithium alkoxide (ROLi) into **3** in situ to generate *O*-zincate-*da* **4** resulted in smooth 1,2-alkyl migration to give the final product **5** after quenching.

Enol-zincates were regarded as a special class of the *O*-type, usually generated as products of 1,4-addition between α,β-unsaturated compounds and zincates (Eq. 8) [8, 33]. Generally, such *O*-zincates show similar reactivity to other enolates. However, in 2000, Ryu and co-workers found an exceptional enol-zincate (Fig. 4) [34]. The enol-zincate **6** was synthesized through the corresponding di-lithio species, which occurred as a *C–O*-bidentate structure. Upon treatment with electrophiles such as cyclohex-2-en-1-one, **6** mainly reacted at the γ-position instead of the β-position, generating an allylic anion to give 1,6-diketone as the main product. The chemistry of enol-zincates has been well reviewed by Harada, Lombardo, and Trombini and hence will not be covered in detail here [8, 33].

$$(8)$$
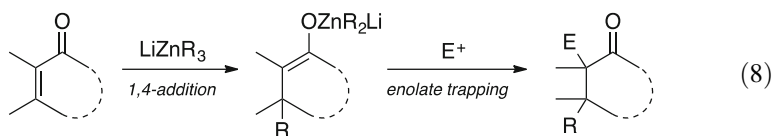
2.4   *Si*-Zincates and *Sn*-Zincates

As an analog of alkyl zincate, *Si*-zincate was synthesized as early as in 1985 by Oshima and co-workers, using ZnR_2 and silyllithium instead of alkyllithium (Eq. 9) [35]. In 1999, Krief and co-workers reported the synthesis of *Sn*-zincates from stannyllithium in a similar way [36]. Such *Si*- and *Sn*-zincates undergo silylzincation or silyl/stannyl Michael addition to unsaturated compounds. The Michael addition employing zincates has been well reviewed elsewhere, so it will not be considered in detail here [8]. Another application of *Si*-zincate, silylzincation, will be discussed later.

$$ZnR_2 \; + R'_3ELi \; \xrightarrow[\text{THF or Et}_2\text{O, 0}^\circ\text{C}]{E=S_i \text{ or } S_n} \; LiZn\left(ER'_3\right)R_2 \qquad (9)$$
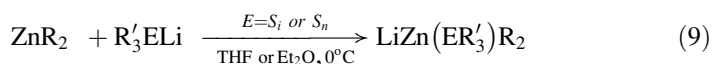
2.5   *X*-Zincates *(X = Halogen and Pseudo-halogen)*

Knochel and co-workers firstly found that adding LiCl could improve the reactivity of organozinc reagents such as ZnR_2 and RZnX [37]. Structural and mechanistic studies from the groups of Hevia, Koszinowski, and Organ revealed that the enhanced reactivity is due to the formation of a series of *X*-zincates (X=Cl or Br) [38–42]. For example, combinations of LiBr and Zn^nBu_2 in different ratios could provide both *Br*-zincate-*ma* and *Br*-zincate-*da*. (Eq. 10).

$$\qquad (10)$$
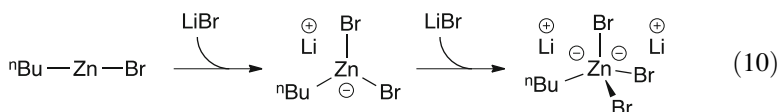
As for *pseudo*-halogens, *X*-zincates (X=CN or SCN) have been reported. Interestingly, $Li_2Zn(SCN)Me_3$ could be smoothly prepared by either adding MeLi to $Zn(SCN)_2$ or treating Li_2ZnMe_4 with $Me_3Si(SCN)$, but the reaction between MeLi and $Zn(CN)_2$ was rather sluggish; $Li_2Zn(CN)Me_3$ could only be synthesized via Me_3Si (CN) and Li_2ZnMe_4 (Fig. 5) [10–12].

A major advantage of Hurd's procedure and related methods is that the zincate is prepared without by-products (in the case of R_2Zn) or with only lithium halide as the by-product (in the case of ZnX_2), and the latter can be easily removed by filtration. Hence, such methods are widely used, especially in preparing compounds for structural research (spectroscopies, X-ray, etc.). However, from the viewpoints of synthetic diversity and functional group compatibility, Hurd's procedure and related methods have obvious limitations. Therefore, alternative synthetic methods for zincates are necessary.
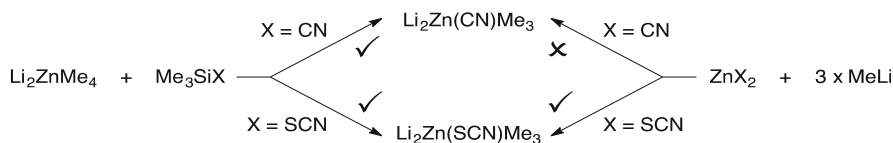
Fig. 5 Synthesis of *pseudo-halogens*-zincates
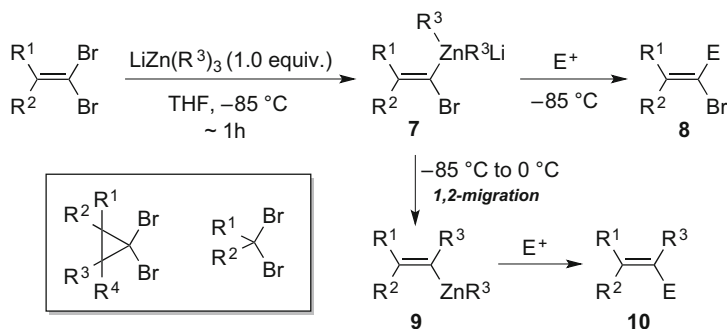
Fig. 6 Br–zincate exchange followed by 1,2-alkyl-migration

3 Halogen–Zinc Exchange of Lithium Zincate and Subsequent Trapping Reactions: Efficient Synthesis and Applications for Aryllithium Zincates

One of the earliest reactions of lithium zincates was halogen–zinc exchange reaction with organohalides. After the exchange, various new substituents could be introduced into the zincates, thus greatly broadening the range of application of such reagents. Harada and co-workers initially examined the exchange reaction between $LiZnR_3$ and *gem*-dibromoalkene [31, 43–46]. At low temperature (−85°C), Br–Zn exchange took place preferentially at the sterically more hindered position to give the vinyl zincate **7**. Trapping of **7** at this low temperature provided 1-bromoalkene substrates **8**. If the temperature was allowed to rise before electrophilic quenching, 1,2-migration would occur to give vinylzinc species **9**, which could be further functionalized to construct multi-substituted alkenes **10** (Fig. 6). *gem*-Dibromocyclopropane and other *gem*-dibromides could also react similarly with $LiZnR_3$ (also see Fig. 3) [46–48]. Since such exchange-migration reactions have been well summarized elsewhere [8, 32], they will not be further discussed in this chapter.

In 1994, Kondo and co-workers reported the first iodine–zinc exchange between aryl iodide and $LiZnMe_3$ [49]. The exchange reaction was completed rapidly at −78°C and its scope was broad (Fig. 7). Not only electron-rich substrates (e.g., 4-iodoanisole) but also those bearing fragile and electron-deficient functional groups (such as COOMe, NO_2, etc.) could smoothly undergo interconversion
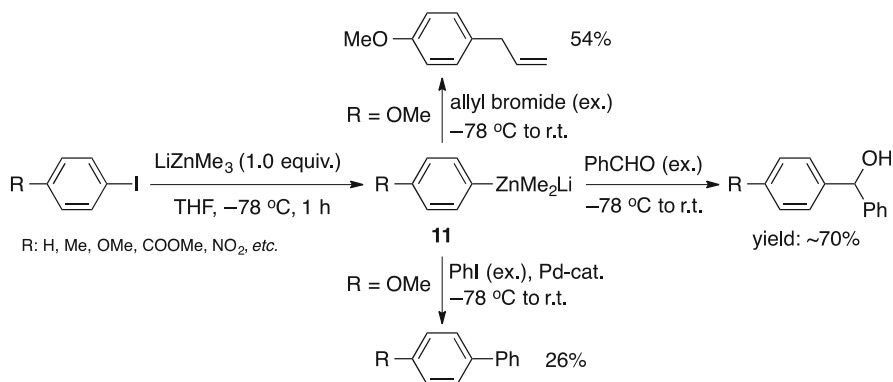
Fig. 7 Br–zincate exchange followed by various trapping

reaction to give the desired aryl zincates **11**, which could be trapped by electrophiles such as aldehyde and allyl bromide, or further participate in cross coupling with aryl halides in the presence of palladium catalyst.

However, the reactivity of zincates **11** is not sufficiently high, as reflected in the moderate/low yields of the trapping/coupling reactions. Another problem with the use of LiZnMe$_3$ is that the exchange with aryl bromide is quite sluggish. In 1996, exchange reactions between aryl bromide or iodide and zincate-*da*, Li$_2$Zn(X)Me$_3$ (X=Me, CN, or SCN), were developed by our group, and these well resolved the problems with zincate-*ma* [10–12]. By treating aryl bromide with Li$_2$Zn(X)Me$_3$ (X=Me, CN, or SCN) in THF at room temperature, the corresponding aryl zincate-*da* **12** could be obtained efficiently and could be further trapped by aldehyde to give the corresponding alcohol in high yield (entries 1–6, Table 2). Due to the high reactivity, some active substituents were not well tolerated. For example, reactions using methyl 4-bromobenzoate and all three types of zincate-*da* give only complex mixtures (entries 7–9, Table 2). It was found that I/Zn exchange using zincate-*da* showed higher tolerance of functional groups, together with higher reactivity of aryl zincate. For example, when aryl iodide **13** was treated with LiZnMe$_3$, only exchange reaction occurred. On the other hand, when Li$_2$ZnMe$_4$ was used, the aryl zincate obtained after exchange reaction could further selectively trigger an intramolecular Michael addition to construct the dihydroindole ring of **14** with the COOMe moiety remaining intact (Eq. 11). Similarly, when iodide **15** was treated with Li$_2$ZnMe$_4$, carbozincation could take place after I/Zn exchange, leading to 3-methyl-2,3-dihydrobenzo[*b*]furan **16**, though no such transformation occurred when LiZnMe$_3$ was used instead (Fig. 8).

Table 2 Reactivities of Li$_2$ZnMe$_4$

Entry	R	X	T (°C)	Yield (%)
1	H	Me	0	90
2	H	CN	r.t.	90
3	H	SCN	r.t.	89
4	MeO	Me	0	84
5	MeO	CN	r.t.	90
6	MeO	SCN	r.t.	92
7	COOMe	Me	0	Trace
8	COOMe	CN	0	Trace
9	COOMe	SCN	0	Trace
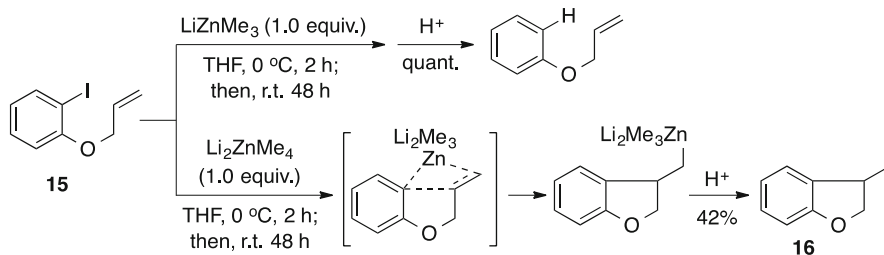
Fig. 8 Intramolecular carbozincation by using zincate-*da*
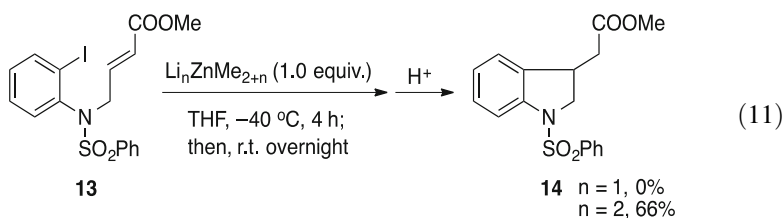
In addition to the activity, the selectivity of the two zincates was also different in some cases [12]. In a representative example, addition of LiZnMe$_3$ to aryl iodide **17** resulted in intramolecular epoxide ring-opening reaction in 86% yield with 96% *endo*-selectivity. In sharp contrast, when Li$_2$Zn(SCN)Me$_3$ was used, the selectivity changed and the *exo*-product became the major one (Eq. 12). Dihydroindole **18** and tetrahydroquinoline **19** structures exist widely in natural products and pharmaceuticals. Hence, combining the complementary results obtained with zincate-*ma* and zincate-*da* would provide an efficient and practically useful protocol for preparation of aryl zincates as well as for further derivatization:
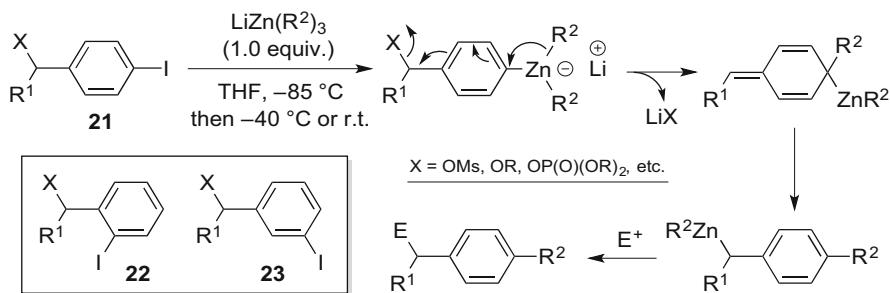
Fig. 9 Dearomatization through alkyl-migration with aryl zincates

$$[Zn] = LiZnMe_3, \mathbf{18} + \mathbf{19}: 86\% \qquad 4 : 96$$
$$[Zn] = Li_2Zn(SCN)Me_3, \mathbf{18} + \mathbf{19}: 92\% \qquad 97 : 3$$
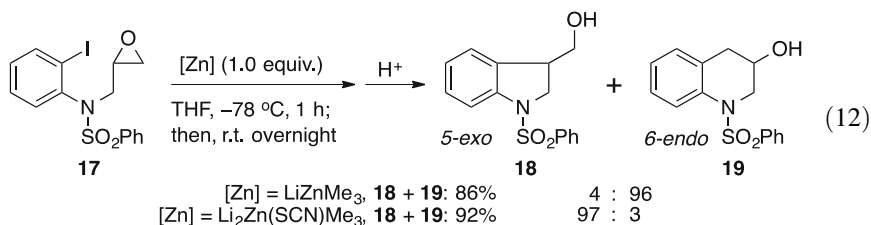
Furthermore, zincate-*da* could also be exploited in exchange reaction with *gem*-dibromocyclopropane at $-78°C$ (Eq. 13) [50]. Adding an oxovanadium (V) compound induced oxidative ligand coupling to give methylated product **20**:
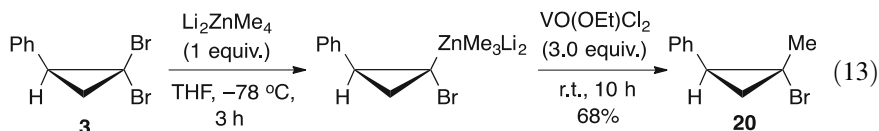
By employing this aryl halide–zincate exchange method, Harada and co-workers expanded the chemistry of exchange-migration from *gem*-dibromide to aryl halide (Fig. 9) [51, 52]. When there was a suitable leaving group at the benzyl position, aryl halides **21** could also undergo exchange-migration with zincate-*ma*, and finally zinc was transferred to the benzyl position. This reaction was regarded as an effective method for preparing benzylzinc compounds, though the yields are not high in some cases. This reaction was applicable to *ortho*-disubstituted benzenes **22**, but not to *meta*-substituted compounds **23**:

It is worth mentioning that zincate-*da* could also take part in tellurium–zinc exchange [12]. Transmetalation is an important synthetic application of organotellurium compounds. When n-butyl 2-pyridyl-telluride **24** was treated with Li_2ZnMe_4 in THF at $0°C$ and then with benzaldehyde, the corresponding alcohol could be obtained in 81% yield (Eq. 14), while the reaction with $LiZnMe_3$ did not proceed at all even under harsher conditions.
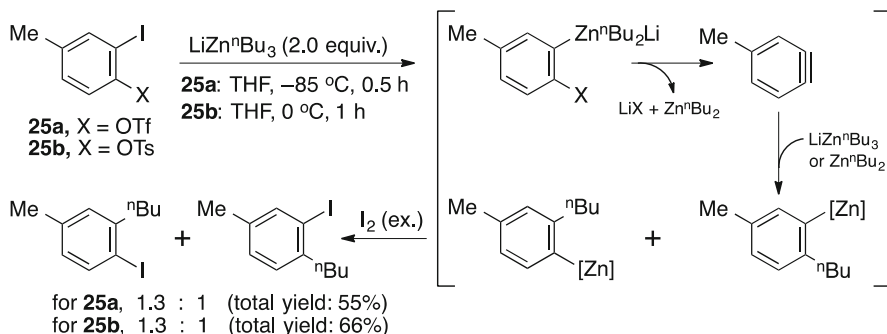
Fig. 10 Benzyne generation via aryl-zincates with leaving groups at *ortho*-position

$$(14)$$
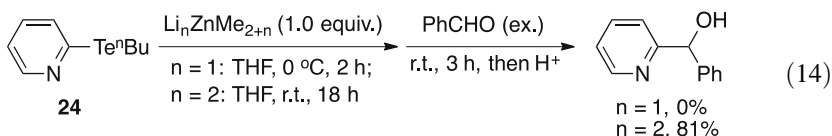
The exchange reaction using zincate was not only influenced by the coordination state of Zn, as reflected in the difference of zincate-*ma* and zincate-*da*, but could also be controlled by the ligand characteristics. In 1999, Harada and co-workers reported I/Zn exchange of 2′-iodophenylsulfonate **25** with LiZn^{n}Bu$_3$, producing 2′-butylphenyl zinc species **26**, which was proposed to be formed through a benzyne intermediate due to the lack of regioselectivity (Fig. 10) [53]. The formation of benzyne via such 1,2-elimination was proved in 2002, when our group examined the exchange reaction of 1,2-dihalobenzene derivatives **26** with LiZnMe$_3$ (Fig. 11a) [54]. After exchange, direct elimination of the zincate occurred to afford benzyne, which could be trapped by reactive diene **27**, forming the Diels–Alder adducts **28** in good to excellent yields. This reaction was later developed into an efficient method for releasing a functionalized benzyne intermediate. In contrast, when LiZn^{t}Bu$_3$ was used instead, the steric hindrance of the ^{t}Bu group resulted in highly stable 2′-haloaryl zincates **29**, which could be captured by aldehyde to give alcohols **30** in high yields (Fig. 11b).

Inspired by this result, a major improvement in exchange using zincate was achieved by our group in 2006 [14, 15]. By using an extremely bulky zincate-*da*, Li$_2$Zn^{t}Bu$_4$, halogen–zinc exchange could be achieved with both bromides and iodides with excellent functional group compatibility (Fig. 12). It is most surprising that no protecting groups were needed for those halides bearing active proton(s), such as amide (N-H), alcohol (O-H), and even rather acidic phenol. On the other hand, no racemization occurred at some sensitive chiral centers, such as the C-2 position of glycerol. Among various trapping reactions of the aryl zincate, the S$_N$2′ reactivity is particularly interesting (Table 3) [15]. After exchange reaction, treatment of the resultant zincate with propargyl bromide afforded the allene products in almost quantitative yield, in sharp contrast with the reaction using
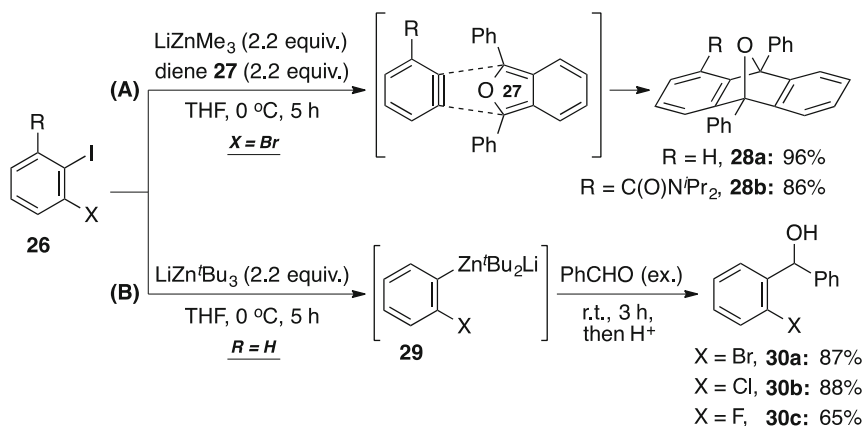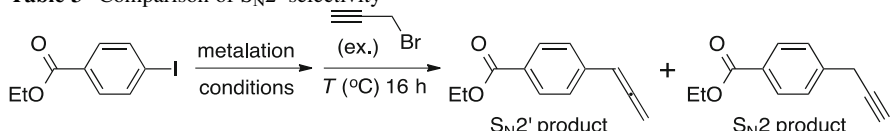
Fig. 11 Benzyne generation and suppression
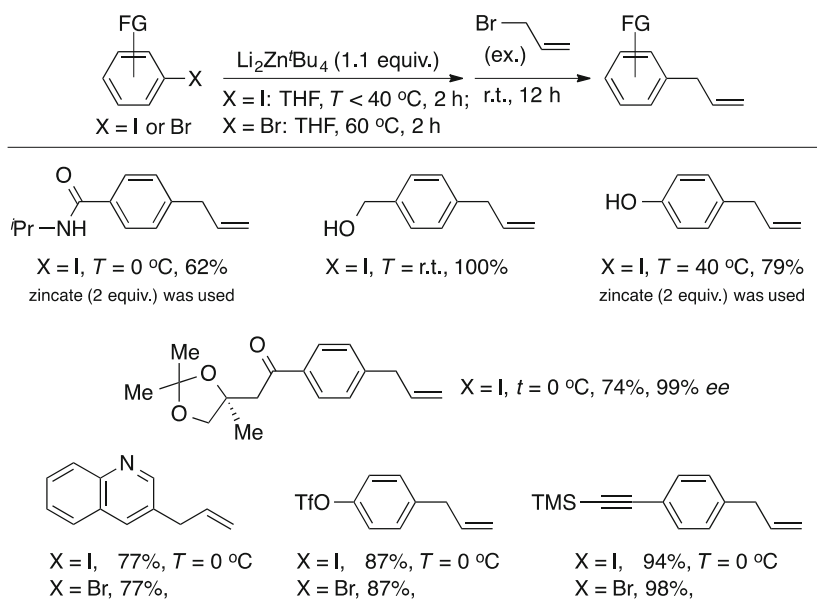
Fig. 12 Halogen–zinc exchange by using $Li_2Zn^tBu_4$

Grignard reagent or organocopper compounds. Therefore, the new approach is potentially applicable as a synthetic method for functionalized allenes. The exchange mechanism was also investigated by means of DFT calculations [55].

In 2010, Gros and co-workers further developed the chemistry of bromide–zincate exchange [56]. Although $Li_2Zn^tBu_4$ showed excellent exchange reactivity toward most iodides and bromides, its application to bromopyridines was unsatisfactory. Instead, $Li_2Zn^nBu_4$ provided much better yield and selectivity (Fig. 13).

Table 3 Comparison of S_N2' selectivity

Entry	Metalation reagent and conditions	t (°C)	Yield (%)	Ratio (S_N2'/S_N2)
1	$Li_2Zn'Bu_4$ (1.1 equiv.), THF, 0°C, 2 h	25	100	98:2
2	^iPrMgBr (1.1 equiv.), THF, −40°C, 1 h, then CuCN (10 mol%)	−40	76	79:21
3	$Li_2Cu(CN)Me_2$ (1.1 equiv.), THF, 0°C, 2 h	25	54	63:37
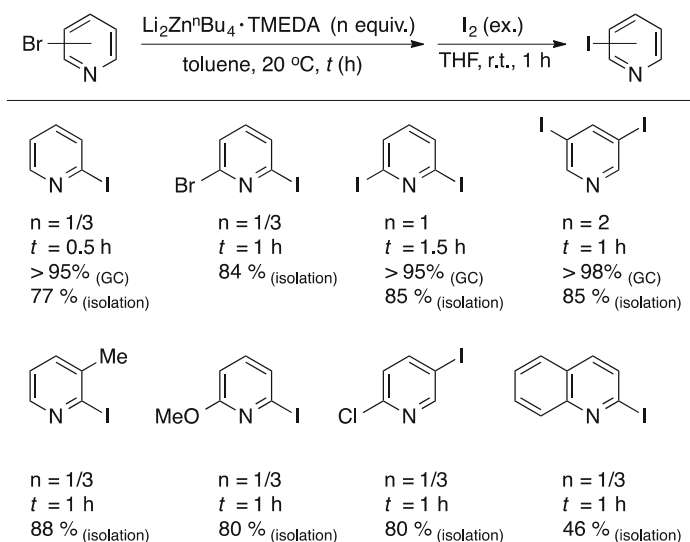
Fig. 13 Exchange reaction between bromopyridines and $Li_2Zn^nBu_4$

The reaction is essentially complete, and $Li_2Zn^nBu_4$ could be used at less than 1 equiv. (two or more ^nBu groups could react in the same molecule).

Besides the halogen–zinc exchange reaction where stoichiometric zincate was used, Knochel and co-workers also reported a catalytic protocol. Treating aryl iodide with ZnR_2 in presence of 10 mol% of lithium acetylacetonate, Li(acac), the exchange reaction could take place smoothly to give corresponding $ZnAr_2$ with excellent functional group tolerance [57, 58].

In general, exchange between aryl halide and zincate is an efficient and broad-spectrum method for synthesis of aryl zincates, with wide applications. Research in this area is continuing, aimed at development of new exchange methods and synthetic applications.
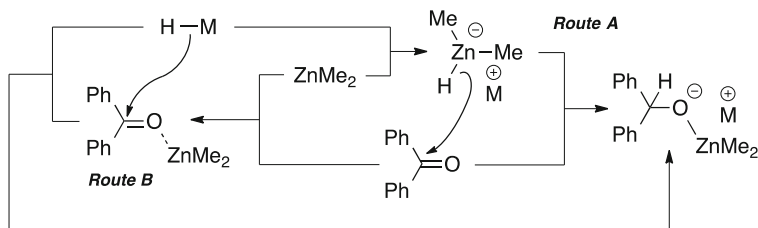
Fig. 14 Possible reaction pathways for reduction of carbonyl compounds by using H-zincate

Table 4 Diastereoselective reduction of β-hydroxy ketone

Entry	Hydride	Combined yield (%)	Ratio (*anti*:*syn*)
1	NaH $_{(2 \text{ equiv.})}$ + ZnMe$_2$ $_{(1 \text{ equiv.})}$	65	83:17
2	LiH $_{(2 \text{ equiv.})}$ + ZnMe$_2$ $_{(1 \text{ equiv.})}$	57	59:14
3	NaBH$_4$ $_{(2 \text{ equiv.})}$	91	50:50

4   Reduction Using *H*-Zincate

Although *H*-zincates have been known since the 1950s, their reactivity was little explored until 1997, when our group systematically examined the reaction scope of *H*-zincate as a highly efficient reducing agent [19]. Careful screening of the components/conditions for the *H*-zincate MZn(H)R$_2$, including ligand (R$^-$), counter cation (M$^+$), solvents, etc., revealed that MZn(H)Me$_2$ (M=Li or Na) operated with highest efficiency in THF (Eq. 15). Transfer of the methyl group was not observed at all. Two possible reaction pathways were considered (Fig. 14), i.e., synergistic action of the ate complex (A) and nucleophilic attack from hydride (NaH or LiH) promoted by ZnMe$_2$ as a Lewis acid (B). To clarify the mechanisms, we focused on the reaction of β-hydroxy ketones with *H*-zincate (Table 4). In this system, the stereochemistry in the 1,3-diol reduction products would be determined by the different reaction routes (Fig. 15). We found that the *anti*-diol **32a** occurred as the main product, while *syn*-diol **32b** was also obtained as a minor product. This result strongly supported the involvement of Path A, in which the active species is the ate complex, while path B was also a possible but minor route, since the residual ZnMe$_2$, Li$^+$, or Na$^+$ could be chelated by **31** and allow attack of external hydride to give the *syn*-product.
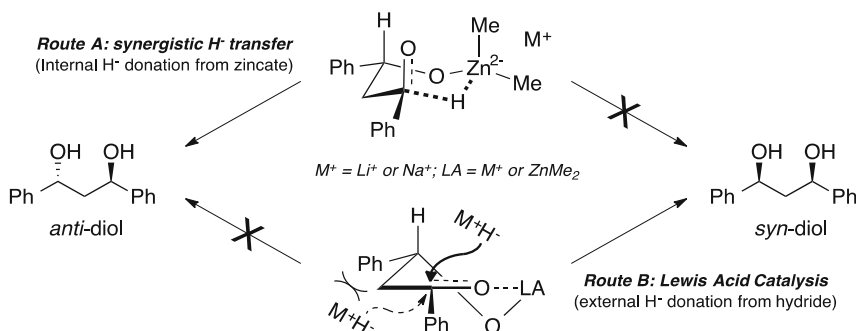
Fig. 15 Stereochemistry of reduction products determined by different reaction routes
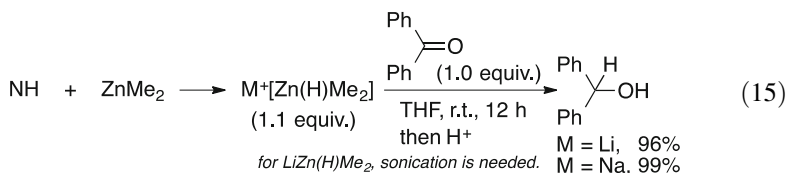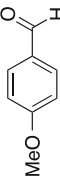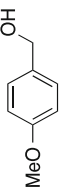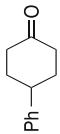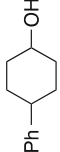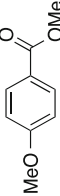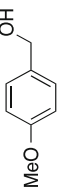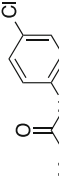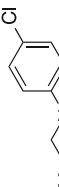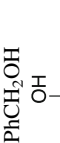
To clarify the mechanism involving *H*-zincate as the active species, a catalytic protocol was designed (Eq. 16). In the catalytic reaction, LiH seemed to be superior to NaH, as reflected in the much higher efficiency.
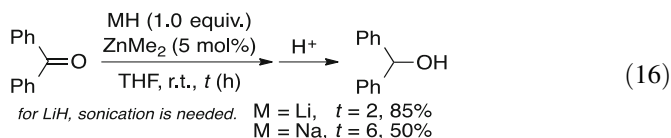
The reaction scope for the reduction using *H*-zincate was broad, whether the reaction was stoichiometric (Table 5) or catalytic (Table 6). In general, this method was not only very effective but also highly selective toward a wide variety of substrates. In some cases it was superior to the classic reduction protocols (entries 11–12, Table 5; entries 7–8, Table 6). Interestingly, this method also exhibited some special reactivities. For example, the reaction of *N,N*-dialkylamide with NaZn (H)Me$_2$ could generate alcohol as the product in high yield, which is abnormal for amide reduction (entry 10, Table 5). In another case, treating carboxylic acid with LiH in the presence of ZnMe$_2$ as a catalyst afforded aldehyde after quenching (entries 9–10, Table 6). The mechanism was considered to involve formation of the ZnMe$_2$-acetal complex intermediate **33** to prevent over-reduction (Fig. 16).
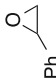
Besides β-hydroxy ketones **31**, α-hydroxy ketone **34a** and its silyl ether **34b** were also used for diastereoselective reduction, generating *anti*- and *syn*-1,2-diol **35a-b**. In these cases, NaZn(H)Me$_2$ gave the best yields and selectivity (Table 7). Opposite diastereoselectivity was observed for **34a** and **34b**, which could be explained in terms of different reduction models (Fig. 17). Different from **34a**, silyl ether **34b** showed weaker coordination ability from oxygen to zinc, and thus the reduction of

Table 5 Scope of reduction with NaZn(H)Me$_2$[a]

Entry	Substrate	Reduction product		Yield[b] (%)
1	Aldehyde	1°-Alcohol	MeO–C$_6$H$_4$–CH$_2$OH	96[c]
2	PhCH$_2$CH$_2$CHO		PhCH$_2$CH$_2$CH$_2$OH	85[c]
3	PhCH(Me)CHO		PhCH(Me)CH$_2$OH	91[c]
4	Ketone — PhCOMe	2°-Alcohol	PhCH(OH)Me	91
5	Ph–cyclohexanone		Ph–cyclohexanol (OH)	95
6	Ester — PhCOOMe	1°-Alcohol	PhCH$_2$OH	97[d]
7	MeO–C$_6$H$_4$–COOMe		MeO–C$_6$H$_4$–CH$_2$OH	98[d]
8	phthalide (lactone)		benzene-1,2-diyldimethanol	100[d]
9	1°-Amide	2°-Amine	Et–NH–C$_6$H$_4$–Cl	68[e, f]
10	2°-Amide — PhCONMe$_2$	1°-Alcohol	PhCH$_2$OH	88[e]
11	α,β-Unsaturated compound — Me–CO–CH=CH–Ph	1°-Alcohol (1,2-addition)	Me–CH(OH)–CH=CH–Ph	90[g] (73%)[h, i]

(continued)

Table 5 (continued)

Entry	Substrate	Reduction product		Yield[b] (%)
			2°-Alcohol	
12	Epoxide		PhCH(OH)Me	92 (0%)[h]

[a]Unless otherwise noted, the reaction was carried out using NaH (1.2 equiv.), $ZnMe_2$ (1.1 equiv.), and substrate (1.0 equiv.) in THF at room temperature for 12 h

[b]Isolated yield

[c]The reaction was carried out at 0°C for 1 h

[d]The reaction was carried out using NaH (2.2 equiv.) and $ZnMe_2$ (2.0 equiv.) at 0°C for 6 h

[e]The reaction was carried out using NaH (3.0 equiv.) and $ZnMe_2$ (3.0 equiv.)
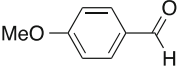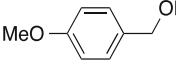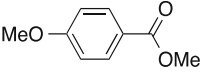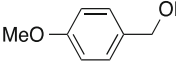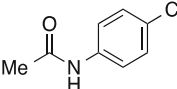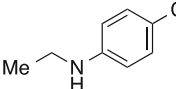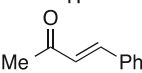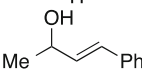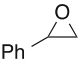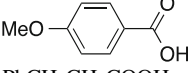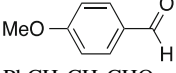
[f]4-Chloroacetanilide was recovered in 28% yield

[g]No conjugate reduction product was obtained

[h]Values in parentheses are yields of reduction using $NaBH_4$ under the same conditions

[i]4-Phenyl-2-butanone was also obtained in 25% yield when using $NaBH_4$ under the same conditions

Table 6 Scope of reduction with LiH catalyzed by $ZnMe_2$[a]

Entry	Substrate		Reduction product		Yield[b] (%)
1	Aldehyde	MeO—C6H4—CHO (O, H)	1°-Alcohol	MeO—C6H4—CH2OH (OH)	92
2		$PhCH_2CH_2CHO$		$PhCH_2CH_2CH_2OH$	93[c]
3		$PhCH(Me)CHO$		$PhCH(Me)CH_2OH$	94[c]
4	Ketone	$PhCOMe$	2°-Alcohol	$PhCH(OH)Me$	84
5	Ester	MeO—C6H4—C(O)OMe	1°-Alcohol	MeO—C6H4—CH2OH (OH)	95[d]
6	1°-amide	Me—C(O)—N(H)—C6H4—Cl	2°-Amine	Me—CH2—N(H)—C6H4—Cl	46[e]
7	α,β-Unsaturated compound	Me—C(O)—CH=CH—Ph	1°-Alcohol (1,2-addition)	Me—CH(OH)—CH=CH—Ph	88[f]
8	Epoxide	Ph—epoxide (O)	2°-Alcohol	$PhCH(OH)Me$	94[g]
9	Carboxylic acid	MeO—C6H4—C(O)OH	Aldehyde	MeO—C6H4—CHO (O, H)	82[h]
10		$PhCH_2CH_2COOH$		$PhCH_2CH_2CHO$	68[h]

[a]Unless otherwise noted, the reaction was carried out using LiH (1.2 equiv.), $ZnMe_2$ (20 mol%), and substrate (1.0 equiv.) in THF at room temperature for 12 h
[b]Isolated yield
[c]The reaction was carried out at 0°C for 1 h
[d]The reaction was carried out using LiH (3.0 equiv.) and $ZnMe_2$ (30 mol%) at 0°C for 6 h
[e]The reaction was carried out using LiH (3.0 equiv.) and $ZnMe_2$ (30 mol%) at room temperature for 48 h. N-Ethyl-4-chloroaniline was the sole product, and 4-chloroacetanilide was recovered in 32% yield
[f]Ratio of 1,2-reduction and 1,4-reduction: 96:4
[g]Ratio of 1-phenethyl alcohol and 2-phenethyl alcohol: 97:3
[h]The reaction was carried out using LiH (3.0 equiv.) and $ZnMe_2$ (100 mol%) at room temperature for 24 h
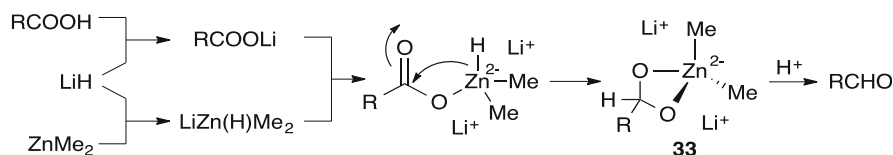
Fig. 16 Mechanism for reduction of carboxylic acid into aldehyde by using H-zincate

34b mainly occurred through a Felkin–Anh model via external hydride donation. In a similar way, reduction of 1,2-diketone **36** with $NaZn(H)Me_2$ was also diastereoselective, affording *anti-diol* **35a** as the main product (Eq. 17).

Table 7 Diastereoselective reduction of α-hydroxy ketone

34a, R = H
34b, R = Si^{i}Pr$_3$
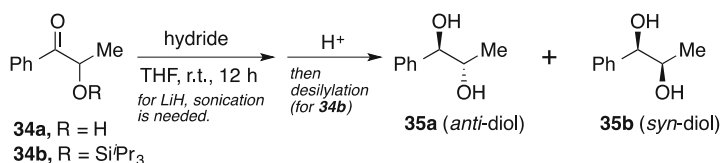
Entry	R	Hydride	Combined yield (%)	Ratio (*anti*:*syn*)
1	H	NaH $_{(2 \ equiv.)}$ + ZnMe$_2$ $_{(1 \ equiv.)}$	99	99:1
2	H	LiH $_{(2 \ equiv.)}$ + ZnMe$_2$ $_{(1 \ equiv.)}$	72	8:1
3	H	LiAlH$_4$ $_{(2 \ equiv., \ at \ -78°C)}$	92	7:1
4	H	NaBH$_4$ $_{(2 \ equiv.)}$	96	12:1
5	Si^{i}Pr$_3$	NaH $_{(2 \ equiv.)}$ + ZnMe$_2$ $_{(1 \ equiv.)}$	70	1:24
6	Si^{i}Pr$_3$	LiH $_{(2 \ equiv.)}$ + ZnMe$_2$ $_{(1 \ equiv.)}$	85	1:4
7	Si^{i}Pr$_3$	NaBH$_4$ $_{(2 \ equiv.)}$	64	1:4
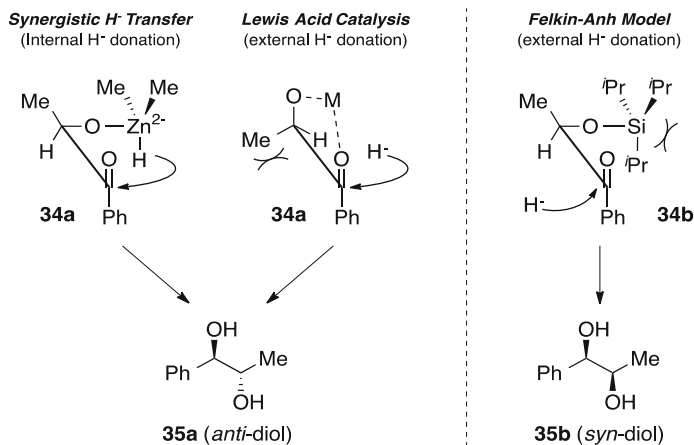
Fig. 17 Stereochemistry of reduction products determined by different reaction routes

(17)
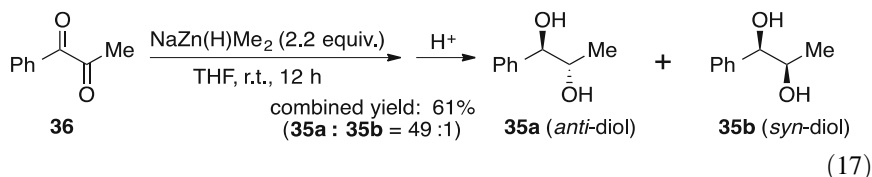
In short, reduction by using *H*-zincate showed high selectivity and remarkable reactivity, being both competitive with and complementary to the commonly used hydride process.
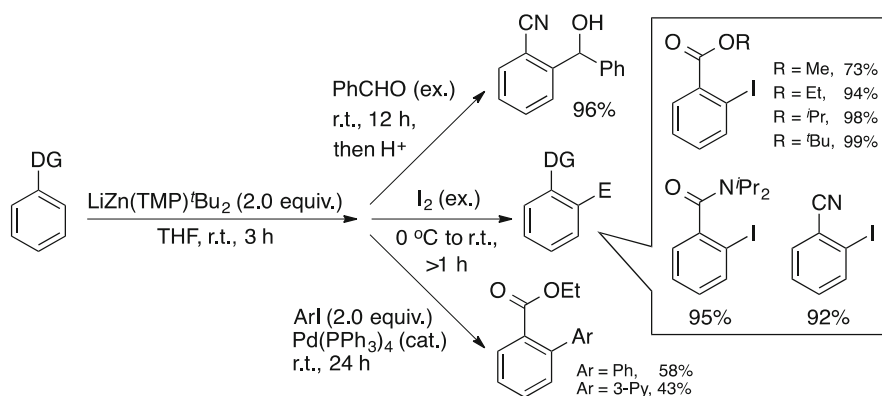
Fig. 18 Synthesis of lithium TMP-zincate and applications in deprotonative metalation of arenes

5 Deprotonation of Arenes by *N*-Zincate

Within the field of zincate chemistry, *N*-zincates and their applications as deprotonating reagents have probably received the most attention, because such reactions provide a straightforward route for chemoselective functionalization of arenes [8, 59–61]. Widely used *N*-zincates include sodium complexes and potassium complexes, as well as lithium complexes. The structures of these ate complexes have also been well characterized, in view of their significance for organometallic chemistry and their mechanistic value for understanding the deprotonation process. Since structural investigations as well as the reactions of sodium and potassium zincate complexes have been extensively reviewed elsewhere [59, 60], this section is mainly focused on the synthetic applications of lithium zincates, particularly for obtaining functionalized arenes.

In 1999, Kondo and our group reported the synthesis of lithium *TMP*-zincate from Zn^{t}Bu$_2$ and LiTMP (Eq. 7) [28] and its application in deprotonative metalation of a series of arenes (Fig. 18). Due to the high selectivity, a variety of polar moieties such as COOR (ester), CONR$_2$ (amide), and CN (nitrile) can be tolerated in arene substrates, behaving as directing groups (DG). Trapping of the metalated species with iodine or aldehyde proceeded in high yield. The metalation could also be followed by palladium-catalyzed cross coupling, though the yields were low in initial tests.

In the metalation, hydrogen in the *ortho*-position of DG in the arenes was abstracted by TMP anion and thus TMPH was released. At that time, aryl zincate **37** was supposed to be the metalated product. Later, mechanistic explorations by Mulvey, Wheatley, and our groups, using both experimental and theoretical methods, established that **37** was formed initially as a kinetic intermediate but then exchanged with TMPH and was transformed into a new *TMP*-zincate **38** as the thermodynamically stable species [62–69].
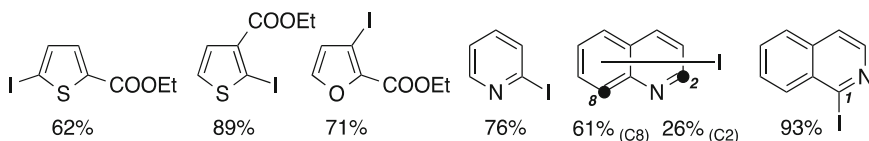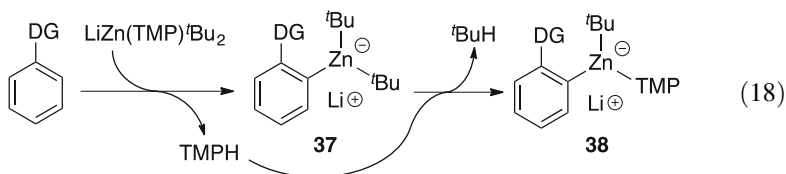
Fig. 19 Deprotonative metalations of heteroaromatic compounds by using TMP-zincate

Various heteroaromatic compounds were similarly deprotonated (Fig. 19) [28]. Among electron-rich cases, thiophene- and furan-carboxylate provided the iodo derivatives after treatment of the intermediate zincates with iodine. Interestingly, bare π-deficient heteroaromatic compounds were also readily deprotonated. With *TMP*-zincate as a base and conducting the reactions at room temperature followed by addition of iodine, pyridine, quinoline, and isoquinoline could be efficiently metalated–iodinated. Under the same conditions, quinoline was deprotonated at both C2 and C8 in a 7:3 ratio, whereas isoquinoline was deprotonated specifically at C1.

Similar examples of regioselective metalation of 3-alkylpyridine-BF_3 complexes with the use of *TMP*-zincate were reported by Michl and co-workers in 2002 [70]. The reaction occurred at the less hindered one of the two reactive positions, as evidenced by trapping of the pyridyl zincates with iodine to afford the 2-iodo-5-alkyl pyridine derivatives in good yields (Eq. 19).
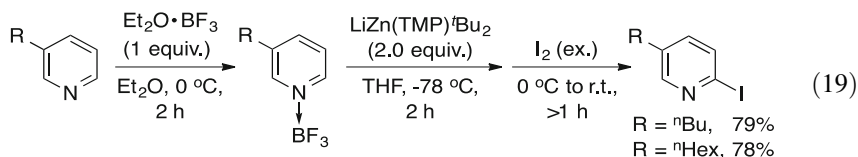
Very recently, Namgoong and co-workers reported a homologation reaction via further utilization of these zincated heterocyclic intermediates with trimethyl borate [71]. For example, treatment of isoquinoline with TMP-zincate $LiZn(TMP)^tBu_2$ followed by addition of $B(OMe)_3$ triggered migration of both the ^tBu group and zinc moiety to produce a 1,2-bismetallic species **39**, which could be further quenched to give a 3,4-dihydroisoquinoline product (Fig. 20). These reactions could also take place with quinolone, but with lower selectivity, as mentioned above.

In 2011, Hevia and co-workers reexamined the deprotonation of aromatic heterocyclics with zincate, compared with the cases of other ate complexes or mixed bases [72]. When the reaction conditions were altered, the selectivity changed drastically. In previous results from Kondo and co-workers (Figs. 18 and 19),
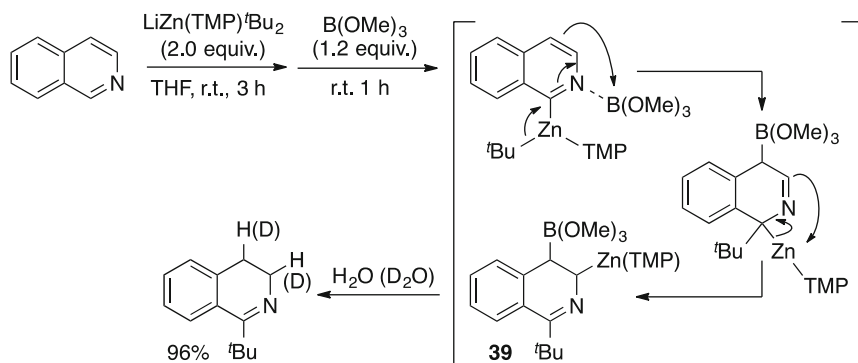
Fig. 20 Homologation reaction after deprotonative metalation of isoquinoline by using TMP-zincate

where the reaction was done at room temperature, pyridine underwent zincation at the 2-position. However, at lower temperature and in a shorter time, it was found that zincation of pyridine took place only at the 4-position, namely, 4-iodopyridine was produced after addition of iodine (Eq. 20). The difference was explained in terms of a switch between kinetic and thermodynamic control. In pyridine, the acidity ratios of the protons at the 4/3/2 positions are 700/72/1, respectively. On the other hand, in the *ortho*-product the sp^2-lone-pair nitrogen is supposed to interact with lithium and thus stabilize the intermediate, which is consistent with the experimental/computational results reported for the deprotonative metalation of trifluoromethylbenzene by the sodium zincate NaZn(TMP)^{t}Bu$_2$(TMEDA) [73]. Therefore, C-4 zincated species were formed under kinetic control, while C-2 zincated species were formed under different conditions, under thermodynamic control.

(20)
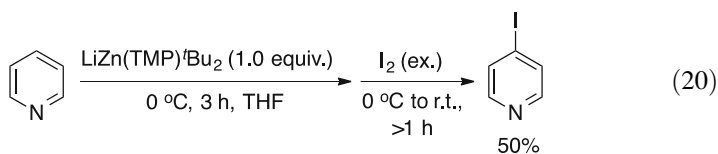
Another interesting result from Hevia's group was the zincation of 2-, 3-, or 4-methoxypyridine, since these compounds possess two directing groups [72]. With LiZn(TMP)^{t}Bu$_2$ at room temperature, the zincation proceeded specifically at the sterically less hindered *ortho*-position from the OMe groups (Eq. 21).
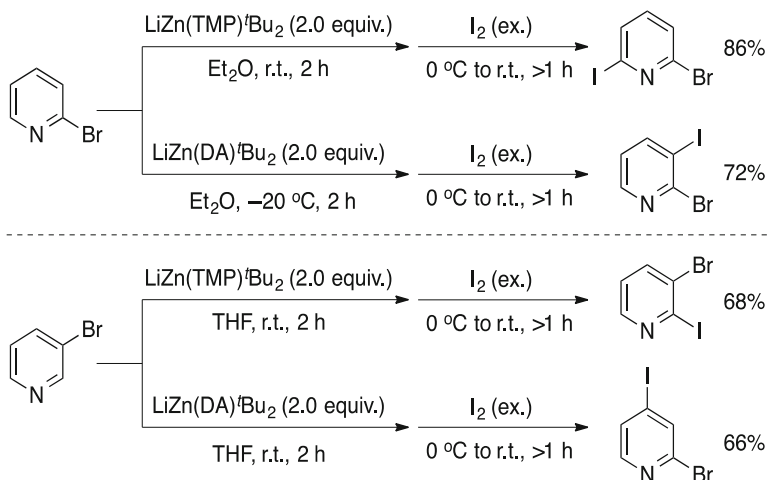
Fig. 21 Deprotonative metalations by using *DA*-zincate
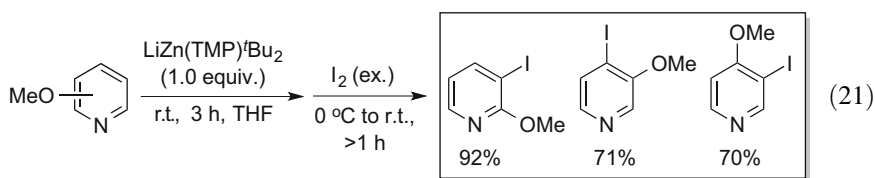
After the discovery of *TMP*-zincate, Kondo and co-workers reported another *N*-zincate containing the diisopropylamino (DA) ligand, LiZn(DA)^{t}Bu$_2$, and compared its reactivity with that of *TMP*-analogs (Fig. 21) [29]. In the reactions with 2-bromopyridine in diethyl ether solution at room temperature, *TMP*-zincate mainly underwent deprotonation at the 6-position, while in the case using *DA*-zincate at −20°C, the abstraction of hydrogen preferentially occurred at the 3-position. More interestingly, in the case of 3-bromopyridine in THF solution at room temperature, the deprotonation occurred at the sterically most hindered 2-position if *TMP*-zincate was employed, whereas, in contrast, utilization of *DA*-zincate resulted in specific metalation at the 4-position, which is least sterically hindered. These results provide diverse possibilities for selective synthesis of multifunctionalized pyridines. It is noteworthy that formation of pyridyne was never suspected during these reactions, even at room temperature, probably because the bulkiness of the *t*-Bu group prohibits the elimination.

Since 2002, our group broadened the scope of the above reaction from bromopyridine to various 1-substituted-3-bromobenzene derivatives. After deprotonation with LiZn(TMP)^{t}Bu$_2$ followed by iodination, the corresponding 1-substituted-3-bromo-2-iodobenzene derivatives were obtained in high yields (Fig. 22) [54, 74].
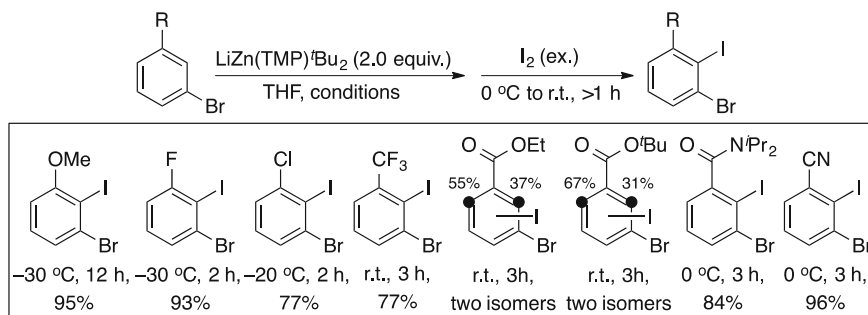
Fig. 22 Deprotonative metalations of 1-substituted-3-bromobenzenes by using bulky TMP-zincate

Surprisingly, when deprotonation was conducted with a smaller *TMP*-zincate, LiZn(TMP)Me$_2$, elimination could not be avoided [54, 74]. Raising the temperature of the reaction mixture in the presence of 1,3-diphenylisobenzofuran **27** resulted in the formation of the Diels–Alder adducts **28** from the intermediate substituted benzynes in high yields in a regioselective manner (Table 8). The elimination to benzyne normally occurred at the C2–C3 position, except for some special cases (e.g., run 4). This method using LiZn(TMP)Me$_2$ is particularly useful for the synthesis of functionalized benzyne, since conventional methods require highly substituted benzenes and can hardly tolerate electrophilic substituents.

As shown in Eq. 18, *TMP*-zincates such as LiZn(TMP)^{t}Bu$_2$ turned out to act as "multi-basic" reagents. In 2006, Mulvey et al. proposed that *TMP*-zincates deprotonate with their *C*-ligand based on the following results (Fig. 23). With LiZn (TMP)^{t}Bu$_2$ as the deprotonating reagent for anisole in 1:2 ratio, the double-DoM product **40** was obtained [62]. When benzamide was treated with LiZn(TMP)^{t}Bu$_2$ in 1:2 ratio in the presence of TMEDA, the double-DoM product **41** was also acquired [64]. However, our computational studies indicated that direct alkyl basicity is kinetically disfavored and instead pointed to a stepwise mechanism whereby *TMP*-zincate acts as an amido base, liberating HTMP during the first DoM event [65–68]. Re-coordination of the amine at lithium then leads to elimination of alkane (from alkyl anion ligand) and regeneration of the TMP base. Indeed, when benzamide was treated with LiZn(TMP)Et$_2$ in THF, the reaction afforded tris(amidoaryl)zincate **42**, which exhibited a tripodal structure in which lithium was stabilized by all three carbonyl *O*-centers, as determined by X-ray crystallography [67].

Considering that TMP anion ligand is the real active species in deprotonation, Mongin and co-workers have reported several studies on deprotonation using LiTMP/Zn(TMP)$_2$ (1/1) mixture since 2007 [75–79]. This protocol is applicable to various arenes and aromatic heterocycles (Fig. 24). In sharp contrast, usage of LiTMP or Zn(TMP)$_2$ alone resulted in very sluggish reaction.

Alkali-metal triamidozincates have been reported [80–82], but sterically hindered lithium dialkylamide and diamidozinc, e.g., LiHDMS and Zn(HDMS)$_2$, are rarely stabilized as lithium triamidozincate [83]. In the case of TMP, although LiZn

Table 8 Direct generation of 3-functionalized benzene using TMP-zincate followed by cycloaddition

Run	1	2	3	4	5	6	7	8
Substrate	OMe	F	Cl	CF$_3$	O=C–OEt	O=C–O^{t}Bu	O=C–N^{i}Pr$_2$	CN
Benzyne	OMe	F	Cl	CF$_3$	OEt	O^{t}Bu	N^{i}Pr$_2$	CN
Conditions	r.t., 12 h	60°C, 15 h	r.t., 48 h	r.t., 12 h	Reflux, 3 h	Reflux, 6 h	Reflux, 12 h	Reflux, 12 h
Yield of **28** (%)	100	71	72	100	55	88	100	90

Conditions:
PhOMe (2.0 equiv.)
LiZn(TMP)^{t}Bu$_2$ (1.0 equiv.)
THF (1.0 equiv.)
in hexane

Conditions:
PhCON^{i}Pr$_2$ (2.0 equiv.)
LiZn(TMP)^{t}Bu$_2$ (1.0 equiv.)
TMEDA (1.0 equiv.)
in hexane

Conditions:
PhCON^{i}Pr$_2$ (3.0 equiv.)
LiZn(TMP)Et$_2$ (1.0 equiv.)
in THF
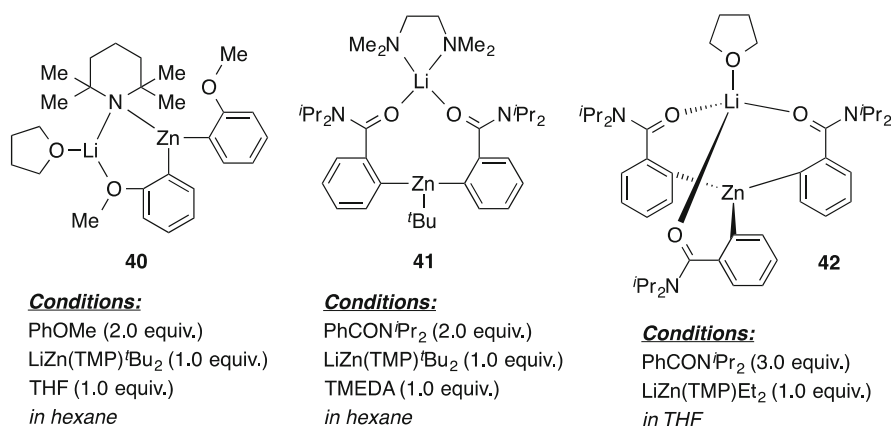
Fig. 23 Double and triple DoM reactions by using TMP-zincate
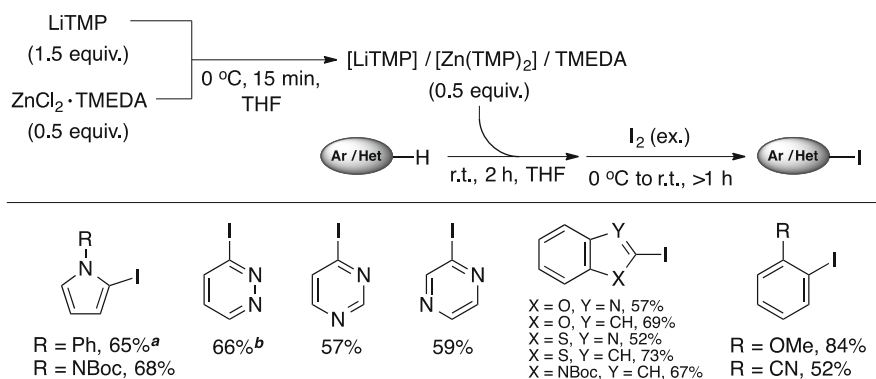
a. The reaction was done in hexane with TMEDA (5.0 equiv.); *b.* The reaction was refluxed in THF with TMEDA (5 equiv.)

Fig. 24 Deprotonative metalations of heteroaromatic compounds by using LiTMP/Zn(TMP)$_2$ (1/1) mixture

(TMP)$_3$ was initially proposed as the formula of the mixture, calculation and NMR analysis ruled out this possibility [76–78, 84]. For example, computational study showed clearly that the equilibrium between LiTMP/Zn(TMP)$_2$ and LiZn(TMP)$_3$ thermodynamically favors the mixture, in sharp contrast to the case of *TMP*-zincate LiZn(TMP)Me$_2$ (Eq. 22) [77]. However, compared with the low reactivity of LiTMP or Zn(TMP)$_2$, the LiTMP/Zn(TMP)$_2$ mixture showed surprisingly improved activity, implying a synergy between the two components. Hence, it is suggested that the deprotonation proceeds with LiTMP, and the resultant aryllithium intermediate is converted quickly to the more stabilized aryl diaminozincate **43** by in situ trapping with neutral Zn species, e.g., Zn(TMP)$_2$ (Eq. 23) [78].

$$ \text{Me}-\text{Zn}\underset{\text{Me}}{\overset{N}{\diagdown}}\text{Li} \xleftarrow[R = Me]{\Delta G = -12.0} \text{LiTMP} + \text{ZnR}_2 \xrightarrow[R = TMP]{\Delta G = +3.8} \textbf{N}-\text{Zn}\diagdown \text{Li} $$

N = TMP; B3LYP/6-31G*; ΔG: kcal/mol.

(22)

(23)

43
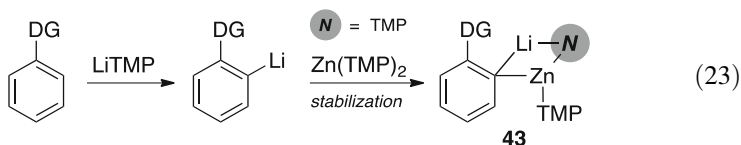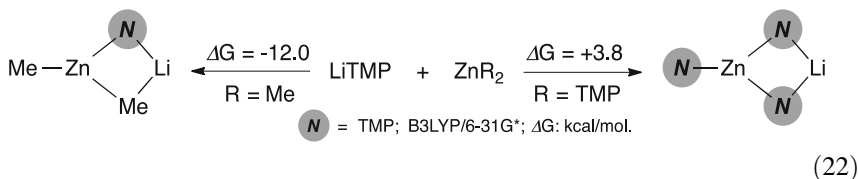
In 2010, Mongin and co-workers expanded this amino Li/Zn mixture model to a new combination alkyl/amino Li/Zn model, LiR/Zn(TMP)$_2$ (1/1) [78]. NMR analysis and calculation indicated formation of the zincate LiZn(TMP)$_2$R in these circumstances. Exceptionally, when (trimethylsilyl)methyllithium was used instead, the calculation showed that formation of a lithium zincate became unlikely and thus the reaction route may then be similar to that of the LiTMP/Zn(TMP)$_2$ combination. Nevertheless, these zincates or base mixtures are also effective for deprotonation of arenes (Eq. 24).

Ar /Het —H $\xrightarrow[\text{r.t., 2 h, THF}]{\substack{\textbf{A or B} \\ (1.0\ \text{equiv.})}}$ $\xrightarrow[\text{0 °C to r.t., >1 h}]{I_2\ (\text{ex.})}$

A: LiZn(TMP)$_2$^{n}Bu
B: (TMS)CH$_2$Li / Zn(TMP)$_2$ (1 : 1)

OMe —I   79% (**A**)   74% (**B**)

CN —I   100% (**A**)   90% (**B**)

58%   10%   mixture (**A**)

(24)
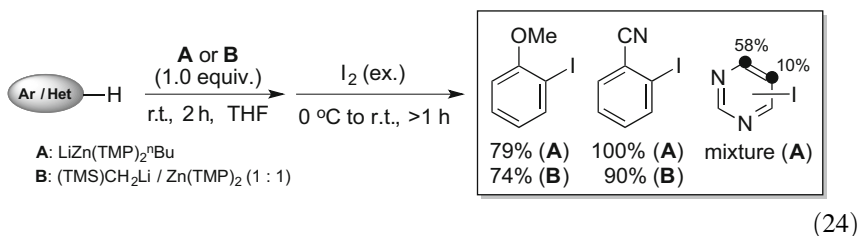
As an application of this work, deprotonation of metallocenes by use of *TMP*-zincate is appealing. Metallocenes, especially ferrocene, are widely employed in catalysis, materials science, and bioorganometallic chemistry, so their functionalization is considered important. In 2005, Mulvey, Hevia, and co-workers reported the first example of direct zincation of a metallocene, by using LiZn(TMP)^{n}Bu$_2$ and TMEDA as a ligand/cosolvent (Fig. 25) [85]. The result was significant but rather surprising, since the intermediate metallo-product from the deprotonative metalation was not the proposed ferrocenyl (Fc) zincate LiZn(TMP)(Fc)^{n}Bu **44** but a mixture of Li$_2$Zn(TMP)$_2$^{n}Bu$_2$(TMEDA) and a neutral Zn(Fc)$_2$(TMEDA) species. This mixture could further react with additional ferrocene to give a new zincate complex of [Li(THF)$_4$][Zn(Fc)$_3$]. Hence, it was hypothesized that the formation of LiZn(TMP)(Fc)^{n}Bu was followed by rapid disproportionation reaction to the neutral Zn(Fc)$_2$(TMEDA) and the zincate Li$_2$Zn(TMP)$_2$^{n}Bu$_2$(TMEDA). This result established for the first time that products of such deprotonative zincation (of course prior to any electrophilic capture) are not necessarily zincates themselves, in contrast to the case of normal arenes with LiZn(TMP)^{t}Bu$_2$ and related
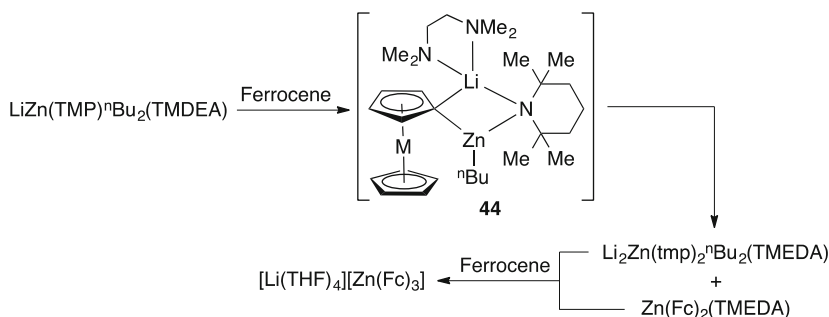
Fig. 25 Deprotonative metalations of ferrocene by using TMP-zincate

reagents. Later, in 2010, Mongin and co-workers reported the deprotonative zincation of substituted ferrocene by utilizing the combination of LiTMP/Zn (TMP)$_2$ (Eq. 25) [79]. The zincation exhibited a broad functional group tolerance, occurring efficiently and selectively at the *ortho*-position of the directing group to provide high yields of iodides after iodination. This reaction provided multiple choices for synthesis of functionalized ferrocene derivatives.

R = COOMe, 83%; R = CONEt$_2$, 81%; R = CN, 87%; R = Br, 64%
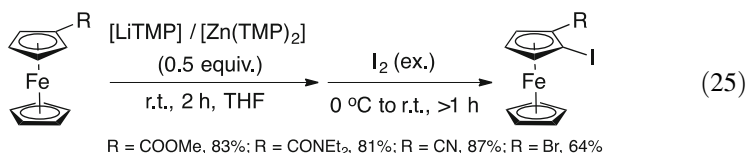
In 2009, Hevia and co-workers presented a new model for deprotonative zincation reaction (Eq. 26) [86]. Although TMP-zincates mediate highly chemo- and regioselective deprotonative zincation reactions for a wide range of aromatic substrates, treatment of LiZn(TMP)^{t}Bu$_2$ with phenyl trimethylsilyl ether did not lead to DoM reaction at the aromatic ring. Instead, a direct lateral metalation (DlM) took place at one of the methyl groups of the TMS group to generate a new zincate **45**. This was the first example of TMP-zincate expressing such DlM reactivity, illustrating the huge synthetic potential that ate complexes can offer.
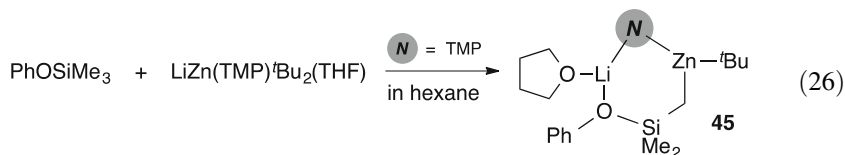
Besides these alkyl N-zincates, halo-N-zincate, i.e., combination of lithium halide and Zn(TMP)$_2$ or related compounds developed by Knochel et al. was also widely used for deprotonation of arenes and exhibited excellent reactivity and selectivity, especially for those arenes bearing functional groups. Such method has been well reviewed [61] and thus will not be extended in this chapter.

Table 9 Copper-catalyzed regioselective silylzincation of alkynes using *Si*-zincate

$$R^1 \!\!-\!\!\!\equiv\!\!\!-\!\! R^2 \xrightarrow[\text{THF, r.t., ~2 h, then H}^+]{\substack{\textit{\textbf{Si}}\text{-zincate (1.1 equiv.)} \\ \text{CuX (2.0 mol\%)}}} \underset{\underset{\textbf{\textit{L}}\text{inear}}{\overset{H}{\underset{Si}{}}}{\overset{R^1 \quad R^2}{}} + \underset{\underset{\textbf{\textit{B}}\text{ranched}}{\overset{Si}{\underset{H}{}}}{\overset{R^1 \quad R^2}{}}$$

Entry	R^1	R^2	*Si*-zincate	X	Yield (%)	*L:B*
1	$^nC_{10}H_{21}$	H	$LiZn(SiPh_3)Et_2$	I	90	100:0
2			$LiZn(SiMe_2Ph)^tBu_2$	CN	92	1:99
3	$BnO(CH_2)_2$	H	$LiZn(SiPh_3)Et_2$	I	87	100:0
4			$LiZn(SiMe_2Ph)^tBu_2$	CN	98	5:95
5	$THPO(CH_2)_2$	H	$MeMgZn(SiMe_3Ph)_3$	CN	97	100:0
6			$LiZn(SiMe_2Ph)^tBu_2$	CN	87	1:99
7	$HOCH_2$	H	$LiZn(SiMe_2Ph)Et_2$	CN	82	100:0
8	$HOCH_2$	Me	$LiZn(SiMe_2Ph)Et_2$	CN	85	100:0
9	$HO(CH_2)_2$	Me	$LiZn(SiMe_2Ph)_3$	CN	89	100:0
10	^{n}Hex	$SiMe_3$	$LiZn(SiMe2Ph)_3$	CN	42	0:100
11	^{n}Pen	^{n}Pen	$LiZn(SiMe_2Ph)Et_2$	CN	90	–

In summary, deprotonative zincation is a major focus of research in zincate chemistry and is practically very useful from the synthetic viewpoint.

6 Silylzincation of C–C Unsaturated Bonds with *Si*-Zincate

Elementometalation of C–C unsaturated bonds is a fundamentally important reaction for organic synthesis. In 1985, Oshima and co-workers reported the first silylzincation of alkyne with *Si*-zincate catalyzed by copper salts (Table 9) [35, 87]. Pd and Co catalysts were also effective, while Rh and Ru compounds showed little catalytic activity. The regioselectivity depended strongly on the nature of the *Si*-zincates. For terminal alkynes, the usage of less bulky zincates, e.g., $LiZn(SiPh_3)$ Et_2, favored the formation of 1-silylalkenes (linear), while 2-silylalkenes (branched) were the main products of bulkier zincates such as $LiZn(SiMe_2Ph)^tBu_2$ (entries 1–6). Internal alkynes could also react smoothly (entries 7–11). Generally, this method is used for alkynes such as propargylic or homopropargylic alcohols and their derivatives, since these reactions showed more regioselectivity than those with other types of alkynes (entries 3–9). The silyl-substituted acetylene could also undergo regiospecific silylzincation, albeit the yields were low (entry 10).

Important and interesting as this reaction was there was little follow-up. In 2004, our group reported a new method for such silylzincation (Table 10) [88], which proceeded without any TM catalyst via the dianion-type *Si*-zincates in just 1.1 equiv., in sharp contrast with Oshima's initial work, which required an excess amount of (2–3 equiv.) zincates and addition of copper salts as a catalyst. The SiBNOL-zincate showed the highest reactivity, and its reaction toward various

Table 10 Direct silylzincation of alkynes

$$R\text{—}\equiv\text{—}H \xrightarrow[\substack{\text{THF, r.t., 12 h,} \\ \text{then H}^+}]{\substack{\text{SiBNOL-zincate} \\ \text{(1.1 equiv.)}}} \begin{array}{c} R \quad H \\ \diagdown \diagup \\ \diagup \diagdown \\ H \quad SiMe_2Ph \\ \textit{Linear} \end{array} + \begin{array}{c} R \quad H \\ \diagdown \diagup \\ \diagup \diagdown \\ PhMe_2Si \quad H \\ \textit{Branched} \end{array}$$

SiBNOL-zincate: Li+ and ClMg+, with biphenyl-diolate O,O bound to Zn^{2-} bearing ^tBu and $SiMe_2Ph$

Entry	R	Yield (%)	L:B
1	^nBu	88	95:5
2	Cy	94	92:8
3	Bn	100	75:25
4	$Cl(CH_2)_3$	89	94:6
5	$Et_2NOC(CH_2)_4$	92	74:26
6	$EtOOC(CH_2)_4$	100	86:14
7	$HOOC(CH_2)_2$	99	81:19[a]
8	$HO(CH_2)_3$	80	85:15[a]
9	Me_3Si	73	0:100
10	Ph	100	12:98
11	$3'$-Py	100	0:100
12	Fc	92	50:50
13	$MeOCH_2$	83	12:88[b]
14	$HOCH_2$	100	15:95
15	H_2NCH_2	99	8:92
16	Me_2NCH_2	76	0:100

[a]2.2 equiv. of zincates were used
[b]The reaction was carried out at $-78°C$ for 4 h
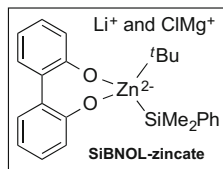
terminal alkynes preferentially gave 2-silylalkenes (branch selectivity). Propargylic alcohols, ethers, amines, or silylacetylene tended to form 1-silylalkenes through reversed regioselectivity, probably due to chelation from oxygen and nitrogen, or α-stabilization from silicon. Internal alkyne did not react at room temperature (Eq. 27), but could participate in the reaction if the mixture was slightly heated (Eq. 28). The yield for reaction of internal alkyne is lower, due to its weaker reactivity compared with terminal alkynes. The potential for further functionalization of the Zn site in the silylzincation products (before quenching) was also tested.

$$^nPr\text{—}\equiv\text{—}CH_2\text{—}\equiv \xrightarrow[\text{THF, r.t., 12 h, then H}^+]{\text{SiBNOL-zincate (1.1 equiv.)}} {}^nPr\text{—}\equiv\text{—}CH_2\text{—}C(=CH_2)SiMe_2Ph \quad 85\% \qquad (27)$$

$$Et\text{—}\equiv\text{—}Et \xrightarrow[\text{THF, 40 °C, 12 h, then H}^+]{\text{SiBNOL-zincate (1.1 equiv.)}} \begin{array}{c} Et \quad Et \\ \diagdown \diagup \\ \diagup \diagdown \\ H \quad SiMe_2Ph \end{array} \quad 58\% \qquad (28)$$
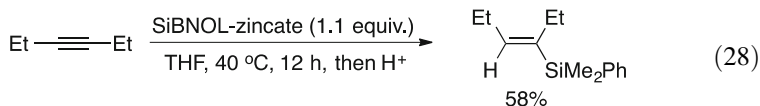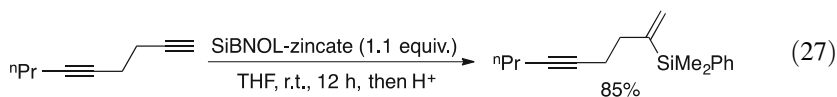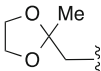
Table 11 Cp$_2$TiCl$_2$-catalyzed silylzincation of alkenes

R $\diagdown\diagup$ $\xrightarrow[\text{THF, r.t., 18 h}]{\substack{\text{SiSiNOL-zincate (1.1 equiv.)} \\ \text{Cp}_2\text{TiCl}_2 \text{ (5 mol\%)}}}$ R $\diagup\diagdown\diagup$ SiMe$_2$Ph
E / Z

SiSiNOL-zincate

Entry	R	Yield (%)	*E:Z*
1	TBDPSO(CH$_2$)$_2$	95	24:76
2	BnO(CH$_2$)$_3$	92	28:72
3	^{t}BuCO(CH$_2$)$_2$	94	29:71[a]
4	^{t}BuS(CH$_2$)$_2$	88	26:74
5	Bn$_2$N(CH$_2$)$_2$	75	21:79
6	HO(CH$_2$)$_2$	55	26:74[b]
7	HOOC(CH$_2$)$_2$	100	24:76[b]
8	Me$_2$NCOO(CH$_2$)$_2$	95	24:76
9	EtOCOO(CH$_2$)$_2$	79	27:73
10	MeOOC(CH$_2$)$_2$	80	23:77
11	Ph	84	N.D.
12	Cy	47	49:51[c]
13	Bn	71	26:74[d]
14	(dioxolane-O,O)C(Me)CH$_2$CH$_2$	81	21:79[e]

[a]The reaction was carried out under reflux
[b]3.0 equiv. of zincates were used
[c]The reaction was carried out at 45°C, where vinylsilane was isolated in 18% yield (*E:Z* = 64:36)
[d]Vinylsilane was isolated in 8% yield (*E:Z* = 58:42)
[e]Vinylsilane was isolated in 19% yield (*E:Z* = 50:50)

The *Si*-zincate could not react directly with alkenes [89]. However, in the presence of TM catalyst, the silylzincation could also take place at terminal alkenes. The first such example was reported in 2005 by our group (Table 11) [90]. Catalyzed by Cp$_2$TiCl$_2$, SiSiNOL-zincate and terminal alkenes could be regio- and chemoselectively transformed into allylsilanes. It seemed that in the metalation, the silyl group was specifically introduced at the 1-position and the elimination at the 3-position was favored to form *E*- or *Z*-alkenes. Many active groups could be compatible with these reactions.

The mechanism was initially proposed to be a silylmetalation–β-H-elimination process. The selectivity for elimination switched when a large group was attached adjacent to the double bond (entries 12–14). On the other hand, in the reaction of substrates without hydrogen at the 3-position, such as styrene, the transformation was complete, and a mixture of alkylsilane and vinylsilane was obtained, in which the latter was the major product (Eq. 29). These results provided some support for the proposed mechanism, though the details remain unclear. Finally, only *mono*-substituted alkenes worked in this method, and 1,1-disubstituted and 1,2-disubstituted alkenes were unreactive even if heated.

Table 12 CuCN-catalyzed silylzincation of alkenes

Entry	R	Yield (%)	*L:B*
1	$2'$-MeOC$_6$H$_4$CH$_2$	81	90:10
2	$4'$-MeOC$_6$H$_4$CH$_2$	97	86:14
3	$3',4'$-(MeO)$_2$C$_6$H$_3$CH$_2$	88	84:16
4	BnCH$_2$	85	81:19
5	Cl(CH$_2$)$_4$	73	84:16
6	TBSO(CH$_2$)$_4$	85	87:13
7	BnO(CH$_2$)$_2$	66	86:14
8	^{t}BuS(CH$_2$)$_3$	76	79:21
9	BnNHCO(CH$_2$)$_3$	77	92:8
10	MeCOO(CH$_2$)$_4$	80	83:17
11	Me$_2$NCOO(CH$_2$)$_3$	90	82:18
12	EtOCOO(CH$_2$)$_3$	94	78:22
13	NC(CH$_2$)$_2$	85	99:1
14	Ph$_2$P(O)CH$_2$	79	99:1

(29)

In 2007, our group demonstrated another alkene silylmetalation. When CuCN was employed as the catalyst, the reaction between SiBNOL-zincate and mono-substituted alkenes stopped after silylzincation and further elimination did not occur (Table 12) [91]. Similar to the Cp$_2$TiCl$_2$-catalyzed reaction, this reaction was selective but not specific, giving a mixture in which 1-silylalkane (linear) was the major product. The silylation occurred to give the branched 2-silylalkane in a regiospecific manner only when strongly coordinative groups such as cyano or phosphine oxide existed at a suitable position (entries 13–14). 1,2-Disubstituted alkenes showed sluggish reactivity, except for those with unusual structures (Eq. 30).

(30)

In 2010, our group examined the silylzincation of allenes (Table 13) [92]. Since there were two double bonds in allene molecules involving an *sp*-carbon, the

Table 13 CuCN-catalyzed silylzincation of allenes

Entry	R^1	*Si*-zincate	t (h)	T (°C)	Yield (%)	*I:T*
1	Me	MeZn(SiMe$_2$Ph)	1	25	90	81:73
2		LiZn(SiMe$_2$Ph)$_3$	24	25	92	1:99
3	^{t}Bu	MeZn(SiMe$_2$Ph)	1	25	87	94:6
4		LiZn(SiMe$_2$Ph)$_3$	24	25	98	12:88
5	F	MeZn(SiMe$_2$Ph)	24	−78	97	98:2
6		LiZn(SiMe$_2$Ph)$_3$	24	25	87	16:84
7	Cl	MeZn(SiMe$_2$Ph)	24	−78	82	94:6
8		LiZn(SiMe$_2$Ph)$_3$	24	25	85	16:84
9	Br	MeZn(SiMe$_2$Ph)	24	−78	89	97:3
10		LiZn(SiMe$_2$Ph)$_3$	24	25	42	12:88
11	EtOOC	MeZn(SiMe$_2$Ph)	1	−100	55	64:36
12		LiZn(SiMe$_2$Ph)$_3$	24	25	72	15:85
13	^{i}Pr$_2$NOC	MeZn(SiMe$_2$Ph)	1	−78	44	89:11
14		LiZn(SiMe$_2$Ph)$_3$	24	−40	75	28:72
15	MeO	MeZn(SiMe$_2$Ph)	1	25	58	90:10
16		LiZn(SiMe$_2$Ph)$_3$	24	25	100	1:99
17	Ph	MeZn(SiMe$_2$Ph)	1	25	76	95:5
18		LiZn(SiMe$_2$Ph)$_3$	24	25	92	10:90
19		MeZn(SiMe$_2$Ph)	6	25	46	93:7
20		LiZn(SiMe$_2$Ph)$_3$	24	25	78	19:81

selectivity was particularly abstractive. Very different from the cases of alkynes and alkenes, the TM-catalyst-free silylzincation of allenes could even take place smoothly and selectively at internal double bonds with MeZn(SiMe$_2$Ph), a neutral zinc species (such Zn compound was also effective for silylzincation of alkenes and alkyne with CuI as catalyst [93]). Surprisingly, tuning the coordination of zinc could further change the selectivity. When *Si*-zincate-*ma*, LiZn(SiMe$_2$Ph)$_3$, was used, addition toward the terminal double bonds became the main route. However, the reaction became inefficient and unselective when *Si*-zincate-*da* was employed.

Beside silylzincation, Michael addition using *Si*-zincate could also introduce silyl groups into C–C unsaturated bonds. 1,4-Addition by using *Sn*-zincate was also reported. Since studies on Michael addition using (heteroelement)-zincates have been well summarized elsewhere [8], the reaction will not be considered in detail in this chapter.

In general, silylzincation is a useful synthetic method for a variety of silanes. The intermediate before quenching, 1-silyl-2-zinc species, could be further functionalized at both the Si and Zn sites, so there is potential for diverse synthetic applications.
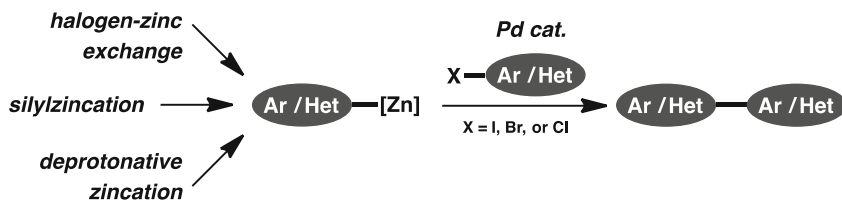
Fig. 26 Negishi coupling by using zincate

7 Applications of Lithium Zincates for Developing New Cross-Coupling Reactions

Zincates have been used as Negishi coupling partners, as described above, where we have mainly presented examples of successive transformations of zincates generated from halogen–zinc exchanges, deprotonative zincations, or silylzincations to show potential utility (Fig. 26). In such reactions, traditional coupling protocols such as palladium catalyst and aryl iodides or bromides were used. In recent years, investigations focused on new cross-coupling methods using zincates have also been reported.

As mentioned in the beginning of this chapter, improvements of the reactivity of organozinc reagents by adding lithium chloride were reported, and the mechanism involving *halogen*-zincate was also proved. [37–42, 94] This LiX-mediated protocol has been widely used for classic Negishi coupling, and details of which will not be extended here due to many previous reviews on this topic. Very recently, Organ et al. reported and clarified an interesting improvement for alkyl–alkyl Negishi coupling [40, 41]. When alkyl bromide and lithium-free RZnBr were treated with Pd catalyst, no coupling occurred at all. When 1 equiv. of LiX (X=Cl or Br) was added, the reaction still did not proceed. However, when 2 equiv. of LiX were added, alkyl–alkyl cross coupling proceeded smoothly with quantitative conversion (Fig. 27). These results suggested the involvement of higher-order X-zincates-*da* Li_2ZnRX_3 (X=Br or Cl) as active species. Later in 2012, Organ's group reported that ammonium salts were effective for preparing *halogen*-zincate-*da* as well. Ammonium zincate underwent alkyl–alkyl cross coupling with alkyl bromides under mild conditions and in high yields (Fig. 28) [95].

In 2012, our group reported a new type of Negishi coupling reaction between zincate and aryl ether (Eq. 31) [96]. Due to the inertness of etheric C–O bond, developments in cross coupling of aryl ethers as electrophiles via C–O bond cleavage have been rather limited. Indeed, when neutral arylzinc reagents such as ArZnX, ZnAr$_2$, zincate-*ma*, and LiZnMe$_2$Ar were treated with aryl ether in the presence of nickel catalyst, no reaction took place. However, when zincate-*da* Li_2ZnMe_3Ar was used, coupling reaction proceeded smoothly at room temperature to provide the corresponding biaryl products.

$$^nBuZnBr \quad + \quad 2 \times LiX$$

Ph⁓⁓Br + LiZn^{n}BuX$_3$ $\xrightarrow[\text{THF/DMI (2 : 1), r.t., 2 h}]{\text{Pd-PEPPSI-IPr (1.0 mol\%)}}$ Ph⁓⁓^{n}Bu

(1.0 equiv.)   (1.6 equiv.)   X = Cl or Br, 100%
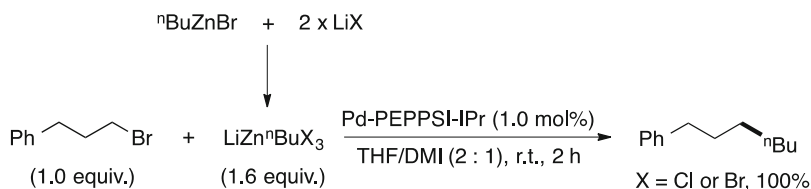
Fig. 27 Alkyl–alkyl Negishi coupling promoted by lithium halides

R^1—Br   + $(^nBu_4N^+)_2[ZnR^2X_3]^{2-}$ $\xrightarrow[\text{THF, r.t., 2 h}]{\text{Pd-PEPPSI-IPent (5.0 mol\%)}}$ R^1—R^2

(1.0 equiv.)   (1.1 equiv.)
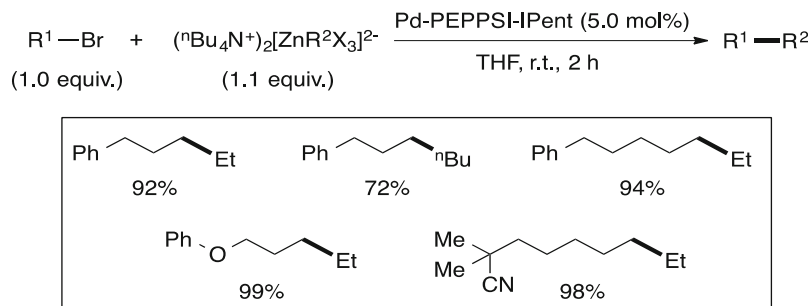
Fig. 28 Alkyl–alkyl Negishi coupling promoted by ammonium halides

Ar¹—OMe   +   Li₂Me₃Zn—Ar² $\xrightarrow[\text{toluene, r.t., 6-12 h}]{\substack{\text{Ni(cod)}_2 \text{ (4 mol\%)} \\ \text{PCy}_3 \text{ (8 mol\%)}}}$ Ar¹—Ar² (31)

(1.0 equiv.)   (2-3 equiv.)   (up to 88%)
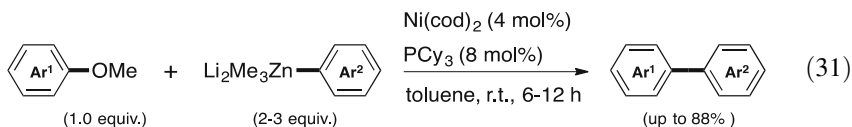
To test the utility of this cross-coupling method, the phenylation of (+)-naproxen amide was examined (Eq. 32). (+)-Naproxen is a commonly used drug for relief of pain, fever, inflammation, and stiffness. Using this coupling method, C–C bond formation was achieved efficiently, under very mild conditions, at the methoxy group of (+)-naproxen, which is generally regarded as unreactive. Further, almost no racemization occurred at the sensitive benzylic and α-ketonic positions. These results demonstrate the potential applicability of this method for late-stage derivatization of functional molecules.

(32)
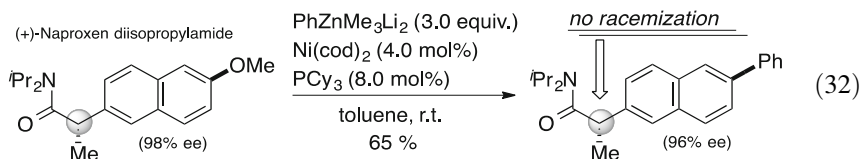
Table 14 Polymerization of NIPAm initiated by zincate

Entry	Solvent	Time (h)	Yield (%)	M_n	PDI
1	THF	24	8	7,000	1.50
2	THF	168	33	7,000	2.71
3	MeOH	3	76	18,000	1.65
4	H$_2$O	<1	92	27,000	2.72

8 Applications of Lithium Zincate in Synthesis of Polymers

In 2004, our group described a new organozincate-mediated anionic polymerization using Li$_2$Zn^{t}Bu$_4$ as an initiator [97]. Acrylic acid derivatives behaved as activated olefins owing to their conjugated carbonyl groups, and hence *N*-isopropyla-crylamide (NIPAm) was chosen as a representative target monomer for polymerization (Table 14). Poly(*N*-isopropylacrylamide) (PNIPAm) exhibits unique temperature-sensitive properties. It has been applied in various ways in organic chemistry, material science, and biotechnology. The ^{t}Bu ligand and the zincate character were very important for this polymerization, since other zincates such as LiZnMe$_3$ or Li$_2$ZnMe$_4$ and simple species such as ^{t}BuLi, ZnCl$_2$, LiCl, or LiOH did not initiate polymerization at all. The reaction was quite sluggish in THF, and the product could be obtained only in low yield (entries 1–2). However, the reaction was dramatically promoted when a protic solvent (MeOH or H$_2$O) was used (entries 3–4). Other acryl acid derivatives were also available for polymerization with this method, including *N,N*-dimethylacrylamide (DMA, 74%), acrylamide (AM, 84%), and 2-hydroxyethylmethacrylate (HEMA, 92%).

Unlike acrylic acid derivatives, styrene is not activated by a conjugated carbonyl group, and therefore it was of interest to know whether the present anionic polymerization method is applicable to polystyrene synthesis. Poly(styrene) is among the most important synthetic polymers, being encountered ubiquitously in daily life. The control of its polymerization is of great commercial significance. Whereas controlled thermal polymerization produces the highest molecular weight product in radical-initiated synthesis of polystyrene, undesirable spontaneous polymerizations can clog styrene production facilities. Indeed, the Li$_2$Zn^{t}Bu$_4$-initiated polymerization of styrene could take place in a protic solvent (MeOH or H$_2$O) [15], but the yield was extremely low, probably because deprotonation reaction of solvents took place prior to carbozincation (polymerization) reaction between styrene and zincate (entries 1–2, Table 15). In aprotic solvent (e.g., Et$_2$O) or under bulk polymerization (neat) conditions, polymerization proceeded smoothly at room temperature to give polystyrene with low polydispersity in high yield (entries 3–4).

Table 15 Polymerization of styrene initiated by zincate
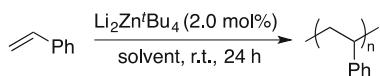
Entry	Solvent	Yield (%)	M_n	PDI
1	H_2O	3.9	5,500	1.58
2	MeOH	0.2	–	–
3	Et_2O	76	3,500	1.02
4	Neat	92	4,200	1.13

Table 16 Halogen–zinc exchange and catalyst-transfer polycondensation for synthesis of regioregular P3HT using zincate
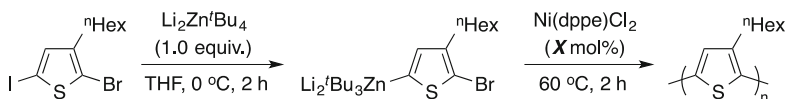
Entry	Cosolvent	Yield (%)	X mol%	M_n	PDI	r.r
1	–	90	6.67	2,500	1.20	90
2	–	88	3.33	5,400	1.18	94
3	–	89	1.67	10,200	1.15	97
4	–	85	0.83	21,700	1.15	98
5	–	80	0.56	30,700	1.19	99
6	^{i}PrOH (1.0 equiv.)	60	1.67	10,900	1.15	97
7	MeOH (1.0 equiv.)	52	1.67	11,900	1.19	97
8	H_2O (1.0 equiv.)	50	1.67	16,800	1.72	97

In 2012, Higashihara and co-workers reported another possibility for application of zincate in polymerization, through an exchange–cross-coupling process (Table 16) [98]. When 2-bromo-3-hexyl-5-iodothiophene was treated with $Li_2Zn^tBu_4$, iodine–zinc exchange reaction took place specifically. When the resultant zincate was heated with nickel catalyst at 60°C, polymerization proceeded in a controlled manner to afford poly(3-n-hexylthiophene) (P3HT) with the predicted M_n values (2.50−30.7 kDa) and low PDIs (<1.2) in high yields (entries 1–5). Due to the stability of $Li_2Zn^tBu_4$ and related zincate species, similar experiments in THF containing a protic impurity (^{i}PrOH or MeOH) were also successful (entries 7–8). In addition, high-molecular-weight P3HT could be obtained in 50% yield in THF containing a small amount of water (1.0 equiv.), although the PDI increased to 1.72, probably due to competitive termination reactions with water during the polymerization (entry 9).

Since $Li_2Zn^tBu_4$ could well tolerate substrates bearing an acidic proton (Fig. 12), the protection-free synthesis of poly[3-(6-hydroxyhexyl)thiophene] (P3HHT), with hydroxyhexyl side chains, was also successful (Fig. 29). After halogen–metal exchange reaction of 2-bromo-3-(6-hydroxyhexyl)-5-iodothiophene with
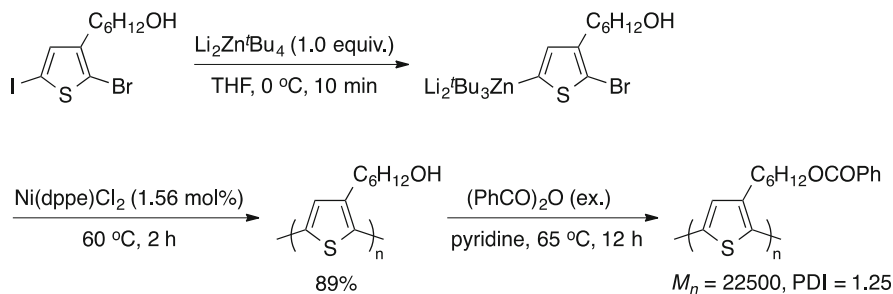
Fig. 29 Protection-free polymerization leading to poly[3-(6-hydroxyhexyl)thiophene] by using $Li_2Zn^tBu_4$

$Li_2Zn^tBu_4$, the resultant monomer could further undergo polymerization catalyzed by Ni to afford P3HHT in 89% yield. However, due to the poor solubility of P3HHT, SEC and NMR characterizations were very difficult. Hence, the product was further derivatized to benzoylated P3HHT (P3HHT-Bz), which was easily characterized due to its excellent solubility.

References

1. Frankland E (1850) On the isolation of the organic radicals. Quart J Chem Soc 2:263–296. doi:10.1039/QJ8500200263
2. Seyferth D (2001) Zinc alkyls, Edward Frankland, and the beginnings of main-group organometallic chemistry. Organometallics 20:2940–2955. doi:10.1021/om010439f
3. Wanklyn JA (1858) Ueber einige neue aethylverbindungen, welche alkalimetalle enthalten. Liebigs Ann 108:67–79. doi:10.1002/jlac.18581080116
4. Hurd DT (1948) Complex metal alkyls. J Org Chem 13:711–713. doi:10.1021/jo01163a015
5. Wittig G, Meyer FJ, Lange G (1951) Über das verhalten von diphenylmetallen als komplexbildner. Liebigs Ann 571:167–201. doi:10.1002/jlac.19515710302
6. von Wittig G (1958) Komplexbildung und Reaktivität in der metallorganischen Chemie. Angew Chem 70:65–71. doi:10.1002/ange.19580700302
7. Wheatley AEH (2004) Recent developments in the synthetic and structural chemistry of lithium zincates. New J Chem 28:435–443. doi:10.1039/b314042c
8. Harada T (2006) The chemistry of organozincate compounds. In: Rappoport Z, Marek I (eds) The chemistry of organozinc compounds. Wiley, West Sussex, pp 685–712
9. Mulvey RE, Mongin F, Uchiyama M, Kondo Y (2007) Deprotonative metalation using ate compounds: synergy, synthesis, and structure building. Angew Chem Int Ed 46:3802–3824. doi:10.1002/anie.200604369
10. Uchiyama M, Koike M, Kameda M et al (1996) Unique reactivities of new highly coordinated ate complexes of organozinc derivatives. J Am Chem Soc 118:8733–8734. doi:10.1021/ja961320e
11. Uchiyama M, Kondo Y, Miura T, Sakamoto T (1997) First observation of Zn−CN Bond in "highly coordinated" mixed organozincates by exafs spectroscopy. J Am Chem Soc 119:12372–12373. doi:10.1021/ja971502o

12. Uchiyama M, Kameda M, Mishima O et al (1998) New formulas for oganozincate chemistry. J Am Chem Soc 120:4934–4946. doi:10.1021/ja973855t

13. Isobe M, Kondo S, Nagasawa N, Goto T (1977) Trialkylzinclithium [R3ZnLi]: a new reagent for conjugate addition to α, β-unsaturated ketones. Chem Lett 6:679–682. doi:10.1246/cl.1977.679

14. Uchiyama M, Furuyama T, Kobayashi M et al (2006) Toward a protecting-group-free halogen−metal exchange reaction: practical, chemoselective metalation of functionalized aromatic halides using dianion-type zincate, $^{t}Bu_4ZnLi_2$. J Am Chem Soc 128:8404–8405. doi:10.1021/ja058246x

15. Furuyama T, Yonehara M, Arimoto S et al (2008) Development of highly chemoselective bulky zincate complex, $^{t}Bu_4ZnLi_2$: design, structure, and practical applications in small-/macromolecular synthesis. Chem Eur J 14:10348–10356. doi:10.1002/chem.200800536

16. Aldridge S, Downs AJ (2001) Hydrides of the main-group metals: new variations on an old theme. Chem Rev 101:3305–3366. doi:10.1021/cr960151d

17. Kobetz P, Becker WE (1963) Preparation of sodium hydride complexes of diethylzinc and zinc chloride. Inorg Chem 2:859–859. doi:10.1021/ic50008a046

18. Kubas GJ, Shriver DF (1970) Nature of dialkyl- and diarylzinc hydride complexes. J Am Chem Soc 92:1949–1954. doi:10.1021/ja00710a028

19. Uchiyama M, Furumoto S, Saito M et al (1997) Design, reactivities, and practical application of dialkylzinc hydride ate complexes generated in situ from dialkylzinc and metal hydride: a new methodology for activation of NaH and LiH under mild conditions. J Am Chem Soc 119:11425–11433. doi:10.1021/ja9718477

20. Aida T, Kuboki N, Kato K et al (2005) Use of CaH_2 as a reductive hydride source: reduction of ketones and imines with CaH_2/ZnX_2 in the presence of a Lewis acid. Tetrahedron Lett 46:1667–1669. doi:10.1016/j.tetlet.2005.01.058

21. Tsuhako A, He J-Q, Mihara M et al (2007) Carbonyl reduction with CaH_2 and R_3SiCl catalyzed by $ZnCl_2$. Tetrahedron Lett 48:9120–9123. doi:10.1016/j.tetlet.2007.10.123

22. Lennartson A, Håkansson M, Jagner S (2007) Facile synthesis of well-defined sodium hydridoalkylzincates(II). Angew Chem Int Ed 46:6678–6680. doi:10.1002/anie.200701477

23. Spielmann J, Piesik D, Wittkamp B et al (2009) Convenient synthesis and crystal structure of a monomeric zinc hydride complex with a three-coordinate metal center. Chem Commun 3455–3456. doi:10.1039/b906319f

24. Kahnes M, Görls H, González L, Westerhausen M (2010) Synthesis and catalytic reactivity of Bis(alkylzinc)-hydride-di(2-pyridylmethyl)amides. Organometallics 29:3098–3108. doi:10.1021/om100153z

25. Campbell R, Cannon D, García-Álvarez P et al (2011) Main group multiple C–H/N–H bond activation of a diamine and isolation of a molecular dilithium zincate hydride: experimental and DFT evidence for alkali metal–zinc synergistic effects. J Am Chem Soc 133:13706–13717. doi:10.1021/ja205547h

26. Coles MP, El-Hamruni SM, Smith JD, Hitchcock PB (2008) An organozinc hydride cluster: an encapsulated tetrahydrozincate? Angew Chem Int Ed 47:10147–10150. doi:10.1002/anie.200804224

27. Marciniak W, Merz K, Moreno M, Driess M (2006) Convenient access to homo- and heterobimetallic alkoxo hydridozinc clusters of formula $[(HZnO^tBu)_{4-n}(LiO^tBu)_n]$ (n = 0, 1, 2, 3). Organometallics 25:4931–4933. doi:10.1021/om060443x

28. Kondo Y, Shilai M, Uchiyama M, Sakamoto T (1999) TMP−zincate as highly chemoselective base for directed ortho metalation. J Am Chem Soc 121:3539–3540. doi:10.1021/ja984263t

29. Imahori T, Uchiyama M, Sakamoto T, Kondo Y (2001) Regiocontrolled deprotonative-zincation of bromopyridines using aminozincates. Chem Commun 2450–2451. doi:10.1039/b108252n

30. Fabicon RM, Parvez M, Richey HG Jr (1991) Formation of organozincate ions from diorganozinc compounds and potassium alkoxides. J Am Chem Soc 113:1412–1414. doi:10.1021/ja00004a053

31. Harada T, Katsuhira T, Hattori K, Oku A (1993) Stereoselective carbon-carbon bond-forming reaction of 1,1-dibromocyclopropanes *via* 1-halocyclopropylzincates. J Org Chem 58:2958–2965. doi:10.1021/jo00063a010

32. Aggarwal VK, Sommer K (2006) Rearrangements of organozinc compounds. In: Rappoport Z, Marek I (eds) The chemistry of organozinc compounds. Wiley, West Sussex, pp 595–640

33. Lombardo M, Trombini C (2006) The chemistry of zinc enolates. In: Rappoport Z, Marek I (eds) The chemistry of organozinc compounds. Wiley, West Sussex, pp 797–862

34. Ryu I, Ikebe M, Sonoda N, Yamato S, Yamamura G, Komatsu M (2000) Conjugate addition of zincates derived from ketone α, β-dianions to enones. An access to unsymmetrical 1,6-diketones. Tetrahedron Lett 41:5689–5692. doi:10.1016/S0040-4039(00)00925-4

35. Okuda Y, Wakamatsu K, Tűckmantel W, Oshima K, Nozaki H (1985) Copper catalyzed silylzincation of acetylenes. Tetrahedron Lett 26:4629–4632. doi:10.1016/S0040-4039(00)98770-7

36. Krief A, Provins L, Dumont W (1999) Metal-mediated, completely diastereofacial conjugate addition of trialkylstannylmetal reagents to γ-alkoxy-α, β-unsaturated esters. Angew Chem Int Ed 38:1946–1948. doi:10.1002/(SICI)1521-3773(19990712)38:13/14<1946::AID-ANIE1946>3.0.CO;2-9

37. Krasovskiy A, Malakhov V, Gavryushin A, Knochel P (2006) Efficient synthesis of functionalized organozinc compounds by the direct insertion of zinc into organic iodides and bromides. Angew Chem Int Ed 45:6040–6044. doi:10.1002/anie.200601450

38. Koszinowski K, Böhrer P (2009) Aggregation and reactivity of organozincate anions probed by electrospray mass spectrometry. Organometallics 28:100–110. doi:10.1021/om8007037

39. Koszinowski K, Böhrer P (2009) Formation of organozincate anions in LiCl-mediated zinc insertion reactions. Organometallics 28:771–779. doi:10.1021/om800947t

40. Achonduh GT, Hadei N, Valente C et al (2010) On the role of additives in alkyl–alkyl Negishi cross-couplings. Chem Commun 46:4109–4111. doi:10.1039/c002759f

41. Hunter HN, Hadei N, Blagojevic V et al (2011) Identification of a higher-order organozincate intermediate involved in Negishi cross-coupling reactions by mass spectrometry and NMR spectroscopy. Chem Eur J 17:7845–7851. doi:10.1002/chem.201101029

42. Fleckenstein JE, Koszinowski K (2011) Lithium organozincate complexes LiRZnX$_2$: common species in organozinc chemistry. Organometallics 30:5018–5026. doi:10.1021/om200637s

43. Harada T, Hara D, Hattori K, Oku A (1988) Generation and alkylation reaction of 1-bromoalkenylzincate. Tetrahedron Lett 29:3821–3824. doi:10.1016/S0040-4039(00)82124-3

44. Harada T, Katsuhira T, Oku A (1992) Stereochemistry in carbenoid formation by bromine/lithium and bromine/zinc exchange reactions of 1,1-dibromoalkenes: higher reactivity of the sterically more hindered bromine atom. J Org Chem 57:5805–5807. doi:10.1021/jo00048a002

45. Harada T, Katsuhira T, Hara D, Kotani Y, Maejima K, Kaji R, Oku A (1993) Reactions of 1,1-dihaloalkenes with triorganozincates: a novel method for the preparation of alkenylzinc species associated with carbon-carbon bond formation. J Org Chem 58:4897–4907. doi:10.1021/jo00070a027

46. Harada T, Katsuhira T, Hattori K, Oku A (1994) Stereochemistry in carbenoid formation by bromine/lithium and bromine/zinc exchange reactions of gem-dibromo compounds. Tetrahedron 50:7987–8002. doi:10.1016/S0040-4020(01)85284-4

47. Harada T, Hattori K, Katsuhira T, Oku A (1989) Generation and alkylation reaction of lithium 1-halocyclopropylzincate. Tetrahedron Lett 30:6035–6038. doi:10.1016/S0040-4039(01)93847-X

48. Harada T, Kotani Y, Katsuhira T, Oku A (1991) Novel method for generation of secondary organozinc reagent: application to tandem carbon-carbon bond formation reaction of 1,1-dibromoalkane. Tetrahedron Lett 32:1573–1576. doi:10.1016/S0040-4039(00)74275-4

49. Kondo Y, Takazawa N, Yamazaki C, Sakamoto T (1994) Halogen-zinc exchange reaction of haloaromatics with lithium trimethylzincate. J Org Chem 59:4717–4718. doi:10.1021/jo00096a005

50. Takada T, Sakurai H, Hirao T (2001) Oxovanadium(V)-induced oxidative ligand coupling of aryltrimethylzincates prepared from bromoarenes and dilithium tetramethylzincate. J Org Chem 66:300–302. doi:10.1021/jo000976u

51. Harada T, Kaneko T, Fujiwara T, Oku A (1997) A new method for preparing benzylzinc reagents *via* homologation of triorganozincates. J Org Chem 62:8966–8967. doi:10.1021/jo971615q

52. Harada T, Kaneko T, Fujiwara T, Oku A (1998) A novel 1,2-migration of arylzincates bearing a leaving group at benzylic position: application to a three-component coupling of p-iodobenzyl derivatives, trialkylzincates, and electrophiles leading to functionalized p-substituted benzenes. Tetrahedron 54:9317–9332. doi:doi: 10.1016/S0040-4020(98)00569-9

53. Harada T, Chiba M, Oku A (1999) Novel homologation reaction of arylzincates bearing a leaving group at the ortho and meta positions. J Org Chem 64:8210–8213. doi:10.1021/jo990937m

54. Uchiyama M, Miyoshi T, Kajihara Y et al (2002) Generation of functionalized asymmetric benzynes with TMP-zincates: effects of ligands on selectivity and reactivity of zincates. J Am Chem Soc 124:8514–8515. doi:10.1021/ja0202199

55. Nakamura S, Liu C-Y, Muranaka A, Uchiyama M (2009) Theoretical study on the halogen-zinc exchange reaction by using organozincate compounds. Chem Eur J 15:5686–5694. doi:10.1002/chem.200802393

56. Chau NTT, Meyer M, Komagawa S et al (2010) Homoleptic zincate-promoted room-temperature halogen-metal exchange of bromopyridines. Chem Eur J 16:12425–12433. doi:10.1002/chem.201001664

57. Kneisel FF, Dochnahl M, Knochel P (2004) Nucleophilic catalysis of the iodine–zinc exchange reaction: preparation of highly functionalized diaryl zinc compounds. Angew Chem Int Ed 43:1017–1021. doi:10.1002/anie.200353316

58. Kneisel FF, Leuser H, Knochel P (2005) Preparation and reactions of highly functionalized bis-arylzinc reagents using a Li(acac)-catalyzed iodine-zinc exchange. Synthesis 2625–2629. doi:10.1055/s-2005-872097

59. Mulvey RE (2009) Avant-garde metalating agents: structural basis of alkali-metal-mediated metalation. Acc Chem Res 42:743–755. doi:10.1021/ar800254y

60. Mulvey RE (2013) An alternative picture of alkali-metal-mediated metallation: cleave and capture chemistry. Dalton Trans 42:6676–6693. doi:10.1039/c3dt00053b

61. Haag B, Mosrin M, Ila H et al (2011) Regio- and chemoselective metalation of arenes and heteroarenes using hindered metal amide bases. Angew Chem Int Ed 50:9794–9824. doi:10.1002/anie.201101960

62. Clegg W, Dale SH, Drummond AM et al (2006) Alkali-metal-mediated zincation of anisole: synthesis and structures of three instructive ortho-zincated complexes. J Am Chem Soc 128:7434–7435. doi:10.1021/ja061898g

63. Clegg W, Dale SH, Hevia E et al (2006) Pre-Metalation structural insights into the use of alkali-metal-mediated zincation for directed ortho-metalation of a tertiary aromatic amide. Angew Chem Int Ed 45:2370–2374. doi:10.1002/anie.200503202

64. Clegg W, Dale SH, Harrington RW et al (2006) Post-metalation structural insights into the use of alkali-metal-mediated zincation for directedortho-metalation of a tertiary aromatic amide. Angew Chem Int Ed 45:2374–2377. doi:10.1002/anie.200503213

65. Uchiyama M, Matsumoto Y, Nobuto D et al (2006) Structure and reaction pathway of TMP-zincate: amido base or alkyl base? J Am Chem Soc 128:8748–8750. doi:10.1021/ja060489h

66. Uchiyama M, Matsumoto Y, Usui S et al (2007) Origin of chemoselectivity of TMP zincate bases and differences between TMP zincate and alkyl lithium reagents: a DFT study on model systems. Angew Chem Int Ed 46:926–929. doi:10.1002/anie.200602664

67. Kondo Y, Morey JV, Morgan JC et al (2007) On the kinetic and thermodynamic reactivity of lithium di(alkyl)amidozincate Bases in directed ortho metalation. J Am Chem Soc 129:12734–12738. doi:10.1021/ja072118m

68. García F, McPartlin M, Morey JV et al (2008) Suppressing the anionic fries rearrangement of aryl dialkylcarbamates; the isolation of a crystalline ortho-deprotonated carbamate. Eur J Org Chem 2008:644–647. doi:10.1002/ejoc.200701096

69. Clegg W, Conway B, Hevia E et al (2009) Closer insight into the reactivity of TMP−dialkyl zincates in directed ortho-zincation of anisole: experimental evidence of amido basicity and structural elucidation of key reaction intermediates. J Am Chem Soc 131:2375–2384. doi:10.1021/ja8087168

70. Schwab PFH, Fleischer F, Michl J (2002) Preparation of 5-brominated and 5,5′-dibrominated 2,2′-bipyridines and 2,2′-bipyrimidines. J Org Chem 67:443–449. doi:10.1021/jo010707j

71. Seo HJ, Yoon SJ, Jang SH, Namgoong SK (2011) Trimethyl borate-induced one-pot homologation reactions of isoquinoline with di-tert-butyl-TMP zincate. Tetrahedron Lett 52:3747–3750. doi:10.1016/j.tetlet.2011.05.045

72. Blair VL, Blakemore DC, Hay D et al (2011) Alkali-metal mediated zincation of N-heterocyclic substrates using the lithium zincate complex, $(THF)Li(TMP)Zn({}^{t}Bu)_2$ and applications in in situ cross coupling reactions. Tetrahedron Lett 52:4590–4594. doi:10.1016/j.tetlet.2011.06.090

73. Armstrong DR, Blair VL, Clegg W et al (2010) Structural basis for regioisomerization in the alkali-metal-mediated zincation (AMMZn) of trifluoromethyl benzene by isolation of kinetic and thermodynamic intermediates. J Am Chem Soc 132:9480–9487. doi:10.1021/ja1038598

74. Uchiyama M, Kobayashi Y, Furuyama T et al (2008) Generation and suppression of 3-/ 4-functionalized benzynes using zinc ate base (TMP−Zn−ate): new approaches to multisubstituted benzenes. J Am Chem Soc 130:472–480. doi:10.1021/ja071268u

75. Seggio A, Chevallier F, Vaultier M, Mongin F (2007) Lithium-mediated zincation of pyrazine, pyridazine, pyrimidine, and quinoxaline. J Org Chem 72:6602–6605. doi:10.1021/jo0708341

76. Seggio A, Lannou M-I, Chevallier F et al (2007) Ligand-activated lithium-mediated zincation of n-phenylpyrrole. Chem Eur J 13:9982–9989. doi:10.1002/chem.200700608

77. L'Helgoual'c J-M, Seggio A, Chevallier F et al (2008) Deprotonative metalation of five-membered aromatic heterocycles using mixed lithium−zinc species. J Org Chem 73:177–183. doi:10.1021/jo7020345

78. Snégaroff K, Komagawa S, Chevallier F et al (2010) Deprotonative metalation of substituted benzenes and heteroaromatics using amino/alkyl mixed lithium-zinc combinations. Chem Eur J 16:8191–8201. doi:10.1002/chem.201000543

79. Dayaker G, Sreeshailam A, Chevallier F et al (2010) Deprotonative metallation of ferrocenes using mixed lithium–zinc and lithium–cadmium combinations. Chem Commun 46:2862–2864. doi:10.1039/b924939g

80. Putzer MA, Neumüller B, Dehnicke K (1997) Synthese und kristallstrukturen der zinkate [Na (12-Krone-4)₂][Zn{N(SiMe₃)₂}₃] und [Na(12-Krone-4)₂]₂[Zn(CC−Ph)₃(THF)][Zn (CCPh)₃]. Anorg allg Chem 623:539–544. doi:10.1002/zaac.19976230184

81. Forbes GC, Kennedy AR, Mulvey RE, Rodger PJA (2001) TEMPO: a novel chameleonic ligand for s-block metal amide chemistry. Chem Commun 1400–1401. doi:10.1039/b104937m

82. Clegg W, Forbes GC, Kennedy AR et al (2003) Potassium–zinc induced synergic enhancement of the basicity of hexamethyldisilazide (HMDS) towards methylbenzene molecules. Chem Commun 406–407. doi:10.1039/b211392a

83. Mulvey RE (2001) s-Block metal inverse crowns: synthetic and structural synergism in mixed alkali metal–magnesium (or zinc) amide chemistry. Chem Commun 1049–1056. doi:10.1039/b101576l

84. García-Álvarez P, Mulvey RE, Parkinson JA (2011) "LiZn(TMP)3", a zincate or a turbo-lithium amide reagent? Dosy NMR spectroscopic evidence. Angew Chem Int Ed 50:9668–9671. doi:10.1002/anie.201104297

85. Barley HRL, Clegg W, Dale SH et al (2005) Alkali-metal-mediated zincation of ferrocene: synthesis, structure, and reactivity of a lithium-TMP-zincate reagent. Angew Chem Int Ed 44:6018–6021. doi:10.1002/anie.200501560

86. Hevia E, Kennedy AR, Klett J, McCall MD (2009) Direct lateral metallation using alkali-metal mediated zincation (AMMZn): SiC–H vs.Si–O bond cleavage. Chem Commun 3240–3242. doi:10.1039/b903592c

87. Wakamatsu K, Nonaka T, Okuda Y, Tückmantel W, Oshima K, Utimoto K, Nozaki H (1986) Transition-metal catalyzed silylzincation and silylalumination of acetylenic compounds. Tetrahedron 42:4427–4436. doi:10.1016/S0040-4020(01)87282-3

88. Nakamura S, Uchiyama M, Ohwada T (2004) Chemoselective silylzincation of functionalized terminal alkynes using dianion-type zincate (SiBNOL-Zn-ate): regiocontrolled synthesis of vinylsilanes. J Am Chem Soc 126:11146–11147. doi:10.1021/ja047144o

89. Nakamura S, Yonehara M, Uchiyama M (2008) Silylmetalation of alkenes. Chem Eur J 14:1068–1078. doi:10.1002/chem.200701118

90. Nakamura S, Uchiyama M, Ohwada T (2005) Cp_2TiCl_2-catalyzed regio- and chemoselective one-step synthesis of γ-substituted allylsilanes from terminal alkenes using dianion-type zincate (SiSiNOL-Zn-ate). J Am Chem Soc 127:13116–13117. doi:10.1021/ja0541074

91. Nakamura S, Uchiyama M (2007) Regio- and chemoselective silylmetalation of functionalized terminal alkenes. J Am Chem Soc 129:28–29. doi:10.1021/ja066864n

92. Yonehara M, Nakamura S, Muranaka A, Uchiyama M (2010) Regioselective silylzincation of phenylallene derivatives. Chem Asian J 5:452–455. doi:10.1002/asia.200900452

93. Auer G, Oestreich M (2006) Silylzincation of carbon–carbon multiple bonds revisited. Chem Commun 311–313. doi:10.1039/b513528a

94. Ochiai H, Jang M, Hirano K et al (2008) Nickel-catalyzed carboxylation of organozinc reagents with CO_2. Org Lett 10:2681–2683. doi:10.1021/ol800764u

95. McCann LC, Hunter HN, Clyburne JAC, Organ MG (2012) Higher-order zincates as transmetalators in alkyl-alkyl Negishi cross-coupling. Angew Chem Int Ed 51:7024–7027. doi:10.1002/anie.201203547

96. Wang C, Ozaki T, Takita R, Uchiyama M (2012) Aryl ether as a Negishi coupling partner: an approach for constructing C-C bonds under mild conditions. Chem Eur J 18:3482–3485. doi:10.1002/chem.201103784

97. Kobayashi M, Matsumoto Y, Uchiyama M, Ohwada T (2004) A new chemoselective anionic polymerization method for poly(N-isopropylacrylamide) (PNIPAm) in aqueous media: design and application of bulky zincate possessing little basicity. Macromolecules 37:4339–4341. doi:10.1021/ma0400261

98. Higashihara T, Goto E, Ueda M (2012) Purification-free and protection-free synthesis of regioregular poly(3-hexylthiophene) and poly(3-(6-hydroxyhexyl)thiophene) using a zincate complex of $^tBu_4ZnLi_2$. ACS Macro Lett 1:167–170. doi:10.1021/mz200128d

Index